

## University of Southampton Research Repository ePrints Soton

Copyright © and Moral Rights for this thesis are retained by the author and/or other copyright owners. A copy can be downloaded for personal non-commercial research or study, without prior permission or charge. This thesis cannot be reproduced or quoted extensively from without first obtaining permission in writing from the copyright holder/s. The content must not be changed in any way or sold commercially in any format or medium without the formal permission of the copyright holders.

When referring to this work, full bibliographic details including the author, title, awarding institution and date of the thesis must be given e.g.

AUTHOR (year of submission) "Full thesis title", University of Southampton, name of the University School or Department, PhD Thesis, pagination

**UNIVERSITY OF SOUTHAMPTON**

School of Medicine / School of Health Sciences

**Altered cutaneous vasoreactivity and  
microvascular control mechanisms as a risk  
factor for pressure ulcer development**

by

Miriam Avery

Thesis for the degree of Doctor of Philosophy

April 2010



UNIVERSITY OF SOUTHAMPTON

ABSTRACT

SCHOOL OF MEDICINE / SCHOOL OF HEALTH SCIENCES

Doctor of Philosophy

ALTERED CUTANEOUS VASOREACTIVITY AND  
MICROVASCULAR CONTROL MECHANISMS AS A  
RISK FACTOR FOR PRESSURE ULCER  
DEVELOPMENT

by Miriam Avery

Pressure ulcers are a universal problem affecting patients in both hospital (Clark and Watts., 1991) and community settings (Margolis et al., 2002). They have a detrimental effect on quality of life (Gorecki et al., 2009) causing increased burden on carers and pain for the sufferer (Hopkins et al., 2006; Girouard et al., 2008). Tissue breakdown, specifically pressure ulcer development, results from an inadequate cutaneous vascular perfusion, caused by external forces such as pressure, friction and shear. The aim of this thesis is to investigate the impact of smoking on vascular responsiveness and microvascular control mechanisms, as a potential method to assess pressure ulcer risk.

The vasoreactivity of the skin was measured in smokers and non-smokers using laser Doppler fluximetry (LDF) following removal of an external pressure load and after local heating of the skin to 43°C. The pressure loading studies produced variable results and the LDF trace was difficult to analyse using spectral analysis, so local heating is the main focus of this thesis. The hyperaemic response to local heating to 43°C was compared at the sacrum and forearm of 9 participants. The sacrum site showed significantly reduced responses compared to the forearm, but there was also a significant correlation between the sites. The forearm site was used in the remainder of the studies.

The response to local heating to 43°C for 10 minutes was measured in heavy smokers and matched non-smokers (n=8 pairs); this was increased to 20 minutes in light/moderate (LM) smokers and matched non-smokers (n=20 pairs) at the volar forearm. The response was significantly attenuated in the heavy smokers in terms of peak hyperaemia and total response (AUC) ( $p < 0.05$ ) and there was a trend towards reduced responses in the LM smokers. When considering all 56 participants in median regression analysis, increasing smoking intensity and longevity (packyears) was significantly predictive for reducing responses to the local heating stimulus.

The mechanisms underlying these altered vascular responses were explored using spectral analysis of the LDF signal. Previous studies have shown oscillations in the LDF signal with frequencies around 1, 0.3, 0.1, 0.04 and 0.01Hz related to the heart beat, respiration, myogenic, neurogenic and endothelium-mediated control mechanisms, respectively (Kvernmo et al, 1999). The relative power in the frequency band which originates from the endothelium increased significantly during heating compared to resting flux in the heavy smoker controls, but not in the heavy smokers. This suggests that the attenuated responses were due to endothelial dysfunction in the heavy smokers. There were no significant differences in the spectral analysis of the heating flux in the LM smokers compared to their controls. However, when considering all smokers, both heavy and LM, compared to all the non-smokers, the non-smokers showed an increased median relative power in the 0.01Hz frequency band, but the smokers showed a decrease in this band from resting to heating flux. This difference between the smokers and non-smokers was significant.

The results show that smoking reduces the vasoreactivity of the skin microcirculation and increasing intensity of smoking, measured by packyears, is significantly predictive for this attenuation. The spectral analysis showed that dysfunctional endothelium may be the reason for the reduced responses in the heavy smoker group. When considering the heavy and LM smokers together versus their controls, the findings showed that the relative power of the frequency, related to the endothelial control of blood flow, was reduced in the smoker group during heating, but increased in the non-smokers, and this difference was significant. This suggests that altered endothelial function causes the reduced vasoreactivity of the skin microcirculation in smokers. Smoking may increase the risk of developing a pressure ulcer through modulating cutaneous vascular control, potentially through its effects on endothelial function. The measurement of the endothelial function of the skin microcirculation may be a potential method for pressure ulcer risk assessment.

## List of Contents

<b>SECTION</b>	<b>PAGE</b>
<b>Title Page</b>	<b>1</b>
<b>Abstract</b>	<b>3</b>
<b>List of Contents</b>	<b>5</b>
<b>List of Figures</b>	<b>11</b>
<b>List of Tables</b>	<b>15</b>
<b>Author's declaration</b>	<b>17</b>
<b>Acknowledgements</b>	<b>19</b>
<b>List of Abbreviations</b>	<b>21</b>
<b>Chapter 1: Introduction</b>	<b>23</b>
<b>1.1 Pressure ulcers</b>	<b>24</b>
1.1.1 Pressure ulcers: the definition	24
1.1.2 Pressure ulcers: the problem	24
1.1.3 Pressure ulcers: the skin	25
<b>1.2 The skin</b>	<b>25</b>
1.2.1 Anatomy of the skin	25
1.2.2 Skin microvasculature	26
1.2.3 Control and regulation of skin blood flow	30
1.2.4 Vasomotion	32
1.2.5 Effect of external stimuli on skin blood flow	33
<b>1.3 Pressure ulcer development</b>	<b>35</b>
1.3.1 Intrinsic factors that increase risk of pressure ulcers	37
<b>1.4 Smoking</b>	<b>39</b>
1.4.1 Smoking background	39
1.4.2 Smoking and cardiovascular risk assessment	40
1.4.3 Smoking and the skin	40
1.4.4 The effects of smoking on the endothelium	41
1.4.5 Nitric oxide and smoking	42

1.4.6	Oxidative stress and smoking	43
<b>1.5</b>	<b>Measurement of skin blood flow</b>	<b>44</b>
1.5.1	Laser Doppler fluximetry	45
1.5.2	Laser Doppler fluximetry and skin challenge	46
1.5.3	Laser Doppler fluximetry and spectral analysis	48
1.5.4	Laser Doppler fluximetry and spectral analysis in patient studies	51
<b>1.6</b>	<b>Hypothesis and aims</b>	<b>52</b>
<b>Chapter 2: Methods</b>		<b>55</b>
<b>2.1</b>	<b>Generic participants details</b>	<b>56</b>
2.1.1	Inclusion/exclusion criteria	56
2.1.2	Matched pairs	56
2.1.3	Smoking status	57
2.1.4	Controlling variables	57
<b>2.2</b>	<b>Skin blood flow measurement methods</b>	<b>58</b>
2.2.1	Laser Doppler fluximetry	61
2.2.2	Biological Zero	61
2.2.3	Repeatability and Coefficient of Variance in the participants	62
<b>2.3</b>	<b>Local skin loading and LDF protocol</b>	<b>62</b>
2.3.1	Development of loading protocol	62
2.3.2	Protocol for local pressure loading study	63
2.3.3	Parameters measured in loading studies	63
<b>2.4</b>	<b>Local skin heating and LDF protocol</b>	<b>64</b>
2.4.1	The local heating block at the forearm and sacrum	65
2.4.2	Protocol for local heating study	67
2.4.3	Parameters measured in local heating studies	68
2.4.4	Local nature of the heating response	70
<b>2.5</b>	<b>Spectral analysis methods</b>	<b>70</b>
2.5.1	The LDF signal	71
2.5.2	The Power Spectral Density of the LDF signal	72

2.5.3	Protocol for spectral analysis: PSD estimate using FFT	75
<b>2.6</b>	<b>Data analysis and statistical methods</b>	<b>77</b>
2.6.1	Sample size	77
2.6.2	Statistics	78
2.6.3	Graphical representation	79
<b>2.7</b>	<b>Layout of the results chapters</b>	<b>79</b>
<b>Chapter 3: Skin blood flow response to loading the skin</b>		<b>81</b>
<b>3.1</b>	<b>Introduction</b>	<b>82</b>
<b>3.2</b>	<b>Hypothesis</b>	<b>83</b>
<b>3.3</b>	<b>Objectives</b>	<b>83</b>
<b>3.4</b>	<b>Methods</b>	<b>84</b>
3.4.1	Participants	84
3.4.2	Summary protocol	84
3.4.3	Statistics	85
<b>3.5</b>	<b>Results</b>	<b>86</b>
3.5.1	Summary of results	87
3.5.2	Pressure loading at the forearm of heavy smokers and matched non-smokers	87
3.5.3	Pressure loading at the sacrum of heavy smokers and matched non-smokers	91
<b>3.6</b>	<b>Discussion</b>	<b>94</b>
<b>Chapter 4: Investigation into vasoreactivity of different skin sites</b>		<b>105</b>
<b>4.1</b>	<b>Introduction</b>	<b>106</b>
<b>4.2</b>	<b>Hypothesis</b>	<b>108</b>

<b>4.3</b>	<b>Objectives</b>	<b>109</b>
<b>4.4</b>	<b>Methods</b>	<b>109</b>
4.4.1	Participants	109
4.4.2	Study protocol	110
4.4.3	Spectral analysis methods	110
4.4.4	Statistics	112
<b>4.5</b>	<b>Results</b>	<b>113</b>
4.5.1	Summary of the results	113
4.5.2	Time domain analysis: Resting/heating flux at forearm and sacrum	115
4.5.3	Correlations between heating responses at the forearm and sacrum	119
4.5.4	Spectral analysis of the resting and local heating responses at forearm and sacrum between 0 and 2Hz.	121
4.5.5	Spectral analysis of the resting/heating flux between 0 and 0.2Hz	127
<b>4.6</b>	<b>Discussion</b>	<b>132</b>
<b>Chapter 5: The cutaneous vascular response to local heating in smokers</b>		<b>137</b>
<b>5.1</b>	<b>Introduction</b>	<b>138</b>
<b>5.2</b>	<b>Hypothesis</b>	<b>139</b>
<b>5.3</b>	<b>Objectives</b>	<b>140</b>
<b>5.4</b>	<b>Methods</b>	<b>140</b>
5.4.1	Participants	140
5.4.2	Participant smoking history	142
5.4.3	Protocol	142
5.4.4	Statistical analysis	143
<b>5.5</b>	<b>Results</b>	<b>144</b>
5.5.1	Summary of results	145
5.5.2	Heavy smoker study	145
5.5.3	Light/moderate smoker study	150
5.5.4	Analysis of all control participants only	155

5.5.5	All smokers compared with controls	157
<b>5.6</b>	<b>Discussion</b>	<b>161</b>
<b>Chapter 6: Mechanisms underlying altered vasoreactivity in heavy and light/moderate smokers: Spectral analysis</b>		<b>169</b>
<b>6.1</b>	<b>Introduction</b>	<b>170</b>
<b>6.2</b>	<b>Hypothesis</b>	<b>171</b>
<b>6.3</b>	<b>Objectives</b>	<b>172</b>
<b>6.4</b>	<b>Methods</b>	<b>172</b>
<b>6.5</b>	<b>Results</b>	<b>175</b>
6.5.1	Summary of results	175
6.5.2	Spectral analysis in heavy smokers and controls	176
6.5.3	Spectral analysis in light/moderate smokers and controls	182
6.5.4	All smokers compared with matched non-smokers	187
<b>6.6</b>	<b>Discussion</b>	<b>189</b>
<b>Chapter 7: General discussion</b>		<b>197</b>
<b>7.1</b>	<b>The concept of the thesis</b>	<b>198</b>
<b>7.2</b>	<b>Summary of findings</b>	<b>199</b>
<b>7.3</b>	<b>Implications of the findings</b>	<b>200</b>
<b>7.4</b>	<b>Implications of the findings for clinical practice</b>	<b>205</b>
<b>7.5</b>	<b>Future Work</b>	<b>206</b>
7.5.1	Nitric oxide and microdialysis studies	206
7.5.2	Stage 1 pressure ulcers	207
7.5.3	Smoking cessation and health promotion	207

<b>Appendix 1: Detail of Parameter calculations</b>	<b>209</b>
A1.1 Area under curve analysis (local heating)	210
A1.2 Maximum hyperaemia during heating	210
A1.3 Mean flux during heating	211
<b>Appendix 2: List of materials</b>	<b>213</b>
<b>Appendix 3: Matlab functions and programs</b>	<b>215</b>
A3.1 Detrend program	216
A3.2 Poly detrend function	216
A3.3 Spectrogram function	217
A3.4 PSD estimation program	218
A3.5 Saving PSD as a text file	218
A3.6 Image of median PSD	219
<b>Appendix 4: A pilot study to consider the neurogenic mechanisms in local heating</b>	<b>221</b>
A4.1 Introduction	222
A4.2 Methods	222
A4.3 Results	224
<b>Appendix 5: Cutaneous microdialysis for the measurement of nitric oxide</b>	<b>227</b>
A5.1 Introduction	228
A5.2 Objectives	229
A5.3 Methods	229
A5.4 Results	235
A5.5 Discussion	239
<b>Appendix 6: List of publications</b>	<b>245</b>
<b>Reference List</b>	<b>247</b>

## List of Figures

<b>FIGURE</b>		<b>PAGE</b>
<i>Chapter 1: Introduction</i>		
1.1	A diagram of the skin and hypodermis	27
1.2	A diagram to show the anatomy of the skin microvasculature	27
1.3	A diagram to show pressure, friction and shear forces	37
1.4	A diagram to show the functioning of the laser Doppler fluximeter (LDF)	45
<i>Chapter 2: General Methods</i>		
2.1	The experimental equipment used in the loading studies	63
2.2	The parameters of the reactive hyperaemic response	64
2.3	A diagram of LDF skin heating probe	65
2.4	A graph showing temperature of local heating probe during the skin heating protocol	66
2.5	A graph to show the temperature rise of the heating probe	67
2.6	The parameters of the local heating-induced vasodilatation response	69
2.7	A graph to show the local nature of the heating response	70
2.8	Graphs to show the effect of detrending the LDF signal	75
2.9	A schematic diagram showing the content of the results chapters	80
<i>Chapter 3: Skin blood flow response to loading the skin in heavy smokers and non-smokers</i>		
3.1	A diagram to show the timeline of the loading protocol	85
3.2	An image of an LDF trace during the loading protocol in a participant	86
3.3	A graph of resting and loading flux at forearm of heavy smokers and non-smokers	88
3.4	A scatter graph of the correlation between body mass index (BMI) and fall in flux with loading in non-smokers	89
3.5	A scatter graph to show effect of BMI on the area under the curve of the reactive hyperaemic response at the forearm	90
3.6	A graph to show the oscillations in the LDF trace	91
3.7	A graph of resting and loading flux at the sacrum of heavy smokers and non-smokers	92
3.8	A scatter graph of the correlation between BMI and fall in flux with loading in non-smokers at the sacrum	93

<b>3.9</b>	A scatter graph to show effect of BMI on area under the hyperaemia curve at the sacrum	<b>94</b>
<b>3.10</b>	A figure from a paper	<b>99</b>
 <i>Chapter 4: Investigation of site differences in cutaneous vasoreactivity</i>		
<b>4.1</b>	A diagram of the timeline of events in the local heating protocol when comparing forearm and sacrum	<b>110</b>
<b>4.2</b>	A flowchart to demonstrate the pathway of data processing for the spectral analysis	<b>111</b>
<b>4.3</b>	Examples of LDF trace at the forearm and the sacrum	<b>113</b>
<b>4.4</b>	A graph to show heating and resting flux at the forearm and sacrum	<b>115</b>
<b>4.5</b>	A graph to show resting flux at the forearm and sacrum	<b>116</b>
<b>4.6</b>	A graph to show increase in flux at the forearm and sacrum	<b>117</b>
<b>4.7</b>	A graph to show area under the heating curve (AUC) at the forearm and sacrum	<b>118</b>
<b>4.8</b>	A graph to show time to 50% recovery at the forearm and sacrum	<b>119</b>
<b>4.9</b>	A scatter graph to show AUC at the sacrum and forearm	<b>120</b>
<b>4.10</b>	Graphs to show absolute power spectral density (PSD) between 0 and 2Hz at the forearm and sacrum during resting flux	<b>122</b>
<b>4.11</b>	A graph to show the relative PSD of the 5 frequency bands during resting flux at the forearm and sacrum	<b>123</b>
<b>4.12</b>	Graphs to show absolute power spectral density (PSD) between 0 and 2Hz at the forearm and sacrum during heating flux	<b>124</b>
<b>4.13</b>	Graphs to show the relative PSD of the 5 frequency bands during resting and heating at the forearm and sacrum	<b>126</b>
<b>4.14</b>	Graphs to show absolute PSD between 0 and 0.2Hz during resting at the forearm and sacrum	<b>128</b>
<b>4.15</b>	Graph to show the relative power of the low frequency bands in the resting flux at the forearm and sacrum	<b>129</b>
<b>4.16</b>	Graphs to show the absolute PSD between 0 and 0.2Hz in the heated flux at the forearm and the sacrum	<b>130</b>
<b>4.17</b>	Graph to show change in relative power from resting to heating at the sacrum	<b>131</b>

***Chapter 5: The cutaneous vascular response to local heating in smokers***

<b>5.1</b>	A diagram of timeline of the local heating in heavy smokers' protocol	<b>143</b>
<b>5.2</b>	Examples of the LDF trace in a heavy smoker and non-smoker	<b>146</b>
<b>5.3</b>	A graph to show the resting and heating flux in heavy smokers and non-smokers	<b>147</b>
<b>5.4</b>	A graph to show peak flux above resting in the heavy smokers and non-smokers	<b>148</b>
<b>5.5</b>	A graph to show average heated flux above resting	<b>149</b>
<b>5.6</b>	A graph to show the AUC in heavy smokers and non-smokers	<b>150</b>
<b>5.7</b>	Examples of the LDF trace in a light/moderate smoker and non-smoker	<b>151</b>
<b>5.8</b>	A graph to show resting and heated flux in the light/moderate smokers and non-smokers	<b>152</b>
<b>5.9</b>	A graph to show peak flux above resting in light/moderate smokers and matched non-smokers	<b>153</b>
<b>5.10</b>	A graph to show the average heated flux above resting in light/moderate smokers and matched non-smokers	<b>154</b>
<b>5.11</b>	A graph to show the AUC in the light/moderate smokers and matched non-smokers	<b>155</b>
<b>5.12</b>	Graphs to show the effect of age on BMI and resting flux in control participant's only	<b>156</b>
<b>5.13</b>	A graph to show the AUC in all smokers (heavy/moderate/light) and their matched controls	<b>157</b>

***Chapter 6: Mechanisms underlying altered vasoreactivity in heavy and light/moderate smokers***

<b>6.1</b>	A graph to show absolute PSD of heated flux in the heavy and matched non-smokers	<b>177</b>
<b>6.2</b>	A scatter graphs of absolute power against AUC heating response in heavy smokers and non-smokers	<b>178</b>
<b>6.3</b>	A graph to show absolute power of low frequency bands in the heavy smokers and matched non-smokers	<b>179</b>
<b>6.4</b>	Graphs to show the relative power between 0 and 0.2Hz of the heating flux in heavy smokers and non-smokers	<b>180</b>
<b>6.5</b>	A graph to show the change in relative PSD from resting to heating in the heavy smokers and non-smokers	<b>181</b>

<b>6.6</b>	A graph to show the absolute PSD of heated flux in LM smokers and matched non-smokers	<b>183</b>
<b>6.7</b>	A scatter graph to show the absolute power and AUC in LM smokers and non-smokers	<b>184</b>
<b>6.8</b>	Graphs to show the change in relative power from resting to heating in the LM smokers and non-smokers	<b>186</b>
<b>6.9</b>	A scatter graph to show the AUC against the absolute power in all smokers (heavy/moderate/light) and their controls	<b>187</b>
<b>6.10</b>	A graph to show change in relative power of frequency around 0.01Hz in all smokers and their controls	<b>188</b>
<b><i>Appendix 4: A pilot study to consider the neurogenic mechanisms in local heating</i></b>		
<b>A4.1</b>	An LDF traces to demonstrate effects of EMLA on the local heating Response	<b>224</b>
<b>A4.2</b>	A graph to show the relative PSD 0.04Hz at EMLA site versus control site during local heating	<b>226</b>
<b><i>Appendix 5: Cutaneous microdialysis for the measurement of nitric oxide</i></b>		
<b>A5.1</b>	The calibration curve for analysis of nitric oxide	<b>234</b>
<b>A5.2</b>	A line graph of microdialysate collection over 30 minutes in smokers and non-smokers	<b>236</b>
<b>A5.3</b>	A bar graph to show area under the microdialysate collection curve	<b>237</b>
<b>A5.4</b>	A line graph to show microdialysate nitric oxide concentration following a 30 minute interruption in perfusion	<b>238</b>
<b>A5.5</b>	A bar graph to show the build-up of nitric oxide during 30 minutes interruption in perfusion	<b>239</b>

## List of Tables

<b>TABLE</b>	<b>PAGE</b>
<i>Chapter 1: Introduction</i>	
1.1 The 5 frequencies demonstrated by spectral analysis	48
<i>Chapter 2: General methods</i>	
2.1 The Accutest Nicometer® levels	57
2.2 A table to show the advantages and disadvantages of different methods to measure skin blood flow	60
2.3 The effects of the different orders of detrend	74
<i>Chapter 3: Skin blood flow response to loading the skin in heavy smokers and non-smokers</i>	
3.1 The baseline parameters of the participants involved in the loading studies	84
<i>Chapter 4: Investigation into vasoreactivity of different skin sites: the local heating response at the sacrum and forearm</i>	
4.1 The baseline parameters of the participants involved in the studies comparing local heating response at the forearm and sacrum	109
<i>Chapter 5: The cutaneous vascular response to local heating in smokers</i>	
5.1 The baseline parameters of the heavy smoker participants and matched non-smokers in the local heating studies	141
5.2 The baseline parameters of the light/moderate smoker participants and matched non-smokers in the local heating studies	142
5.3 The univariate analysis assessing predictive value of the variables in the study on mean heated flux	158
5.4 The multivariate analysis assessing predictive value of the variables in the study on the mean heated flux	158
5.5 The univariate analysis assessing the predictive value of the variables on AUC of the local heating response	159
5.6 The multivariate analysis assessing the predictive value of the variables on AUC of the local heating response	160

<b>5.7</b>	Age and smoking intensity distribution of the participants	<b>165</b>
<b><i>Chapter 6: Mechanisms underlying altered vasoreactivity in heavy and light/moderate smokers</i></b>		
<b>6.1</b>	The average coefficient of variance of the absolute and relative power at the forearm of 17 participants	<b>175</b>
<b><i>Appendix 4: A pilot study to consider the neurogenic mechanisms in local heating</i></b>		
<b>A4.1</b>	The participants' baseline parameters	<b>223</b>
<b><i>Appendix 5: Cutaneous microdialysis for the measurement of nitric oxide</i></b>		
<b>A5.1</b>	The participants' baseline parameters	<b>230</b>

# Academic Thesis: Declaration Of Authorship

I, .....  
[please print name]

declare that this thesis and the work presented in it are my own and has been generated by me as the result of my own original research.

[title of thesis]  
.....  
.....

I confirm that:

1. This work was done wholly or mainly while in candidature for a research degree at this University;
2. Where any part of this thesis has previously been submitted for a degree or any other qualification at this University or any other institution, this has been clearly stated;
3. Where I have consulted the published work of others, this is always clearly attributed;
4. Where I have quoted from the work of others, the source is always given. With the exception of such quotations, this thesis is entirely my own work;
5. I have acknowledged all main sources of help;
6. Where the thesis is based on work done by myself jointly with others, I have made clear exactly what was done by others and what I have contributed myself;
7. Either none of this work has been published before submission, or parts of this work have been published as: [please list references below]:

Avery, M., Voegeli, D. and Clough, G.F. 2004. Evidence for endothelial dysfunction in the skin microvasculature of long-term smokers. Proceedings of The Physiological Society. PC153A pp170P

Avery MR, Voegeli D & Clough GF. 2005, Endothelial dysfunction in long-term smokers. Proceedings joint meeting Microcirc Inc and BMS, *J Vasc Res* ;12, 670.

Avery, M., Voegeli, D., Byrne, C., Simpson, D. and Clough, G. 2009. Age and cigarette smoking are independently associated with the cutaneous vascular response to local warming. *Microcirculation.*, 16, (8) 725-734

Signed:.....

Date: .....



## **Acknowledgements**

I would like to thank my supervisors, Professor Geraldine Clough and Dr David Voegeli, for their continued support and encouragement throughout the completion of this thesis.

I am also most thankful to Dr David Simpson for all his help and advice relating to the signal processing aspects of this thesis, and for the extremely useful 'demystifying biomedical signals' course that I attended in the earlier stages of this thesis.

Most of all I am thankful to my husband, Simon, for his patience and encouragement when it was most needed.



## List of Abbreviations

<b>ACh</b>	Acetylcholine
<b>ADP</b>	Adenosine Diphosphate
<b>ANS</b>	Autonomic Nervous System
<b>AUC</b>	Area under Curve
<b>AVA</b>	Arteriovenous Anastomosis
<b>BH4</b>	Tetrahydrobiopterin
<b>BMI</b>	Body Mass Index
<b>BZ</b>	Biological Zero
<b>CAT1</b>	Cationic amino acid transporter
<b>CAD</b>	Coronary Artery Disease
<b>CHD</b>	Coronary Heart Disease
<b>cGMP</b>	Cyclic Guanosine Monophosphate
<b>CGRP</b>	Calcitonin Gene-Related Peptide
<b>COX</b>	Cyclooxygenase
<b>CSE</b>	Cigarette Smoke Extract
<b>CV</b>	Coefficient of Variance
<b>DFT</b>	Discrete Fourier Transform
<b>EC</b>	Endothelial Cell
<b>ECG</b>	Electrocardiography
<b>EDHF</b>	Endothelium derived hyperpolarizing factor
<b>EHT</b>	Essential Hypertension
<b>EMLA</b>	Eutectic mixture of lidocaine and prilocaine
<b>eNOS</b>	Endothelial nitric oxide synthase
<b>EPUAP</b>	European Pressure Ulcer Advisory Panel
<b>FFT</b>	Fast Fourier Transform
<b>HUVEC</b>	Human Umbilical Vein Endothelial Cells
<b>iNOS</b>	Inducible Nitric Oxide Synthase
<b>IQR</b>	Interquartile Range
<b>IR</b>	Ischaemia Reperfusion
<b>ISVR</b>	Institute of Sound and Vibration Research
<b>LDF</b>	Laser Doppler Fluximetry
<b>LDI</b>	Laser Doppler Imaging
<b>LM</b>	Light/moderate
<b>L-NAME</b>	L-Nitro-Arginine Methyl Ester

<b>L-NMMA</b>	L-N <sup>G</sup> -monomethyl Arginine
<b>MAP</b>	Mean Arterial Pressure
<b>MDA</b>	Malondialdehyde
<b>MMP</b>	Membrane metalloproteinases
<b>MWU</b>	Mann Whitney U
<b>NADH</b>	Nicotinamide Adenine Dinucleotide
<b>NADPH</b>	Nicotinamide Adenine Dinucleotide Phosphate
<b>NICE</b>	National Institute for Clinical Excellence
<b>NO</b>	Nitric Oxide
<b>NOS</b>	Nitric Oxide Synthase
<b>NPUAP</b>	National Pressure Ulcer Advisory Panel
<b>PAOD</b>	Peripheral Arterial Obstructive Disease
<b>PIV</b>	Pressure Induced Vasodilatation
<b>PSD</b>	Power Spectral Density
<b>RCN</b>	Royal College of Nursing
<b>RH</b>	Reactive Hyperaemia
<b>ROS</b>	Reactive Oxygen Species
<b>SAC</b>	Stretch Activated Cell
<b>SCI</b>	Spinal Cord Injury
<b>SMC</b>	Smooth Muscle Cell
<b>SNP</b>	Sodium Nitroprusside
<b>SNS</b>	Sympathetic Nervous System
<b>SOD</b>	Superoxide Dismutase
<b>SPSS</b>	Statistics Package for the Social Sciences
<b>SWILK</b>	Shapiro-Wilk Test for normality
<b>UK</b>	United Kingdom
<b>WTCRF</b>	Wellcome Trust Clinical Research Facility

# **Chapter 1**

## **General Introduction**

## **1.1 Pressure Ulcers**

### **1.1.1 Pressure ulcers: the definition**

The American National Pressure Ulcer Advisory Panel (NPUAP) and the European Pressure Ulcer Advisory Panel (EPUAP) have defined a pressure ulcer as:

‘localized injury to the skin and/or underlying tissue usually over a bony prominence, as a result of pressure, or pressure in combination with shear’ (EPUAP-NPUAP, 2009).

### **1.1.2 Pressure ulcers: the problem**

Pressure ulcers remain a significant problem in the United Kingdom (UK). This is despite there being an increased focus on research, developments in the technology of patient support surfaces and the introduction of guidelines for practice by the Royal College of Nursing (RCN) and National Institute for Health and Clinical Excellence (NICE) (RCN and NICE, 2005). When data from pressure ulcer audits completed in 44 acute hospitals in England and Wales between 2005 and 2007 was compiled, there was found to be an overall pressure ulcer prevalence of 10.2 - 10.3%; this was despite increased awareness and new NICE guidelines during that period (Phillips and Buttery, 2009). The problem of pressure ulcer development is not confined to the UK, but is evident worldwide. In a recent study of 253 patients in an Indonesian Intensive Therapy Unit (ITU), 72 (28.4%) developed pressure ulcers (Suriadi et al., 2008). In a study of 535 patients in a hospital in Sweden, 27% of the patients developed one or more pressure ulcers (Wann-Hansson et al., 2008). Throughout the world and in a range of different settings (Clark and Watts, 1991; Margolis et al., 2002) pressure ulcers remain a huge problem.

Pressure ulcers result in reduced quality of life for patients (Gorecki et al., 2009) and increased workload for their carers. They cause significant morbidity due to pain (Girouard et al., 2008, Gunes, 2008), infection and immobility (Spilsbury et al., 2007), and in some circumstances, may contribute to a patients’ death (Tingle, 1997). The financial implication of pressure ulcers to the health and social care system in the UK is considerable. The annual cost of treating pressure ulcers in 2004 was estimated to be approximately £1.4 - 2.1 billion a year (Bennett et al., 2004), which was 4% of the total health care expenditure.

### **1.1.3 Pressure ulcers: the skin**

The skin is the largest organ of the human body and is a physical barrier to the external environment. The skin has an important role in maintaining homeostasis through temperature regulation and protection. The skin undergoes constant repair and remodelling to maintain it as a barrier and allow it to fulfil its role. Pressure ulcers occur when external forces on the skin, such as pressure, friction and shear, cause skin breakdown and disruption of this physical barrier.

Many factors, including age, disease status, body mass index (BMI) and smoking, affect the risk of tissue breakdown by modulating skin structure and the control and function of the cutaneous microvasculature. Monitoring and sampling the cutaneous environment and microvascular responses to certain stimuli can be used to further inform patient care regarding skin health.

## **1.2 The skin**

In adults, the skin covers an area of approximately 2 square metres and has a variable thickness ranging from 0.5mm to 4.0mm (Tortora and Derrickson, 2009). The skin is divided into two main sections: the superficial epidermis (40-80 $\mu$ M) and the deeper and thicker dermis (100-200  $\mu$ M). The dermis is attached to a subcutaneous layer composed of areolar and adipose tissue (Tortora and Derrickson, 2009).

### **1.2.1 Anatomy of the skin**

The epidermis is composed of keratinized stratified squamous epithelium and is divided into five layers. The deepest layer of the epidermis is the stratum basale. Cells are formed in the stratum basale and are pushed through the remaining four layers of the epidermis; the stratum spinosum, stratum granulosum, stratum lucidum and the stratum corneum. As the cells move through the layers, they accumulate keratin. When they reach the epidermal surface, they are sloughed off and replaced by underlying cells moving to the surface. This whole cycle takes four weeks in an average epidermis (Tortora and Derrickson, 2009) (*Figure 1.1*).

The dermis is mainly composed of connective tissue containing collagen and elastic fibres, which ensure that the skin has high tensile strength and the ability to stretch and recoil. The dermis also contains blood vessels, nerves, glands and hair follicles. It is divided into the superficial papillary

region and the deeper reticular region. The papillary region has a large surface area due to small projections called dermal papillae; these are small structures that protrude into the epidermis and some of these contain capillary loops. The collagen and elastic fibres in the papillary layer are not as dense as in the reticular layer (Stevens and Lowe, 1997). The connective tissue of the reticular layer is composed of fibroblasts, collagen and elastic fibres. There are also adipose cells, hair follicles, nerves, sebaceous glands and sweat glands scattered amongst the collagen and elastic fibres (Tortora and Derrickson, 2009). The reticular layer is attached to underlying bone and muscle by the subcutaneous layer (*Figure 1.1*).

It is estimated that the skin layers contain approximately one million nerve fibres. The majority of these free sensory nerve endings are in the dermis, but a few unmyelinated nerve endings can be found in the epidermis. Thermoreceptors are cutaneous free nerve endings that detect coldness and warmth. Cold receptors are activated between 10 and 40°C and are free nerve endings located in the stratum basale layer of the epidermis (Tortora and Derrickson, 2009). There are fewer warmth receptors than cold receptors and these can be found in the dermis. These nerve endings are attached to small diameter unmyelinated C fibres and are activated between 32 - 48°C. The sensation of temperature above 48°C or below 10°C will stimulate pain receptors, known as nociceptors. Thermoreceptors release vasoactive peptides such as calcitonin gene-related peptide (CGRP) and substance P and this can occur in the absence of pain (Magerl and Treede, 1996).

### **1.2.2 Skin microvasculature**

The microcirculation is the section of the vascular system ranging from primary arterioles (~100µm diameter) to capillary venules (Wiernsperger, 2000). The skin microvasculature has important functions; the regulation of body heat, provision of oxygen and nutrients for the epidermis and dermis, metabolic exchange and tissue homeostasis (Wright et al., 2006). The epidermis is avascular; all of the cutaneous blood vessels are found in the dermis and subcutaneous layer (Bircher et al., 1994). The blood vessels in the dermis provide oxygen and nutrients to both the dermis and epidermis. The stratum basale layer of the epidermis is the closest to the vessels in the dermis, so receives most of the oxygen and nutrients for the epidermis. As the cells in the stratum basale move further from the blood vessels and thus oxygen and nutrient supply, they die and are removed from the surface of the epidermis.

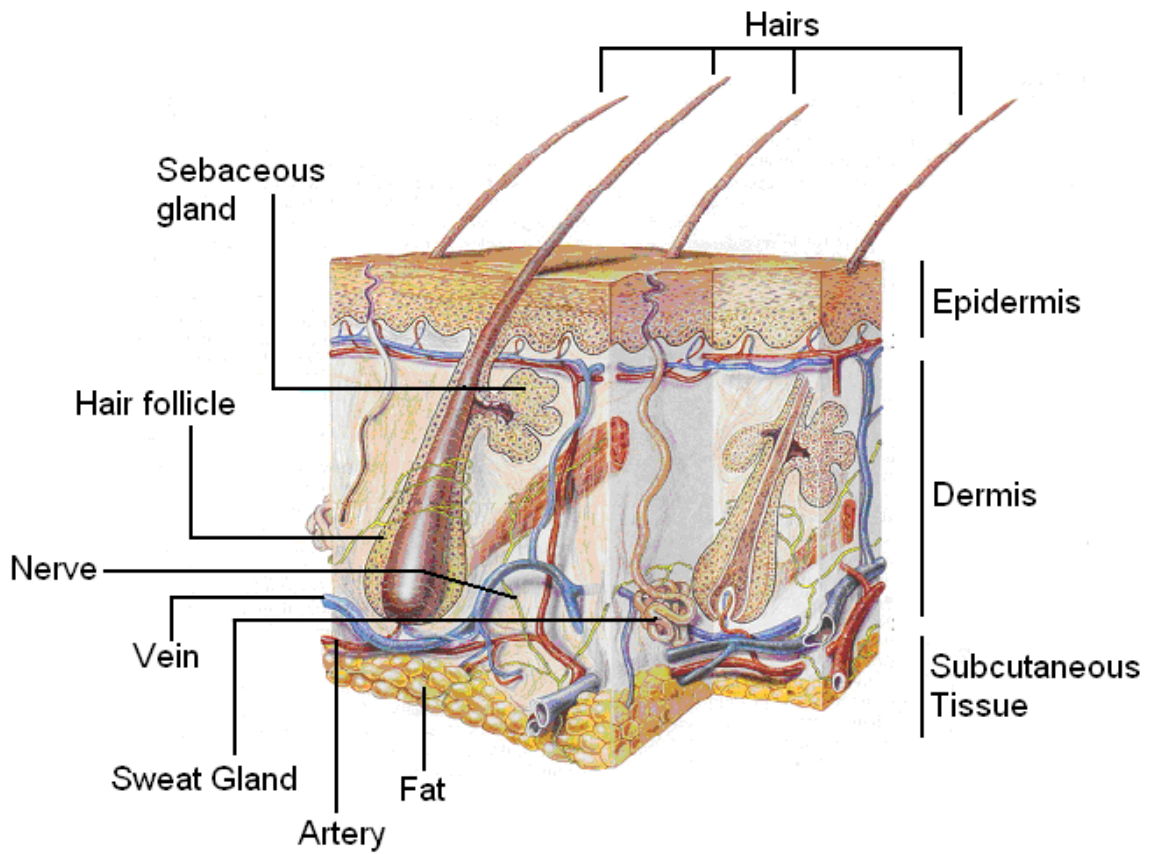


*Figure 1.1* A diagram of the skin and hypodermis (adapted from Seeley et al., 1999).

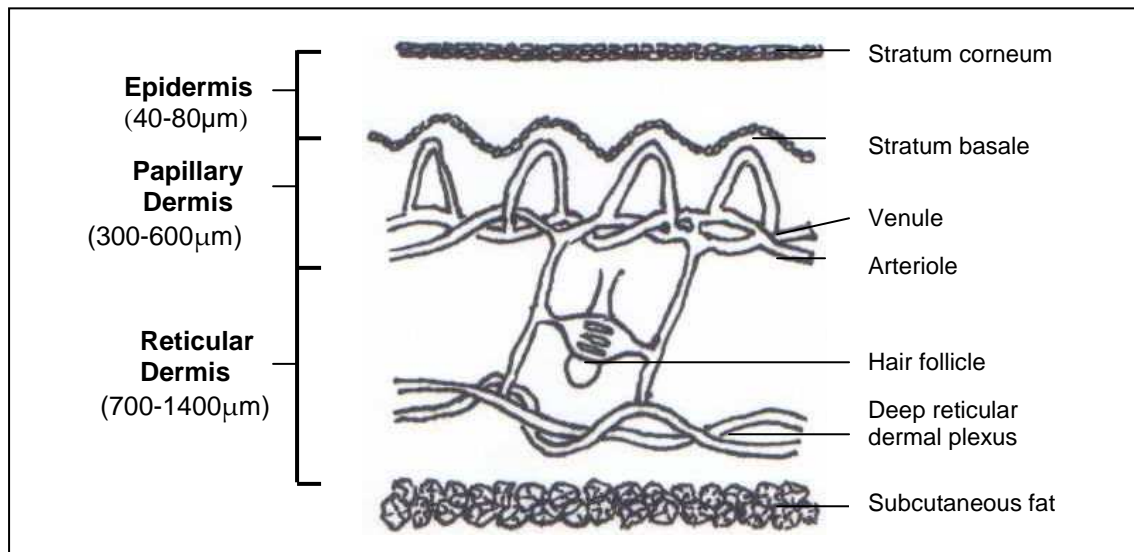


*Figure 1.2* A diagram to show the anatomy of the skin microvasculature (adapted from Swain and Grant, 1989)

The blood vessels in the dermis carry between 8 and 10% of the total cardiac output in a normal resting adult (Tortora and Grabowski, 2000). However, during severe heat stress the human skin can receive up to 70% of cardiac output. When the external temperature is cold, blood flow is able to reduce to nearly zero in the skin (Rowell, 1977).

The skin contains two types of resistance vessels: arteriovenous anastomoses (AVAs) and arterioles. The AVA's have thick muscular walls (Levy et al., 2006); they do not connect to the capillary bed, but shunt blood directly from arterioles to venules (Tortora and Grabowski, 1996). The AVA's are most commonly found in the dermis of the palms, the soles of the feet, the nose and ears. The arterioles transfer blood flow to the venules through the capillaries, and in this way provide for the skin's nutritional needs (Pocock and Richards, 2006).

The AVA's are richly innervated by the sympathetic nervous system (SNS) and the regulation of these vessels is by temperature receptors in the skin or the central nervous system. Substantial changes in vessel diameter can occur in these vessels; stimulation of sympathetic nerve fibres can nearly completely constrict the vessel, but the AVA's will dilate maximally when there is removal of this stimulation.

The arterioles are the main source of vascular resistance within the cutaneous microcirculation. They are innervated by sympathetic nerve fibres and most arterioles are in a state of basal constriction (Pocock and Richards, 2006). However, unlike AVA's, arterioles are also controlled by local metabolic factors (Pocock and Richards, 2006). The arterioles have thick walls; the wall thickness of arterioles is half of the total vessel diameter (Tortora and Derrickson, 2009). The three layers of the wall of the arteriole are the tunica interna, the tunica media and the tunica externa. The tunica interna is composed of a thin internal elastic lamina, the tunica media consists of smooth muscle cells and the tunica externa is composed of collagenous connective tissue and many unmyelinated sympathetic nerves (Tortora and Derrickson, 2009).

The primary arterioles progressively become smaller with less smooth muscle and innervation in their walls as they become secondary, tertiary and then terminal arterioles. The terminal arterioles, called metarterioles feed into capillaries and then the capillaries drain into venules. At the junction between the arteriole and capillary, the final muscle cell forms the pre-capillary sphincter (Tortora and Derrickson, 2009).

The arterioles feed into capillaries, which are the smallest vessels in the microvasculature. The capillaries have a diameter in the range of 5-10 $\mu$ M and they connect the arterioles to the venules.

They have a vast surface area and their narrow diameter means that blood cells usually pass single file through the capillary lumen. The capillaries do not have a tunica media or tunica externa; their walls are composed of a single layer of endothelial cells and a basement membrane. The post-capillary venules have thin walls, but with increasing size the venules have two smooth muscle layers in their walls (Tortora and Derrickson, 2009) (*Figure 1.2*).

The cutaneous arterioles, capillaries and venules form two plexuses in the dermis. The upper horizontal network in the papillary dermis has nutritive capillary loops coming from it; most of the cutaneous microvasculature is found in the papillary dermis (Braverman, 2000). The lower horizontal plexus is at the boundary of the dermal and subcutaneous tissue (Braverman, 1989). The lower plexus, formed by vessels from the underlying muscles and subcutaneous fat, lead into arterioles and venules. These also form connections with the upper horizontal plexus (Braverman, 1989) (*Figure 1.2*). The ascending arterioles are randomly spaced at intervals of 1.5 – 7mm within the dermis. The lower plexus also connects to the hair bulbs and sweat glands (Braverman, 2000) (*Figure 1.2*).

Many of the control mechanisms for regulating skin blood flow and ensuring adequate cutaneous perfusion arise from the endothelial cells lining all blood vessels. The endothelium has been shown to have a number of functions, including angiogenesis, metabolic, anti-inflammatory and anti-thrombogenic processes (O’Riordan et al., 2005). In particular, the endothelium has a vital role to play in the hemodynamics of the circulation. The layer of endothelial cells lining blood vessels contains gap junctions; these allow chemical and electrical communication between cells. Molecules, including metabolites and ions pass through the gap junctions from one cell to another, and facilitate the coordination of responses by the cells (Rumery and Hill, 2004)

Normal endothelial function has been described as the ability of the endothelium to release compounds that cause a direct relaxation of smooth muscle cells within the vascular wall; emphasizing the importance of its role in vasodilation above the other functions (Cracowski et al., 2006). Important endothelium-derived vasoactive compounds, include prostacyclin, thromboxane, nitric oxide (NO), endothelin, angiotensin, endothelium derived hyperpolarizing factor (EDHF), free radicals and bradykinin. NO is thought to be the main endothelium-derived relaxing factor and is known to perform an important role in the maintenance of vascular reactivity (Furchgott, 1999). NO acts to balance out the actions of endothelium-derived contracting factors.

### **1.2.3 Control and regulation of skin blood flow**

In order to sustain tissue perfusion and meet the demands of temperature regulation there must be an appropriate control of vascular responses. In the cutaneous microvasculature, alterations in blood flow in response to changing needs of the tissue are regulated by contraction and relaxation of vascular smooth muscle. This involves a combination of neural, myogenic, hormonal and metabolic mechanisms.

#### ***Neural mechanisms***

The arterioles are in a state of vasoconstrictor tone (Carlson et al., 2008), so that they maintain the capacity to further constrict or dilate. This tone is controlled by the autonomic nervous system (ANS), the metabolic needs of the tissues, local and circulating hormone levels and mechanical factors. The main mechanical factors that influence microvascular tone are pressure and flow. An increase in blood pressure causes a contraction called myogenic tone, and a decrease in blood pressure causes relaxation of the arterioles (Carlson et al., 2008).

The regulation of skin blood flow by the nervous system occurs in two main ways: central control by sympathetic nerve fibres and also by nerve axon reflex. The central control of skin blood flow is through two different pathways of sympathetic nerves; the sympathetic adrenergic vasoconstrictor nerves and the sympathetic vasodilator nerves. The glabrous areas of skin such as the palms, soles and lips, where AVAs are mainly found, are only innervated by the vasoconstrictor nerves; the rest of the skin microvasculature is innervated by both vasodilator and vasoconstrictor nerves (Charkoudian, 2003).

The nerve axon reflex mediates vasodilation of the cutaneous microcirculation. It is neurally mediated by nociceptive C-fibres (Cable, 2006), which are stimulated by heat or other stimuli. These fibres stimulate conduction in the normal direction (orthodromic) to the spinal cord and in the opposite direction (antidromic) to other axon branches. This causes the release of local vasodilator neuropeptides, such as substance P, bradykinin and calcitonin gene-related peptide (CGRP) from the terminals in skin and tissue. These neuropeptides then act on the vascular smooth muscle or through secondary pathways, such as mast cell release of histamine, to cause vasodilation to the area around the sensory neurons (Vinik et al., 2001; Chao and Cheing, 2009).

#### ***Myogenic mechanisms***

The vascular smooth muscle in the wall of blood vessels directly regulates skin blood flow by causing constriction in response to an increase in pressure across the wall and dilation in response

to a decrease in pressure (Bayliss, 1902). The increase in pressure causes an increase in intracellular calcium by activating cell membrane stretch activated channels (SAC) in smooth muscle cells (SMC) and endothelial cells (EC) (Takenaka et al., 1998). The SAC's are permeable to molecules such as potassium, sodium and calcium. The SAC's increase the calcium level in the cells by allowing direct influx of extracellular calcium and by depolarizing the SMC's which then causes an influx of calcium through voltage operated calcium channels. The raised calcium levels results in constriction of the vessel. The change in resistance of the blood vessels does compensate for the changes in arterial pressure, and it is suggested that this may be a form of autoregulation of blood flow (McGeown, 2002; Carlson et al, 2008). The myogenic responses have been shown to be more prominent in smaller vessels (Lagaud et al., 1999), and stronger in males than females (Huang et al., 1997).

Shear stress on the endothelial cells also affects the control of the blood vessels (Widlansky, 2009). The shear stress causes an influx of calcium through SAC's and an increase in calcium in endothelial cells. The mechanism of the shear stress response has been modelled mathematically (Wiesner et al., 1997). The increase in calcium leads to hyperpolarisation of endothelial cells and generation of NO. The propagation of hyperpolarisation and also the effects of the NO cause a decrease in the calcium level of SMCs and relaxation of the vessel (Koenigsberger et al., 2006). The endothelial cells have direct connections with the smooth muscle cells through myoendothelial gap junctions (Dora et al., 2000). Therefore, stress on smooth muscle by changes in intravascular pressure causes increased calcium levels in SMC's and the myogenic response. However, shear stress directly on endothelial cells causes reduced calcium levels in SMC's and the myogenic response is attenuated (Koenigsberger et al., 2006).

Endothelial cells produce NO which acts on smooth muscle cells to cause vasodilation. NO is produced from L-arginine by nitric oxide synthase (NOS) and there are several known isoforms. Endothelial NO causes dilation of blood vessels by stimulation of soluble guanylyl cyclase and also by increasing cyclic guanosine monophosphate (cGMP) within the smooth muscle cells (Forstermann et al., 1994). NO also inhibites platelet aggregation and adhesion. There is evidence that NO inhibits DNA synthesis, mitogenesis and proliferation of vascular SMC's (Forstermann and Munzel, 2006). Due to its dilating effects, NO is important in the control of blood pressure. NO, produced by endothelial cells, is known to regulate vascular tone and is important in the maintenance of vasodilation following local cutaneous heating and loading (Meredith et al., 1996; Kellogg et al., 1999).

### ***Hormonal and Metabolic mechanisms***

The SMC's around the vessel can also be stimulated directly by catecholamines acting on  $\alpha 1$ -adrenoceptors. Inflammation produces vasodilators such as bradykinin that increase blood flow at body sites where there is trauma and infection (McGeown, 2002). Skin blood flow is also regulated by local metabolite production. It has been found that local ischaemia results in the formation of vasodilator metabolites. These metabolites decrease the vascular resistance and cause local dilation of the resistance vessels and the opening of the pre-capillary sphincters in the local area (Berne et al., 1998). These metabolites are thought to include carbon dioxide, lactic acid, adenosine, phosphate,  $K^+$  ions and  $H^+$  ions (Seeley et al., 2000; McGeown, 2002).

#### **1.2.4 Vasomotion**

The regulation of the skin blood vessels results in an oscillatory blood flow pattern termed flowmotion; this flowmotion is in part caused by the rhythmic constriction and dilation of the blood vessels which is called vasomotion (Nilsson and Aalkjoer., 2003; Mauban et al., 2001; Rossi et al., 2006a). There are many different mechanisms for oscillations in blood flow. Mechanical oscillations are present in the blood flow and result from the movements of the heart and respiratory function. There are also oscillations which result from neural discharges (Nilsson and Aalkjoer, 2003). Vasomotion is generated from within the vascular wall and is not a consequence of the heart beat, respiration or neural discharges (Nilsson and Aalkjoer, 2003), but requires some tone to be present in the vessel.

It is possible that neural or hormonal input increases tone to a level where vasomotion can occur (Nilsson and Aalkjoer, 2003). Also, hormonal or neural inputs could influence the frequency or phase of the oscillations in vasomotion (Nilsson and Aalkjoer, 2003).

A number of theories have been suggested for the precise mechanism within the vessel wall that causes vasomotion. One suggestion is that oscillations in membrane potential are responsible for the oscillations in vessel tone in vasomotion. In a study where membrane potential was measured during vasomotion, the membrane potential oscillated at the same frequency as vasomotion (Hill et al., 1999). It is suggested that the coordination of the SMC's in the vessel wall would need to be due to electrical communication for it to be fast enough (Nilsson and Aalkjoer, 2003). A further theory is that the coordination of the SMC's in vasomotion is through gap junctions between the smooth muscles that enable them to quickly synchronise and constrict and dilate together (Hill et al., 1999; Sell et al., 2002; Haddock and Hill, 2005).

The rhythmic constriction and dilation in the skin microcirculation has been shown to be of benefit to microcirculatory flow. A study using theoretical analysis of oscillations in a multibranched network has shown that stimulated vasomotion can cause an increase of 40 - 60% in the mean blood flow when compared to normal, steady state conditions (Ursino et al., 1996). It has been shown mathematically that vasomotion reduces the vascular resistance and results in an increase in the effective diameter of a vessel (Slaaf et al., 1988). Both chaotic and periodic vasomotion increase blood flow compared to steady state (Parthimos et al., 1996). As the cutaneous microcirculation is regulated by a number of different mechanisms, it is considered that chaotic vasomotion will be inevitable (Parthimos et al., 1996). Vasomotion has also been shown to effect the distribution of blood flow; in a mathematical model it was shown that the distribution of flow at bifurcations in the arterioles was altered depending on whether the vasomotion was periodic or chaotic; chaotic vasomotion allowed a constant ratio of blood flow between the branches, but periodic vasomotion was able to increase flow in one branch of the arteriole and not the other (Ursino et al., 1996).

Vasomotion is thought to be beneficial in certain pathological conditions that result in tissue ischaemia. Using theoretical modelling it has been shown that periods of high flow with low frequency oscillations improves long distance diffusion of oxygen to capillaries (Tsai and Intaglietta, 1993). This means that at reduced perfusion levels, oxygen is more evenly distributed, so that there is less tissue with very low oxygen levels. In a study using rat hind limbs, Rucker et al. (2000) demonstrated using Nicotinamide Adenine Dinucleotide (NADH) fluorescence, that vasomotion improved flow to tissues and also maintained the NADH fluorescence in tissues adjacent to muscle; they concluded that vasomotion had a beneficial effect on tissue oxygenation due to improvements in microvascular flow. Other studies have shown the frequency of oscillations in the microvasculature to be significantly enhanced in pathologies where blood flow is reduced such as hypotension (Pajk et al., 2002; Nilsson and Aalkjaer, 2003).

### **1.2.5 Effects of external stimuli on skin blood flow**

#### ***Environmental temperature change***

The primary role of the cutaneous microvasculature is regulation of body temperature. The significant changes in blood flow during temperature regulation are implemented through the AVA's and the arterioles (Pocock and Richards, 2006). When body temperature rises, there is a decrease in SNS activity, the AVA opens and the arterioles vasodilate. When temperature falls, there is an increase in SNS activity, the AVA closes and arterioles constrict. If more heat loss is required then sweating is stimulated. The sweat glands are innervated by cholinergic sympathetic

vasodilator fibres; sweat contains an enzyme which causes the production of bradykinin, which is a strong vasodilator, and the bradykinin acts locally to cause further vasodilation of arterioles (Pocock and Richards, 2006). The sweating also enables evaporation and heat loss.

### ***Local warming***

The skin blood flow response to a local thermal challenge has been investigated in detail in recent years. The response to local heat stimulation involves an initial rapid vasodilation, followed by a short nadir, and then a secondary prolonged vasodilation, which can be described as the plateau. The initial, rapid increase in skin blood flow following local skin heating has been attributed to an axon reflex (Minson et al., 2001; Kellogg et al., 1999). It has been shown that NO does have a role to play in the onset of the local heating response to progressive local heating (Houghton et al., 2006). NO inhibition by L-Nitro-Arginine Methyl Ester (L-NAME) shifted or shutdown the onset of the axon reflex to a higher temperature. Although Minson et al. (2001) showed that NOS inhibition during rapid local heating slightly attenuated the axon reflex response, they found that it reduced the plateau response by approximately 20%, suggesting the role for NO is more significant during this secondary phase.

Some studies have suggested that NO might be indirectly involved in CGRP-induced vasodilation in the skin (Klede et al., 2003) and contributes to vasodilation in response to substance P (Klede et al., 2003). The effect that NO inhibition has in shifting the onset of the vasodilatation to a higher temperature with NO inhibition could be due to a desensitization of C-fibre nociceptors (Houghton et al., 2006). The involvement of prostaglandins in the local heating response is unclear. When the cyclooxygenase (COX) pathway, which is part of the pathway involved in the production of prostaglandins was inhibited, active vasodilation (sympathetic cholinergic) during whole body heating was also inhibited but this had no effect on local skin heating (McCord et al., 2006).

### ***Local pressure loading***

When a load is applied to the surface of the skin, the function of the elastin and collagen fibres in the dermis is to distribute and support the load (Hagisawa et al., 2001; Krouskop, 1983). There is evidence to suggest that application of a load to the skin below a certain pressure does not induce a decrease in blood flow as might be expected, but an increase (Xakellis et al., 1993). A study was performed using a calibrated pressure device to apply progressive amounts of pressure to the human hand, during which skin blood flow under the pressure device was measured using Laser Doppler Fluximetry (LDF) (Fromy et al., 2000). They demonstrated that up to pressures of 25mmHg there was a neurally mediated dilation in the skin of the human hand (Fromy et al.,

2000). In a similar study it was also found that local low level pressure stimuli leads to a slow developing vasodilation in the hand (Abraham et al., 2001).

It is clear that not all localised ischaemia results in cell necrosis. If there is pressure relief and the tissue is allowed to recover, there is a period of increased blood flow called reactive hyperaemia (RH) (Sprigle et al., 2002). It is important that the microcirculation is able to generate an adequate RH response to an interruption in tissue perfusion (Wywiałowski, 1999). The RH response is thought to result from several different mechanisms. The ischaemia caused by blood flow occlusion results in an accumulation of the metabolite adenosine in the ischaemic tissue. More recently it has been suggested that shear stress causes vasodilator prostaglandins to be produced by endothelial cells (Binggeli et al., 2003).

### **1.3 Pressure ulcer development**

Pressure ulcers develop when pressure, shear and friction forces act on the skin (*Figure 1.3*), particularly at areas where there is a bony prominence. The pressure applied to the skin is focused on the skin tissue directly above bony prominences. Kosiak (1961) described the link between pressure and pressure ulcers; they suggested that almost all pressure ulcers develop in the tissue over bony prominences subjected to excessive pressure and healing processes only begin to occur when pressure is removed. It is now generally considered that normal capillary pressure is approximately 32mmHg, which means that external pressures above 32mmHg will cause capillary deformation. The combination of friction and shear exacerbate the effects of pressure and mean that a reduced amount of pressure is required to cause damage (Dinsdale, 1974). Although in some cases only the skin tissue layer is affected in pressure ulceration, deep tissue pressure ulcers which involve muscle tissue can also occur. In the deep tissue pressure ulcers, the damage begins in the tissues under what appears to be intact skin (Ankrom et al., 2005).

A detailed understanding of the nature of the damage that occurs in the development of a pressure ulcer has been difficult to determine due to the difficulty of conducting research studies to investigate the changes that occur to the tissues at different stages of pressure ulcer development (Edsberg, 2007). There have been many *in vitro* studies and *in vivo* studies in animals that have directly measured the effects of pressure on tissue. However, there are ethical issues involved in sampling ulcerated tissue in human participants, so human studies have relied on considering the effects of the ulceration on the surrounding tissue or by conducting studies post-mortem (Edsberg,

2007). The main reasons for pressure ulcer formation are considered to be ischaemia, ischaemia-reperfusion and direct cell deformation.

The direct pressure applied to the supporting skin tissue layers has been shown to cause structural changes to the cutaneous tissue and in particular to the collagen fibres in the dermis. These collagen fibres become densely packed and change their alignment (Edsberg, 2007). It is suggested that the network of collagen and elastin fibres are important in preventing the surface pressures from extending into the deeper tissues; any damage to this tissue layer means that there are difficulties in the support of mechanical loads (Edsberg, 2007).

### ***Ischaemia***

When the tissue can no longer mechanically support the pressure, the result is occlusion of skin blood flow and ischaemia. The cutaneous microcirculation is not able to deliver oxygen and nutrients at a rate that is able to meet the metabolic demands of the tissue (Knight et al., 2001). It has also been suggested that occlusion to the lymphatic system can occur accentuating the accumulation of metabolic waste products (Reddy and Cochran, 1981). The accumulation of metabolic waste products can lead to cell damage. In a study in which 60mmHg was applied to the trochanteric region of dogs for greater than 1 hour, tissue samples from the site showed necrosis of the muscle and venous thrombosis (Kosiak, 1959). The venous thrombi that develop during loading can effect the RH following pressure removal, so that the tissue remains ischaemic for longer (Kosiak, 1961).

### ***Ischaemia-reperfusion***

Ischaemia reperfusion (IR) injury is cellular injury resulting from reperfusion of blood into a previously ischaemic tissue (Pretto, 1991). There is increasing evidence to suggest that IR plays a role in the pathology of skin damage during pressure ulcer formation (Peirce et al., 2001; Reid et al., 2004). The 2 hourly patient turning regimes advocated on many hospital wards mean that although the length of ischaemia to the tissues is reduced, the IR in the skin blood vessels still occurs at certain skin sites. The return of normal blood flow can exacerbate the tissue injury caused by the ischaemia (Bulkley, 1987). It has been shown in a skin rat model that repeated IR injuries are more damaging to tissue than prolonged ischaemia alone (Peirce et al., 2000). There are several proposed mechanisms for the damage caused by IR, but the majority involve the increased presence of reactive oxygen species (ROS) which results from the IR. The injury caused by ROS to the blood vessels includes endothelial cell swelling that limits perfusion (Mazzoni et al., 1995) and changes in the permeability of the post-capillary venules (Pierce et al., 2001).

### ***Deformation damage***

A further theory regarding the aetiology of pressure ulceration is that of direct cell damage caused by deformation. In deep tissue injury, the load on the skin surface is transferred to the muscle and is thought to directly cause cell damage. An *in vitro* study was completed in which compression was applied to engineered skeletal muscle tissue. It was found that direct cell damage occurred within 1-2 hours and they suggest that prolonged deformation of cells leads to cell damage and that this is involved in the onset of pressure damage (Breuls et al., 2003). A further study involving the rat hind-limb also found that above a certain threshold of tissue strain, damage occurred to the skeletal muscle (Ceelen et al., 2008). It is likely that after the initiation of this muscle damage, the development of the damage is accelerated by the effects of ischaemia (Ceelen et al., 2008).

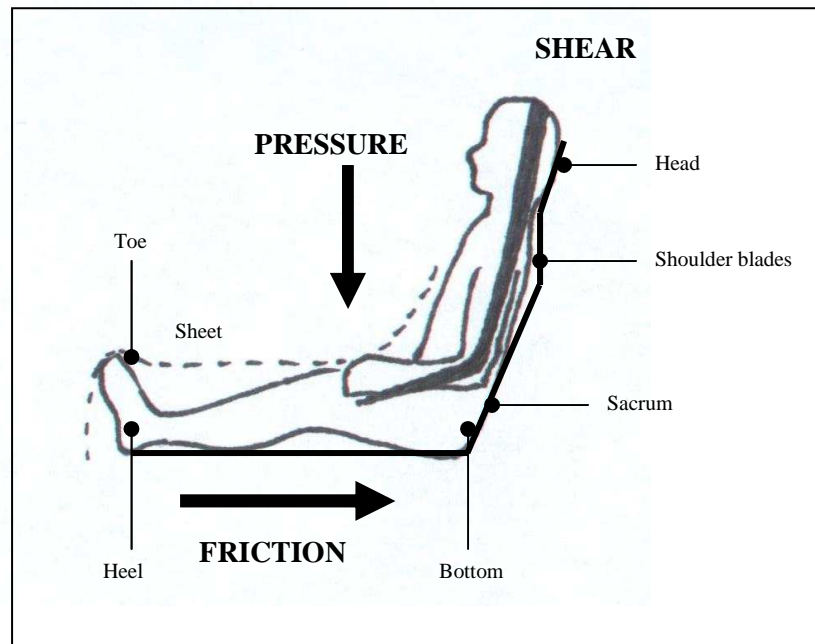


**Figure 1.3** A diagram to show pressure, friction and shear forces (adapted from Russell, 1998).

#### **1.3.1 Intrinsic factors that increase risk of PU**

There are many proposed factors that increase risk of pressure ulcer development, although more research is needed to demonstrate the link between these factors and pressure damage (Moore and Cowman, 2008). Certain population groups have altered skin microcirculation which can potentially increase risk of pressure ulcer development. The risk of pressure ulcer damage to the skin is difficult to predict due to the range of factors, both intrinsic and extrinsic, that affect the skin and specifically the skin microcirculation.

### ***Cardiovascular disease***

Cardiovascular disease may increase risk of pressure ulcer formation. Several studies have demonstrated changes in skin blood flow and vasoreactivity in patients with cardiovascular disease. A study has shown that the responsiveness of the forearm cutaneous microvasculature in a group of patients with essential hypertension to both CGRP and also a local warming stimulus, measured using LDF, was significantly reduced compared to a normotensive group (Lindstedt et al., 2006). Patients with peripheral arterial obstructive disease (PAOD) have shown delayed RH and reduced vasodilatory response to both acetylcholine (ACh) and Sodium Nitroprusside (SNP). The cutaneous blood flow was not impaired during baseline measurements in these patients, but only during the skin challenge. This may suggest that compensatory mechanisms were sustaining baseline flow at normal levels, and that these compensatory mechanisms have become exhausted during the challenge of post-occlusive hyperaemia (Rossi et al., 2005).

### ***Diabetes***

Diabetes is commonly considered to be a risk factor for pressure ulcer development. This is due in part to the effects of diabetes on the skin microcirculation. Studies have shown reduced sympathetically-mediated vasomotion in the foot skin microcirculation and increased capillary permeability in diabetic patients with neuropathy (Lefrandt et al., 2003). However, a further study has shown significant reduction in skin arteriolar vasomotion in diabetic patients without neuropathy (Meyer et al., 2003), suggesting that sympathetic peripheral dysfunction occurs earlier than parasympathetic diabetic neuropathy.

A study was completed in which progressive pressure was diabetic patients compared with the matched control subjects (Fromy et al., 2002). This suggests that the tissues of diabetic patients are potentially more susceptible to external pressure application and thus increased risk for pressure damage.

### ***Age***

Pressure ulcers are more common in the elderly and age is a predictive indicator included in most pressure ulcer risk assessment tools. In a study by Whittington et al. (2000), 17,560 patients in hospitals in the USA were studied for pressure ulcer development and 7% of the patients developed pressure applied to the ankle bone of diabetic patients without neuropathy and controls. It was found that the skin blood flow decreased to baseline with much lower applied pressure in the ulcers; 73% of these were in patients over 65 years. With the increased life expectancy of the population there is potential for a vast increase in the prevalence of pressure ulcers and an increase in the financial and personal costs that pressure ulcers cause.

There has been much investigation into the effect of ageing on the skin blood flow. Maximal cutaneous blood flow was shown to decrease linearly with age (Martin et al., 1995) in laser Doppler measures of skin blood flow. The ability to increase skin blood flow in response to environmental heat stress has been shown to be compromised with advanced age (Minson et al., 1998; Minson et al., 2002). In a study where a load was applied to the forearm skin of younger (mean age: 25.2 years) and older (mean age: 64.6 years) volunteers, the RH response as a result of the removal of the load was significantly reduced in the older group (Hagisawa et al., 1991).

There are structural changes in the skin tissue and the microcirculation that may increase the risk of pressure damage with advancing age. The number of capillary loops in skin decreases significantly with age, resulting in an increased inter-capillary distance (Li et al., 2006a). It has also been shown that aged skin is characterized by a flat dermal-epidermal junction with the disappearance of capillary loops, so there is loss of dermal nutritional vessel density and a reduction in the surface area for gas exchange. The density of capillary loops is shown to correlate negatively with age (Li et al., 2006a). The microvasculature is thicker and more twisted with increasing age, but there is an increase in total vascular length with increasing age (Li et al., 2006a).

## **1.4 Smoking**

### **1.4.1 Smoking background**

Smoking is also thought to be a factor effecting skin blood flow and skin blood flow responses to external stimuli. In 2006, approximately 23% of men and 21% of women smoked cigarettes in the United Kingdom, and there was an estimated 12 million cigarette smokers in the UK in 2008 (Allender et al., 2008). Others have suggested that worldwide, 47.5% of men and 10.3% of women smoke cigarettes (Yanbaeva et al., 2007). Smoking affects many of the human body organs and functions and is related to many diseases.

It has been well known since the 1950's that there is a link between cigarette smoking and cardiovascular disease (Doll and Hill, 1956). The epidemiological evidence for this is strong. A 50 year cohort study of UK doctors considered the long term risk of smoking and found that the mortality from coronary heart disease was around 60% higher in smokers and 80% higher in heavy smokers compared with non-smokers (Doll et al., 2004).

### **1.4.2 Smoking and cardiovascular risk assessment**

There has been much research on the effects of smoking on the cardiovascular system and the more recent work has explored the method of using measurements of skin blood flow to predict risk of cardiovascular disease. The skin is easily accessible and can be investigated non-invasively (Holowatz et al., 2008). As far back as the 1980's, Sax et al. (1987) showed using the technique of plethysmography, that patients with microvascular angina had an impaired forearm vasodilator reserve following forearm ischaemia. In a further study in children with diabetes, it was shown that they had impaired microvascular hyperaemic response to local heat compared to matched controls (Shore et al., 1991). Also, using iontophoresis coupled with LDF, it was found that an increased risk of coronary heart disease was associated with a smaller endothelium-dependent dilation and less capillary recruitment in the skin (IJerman et al., 2003a). In fact, a study has shown that patients with abnormal LDF measurement of the thermal hyperaemia showed increased cardiovascular mortality, and it is suggested that its use could improve risk assessment, alongside current assessments such as Framingham (Kruger et al., 2006). These studies suggest that patients with increased risk of cardiovascular disease have abnormal skin microcirculation and that this can be detected non-invasively.

### **1.4.3 Smoking and the skin**

Although smoking is a risk factor for cardiovascular disease it has also been shown that smoking has specific local effects on the skin. The effects on the skin can be seen in both the structural anatomy and the microcirculation and both these effects may potentially increase the risk of pressure ulcer development. After sun exposure, it is thought that smoking is the most important contributor to premature skin ageing. A recent study by Helfrich et al. (2007) found that cigarette smoking significantly correlated with skin aging in skin that had not been exposed to the sun. Smoking has been shown to cause reduction in collagen in skin through up-regulation of membrane metalloproteinases (MMP), which breakdown the collagen (Knuutinen et al., 2002; Yin et al., 2000). Several studies have found a significant link between smoking and increasing presence of pressure ulcers in patients (Cakmak et al., 2009; Smith et al., 2008)

There is evidence that smoking has adverse effects on the cutaneous microcirculation, although studies so far have produced conflicting results. In a study investigating the chronic effects of smoking on basal skin blood flow at the sacrum, there was no significant difference between smokers and their matched non-smoking controls (Butler et al., 2001). It was also shown that cutaneous blood flow during and after cigarette smoking was not significantly different from pre-

smoking blood flow levels (Tur et al., 1992). However, others have found that cigarette smoking causes an acute decrease in skin blood flow at the finger, thumb and upper arm body sites (Bornmyr and Svensson, 1991; Richardson, 1987; Goodfield et al., 1990; Monfrecola et al., 1998; Reus et al., 1984; Van Adrichem et al., 1992).

The effect of smoking intensity on skin blood flow has been explored in several studies. In a study considering the flow and nitroglycerin-mediated reactivity of the brachial artery, it was shown that these were significantly reduced in smokers compared to non-smokers, but smoking a small or large number of cigarettes per day caused the same adverse effects on endothelial function (Barua, et al., 2002). However, other studies have shown there to be differences in acute skin blood flow responses to smoking a cigarette between light (10-12 cigarettes/day) and heavy smokers (>20 cigarettes/day) (Midttun et al., 2006). The blood flow in AVA's, measured using the heat washout method, decreased during smoking in the light smokers and returned to pre-smoking levels immediately after smoking, but in heavy smokers it remained unchanged before, during and after smoking. They suggest that this shows that heavy smokers have severe impairments in their peripheral microcirculation (Midttun et al., 2006).

#### **1.4.4 The effects of smoking on the endothelium**

The endothelial lining of skin blood vessels is important in the regulation of skin blood flow. It is thought that smoking causes an alteration in the function of the endothelium. Endothelial dysfunction is primarily considered to be a disease of the microvasculature (Stewart et al., 2004) and means that the blood vessel wall is more susceptible to vasoconstriction, leukocyte adherence, platelet aggregation and thrombosis, vascular inflammation and atherosclerosis (Verma and Anderson, 2002).

The first evidence that cigarette smoking could cause endothelial injury was demonstrated in a study where morphological observations of umbilical arteries taken from smoking mothers were completed (Asmussen and Kjeldsen, 1975). The endothelium was shown to have an irregular appearance. Other studies have shown that morphological changes to aorta endothelium caused reduced production of prostacyclin from the endothelium and platelet adhesion (Pitillo et al., 1982). Rats exposed to nicotine showed increased endothelial cell death which resulted in leakage of macromolecules across the endothelium (Lin et al., 1992). Although the vasodilator capacity of the cutaneous microcirculation has been shown to be reduced in smokers compared to non-smokers (IJzerman et al., 2003b) and also in the infants of smoking mothers compared to non-smoking mothers (Ahlsten et al., 1987); only one study has shown reduction in vasodilation due to

endothelial-dependent mechanisms without reduction in vasodilation due to endothelium-independent mechanisms (Celermajer et al., 1993). However, it is important to clarify that even this study was completed on the brachial artery of participants and not the vessels of the microcirculation.

There are several theories as to how smoking may cause endothelial dysfunction. More recently, the main focus of attention has been on the effects of smoking in reducing nitric oxide levels in the body, through an increase in oxidative stress.

#### **1.4.5 Nitric oxide and smoking**

It has been hypothesised that a reduction in NO production in smokers results in a reduction in the vasodilator capacity of the cutaneous microcirculation. Several studies have shown that smoking affects the intravascular levels of NO. Long term smokers have significantly lower plasma NO (Node et al., 1997) and reduced plasma NOS activity (Barua et al., 2001) than non-smokers. In a recent study, smoking a cigarette decreased nitrate and nitrite concentrations in the plasma by  $3.5 \pm 1.2$  and  $3.4 \pm 1.1$   $\mu\text{mol/L}$  compared to pre-smoking and sham smoking, respectively (Tsuchiya et al., 2002). NO biosynthesis *in vivo* and *in vitro* is adversely affected in light smokers, as well as heavy smokers. A study has shown there to be similar alterations in NO production, endothelial nitric oxide synthase (eNOS) protein expression and activity in light and heavy smokers (Barua et al., 2002). However, there are conflicting findings from another study, in which smokers had increased serum levels of NO compared to non-smokers (Chavez et al., 2007).

The reasons why smokers may have altered vascular NO levels has been explored in much detail. It may be due to reduced intracellular availability of the precursors of NO such as L-arginine (Hutchison et al., 1999), or the cofactors of NO, such as tetrahydrobiopterin (BH<sub>4</sub>) as a result of oxidation by peroxynitrite (Heitzer et al., 2000). The adverse effects of cigarette smoke on endothelial function may be reversed by supplementation of L-arginine (Hutchison et al., 1999) or BH<sub>4</sub> (Heitzer et al., 2000). It has also been shown that cigarette smoke extract (CSE) causes acute reduction in endothelial cell L-arginine transport (Zhang et al., 2006). The cationic amino acid transporter (CAT1) is one of the major transporters for L-arginine for the endothelial cell. CSE caused diminished CAT1 mRNA. They found that CSE was able to reduce endothelial NOS (eNOS) enzymic activity, but not inducible NOS (iNOS) activity (Zhang et al., 2006).

#### 1.4.6 Oxidative stress and smoking

There has been much focus on the effect of oxygen free radicals and oxidative stress on endothelial function, particularly in relation to smokers as it is known that cigarette smoke contains and generates a substantial amount of oxygen free radicals (Smith and Fischer., 2001; Leanderson and Tagesson, 1992). Although it is suggested that when produced in a controlled manner reactive oxygen species (ROS) such as hydrogen peroxide ( $H_2O_2$ ) have important signalling functions in the body (Griendling and Harrison, 1999). Some studies do not agree, and suggest that ROS cause the proliferation and apoptosis associated with cardiovascular diseases such as atherosclerosis (Li et al., 1997).

Although the ROS from cigarette smoke could cause the vascular dysfunction seen in smokers, the specific pathway for this has not been clearly defined. It is believed that the endothelial dysfunction in smokers may result from oxidative damage by ROS on endothelial cells (Heitzer et al., 1996).

ROS may also cause endothelial dysfunction through inactivation of NO. Xanthine oxidase is a multifunctional enzyme present in high concentrations in the endothelial cells of capillaries and can produce free radicals (Guthikonda et al., 2003). Xanthine oxidase derived superoxide radicals are thought to react with NO to form peroxynitrate, which causes inactivation of NO (Guthikonda et al., 2003). When xanthine oxidase is blocked by allopurinol, endothelial dependent vasodilation in smokers is improved (Guthikonda et al., 2003).

Furthermore, other studies have shown that cigarettes smoking cause sticking of leucocytes to the microvascular endothelium in hamsters (Lehr et al., 1993), but vitamin C prevented this (Lehr et al., 1994). This suggests that the anti-oxidants could not act as scavengers of the ROS that were causing the damage. A study has shown significantly improved endothelial function of the brachial artery measured by flow-mediated vasodilation in smokers following vitamin C supplementation (Young et al., 2006).

Recently, the role of nicotinamide adenine dinucleotide phosphate (NADPH) oxidase in generating ROS, and specifically superoxide, has been explored. Although, cigarette smoking was found to cause significant endothelial dysfunction in the carotid arteries of rat, this was reversed with the inhibition of NADPH oxidase (Orosz et al., 2007). It is thought that the water soluble components of cigarette smoke cause increased NADPH oxidase-dependent superoxide generation in the arteries, and so the inhibition of NADPH prevented this (Orosz et al., 2007).

Although cigarette smoke contains large quantities of oxygen free radicals, the role of nicotine has also been explored in relation to oxidative stress. It has been shown that 2 sprays of a nicotine nasal spray (1mg of nicotine) causes endothelial dysfunction as measured in the brachial artery of chronic smokers, using high-resolution ultrasound (Neunteufl et al., 2002). However, they also found that smoking a cigarette with a nicotine yield of 1mg caused a greater amount of endothelial dysfunction compared to the nicotine nasal spray. This suggests that, although nicotine has a role to play in endothelial dysfunction, other constituents of cigarette smoke contribute as the dysfunction was more evident after smoking a cigarette than nicotine spray alone (Neunteufl et al., 2002). Acute infusion of nicotine causes impaired endothelial dependent arteriolar vasodilation, but this was restored by perfusion with superoxide dismutase (SOD) (Mayhan and Sharpe, 1998), which is known to catalyze the removal of superoxide (Csiszar et al., 2009). It has also been found that infusion of nicotine impaired the release of NO from the hamster cheek pouch microcirculation in response to ACh and adenosine diphosphate (ADP) and treatment with SOD prevented this (Mayhan and Sharpe, 1999).

The increased oxidative stress in smokers may be due to an imbalance in oxidants and anti-oxidants. Several studies have shown that smokers have lower levels of antioxidants, which results in an increased susceptibility to the oxidant effects of cigarette smoke (Morrow et al., 1995; Nuttall et al., 2002; Tousoulis et al., 2003). In smokers with a lower NO-mediated vasodilation response, there was a reduction in circulating levels of ascorbic acid, tocopherol, and alpha and beta carotene, which suggests reduced antioxidant capacity (Rocchi et al., 2007). However, other studies have shown increased function of antioxidant mechanisms involving vitamin C in smokers, suggesting that this is a compensatory mechanism against the increased presence of ROS (Chavez et al., 2007). The vitamin C was proposed to prevent accumulation of malondialdehyde and was a protective measure and compensatory mechanism against oxidative damage. Further studies have also demonstrated the potential protective effects of vitamin C against the microvascular effects of cigarette smoking (Gamble et al., 2000).

## **1.5 Measurement of skin blood flow**

There are several techniques currently used to measure the blood flow in the cutaneous microcirculation, including photoplethysmography, laser Doppler imaging (LDI) and LDF. LDF has been used in a large number of studies and in recent years has become a tool by which the oscillatory nature of the blood flow can also be measured by further analysis of the signal. This is the technique used within this thesis, so will be considered in more depth.

### 1.5.1 Laser Doppler fluximetry

Since the 1970's, numerous studies using LDF to monitor the skin microcirculation have been published (Bongard and Bounameaux, 1993; Saumet et al., 1988). LDF has been shown to be an affective and reliable method for the measurement of blood flow in the microcirculation both in medicine and microvascular research (Obeid et al., 1990).

The LDF uses the Doppler affect, where laser light becomes shifted in frequency when it is scattered by moving red blood cells in the tissues. A portion of the backscattered light is detected photoelectrically and a voltage output is obtained (Cooke and Almond, 1990) (*Figure 1.4*). The product of red cell velocity and density is called the flux of red cells which, for a constant haematocrit within the volume of tissue being sampled, should be proportional to red cell flow (Cooke and Almond, 1990).

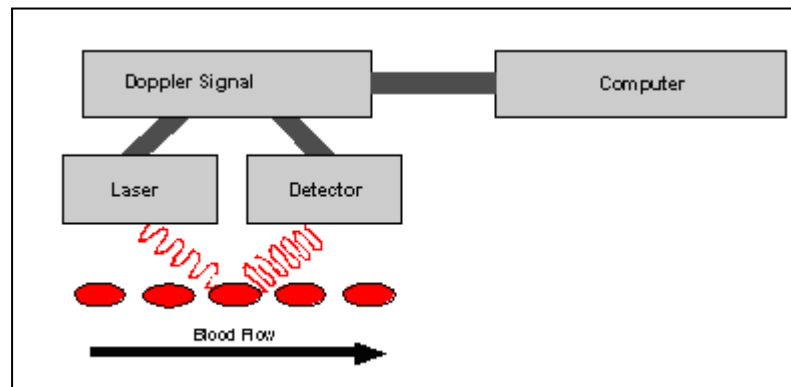


*Figure 1.4* A diagram to show the functioning of the Laser Doppler fluximeter

The LDF is suited to measure relative flow changes in the microvasculature, such as during heating or cooling or during and after ischaemia. The depth of surface penetration is less than 1mm and is dependent on wavelength and number of fibres (Fredriksson et al., 2009). A recent study has shown using Monte Carlo estimation that for a LDF probe with a fibre separation of 0.46mm, the depth of penetration measured is between 0.21-0.39mm (Larsson et al., 2002). The proportion of photons that reach depths greater than 1.4mm when using this probe was found to be 13.7% (Clough et al., 2009). Thus, the majority of the measurement is taken from epidermal and dermal tissue. It measures flow in the capillaries and tertiary arterioles within the upper horizontal plexus (Braverman et al., 1990).

LDF is an established non-invasive procedure which measures both nutritional and non-nutritional blood vessels (Nilsson et al., 1980). This method has advantages over other methods in that it does

not cause tissue trauma or disturb the microcirculation directly (Jan et al., 2005). The blood flow in the arterioles, capillaries and venules is measured, but capillary supply to sweat glands and hair follicles does not contribute as these are 3 - 5mm below the skin surface (Braverman, 2000). LDF has high temporal resolution as measurements can be taken continuously.

The LDF technique does have disadvantages. The LDF probe is prone to effects of movement artefact on the signal. The technique of LDF only gives a relative measure of skin blood flow; the signal does not give absolute values for the blood flow signal, but only measures in arbitrary units. The measurement depth of the laser Doppler probe is also variable due to differences in tissue structure, the heterogeneity of blood flow, the distribution of blood vessels and the measuring probe itself (Wohlrab et al., 2001). As the LDF probes used in the studies in this thesis have diameters of 1.5mm (skin heating) and 8mm (skin loading) and the distribution of blood vessels in the skin is variable, there can be significant site-to-site variations in flux measurements (Bravermann, 2000).

### **1.5.2 Laser Doppler fluximetry and skin challenge**

It is considered that measurements are more accurate when a known challenge is applied to the skin in conjunction with the LDF. These include post-occlusive reactive hyperaemia, local pressure-induced hyperaemia and local thermal challenge.

#### ***Post-occlusive reactive hyperaemia***

Post-occlusive hyperaemia is the increase in skin blood flow above baseline levels after the release of a short arterial occlusion (Cracowski et al., 2006). The test is performed by placing a cuff on the upper arm and increasing the pressure above systolic blood pressure. On removal of the cuff, there is usually an increase in blood flow above baseline levels. The ischaemic period is usually between 3 and 5 minutes; for ischaemic periods that are greater than 5 minutes there has been shown to be a linear correlation between the length of the ischaemia and the amplitude of the response (Wong et al., 2003). A study has shown that NO is not crucial for the response (Wong et al., 2003; Zhao, 2004); the hyperaemia in response to both 5 and 15 minutes occlusion was not significantly different at the L-NAME site compared to the control site (Wong et al., 2003).

#### ***Local pressure induced hyperaemia***

Studies have shown that the RH response in the skin microvasculature following removal of external pressure is different to the response caused by the release of cuff occlusion. External pressure on the skin results in a more prolonged increase in skin blood flow (Rendell and Wells,

1998). When the microvascular response to pressure and cuff-induced ischemia were compared at the finger site of human participants, the pressure induced hyperaemia began later, lasted for longer and was of a greater magnitude compared with the cuff occlusion. The application of direct pressure to the skin causes substantial stress directly on the arterioles themselves (Rendell and Wells, 1998). When cuff occlusion occurs, venous return is blocked, so venous blood remains in venules during occlusion (Capp et al., 2004). However, local pressure forces venous blood out of the venules. Many studies have used measurement of skin blood flow during and after ischaemia caused by cuff occlusion and have demonstrated differences in vasoactivity between groups including smokers and non-smokers; smokers were shown to have reduced response to ischaemia (Rossi et al., 2007a).

Several studies have considered the effect of external pressure on the skin of different body sites and using different methods of loading the skin. In a study, patients lay on a mattress and the skin blood flow was measured using LDF at the trochanter, before, during and after the pressure period (Frantz and Xakellis, 1989). Further studies positioned the heel on a transparent plate to apply the pressure and LDF measured skin blood flow through the plate (Mayrovitz et al., 1997; Mayrovitz and Smith, 1998). Other studies used external loading devices of varied sophistication, which applied given loads to the skin (Schubert and Fagrell, 1991; Colin and Saumet, 1996; Fromy et al., 2000; Abraham et al., 2001). The studies involving external loading and removal have shown light smokers to have attenuated reactive hyperaemic responses (Noble et al., 2003) and a group of elderly patients had diminished responses (Schubert and Fagrell, 1991).

### ***Thermal challenge induced vasodilation***

Several studies have been undertaken to measure the response to local heating in different patient groups and healthy control participants. A study was completed in which local heating was applied to the hand and foot of patients with complete spinal cord injury (SCI) compared to patients with incomplete SCI (Nicotra et al., 2004). They found that the axon-reflex mediated phase was significantly reduced in the foot (below the level of the lesion) of patients with complete SCI compared to those with incomplete SCI. They suggest from this study that the local heating response may be a useful technique to assess the spinal sympathetic pathways in order to classify SCI (Nicotra et al., 2004). The local heating response has also been used to consider the effects of ageing on the skin microcirculation. It was found that the initial rise in blood flow and the prolonged plateau vasodilatation in response to local heating was significantly attenuated in older (69-84 years) participants compared to younger (18-24 years) participants (Minson et al., 2002). The reduced ability to increase blood flow rapidly to a direct heat stimulus and also the attenuated prolonged vasodilatation could make the skin of the elderly group more at risk of damage.

### 1.5.3 Laser Doppler fluximetry and spectral analysis

The LDF signal is composed of a number of oscillations of various frequencies resulting in flowmotion and this is in part due to the constriction and dilation of the blood vessels during vasomotion (Rossi et al., 2006a). In recent years, spectral analysis of the cutaneous LDF signal has been used to investigate skin blood flowmotion in an increasing number of studies. Several studies have shown there to be 5 distinct frequencies of oscillations within the LDF signal (*Table 1.1*).

<i>Frequency</i>	<i>Origin</i>	<i>Research study references</i>
~ 1.0Hz	Cardiac Rhythm	Bracic and Stefanovska, 1999
~ 0.3Hz	Respiratory Rhythm	Bollinger et al., 1993; Bracic and Stefanovska, 1999
~ 0.1Hz	Intrinsic smooth muscle (myogenic) activity of blood vessels	Akselrod et al., 1981; Hyndman et al., 1971
~ 0.04Hz	Neurogenic activity of blood vessels	Kastrup et al., 1989; Soderstrom et al., 2003
~ 0.01Hz	Endothelium-mediated activity of blood vessels	Kvernmo et al., 1999; Kvandal et al., 2003; Stewart et al., 2007

**Table 1.1** A table to show the origin of the 5 frequencies demonstrated by spectral analysis of the skin LDF signal.

#### *Spectral analysis and summary of frequency bands*

The LDF signal is composed of oscillations of different frequencies. The power of the signal at each of the different oscillation frequencies can be calculated using spectral analysis. There have been various studies, using spectral analysis of the LDF signal, that have demonstrated that the frequencies within the LDF signal originate from mechanisms of skin blood flow control, including both local and systemic control mechanisms.

#### *Oscillations around 1Hz (60 beats/min)*

During rest, the cardiac frequency in adult humans is around 60 beats/min (1Hz), ranging from 36 to 96 beats/min (0.6-1.6Hz). The activity of the heart can be detected in all vessels, including the vessels of the cutaneous microcirculation. This was shown in a study in which the electrical activity of the heart measured using electrocardiography (ECG), and peripheral blood flow using LDF, were measured at the same time in a group of human volunteers. The heart rate frequency at ~1Hz was present in the LDF signal of peripheral blood flow (Bracic and Stefanovska, 1999).

### ***Oscillations around 0.4Hz***

The frequency  $\sim 0.4\text{Hz}$  has been shown to represent respiratory function, but it can only be found weakly in the microvascular blood flow signal. A study was completed in which the LDF signal at the dorsum of the foot was measured simultaneously with recordings of respiratory activity using mercury strain gauge. The waves at  $\sim 0.4\text{Hz}$  synchronized with respiration and disappeared during cessation of respiration (Bollinger et al., 1993). It is suggested that the oscillations in the LDF signal at a frequency of  $\sim 0.4\text{Hz}$  result from the changes in thoracic pressure during respiration (Bollinger et al., 1993).

### ***Oscillations around 0.1Hz***

The oscillations detected in microvascular flow at a frequency of  $\sim 0.1\text{Hz}$  have been shown to originate from the vasomotor control of smooth muscle and therefore blood pressure regulation. Hyndman et al. (1971) showed that mean arterial pressure (MAP) contains repetitive fluctuations with a frequency of 1 every 10 seconds ( $0.1\text{Hz}$ ). The parasympathetic and sympathetic nervous system and also the renin-angiotensin system of dogs was blocked while peripheral microvascular flow was measured (Akselrod et al., 1981). They found that there was a peak in the spectral analysis of the microvascular flow at  $\sim 0.12\text{Hz}$ . Parasympathetic blockade caused the frequency at  $0.1\text{Hz}$  and  $0.4\text{Hz}$  to be abolished completely. Others have found that the intensity of this frequency in the peripheral blood flow signal varies with place of observation implying local rather than central origin (Bracic and Stefanovska, 1999).

### ***Oscillations around 0.04Hz***

Using human volunteers, Kastrup et al. (1989) measured peripheral blood flux on the distal forearm using LDF. They detected two categories of oscillations with frequencies  $\sim 0.11\text{Hz}$  and  $\sim 0.03\text{Hz}$ . The oscillations at frequency  $\sim 0.11\text{Hz}$  were shown to have a non-neurogenic origin, as they were unaffected by local nervous and ganglionic blockade. However, in every subject, the oscillation with frequency  $\sim 0.03\text{Hz}$  disappeared in tissue with local lidocaine anaesthesia; these oscillations could only be identified in unanaesthetised skin. This suggests that the oscillations with frequency  $\sim 0.04\text{Hz}$  are neurogenic in origin.

A further study was completed in which blood flow on free flaps which have no sympathetic blood flow control was measured using LDF and compared with intact skin in human volunteers (Soderstrom et al., 2003). There was a significant difference between the free flaps and intact skin in the normalised power (power in the interval divided by total power between  $0.0095$  and  $2\text{Hz}$ ) of two frequency bands:  $0.0095\text{-}0.021\text{Hz}$  and  $0.021\text{-}0.052\text{Hz}$ . The former is attributed to endothelial activity (see next section) and they suggest that this would be due to smaller number of intact

vessels in the implanted skin. They conclude that sympathetic nerve activity influences blood flow oscillations with frequencies of 0.02-0.05Hz.

#### ***Oscillations around 0.01Hz***

A recent study has shown that a NOS inhibitor reduces very low frequency oscillations in the laser Doppler power spectrum (Stewart et al., 2007). They conclude that very low frequency oscillations in the laser Doppler signal (0.0095-0.021Hz) are NO-dependent and that the measurement of this frequency is a potential non-invasive marker for NO-dependent microvascular reactivity. This underlines what has already been shown in a study by Kvandal et al. (2003). They found that iontophoresis of the endothelial-dependent vasodilator ACh, increased the relative power of the oscillations around 0.01Hz in the laser Doppler signal more than an endothelial-independent vasodilator, SNP. The introduction of L-N<sup>G</sup>-monomethyl Arginine (L-NMMA), an NO inhibitor, prevented this difference. In a group of long distance trained athletes, the endothelial-dependent vasodilator ACh enhanced the amplitude of oscillations of around 0.01Hz in the cutaneous microcirculation signal to a significantly greater extent than SNP (endothelium-independent), but did not reach significance in control group (Kvernmo et al., 1999). Therefore, there is evidence from a number of studies for a relationship between ~0.01Hz oscillations and the endothelium.

The spectral analysis of the LDF signal during ACh iontophoresis and ischaemia induced hyperaemia has recently been compared to assess which is most accurate at measuring endothelial function (Rossi et al., 2004). It was found that there was a significant increase in the relative contribution of the ~0.01Hz frequency with ACh, but not with ischaemia induced hyperaemia. They suggest that the skin vasodilation resulting from iontophoresis of ACh is more accurate than post-ischaemic reactive hyperaemia to explore skin microcirculation endothelial function in healthy subjects.

#### ***Oscillations around 0.005-0.0095Hz***

Although the presence of 5 frequency bands within the LDF signal is generally accepted in the literature, there has been recent suggestion of a further very low frequency peak of oscillations between 0.005 and 0.0095Hz. The study showed there to be peak at this frequency at rest and during stimulation with ACh and SNP (Kvandal et al., 2006); it also demonstrated that ACh affects this frequency greater than SNP suggesting that it is endothelium related. However, inhibition of NO or PG synthesis did not reduce the increased response to ACh compared to SNP, which confirms that other endothelium dependent mechanisms must be involved.

### ***Spectral analysis techniques – Fast Fourier Transform versus Wavelets***

There are various methods used to calculate the power spectral density (PSD) of the LDF signal, but the methods most commonly used are the fast Fourier transform (FFT) and Wavelet analysis. There have been several studies in recent years that have used FFT to complete spectral analysis on the LDF signal (de Jongh et al., 2004; Stewart et al., 2007; Cui and Sathishkumar, 2006; Bari et al., 2005).

#### **1.5.4 Laser Doppler Fluximetry and spectral analysis in patient studies**

Several recent studies have measured the oscillatory frequencies in the skin of different patient groups. In a study of critically ill patients, the frequency of vasomotion in the skin microcirculation was increased both during resting conditions and during RH in patients that did not go on to survive when compared to survivors (Knotzer et al., 2007). In patients with chronic kidney disease, a reduced post-ischaemic increase in the PSD of the endothelium-related frequency (0.01Hz) in the LDF signal was observed, and suggested to be an early sign of endothelial dysfunction in these patients (Rossi et al., 2008).

In another study considering patients with PAOD, the patients showed a reduced amplification of flowmotion during RH compared to healthy controls. The study showed there to be amplified flowmotion waves around the frequency 0.01Hz, 0.04Hz and 0.1Hz in these patients at baseline, but not during RH. It may be that during resting conditions there is a compensatory mechanism at work in order to optimize skin blood flow, but that this is exhausted when the blood flow is challenged (Rossi et al., 2005).

These studies show that, in patient groups or sections of the population at risk of changes in skin blood flow such as smokers, the regulation of skin blood flow can be investigated using LDF and spectral analysis. Our current knowledge of the effects of different disease states on vasomotion is not clear and needs further study.

#### ***Rationale for the studies***

There has been much development in the equipment and products used to try to reduce the risk of pressure ulcer development by relieving the pressure, friction and shear forces on the skin of patients both in hospital and the community. There have been improvements in standard hospital mattresses, but also specialised pressure ulcer prevention equipment, such as alternating pressure mattresses. This specialist equipment and patient turning regimes must be directed at those patients particularly at risk. Accordingly it is important to determine the patients that are more at risk and

provide them with specialist products (NICE, 2005). In all of this, the timely assessment of risk for pressure ulcer development is vital and the NICE (2005) guideline recommends that the initial assessment is completed within 6 hours during the first episode of care. The current economic climate has resulted in a reduction in spending in the NHS, which could equate to a reduction in the nurse/patient ratio, which puts increasing pressure on aspects of care such as risk assessment. It is important to ensure risk assessment tools are appropriately validated and research-based.

The current strategies used to assess a patient's susceptibility to pressure ulcer development include formal risk assessment tools, such as the Waterlow score and Braden scale, clinical judgement and general skin inspection of the patient. The assessment process is dynamic; it is ongoing and responsive to changes in patient drugs, treatments and general condition/diagnosis. The public expect value for money and high levels of efficiency from the NHS; it is important to avoid pressure ulcer development, but also to avoid giving expensive, specialist pressure relieving equipment to those that don't require it. This is a very delicate balance as the costs of developing a pressure ulcer in both financial and quality of life terms are high.

There is a need for more accurate assessment of risk of pressure ulcer development. The use of risk assessment tools alongside clinical judgement is not necessarily the answer. There are currently over 40 RAT's in use (Moore and Cowman, 2010); mainly due to the widely varying patient populations in different health care settings with varying risk factors (Moore and Cowman, 2010). However, there is a lack of evidence regarding the sensitivity and specificity of RAT's (Moore and Cowman, 2010). An objective tool to assess the skin microcirculation and its control mechanisms could potentially be used as an objective adjunct to clinical judgement in the quest for sensitive and specific risk assessment.

## **1.6 Hypothesis and aims**

An appropriate blood flow is essential for the maintenance of cutaneous viability and health. Tissue breakdown, specifically pressure ulcer development, results from an inadequate cutaneous vascular perfusion, known to be caused by external forces such as pressure, friction and shear. Although the focus of research is often directed at these forces, it is thought that the risk of developing a pressure ulcer is increased by factors which alter the control of the cutaneous microvasculature. Smoking is a recognised risk factor for cardiovascular disease; it is also a potential risk factor for pressure ulcer development. It is hypothesised that smoking can increase the risk of developing a pressure ulcer through modulating cutaneous vascular control, potentially

through its effects on endothelial function. The aim of this thesis is to investigate the impact of smoking on vascular responsiveness and microvascular control mechanisms and to determine whether measurement of altered cutaneous responses may be an appropriate tool for risk assessment in a clinical setting.

**The specific aims of this thesis are:**

1. To develop a protocol to measure cutaneous vascular responsiveness by applying a reproducible challenge to the cutaneous microvasculature in a clinical setting
2. To investigate differences in the cutaneous vascular responses in healthy habitual smokers and non-smokers using laser Doppler fluximetry
3. To measure the spectral frequencies in the LDF signal during the vascular responses to determine which are responsible for any evident differences between the smokers and non-smokers.
4. To explore the mechanisms underlying the altered vascular responsiveness in smokers and, in particular, the role of endothelial derived factors.
5. To consider the potential use of an objective measurement screening method as an adjunct to the use of pressure ulcer risk scales in the context of clinical practice



## **Chapter 2**

### **General Methods**

The main research studies in this thesis involve the use of LDF to investigate skin blood flow responses. The methods section will first describe the participants involved in general terms, while the specific characteristics of the different groups of participants can be found in the relevant results chapters. Following this, there is an explanation of the techniques used to measure skin blood flow responses to local loading and heating. The spectral analysis technique used to further investigate the responses will be described and finally the data handling used within the thesis is summarised.

## **2.1 Generic Participant Details**

The studies in this thesis were approved by the Southampton and South West Hampshire Joint Research Ethics Committee; the ethics approval numbers were 211/01 and 138/01. The studies conformed to the principles outlined in the Declaration of Helsinki. The participants involved in the studies contained in this thesis were convenience samples of healthy human participants. In each of the different investigations the participants were recruited by advertisement and personal contact. The specific characteristics of the participants in each of the studies are summarized in the relevant chapters of results throughout the thesis.

### **2.1.1 Inclusion/exclusion criteria**

The participants were aged between 18 and 70 years and were able to give their written, informed consent. Those with a history of cardiovascular or respiratory disease, recent illness, taking medication mediating blood flow and with present or previous pressure ulcers were excluded from the studies.

### **2.1.2 Matched pairs**

The 'at risk' groups of smokers were matched as was possible to non-smoking control participants in terms of age, sex and BMI. This is because it is thought that there is a significant impairment in endothelial function with age (Taddei et al., 2000) and the regulation of blood flow is effected by hormones and body fat content (Elliot et al., 1999; Bungum et al., 1996). As age, sex and BMI are factors that could have an effect on vascular responses, matching the groups for these factors controls for their effect. The information related to age, sex and BMI was documented, so that median regression analysis could be completed to determine their importance as independent variables.

### 2.1.3 Smoking status

Participants smoking status was gained from all participants by self-report and, in the heavy smoker group only, this was confirmed by the measurement of urinary cotinine levels (Accutest Nicometer<sup>®</sup>, Jant Pharmacal Corp, USA). This is an immunoassay technique that provides a measurement of a stable metabolite of nicotine. Cotinine has a relatively long half-life of 10-40 hours and is a more sensitive and specific marker of smoking habit than carbon monoxide estimation (Murray et al., 1993). The Accutest<sup>®</sup>Nicometer<sup>®</sup> strip has monoclonal antibodies to cotinine coated to gold particles, so that cotinine in the sample binds to the antibodies on the gold particle. The number of occupied binding sites is a function of the amount of cotinine and thus the distance the gold migrates is directly related to the amount of cotinine in the sample.

The volunteers provided a urine sample, which was tested using the Accutest<sup>®</sup>Nicometer<sup>®</sup> strip according to the manufacturer's protocol. The results are expressed as a level, which corresponds to a concentration range for cotinine. The assigned ranges are shown in *Table 2.1*.

<i>Accutest<sup>®</sup>Nicometer<sup>®</sup></i> <i>Level</i>	<i>Expected Cotinine</i> <i>Range (ng/mL)</i>	<i>Smoking status</i>
0	0 – 100	Non Smoker Levels
1	100 – 250	Smoker Levels
2	250 – 1,000	Smoker Levels
3	1,000 – 2,000	Smoker Levels
4	2,000 – 5,000	Smoker Levels
5	5,000 – 10,000	Smoker Levels
6	> 10,000	Smoker Levels

**Table 2.1** A table to show the Accutest Nicometer<sup>®</sup> levels, the expected cotinine range and the corresponding smoking status.

### 2.1.4 Controlling variables

It is well known that many factors can affect skin blood flow and also LDF measurements. The variables of age, sex and BMI were controlled for by matching the different groups. The experimental conditions were kept as similar as possible for all studies. On arrival, the participants were asked to remain in a semi-recumbent position for 15 minutes to acclimatise and allowed for recovery from physical exercise. As ambient temperature effects skin blood flow, studies were

completed in a temperature-controlled room. Although the participants were asked to abstain from caffeine for 2 hours before the study, some were unable to comply, and blood caffeine levels were not tested to check for compliance. The smokers were originally asked to refrain from smoking for at least 2 hours before the study, but due to compliance issues in heavy smokers, this was reduced to only 1 hour. The heavy smokers had difficulties in refraining from smoking for the hour before the studies.

## **2.2 Skin blood flow measurement methods**

Various methods have been used to measure and compare skin blood flow responses. There are some simple methods such as LDI (Clough et al., 1998; Murray et al., 2009), LDF (Rossi et al., 2009, Debbabi et al., 2010) and transcutaneous oximetry (Bader and Gant, 1988; Svalestad et al., 2010). Photoplethysmography (Bergstrand et al., 2009) and capillaroscopy have also been used (*Table 2.2*).

The LDI is a non-contact device that enables the mapping of skin blood flux over an area of the skin surface. The laser beam is scanned across the skin surface using a moving mirror and the scattered light signal is analysed to give an image of blood flow over the area (Murray et al., 2004; Wright et al., 2006). The method of transcutaneous oxygen tension measurement involves the measurement of oxygen molecules transferred through the skin from capillaries and subcapillary plexuses. It requires the application of heat to the skin surface to enhance oxygen flow through the dermis otherwise the oxygen levels are difficult to measure (Colin and Saumet, 1996).

Capillaroscopy enables real-time visualisation of the capillaries in the skin and therefore is most sensitive for measurement nutritive skin blood flow (Bongard and Bounameaux, 1993; Wright et al., 2006). Historically, the nail-fold has been considered the optimal site to use capillaroscopy as the capillaries lie parallel to the skin surface, but recent developments in the equipment used has meant that other body sites can be interrogated (Wright et al., 2006). A further method to measure skin blood flow is photoplethysmography. This method measures changes in optical density in response to changes in blood volume in the tissue being sampled (Wright et al., 2006). The light is directed at the tissue, scattered, reflected and refracted and absorbed before reaching the detector; the amount of absorption depends on blood volume in the tissues (Wright et al., 2006). LDF provides a continuous, non-invasive, real-time measurement of blood flow in the microvasculature (Obeid et al., 1990) and has been used in the studies in this thesis. It has advantages over other methods in that it does not cause tissue trauma or disturb the microcirculation directly (Jan et al.,

2005). The blood flow in the arterioles, capillaries and venules is measured and LDF has high temporal resolution as measurements can be taken continuously. LDF is ideal for measurement of relative flow changes in the microvasculature, such as during heating or cooling or during and after ischaemia.

Method	Advantages	Disadvantages	References
Laser Doppler Fluximetry	Simple to use and non-invasive Sensitive detection of skin blood flow changes Can be used anywhere on skin Relatively cheap Spectral analysis can be completed on signal	Measurements only in arbitrary units High spatial variation Signal observed when blood flow stopped (BZ) Problems with movement artefact on the signal Potential effects of probe pressure	Obeid et al., 1990 Bongard and Bounameaux, 1993 Wardell et al., 1994 Bircher et al., 1994 Wright et al., 2006
Laser Doppler Imaging	Simple to use and non-invasive Non-contact device Automated analysis by software, reducing operator bias Good spatial resolution (wide field of vision) Can record patterns over skin area	Fewer research studies have used this Movement artefact effects present	Wardell et al., 1994 Wright et al., 2006
Transcutaneous oxygen measurements (electrochemical electrodes)	Simple to use Non-invasive Relatively cheap	Heater system needed to cause local hyperaemia Evaluates oxygenation in skin; not a direct measure of skin blood flow Factors can impair diffusion of oxygen towards the probe, such as local oedema and skin thickness. Not good spatial resolution	Bongard and Bounameaux, 1993 Wright et al., 2006
Capillaroscopy	Relatively simple to use and non-invasive Direct, objective evaluation of capillary bed Can be used at many skin sites Measure diameter, length, density of caps. Measures transit time through individual caps. Good spatial resolution	Restricted to measurement of nutritive portions of skin – not as much depth measured. Potentially some operator bias	Bongard and Bounameaux, 1993 Wright et al., 2006
Photoplethysmography	Simple to use Relatively cheap Free from operator bias	Limited spatial resolution Only assesses blood volume at single point	Wright et al., 2006

**Table 2.2** A critical analysis of the main non-invasive methods currently used to measure skin blood flow. They involve direct measures of blood flow, visualizing the vessels and also measurement of skin oxygen levels

### **2.2.1 Laser Doppler fluximetry (LDF)**

Since the 1970's, numerous studies using LDF to monitor the skin microcirculation have been published (Bongard and Bounameaux, 1993; Saumet et al., 1988). LDF has been shown to be an effective and reliable method for the measurement of blood flow in the microcirculation in medicine and microvascular research (Obeid et al., 1990). A description of the LDF technique can be found in the *Chapter 1, section 1.5.1*.

The LDF (DRT4 Moor Instruments Ltd, UK) used in the studies in this thesis has a wavelength of 785nm, 1mW, and the specific probe used for the loading study is a 0.5mm separation probe with temperature sensor (DP1-V2) (Moor Instruments Ltd). It has been suggested that the LDF measures to a depth of less than 1mm. A recent study has shown using Monte Carlo estimation that for a LDF probe with a fibre separation of 0.46mm, the depth of penetration measured is between 0.21-0.39mm (Larsson et al., 2002). The proportion of photons that reach depths greater than 0.4mm when using this probe was found to be 13.7% (Clough et al., 2009). Thus, the majority of the measurement is taken from epidermal and dermal tissue.

The pinhead LDF probe (VP12) used for the skin heating studies was positioned in the SHP1 heater probe (*Figure 2.3*) and attached to the SHO2™ skin heating unit. The pinhead probe has a short stainless steel tip of 12.7mm and diameter of 1.5mm. In order to improve the accuracy of the results using the LDF technique the same experimenter completed all the studies and the LDF probe was applied to the participants in the same way using a sticky-O ring to maintain its position. The LDF traces were analyzed by the same person.

### **2.2.2 Biological zero (BZ)**

A signal is observed from the LDF when blood circulation is stopped, called the Biological Zero (BZ). It is not related to tissue perfusion and Brownian motion of macromolecules may contribute to it (Bircher et al., 1994). The BZ was measured in a group of seven participants; a sphygmomanometer cuff was inflated to 200mmHg for two minutes to occlude forearm flow. The occluded flux was measured and the BZ was  $5.8 \pm 2.6$  AU (median  $\pm$  Interquartile Range (IQR)).

All methods used to induce an experimental flow perturbation, such as heating and loading the skin, may alter the BZ signal (Kernick et al., 1999). Although BZ should be measured under every experimental condition, it is not possible when responses are transient (Kernick et al., 1999). Therefore, it is not possible to know what the BZ is during heating or loading responses. Some

have suggested that BZ is not used in skin blood flow assessment as it causes the perfusion to be underestimated (Zhong et al., 1998).

### **2.2.3 Repeatability and coefficient of variance (CV) in the participants**

The day-to-day and site-to-site repeatability and coefficient of variance (CV) were measured from resting flux traces from a group of the non-smoking control participants involved in some of the studies in this thesis. The median within site and day to day CV for resting flux measured over 10 minutes in 7 of the non smoking participants were 15% and 12 % respectively. The CV of the spectral analysis of these resting flux traces can be found in *Chapter 5*.

## **2.3 Local skin loading and LDF protocol**

The response of the skin blood flow to external loading using LDF has been evaluated in several studies previously (*Chapter 1, section 1.5.2*) (Mayrovitz et al., 1997). The skin loading protocol attempts to consider the effect of pressure applied directly to the skin on skin blood flow.

### **2.3.1 Development of loading protocol**

The LDF probe used to measure skin blood flow is known to be very sensitive to any movement and it can result in artifact on the LDF trace. The effect of applying and removing the loads to the loading pan in the experimental set-up did cause some artifact to the LDF trace and efforts were made to reduce this to a minimum. A different loading application system was subsequently developed to try to overcome this, but this caused more potential artifact on the LDF probe during application of the loads and was also difficult to maintain its position on the participant. The final loading instruments and experimental set-up was identical to that used in a previous pilot study (Noble et al., 2003).

Skin blood flux was measured using LDF (DRT4, Moor Ltd., Axminster, UK) and a single point fluximeter probe. The probe head was mounted in a rigid plastic indenter which was 50 mm in diameter. The indenter was mounted vertically and supported by a cantilevered arm fixed to the side of the bed (*Figure 2.1*). This ensured that the LDF was recording flux in the central loaded area, where greatest loading occurs (Mayrovitz et al., 1997). The equipment used was borrowed for the purposes of this study from Professor Ian Swain (Salisbury).

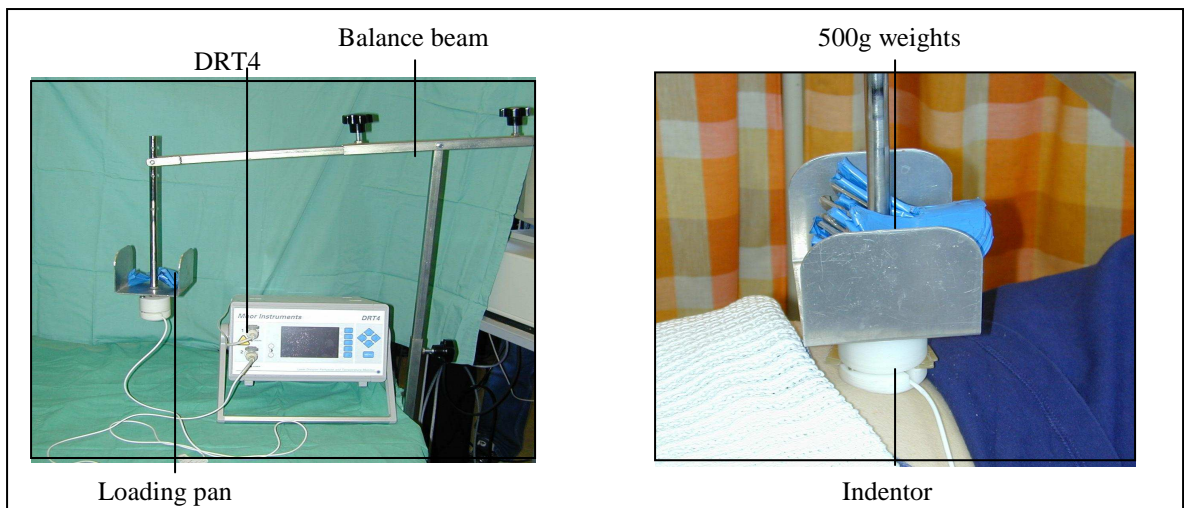


**Figure 2.1** Experimental equipment used in the skin loading studies including the DRT4 machine (Moore Ltd, Devon), LDF probe, balance beam, loading pan and indenter.

### 2.3.2 Protocol for local pressure loading study

The studies were completed in the temperature-controlled environment of the Wellcome Trust Clinical Research Facility (WTCRF). The volunteers gave their written informed consent to take part in the study. Their age, sex, height and weight were then recorded, a smoking history taken and a urine sample was collected. The participants remained in a sitting position on the hospital bed for 15 minutes to allow for acclimatisation.

The participant's forearm was positioned comfortably on a pillow at heart level with the volar surface exposed. The LDF probe, mounted within the indenter, was attached to the skin using a sticky-O ring. The resting flux was recorded, without any weights applied to the loading pan. There was continual recording of skin blood flow during the graduated application of pressure loading (500 g increments every 2 minutes up to a total of 2500g i.e. 25 N after 10 minutes). The load was then removed and the flux continued to be measured for at least ten minutes. The loading pattern used was similar to that used by Schubert and Fagrell (1989).

### 2.3.3 Parameters measured in loading studies

The cutaneous vascular response to loading was characterized by the following parameters, obtained from each experimental tracing. The measurements recorded are illustrated in *Figure 2.2*:

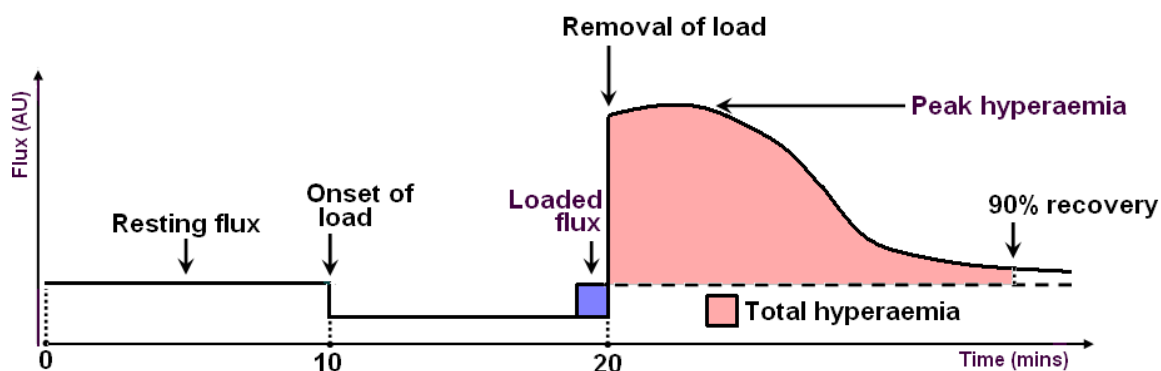


**Figure 2.2** A diagram to illustrate the parameters of the skin loading and off-loading induced reactive hyperaemia adapted from a diagram by Haggisawa et al. (1991)

**Resting flux** – mean flux over the 10 minute measurement period

**Loaded flux** – mean flux measured during the final 30 seconds of the loaded period, when all the loads had been applied.

**Maximum hyperaemia** – measured 3 seconds after the highest flux point is reached (as the initial spike was artefact) and a mean over 2 seconds was calculated.

**Area under response curve to 50% recovery** – the 50% recovery was calculated from the midway point between the maximum hyperaemia and the resting flux. The trapezoid method was used to calculate the area under the hyperaemia curve from off-loading to the point where the 50% recovery value is reached.

**Area under response curve to 90% recovery** - the 90% recovery was calculated and the trapezoid method was used to calculate the area under the hyperaemia curve from off-loading to the point where the 90% recovery value is reached.

#### **2.4 Local skin heating and LDF protocol**

There are now many published studies in which the cutaneous microcirculation has been evaluated by measurements of skin blood flow responses during local heating. The hyperaemic response to local skin heating is a well-characterized response. The local heat causes an initial local vasodilation response to a peak, followed by a prolonged plateau, which then gradually returns to resting flux levels.

Skin blood flow was measured using non-invasive LDF (DRT4, Moor Instruments Ltd, Axminster, UK). A programmable skin heater unit (SHO2), was used with the LDF. This measuring device is 3cm in diameter and contains a circular metal heating disk (1.1cm diameter), in the centre of which is a pin-headed optic probe (1.5mm diameter), which continuously measures blood flux (*Figure 2.3*).

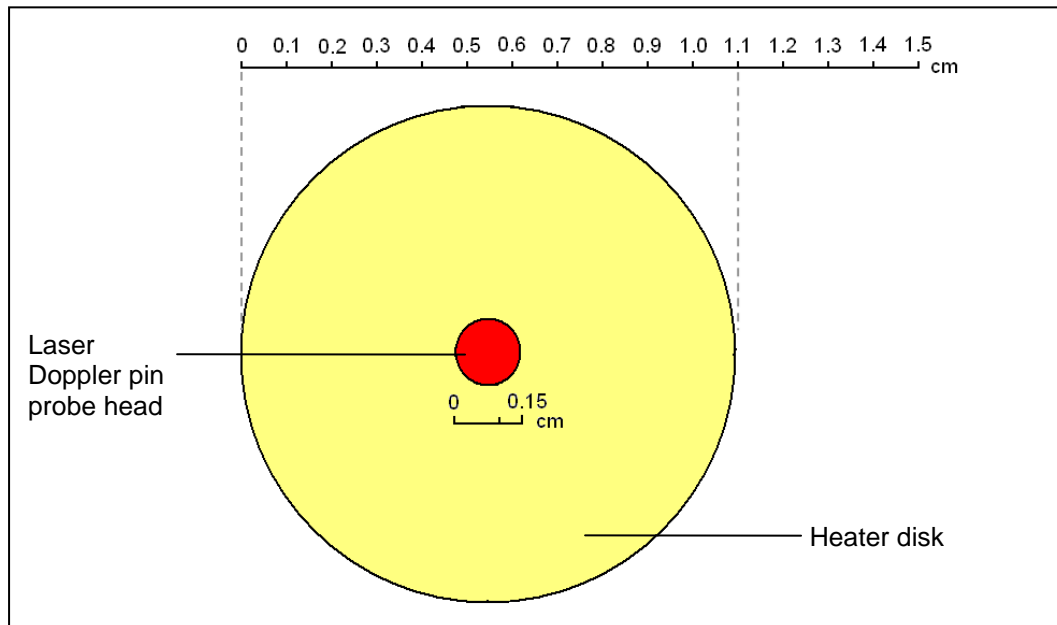


**Figure 2.3** A diagram to show the area of the laser Doppler fluximeter probe and heater that is in contact with the skin. The radius of the skin heater block is 5.5mm and the area of the heated section (red) is 95.1mm<sup>2</sup>. The pinhead laser Doppler probe has a diameter of 1.5mm.

#### 2.4.1 The local heating block at the forearm and sacrum

The local heating protocol was developed following consideration of previous research completed using the local heating response in participants. The temperature of 43 °C was used in order to produce a non-painful vasodilation response and the increase in temperature was completed at a fast enough rate to produce a biphasic response, with an initial axon reflex mediated vasodilation followed by a plateau region, which is considered to be NO-dependent. The studies were completed in the heavy smoker group initially, followed by the spectral analysis on this data. The length of resting and heating flux was then increased to 20 minutes, following advice from the engineering department, to improve the reliability of the spectral analysis and reduce the bias. The aim was to achieve the balance between increased data collection and patient comfort during the studies.

During the local heating studies, the temperature of the heating block was recorded continuously. The temperature of the heating block from the start of heating until approximately 15 minutes after the heater was turned off can be seen in *Figure 2.4*. The shape of the response is different at the 2 skin sites. The mean temperature at the sites immediately before the skin heating began was 28.9 and 33.3°C at the forearm and sacrum respectively. At the sacrum, the time taken to reach a mean temperature of 48.2°C was 78 seconds and at the forearm this was 95 seconds (*Figure 2.5*). At both sites, the rate of heating was around 0.2°C/second, which has been shown to result in a biphasic response (Houghton et al., 2006). A slower, incremental heating protocol of around 0.1°C/min has been shown to produce vasodilation as a result of NO mechanisms only (Houghton et al., 2006).

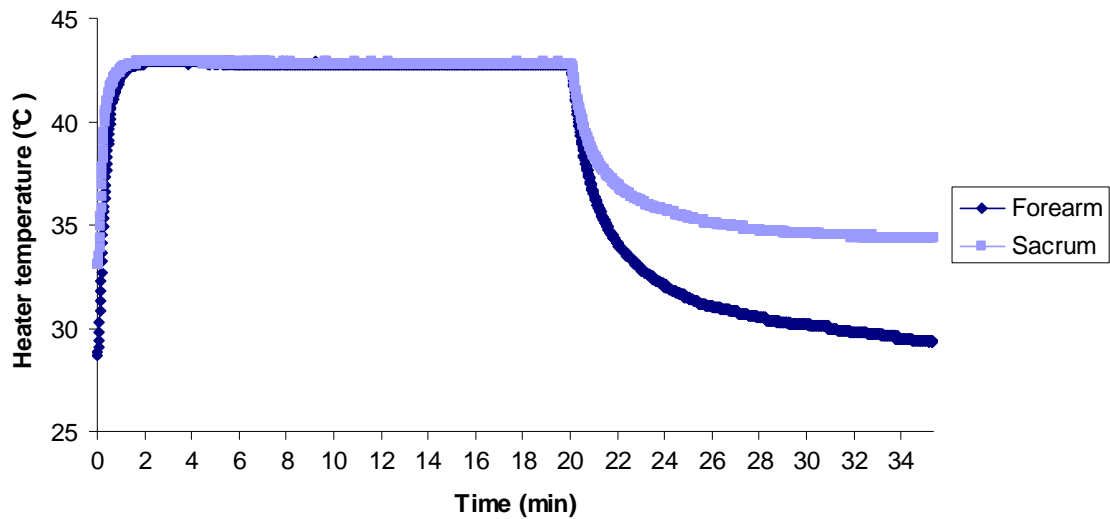


**Figure 2.4** A line graph to show the mean temperature of the heating block from the start of heating at the sacrum and forearm sites of 9 non-smoking control participants.

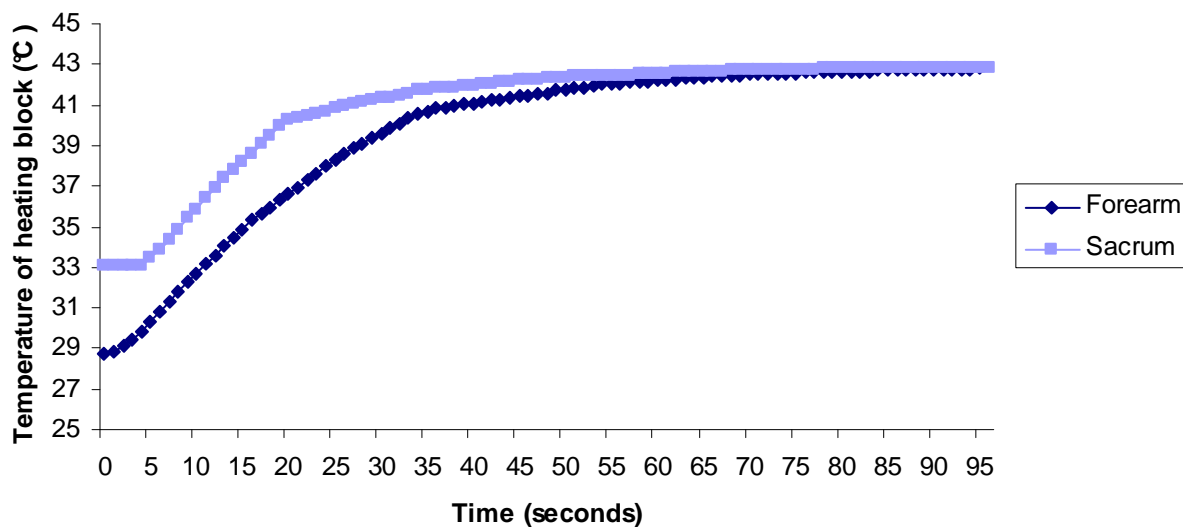


**Figure 2.5** A graph to show the median temperature of the heater block placed on the skin over the sacrum and volar surface of the forearm in 9 non-smoking control participants during the heating up phase. The temperature of the heater block before the heating began was significantly higher at the sacrum compared to the forearm ( $p=0.008$ ) analysed using the Wilcoxon paired test

#### 2.4.2 Protocol for local heating study

The studies were completed in the temperature-controlled environment of the WTCRF. The study was approved by the Southampton and South West Hampshire Joint Research Ethics Committee, approval number 211/01 and 138/01. The volunteers gave their written informed consent to take part in the study. Their age, sex, height and weight were then recorded and smoking history taken. A urine sample was taken from some of the participants to confirm their smoking history.

The participant remained in a sitting position on the hospital bed for approximately 15 minutes to allow for acclimatisation to room temperature. The study was completed at the forearm site and then, in some participants, also the sacrum site. The participant's forearm was positioned comfortably on a pillow at heart level with the volar surface exposed. The heater disk and LDF were attached to the arm using a sticky-O ring, so that it was flush to the skin surface.

#### *Length of measurements taken*

The protocol was initially completed in 8 heavy smokers and their matched controls and the skin blood flow was measured continuously throughout the studies. In these participants, the resting skin blood flow was measured for 10 minutes at the forearm. The skin was then heated up to 43°C

for 10 minutes and skin blood flux was measured during heating. The heater was then switched off and the skin blood flow was continuously measured further for approximately 30 minutes.

The volunteer was made comfortable in a prone position. The sacrum was exposed and the skin heater and LDF probe were attached using a sticky-O ring. The protocol then continued as for the forearm.

Previous studies have shown that local skin heating to 43° C for 60 minutes results in a maximal vasodilation response (Martin et al., 1995; Minson et al., 2001). The skin heater was set to 43° C for 10 minutes (heavy smokers) or 20 minutes (light/moderate (LM) smokers) in this study, inducing a sub-maximal vasodilation. A previous study showed that when skin is heated to 42° C, the skin temperature was only ~40° C at the heating probe-skin surface interface (Minson et al., 2001). The actual skin temperature will be approximately 2-3° C lower than the temperature setting.

The data from the studies in the heavy smokers was analyzed and further spectral analysis was completed. In consideration of these results and in order to improve the accuracy of the spectral analysis, the length of measurements was increased in the studies involving the LM smokers and their controls. The resting skin blood flow was measured for 20 minutes (increased from 10 minutes) in these participants and the skin was heated to 43° C for 20 minutes (increased from 10 minutes) in these participants. The skin blood flow was measured for a further 30 minutes after the skin heater was switched off in these participants.

#### **2.4.3 Parameters measured in local heating studies**

The following parameters were measured from the LDF traces from the local heating studies (*Figure 2.6*). The parameter calculations can be found in *Appendix 1*.

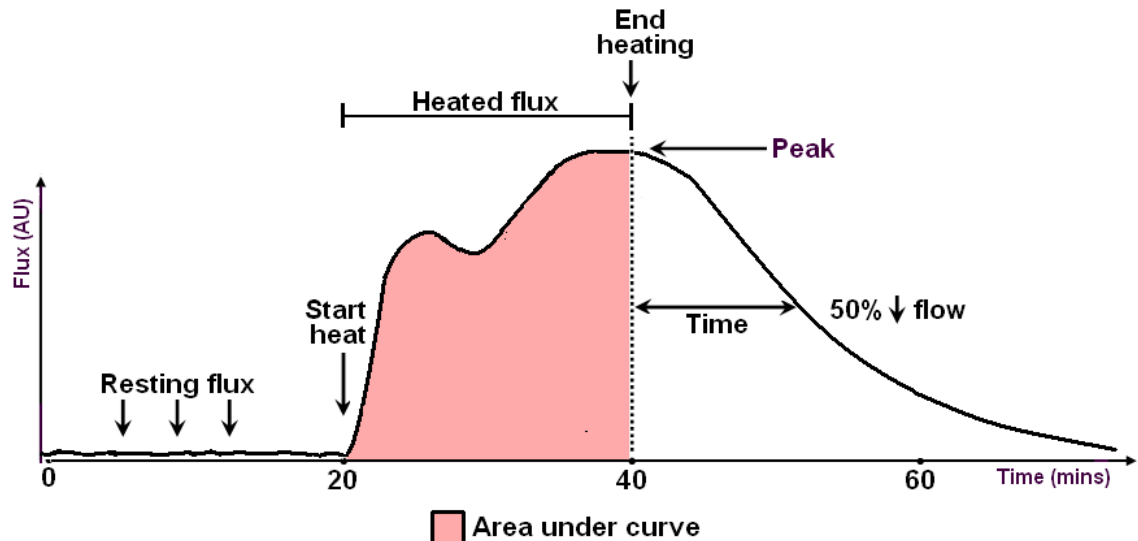


**Figure 2.6** A diagram to illustrate the parameters of the local heating response that were measured.

**Resting flux** - measured over the 10 or 20 minute period immediately prior to heating

**Peak hyperaemic response after skin heating to 43 °C** – the highest flux reached (usually during the plateau part of the response) (*Appendix 1*).

**Mean heated flux** – the mean flux during 10 or 20 min heating (*Appendix 1*)

**Mean heated flux minus the resting flux** – change in flux from resting to heating.

**Duration of hyperaemic response** - time from starting local heating to recovery of flux to resting flux levels (seconds)

**Time to recovery** – time from peak to recovery

**Total hyperaemic response** - area under the hyperaemic response flux curve (AU.second) (*Appendix 1*).

The skin blood flux response to local heating caused a 2-phase response in most participants; an initial steep rise in flux followed by a nadir and then plateau vasodilation. This is similar to previous studies. The initial peak varied in the amount it was distinct from the plateau vasodilation and it was difficult to determine a repeatable method to measure this for each of the LDF traces in the studies in this thesis (*Figure 4.3*). In some cases, this was a pause in the upward rise in flux (*Figure 4.3a*) and in others a definite initial peak (*Figure 4.3b*). This variation was within the groups and was not an observable difference between the forearm and sacrum sites. Thus, for the purposes of this study, the maximum flux, average heated flux and area under the curve during heating were used to define the local heating response. The short, non-stationary LDF trace during the initial peak also made it difficult to complete the spectral analysis on that section of trace separately.

#### 2.4.4 Local nature of the heating response

The local nature of the heating response was investigated in 10 of the participants involved in the studies in this thesis (7 non-smokers and 3 smokers). Two LDF probes were placed less than 5cm apart on the volar surface of the forearm and resting flux was measured for 20 minutes in both probes. The skin was heated to 43°C directly over one of the probes (randomly assigned) and no heat was applied to the adjacent probe. The results showed that the resting flux at the site directly over the local heating challenge and adjacent to it were  $9.2 \pm 2.5\text{AU}$  and  $10.4 \pm 2.5\text{AU}$  (median  $\pm$  IQR) respectively. The flux during the local heating challenge was  $174.0 \pm 83.5\text{AU}$  directly over the local heating site and  $11.0 \pm 5.1\text{AU}$  at the site adjacent to it. There was no change in the flux measured at the adjacent site, but a significant increase in flux at the heated site (*Figure 2.7*).

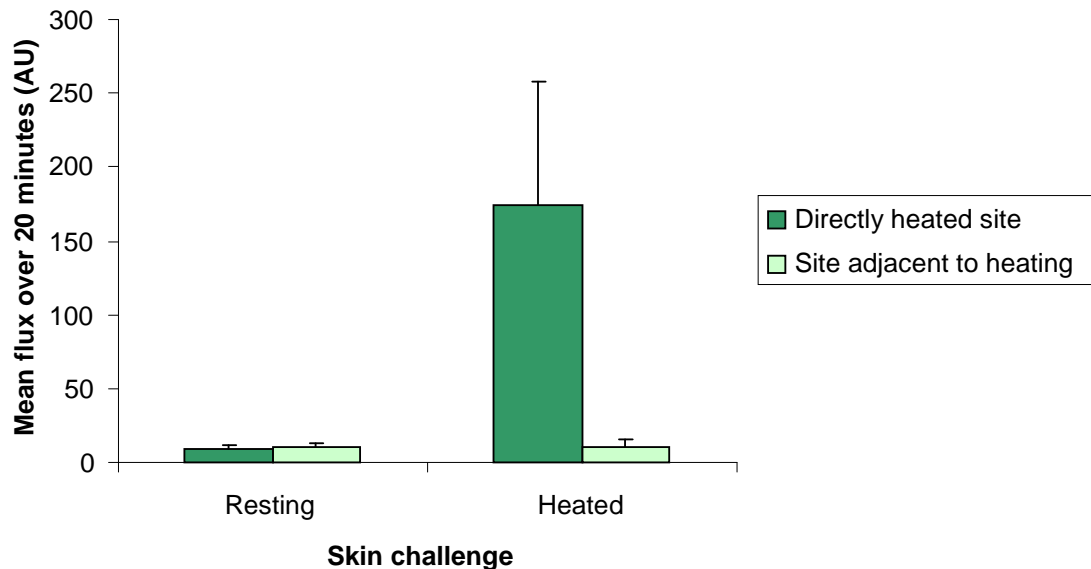


*Figure 2.7* A bar graph to show the LDF flux at rest and then during the local heating response measured directly under the heating challenge (dark green) and adjacent to it (light green) at the volar forearm of 10 participants. The 2 LDF probes were placed less than 5 cm apart on the forearm surface.

#### 2.5 Spectral analysis methods

The LDF signal contains oscillations at different frequencies which can be analysed using spectral analysis and one of the methods used for this is the FFT. A transform is any fixed procedure that

changes one chunk of data into another chunk of data but in a different form. The input signal contains the signal being decomposed; the LDF time domain signal. This produces two output signals containing the amplitudes of the component cosine and sine waves. All the scaled sine and cosine waves added together can produce the time domain signal.

### **2.5.1 The LDF signal**

The LDF signal from the skin is composed of a sum of sinusoidal oscillations, which oscillate at different frequencies. The raw LDF signal gained from the skin is filtered and processed in certain ways within the DRT4 machine and this has important implications for the spectral analysis of the signal using an FFT.

The raw LDF signal is processed within the DRT4 by passage through a band-pass filter set at frequency range 20Hz to 14.9kHz. This processes the raw LDF signal to produce a low frequency Flux signal. The derived Flux signal then goes through a second low pass filter at around 20Hz and is then sampled by A/D conversion and is displayed on the screen. The individual samples are converted into a digital format via the quantizer (Moor Instruments, Ltd).

#### ***Sampling rate of LDF signal***

As the sampling rate increases, the digital signal provides an increasingly improved approximation of the continuous signal. So that there is not loss of information, the digital signal must comply with sampling theorem, which states that the sampling rate must be more than twice the maximum frequency present in the signal. This is important in signal processing to prevent aliasing; this is when oscillations within the signal move and can be shown at a different frequency within the spectrum (Burrus et al., 1994; University of Southampton Course notes, 2005). The Flux signal is passed through a low pass filter at approximately 20Hz in the DRT4, which means that the maximum frequency in the signal is at 20Hz. The signal is then sampled at 40Hz to comply with sampling theorem and ensure that aliasing is prevented.

#### ***LDF signal properties***

The assumption in signal processing is that the signal can be described as stationary and ergodic. The signal is stationary if it does not vary its statistical properties with time and ergodic if the recorded signal is representative of the whole process (Burrus et al., 1994). When analysing physiological signals, such as skin blood flux, this can only be an approximate assumption. In this thesis, the signal processing is completed on the resting LDF signal alone and then on the heated

LDF signal alone, so that the stationarity (constant variance over time) and ergodicity (representative signal) of the signal is optimised.

### **2.5.2 The Power Spectral Density (PSD) of the LDF signal**

The spectral analysis of the LDF data in this thesis was completed with the help and guidance of Dr David Simpson (Institute of Sound and Vibration Research (ISVR), University of Southampton) using the statistical package Matlab<sup>®</sup> version 7, student version, with additional signal processing toolbox.

The PSD is an estimate of the distribution of signal power over the frequency bands in the signal. The PSD of a random signal, which includes all physiological signals, can only be an estimate. All the data would have to be available for the true spectrum to be calculated; as the LDF signal is recorded and then digitised at a certain sampling frequency, the spectrum can only be estimated.

#### ***Frequency domain***

LDF signals are composed of a sum of sinusoidal oscillations, which oscillate at different frequencies. The FFT enables demonstration of a signal in its different frequency bands. Studies have shown that there are 5 different frequency bands within the LDF signal which relate to certain aspects of skin blood flow control. The frequencies around 0.01Hz, 0.04Hz, 0.1Hz, 0.4Hz and 1Hz have been shown to relate to endothelium, neurogenic, myogenic, respiratory and cardiac related mechanisms respectively (Kvernmo et al., 1999) (*Chapter 1, Section 1.5.3*). The band widths for each frequency used for the purposes of this thesis were similar to previous studies (Rossi et al., 2006b; Clough et al., 2009). These bandwidths are: 0.01Hz (0.008-0.2Hz), 0.04Hz (0.2-0.5Hz), 0.1Hz (0.5-0.15Hz), 0.4Hz (0.15-0.4) and 1Hz (0.4-2.0Hz).

#### ***Calculation of the PSD using a fast Fourier transform (FFT)***

The simplest method of calculating the PSD is the periodogram; this is the square of the FFT signal. However, the periodogram is not a good estimate, as it contains a large proportion of random error. This random error cannot be removed by increasing the number of data samples.

The PSD estimation using the Welch method (non-parametric) is the most commonly used method. The digitised sequence of numbers (N samples) is divided into L windows of data (length M samples) that overlap; the periodogram of each window is then calculated using the FFT. The average of all the periodograms is then used as an estimate of the PSD. The power (AU<sup>2</sup>) of the

signal is equal to the area under the PSD curve and the PSD is given in units  $\text{AU}^2/\text{Hz}$ . There are various different window types that can be used with the Welch method of PSD estimation.

The random error in the PSD is dependent on the standard deviation between the estimates. The standard deviation, and therefore also the random error, can be reduced by increasing the number of windows. The bias error depends on the frequency resolution of the estimate. The frequency resolution is equal to the sampling rate divided by the window length  $M$ . The frequency resolution is improved and the bias error reduced by increasing the length of the windows. Therefore, a balance needs to be gained between increasing the number of windows, but at the same time reducing their length, which would reduce the random error, but this would at the same time increase the bias error.

### ***The data manipulation for signal processing and PSD estimation***

The LDF signal was sampled at 40Hz and saved as a text file in the digitised format. This was then saved as an excel file and separated into the baseline Flux section and the Flux during heating section. This was 600 seconds or 24001 data points in length for the heavy smoker study and 1200 seconds or 48002 data points in length for the light smoker study.

The data sections were loaded into Matlab<sup>®</sup> version 7, student version, with additional signal processing toolbox. The mean value was then removed from the signal; making the mean of the signal equal to zero (*Figure 2.8 a2 and b2*). If not removed, the mean Flux of the signal would appear on the power spectrum as a high power frequency at 0Hz and distort the very low frequencies around zero.

The gradient within the heated flux signal following the start of heating would also significantly distort the very low frequencies around zero, so the entire signal also needed to be detrended. The signals were detrended at several powers between 4 and 20 to consider the effectiveness of the different orders of detrend in removing the mean value and the gradient from the signal. The effect the detrend order had on the low frequency components of the signal was also considered. The results show that there is no added benefit in detrending to a power greater than 10. The LDF signals were detrended to a power of 10 in the final analysis (*Table 2.3*).

Order of detrend	Absolute power 0 – 0.2Hz (AU <sup>2</sup> )	Power ~0.01Hz (AU <sup>2</sup> )	Power ~0.04Hz (AU <sup>2</sup> )	Power ~0.1Hz (AU <sup>2</sup> )
4	30.65	3.39	6.25	9.3
8	24.80	2.97	6.27	9.3
10	24.45	2.72	6.27	9.3
15	23	2.51	6.27	9.3
20	24.9	2.4	6.23	9.3

**Table 2.3** A table showing the median absolute power and power of the low frequency bands from 16 volunteers, 8 smokers and 8 non-smokers, with the signal de-trended by an order of 4, 8, 10, 15 and 20.

The de-trending of the heated Flux signal was improved by removing the initial 100 seconds from the signal. The initial 100 seconds contains the sharp increase in flux following onset of local heating and this gradient was difficult to remove from the signal with the de-trend program. An LDF signal that has been de-trended with and without the initial 100 seconds removed can be seen in *Figure 2.8*. The resting and heated Flux sections were de-trended in the same way; both to the power of 10 and both with the initial 100 seconds removed. Therefore, the length of the files analysed in the heavy smoker study were 500 seconds or 20001 data points and in the LM smoker study they were 1100 seconds or 44001 data points.

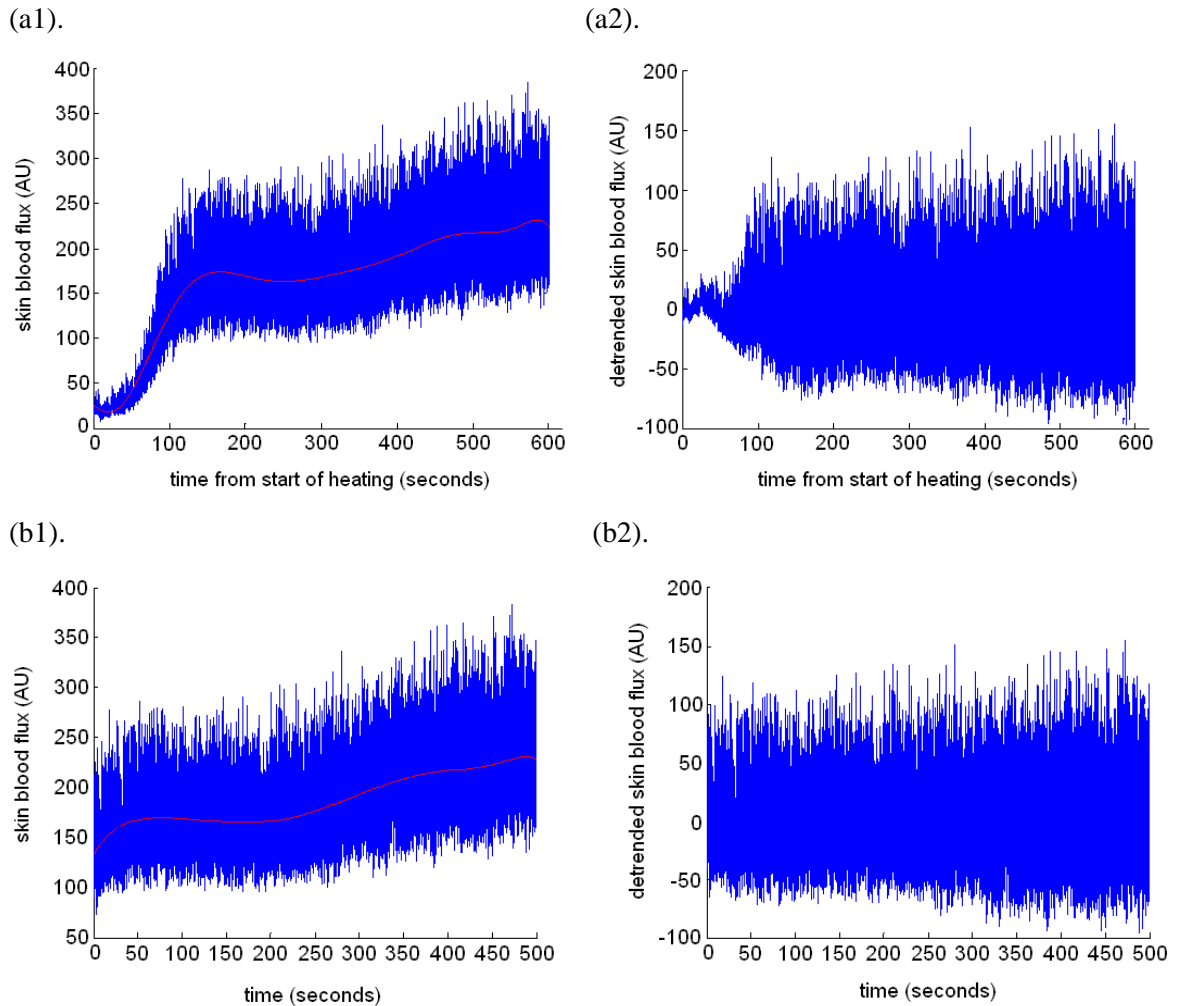


**Figure 2.8** Graph (a1) shows an example of a 600 second signal from a non-smoker volunteer and (a2) is the resultant de-trended signal. Graph (b1) shows the LDF signal from the same volunteer with the initial 100 seconds of the Flux following initiation of heating removed and (b2) shows the result of de-trending that signal.

### 2.5.3 Protocol for spectral analysis: Power Spectral Density (PSD) estimate using FFT (the Welch method)

#### *Heavy smokers and matched non-smoking controls*

The PSD of the LDF signal in the heavy smokers was estimated using the Welch method. The 500 seconds of data or 20001 data points (N) was separated into windows of length 250 seconds (10001 data points) (M) and overlap 50%. The Hanning window was used for the calculations. The number of windows (L) in this analysis was 5 (Equation 2.1). The frequency resolution of the signal is 0.004Hz, which is sufficient to measure the power of the low frequencies around 0.01Hz (Equation 2.2).

$$(L) = (2N/M)+1$$

**Equation 2.1** An equation to calculate the number of windows to be used in the Welch method of PSD analysis, where L is the number of windows, N is the number of data points and M is the window length

$$\text{Frequency resolution} = fs/M$$

**Equation 2.2** An equation to calculate the frequency resolution of the signal, where fs is the sampling rate and M is the window length.

The PSD was calculated over the frequencies 0 - 20Hz. The maximum frequency present in the signal is equal to the half the sampling rate, 20Hz. The program for calculation of the PSD and the function required for that program can be found in *Appendix 3*. The estimated PSD could be saved as an image (*Appendix 3*) and as text, in excel format (*Appendix 3*). The power can be calculated from the PSD using the area under the curve (AUC); this is approximated by integration using the trapezoidal method.

#### ***Light smokers and matched non-smoking controls***

In the LM smokers study, the experimental protocol was changed so that the LDF signal was recorded for 20 minutes at rest and the local heating stimulus to 43°C was applied for 20 minutes, while the flux was continuously measured. The length of data collection was increased to reduce the random error and the bias error within the PSD estimate. As with the heavy smoker study, the initial 100 seconds was removed from the resting and heated Flux data to give 1100 second lengths of data and 44001 data points. The 1100 seconds or 44001 data points (N) was separated into windows of length 400 seconds (M) and overlap 50%. The Hanning window was used for the calculations. The number of windows using the Welch method for PSD estimation was 6 (Equation 2.2), so that there was more windows to reduce the random error. The frequency resolution was 0.0025Hz, so improved resolution to reduce bias error. The Matlab® programs used to calculate the PSD in the light smoker data can be found in *Appendix 3*.

## **2.6 Data analysis and statistical methods**

### **2.6.1 Sample size**

#### **Local skin loading studies**

Previous data had shown that a fall in flux response of 25% with 80% power and significance at  $p < 0.05$  was detectable with a sample size of 15 participants. However, due to the difficulties with the loading apparatus in the group of patients involved in this thesis, many of the participants could not be included, and a sample of 8 was the final sample size included.

#### **Local heating studies**

##### ***Comparing sacrum and forearm sites***

In order to determine the sample size required when comparing the sacrum and forearm skin sites in the same individual, a sample of 4 matched pairs was used. The data used to determine sample size was the maximum hyperaemia during 20 minutes local heating of the forearm skin and the sacrum skin to 43°C in these 4 participants.

A web based power calculator was used entitled: 'Find statistical considerations for a crossover study where the outcome is a measurement' (Schoenfeld, 1995) and can be found at the following web address: [http://hedwig.mgh.harvard.edu/sample\\_size/size.html#minimal](http://hedwig.mgh.harvard.edu/sample_size/size.html#minimal)

The results of the power calculations showed that with a sample size of 7, the probability is 87% that the study will detect a difference at a 2 sided 5% significance level, if the true difference between the site measurements is 107.2AU. This is based on the assumption that the standard deviation of the difference in the 2 sites is 75.5.

##### ***Heavy smokers and controls***

The previous pilot study involving loading the skin of light smokers and matched controls was powered for 9 matched pairs (Noble et al., 2003). With heavy smokers more variability was expected, but also greater differences. There were originally 10 in the sample, but 2 participants were later excluded because of vasoactive medications.

### ***Light/moderate smokers and controls***

In order to determine the sample size required when comparing light smokers and non-smoking controls, a sample of 3 matched pairs was used. The data used to determine sample size was the maximum hyperaemia during 20 minutes local heating of the forearm skin to 43°C in these 3 participants.

A web based power calculator was used entitled: 'Inference for means: comparing 2 independent samples' and can be found at the following web address:

<http://www.stat.ubc.ca/~rollin/stats/ssize/n2.html>. The sample size calculations are based on normal distributions.

The results of the power calculations showed that with a desired power of 80% and  $p < 0.05$ , a sample size of 15 would be required and with a desired power of 90% and  $p < 0.05$ , a sample size of 20 would be required.

### **2.6.2 Statistics**

The data in the studies in this thesis are treated as non-normal. In most of the studies the sample sizes are small and the results skewed; although the LM smoker population has a sample size totalling 40, the Shapiro-Wilk test for normality (SWILK) (Stata version 9.0) and frequency histograms showed the data to be skewed and thus non-normal.

#### ***Swilk Test of Normality***

The Shapiro-Wilk W test for normality (known as the SWILK test in the Stata (version 9.0) statistics package), tests the null hypothesis that a sample came from a normally distributed population. The test gives a W statistic and if this is too small the null hypothesis can be rejected.

The statistics package for the social sciences (SPSS) version 14.0 was used for all of the statistical analysis in this thesis, apart from the median regression analysis. Throughout the thesis, the average for the group data is expressed by the median and the spread of the data by the IQR. The statistical analysis between the smokers and non-smokers was completed using the Mann Whitney U (MWU) test and the statistical analysis within the same individual, comparing sacrum and forearm responses or resting and heating responses was completed using the Wilcoxon paired test. There was a statistically significant difference where  $p < 0.05$ .

The median regression analysis included in this thesis was completed using the data analysis and statistical software package, Stata version 9.0, and with the help of Dr Peter Nicholls (University of Southampton).

### **2.6.3 Graphical representation**

In this thesis, the bar graphs show medians with error bars representing plus IQR.

In this thesis, the line graphs are periodograms produced by Matlab<sup>®</sup> software and show the PSD over a range of frequencies.

### **2.7 Layout of the results chapters**

An overview of the content of the individual studies in this thesis is presented in *Figure 2.9*

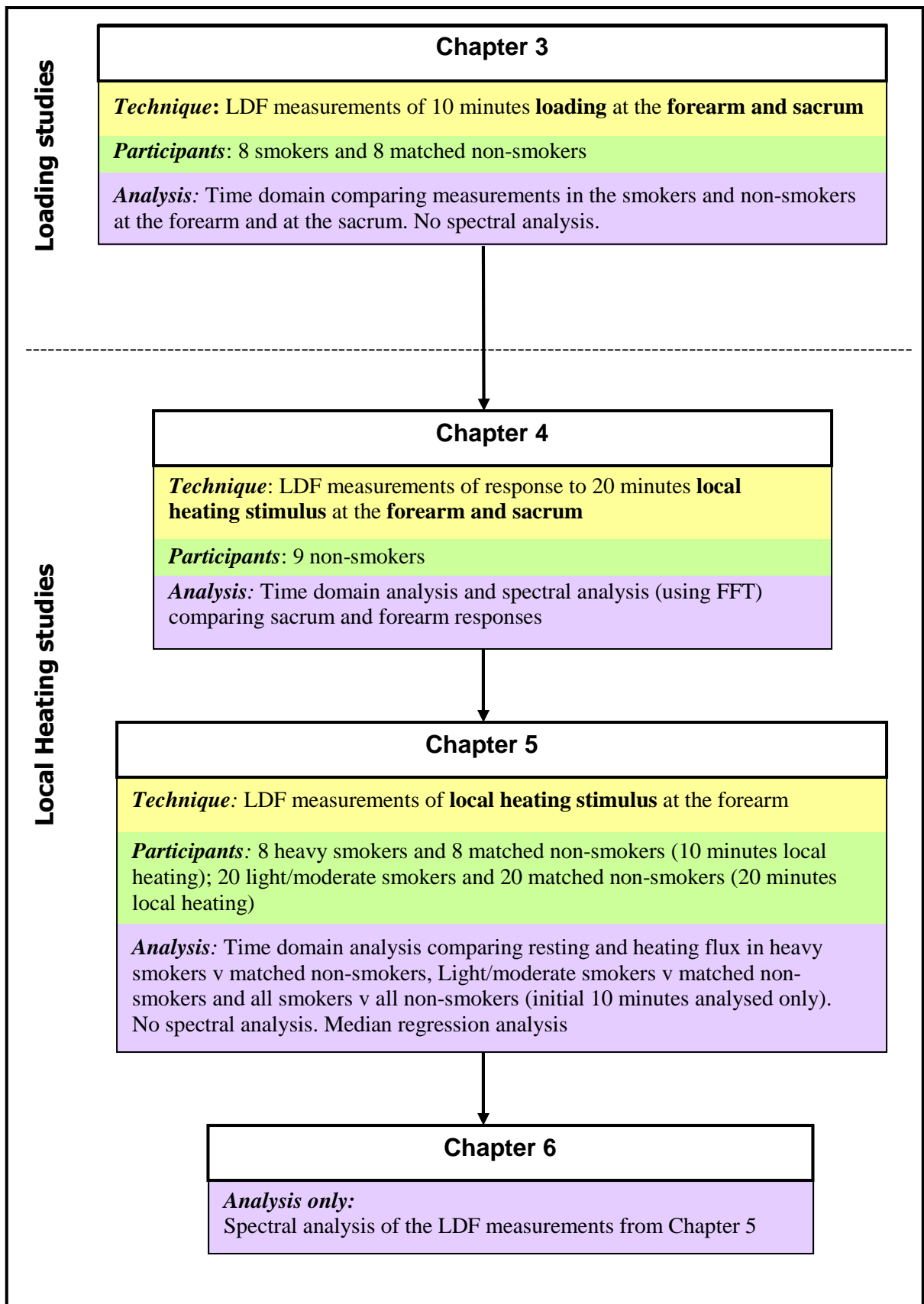


**Figure 2.9** A schematic diagram showing a summary of the content of each of the experimental chapters contained within this thesis.

## **Chapter 3**

### **Skin blood flow response to loading the skin in heavy smokers and non-smokers**

### **3.1 Introduction**

The problem of pressure ulcer development in patients both in hospital and the community remains ever present. Although much research into risk assessment and prevention has been undertaken, pressure ulcers continue to develop in patients in all health care settings. Pressure ulcers are a huge challenge to health care professionals, who face the task of patient risk assessment, prevention and treatment.

Much of the research in this field has focussed on the external forces on the skin that cause damage, such as pressure, friction and shear. Although these are important causes of pressure ulceration, the functioning of the skin microcirculation is a directly relevant measure of skin health due to its pivotal role in maintaining skin health (Brienza et al., 2005). The skin needs oxygen and nutrients via the vasculature to remain healthy; any disruption to this can cause skin breakdown and pressure ulcer development.

Over the last few decades, many studies both in humans and animals have investigated the effects of skin loading, and the resultant blood vessel occlusion, on the cutaneous microcirculation. The rapid increase in blood flow, the RH, following removal of the load has also had much attention. The RH response is considered to be a protective response, in which the ischaemic tissue is quickly re-established with oxygen and nutrients and waste is removed (Xakellis et al., 1993; Mayrovitz et al., 1999). The RH response to a transient pressure load has been shown to be reduced in the elderly (Schubert and Fagrell, 1991), hypotensive patients (Schubert, 1991) and patients with SCI (Sae-Sia et al., 2007).

The reperfusion of tissue during the RH response may be part of the pathology of pressure ulcer formation. A study involving laboratory animals used a computer controlled device to apply 100N pressure to the skin for 2 hours, followed by the collection of biopsy's from the loaded site for histological examination. It was found that the specimens collected immediately following cessation of pressure showed no damage and the first signs of pathology were found at least 2 hours after the pressure was removed. This would suggest that reperfusion into the ischaemic area is a contributing factor in the damage that occurs (Houwing et al., 2000).

Although, there are risk factors that are thought to make an individual more susceptible to the effects of pressure on the skin, more research is needed to demonstrate this. Cigarette smoking may increase the risk of pressure damage due to effects on the skin microcirculation. It is included in some of the risk assessments used by health professionals to assess patients' risk of pressure

damage. A recent study showed a relationship between cigarette smoking and pressure ulcer development; in a sample of participants with SCI, as well as diabetes, injury duration and depressive symptoms, cigarette smoking was significantly associated with the patient report of one or more pressure ulcers (Smith et al., 2008).

Research studies have also shown specific effects of smoking on the RH response to local pressure application. In a study using tissue reflectance spectroscopy, it was shown that smokers had a reduced RH response following 10 minutes of 50mmHg pressure applied to the patellar tendon (Sprigle et al., 2002). However, this study involved 12 smokers and 76 non-smokers, and the main aim of the study was to determine the effect of gender, age, skin pigmentation and diabetes. In another pilot study, using identical apparatus to the studies described in this chapter, the RH response to loading at the sacrum in a group of light smokers and non-smoking controls were compared. There was a significant attenuation in the RH response to loading in the light smokers compared to the non-smoking controls (Noble et al., 2003). As far as it has been possible to ascertain, there have been no studies to investigate skin blood flow response to external pressure application in participants that smoke heavily.

### **3.2 Hypothesis**

The reactive hyperaemic response in the skin microcirculation following removal of a load will be significantly attenuated in heavy smokers compared to non-smokers at both the forearm and sacrum skin sites measured using LDF.

### **3.3 Objectives**

- To measure, using LDF, vascular responses to a loading stimulus in the forearm and sacrum skin of heavy smokers and non-smokers matched for age, sex and BMI.
- To determine whether there are any differences in responses in the heavy smokers compared to the matched non-smokers in the same way they were in the previous pilot study in light smokers (Noble et al., 2003).

### 3.4 Methods

#### 3.4.1 Participants

Although loading studies were completed on a total of 12 smokers and 15 non-smoker controls at the forearm and sacrum, a number of the participants were excluded for matching purposes and due to high levels of movement artifact on LDF traces. The artifact was caused by both participant discomfort and movement of the apparatus during the experimental protocol. Only data from eight matched pairs could be analysed at the forearm and sacrum. The background information relating to the participants is summarised in *Table 3.1*.

<b>Parameter</b>	<b>Control group (n=8)</b>	<b>Smokers (n=8)</b>
<b>Age (years)</b>	38.8 ± 8.8 (30 – 51)	35.3 ± 8.0 (28 – 44)
<b>Sex</b>	7 females / 1 male	7 females / 1 male
<b>Body Mass Index (kg/m<sup>2</sup>)</b>	24.1 ± 4.1 (17.1 – 30.4)	22.6 ± 5.7 (17.5 – 34.1)
<b>Mean Arterial Pressure (mmHg)</b>	82.1 ± 12.3 (63 – 97)	85.1 ± 10.0 (75 – 97)

**Table 3.1** The age, sex, BMI and MAP of the heavy smokers and their matched control participants (n=8 pairs). The data shown is mean ± standard deviation (range) for the smokers and non-smokers. The groups were matched in terms of age, sex and body mass index. The BMI was calculated as [weight (kg)/(height (m))<sup>2</sup>]. The mean arterial pressure was calculated as [(2\*diastolic BP) + systolic BP]/3.

The smokers had smoked for 22.1 ± 13.4 (10-50) packyears. (*Packyears = number packs per day x number of years smoked for*). The control group were all non-smokers.

#### 3.4.2 Summary Protocol

The skin loading protocol has been described in general terms in *Chapter 2, section 2.3*. The specific protocol for the loading studies is as follows (*Figure 3.1*):

The study participants were made comfortable in a head-up tilt position on a hospital mattress, with their arm maintained at heart level on a pillow. They acclimatised to room temperature for 10 - 15

minutes before the skin blood flow measurements began. The loading apparatus was identical to that used in a previous pilot study in light smokers (Noble et al., 2003) (*Chapter 2, section 2.3*). The balance beam ensured that the load was applied perpendicular to the skin to exclude shear forces. The laser Doppler probe, mounted within the indenter, was attached to the skin using a sticky-O ring. The resting skin blood flux was recorded, without any weights applied to the loading pan. Skin blood flux during stepped application of pressure (500 g increments every 2 minutes up to a total of 2500 g i.e. 25 N after 10 minutes) was continuously recorded. The load was then removed and skin blood flow continued to be measured for at least ten minutes. The loading pattern used was similar to that used by Schubert and Fagrell (1989). The above protocol was then completed at the skin site of the sacrum.

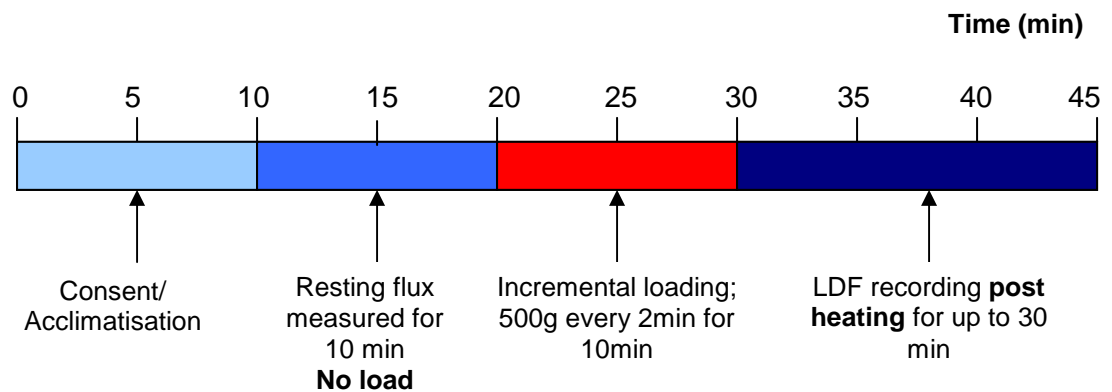


**Figure 3.1** A diagram to show the timeline of events occurring within the loading study protocol

The cutaneous vascular response to loading was characterized by the following parameters, obtained from each experimental tracing using the manufacturer’s software. The measurements recorded can be found in *Figure 2.2* (see *Chapter 2 section 2.3.3* for definition of parameters).

### 3.4.3 Statistics

#### *Statistical analysis*

The data in this chapter is considered to be non-normal; the sample size is small and the results skewed. The average for the group data is quoted by the median and the spread of the data by the interquartile range (IQR). The data are quoted to 1 decimal place.

The statistical analysis to compare the heavy smoker group to the non-smokers was completed using the statistics package SPSS. The MWU test was used to test for differences between the groups and there was considered to be a statistically significant difference where  $p < 0.05$ . The

correlations within the data were measured using the Spearman Rho test. In this chapter the data is represented graphically in the form of bar graphs; the bars represent the median and the error bars represent the IQR.

### 3.5 Results

In a published pilot study, Noble et al. (2003) showed that the hyperaemic response to a loading stimulus was significantly reduced at the sacrum of light smokers compared to their matched controls. We used the same loading apparatus to investigate the effect of loading and unloading on the skin blood flow response in a group of heavy smokers. An example of a LDF trace measured at the forearm of a study participant can be found in *Figure 3.2*.

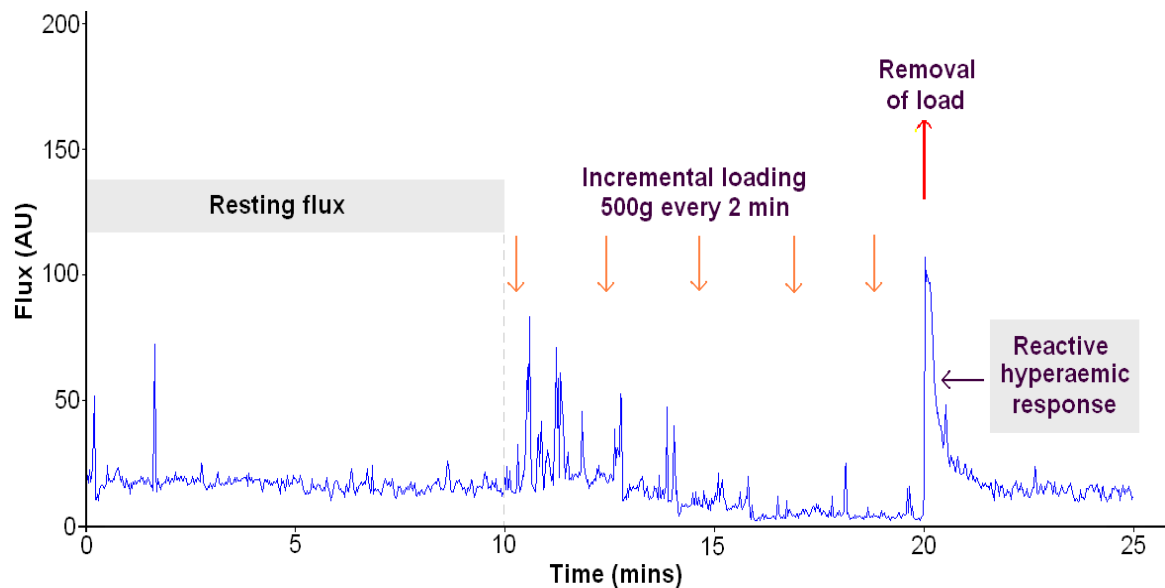


**Figure 3.2** An image of the LDF trace from a loading study at the forearm of a participant. The resting flux was measured for 10 minutes, followed by 10 minutes of incremental loading (identified on the figure by the thin arrows). The total load was 2500g. The load is then removed (thick arrow) the RH response can be seen on the LDF trace and then recording continued for a further 10 minutes. The spikes in the LDF trace are either movement artifact from movement by the participant or movement of the apparatus when the loads are placed onto the loading pan.

### 3.5.1 Summary of the results

The studies in this chapter have shown that the application of gradually applied loads caused a reduction in skin blood flux at the forearm in the non-smokers and heavy smokers; the fall in flux was  $39 \pm 69\%$  and  $58 \pm 59\%$  (median  $\pm$  IQR) in the non-smokers and heavy smokers respectively. The loaded flux tended to be lower in the heavy smoker group, but the results were highly variable in both groups and the difference was not significant. There was no significant difference in the RH response following the removal of the load in the heavy smokers compared with the non-smokers, and this was also highly variable. The variability in the blood flow occlusion caused by the 2500g load would be expected to result in similar variability in the ensuing RH response. The studies at the sacrum site showed similar trends in loading and RH responses and also demonstrated no differences between the heavy smokers and non-smokers.

The participants in both the smoking and non-smoking groups in the study had a broad range of BMI, which may be the reason for the variability in both the loaded flux and the hyperaemic responses in this study (the range of BMI's for the control group was 17.1 – 30.4 and for heavy smokers was 17.5 – 34.1kg/m<sup>2</sup>). The results showed significant correlations between BMI and the area under the response curve to 90% recovery, and this was seen in both the forearm and sacrum results. The higher the participant's BMI, the lower the participants' RH response following off-loading.

It was observed that there was higher resting flux at the sacrum and also a trend for reduced responses at the sacrum in both the heavy smokers and the controls compared to the forearm, but this was not formally tested due to the variability present with the loading challenge in all the groups.

### 3.5.2 Pressure loading at the forearm of heavy smokers and matched non-smokers

The results in this section show the response of the skin blood flux to loading and off-loading at the forearm sites in heavy smokers and non-smokers. A bar chart of the resting and loaded flux in the non-smokers and heavy smokers can be seen in *Figure 3.3*.

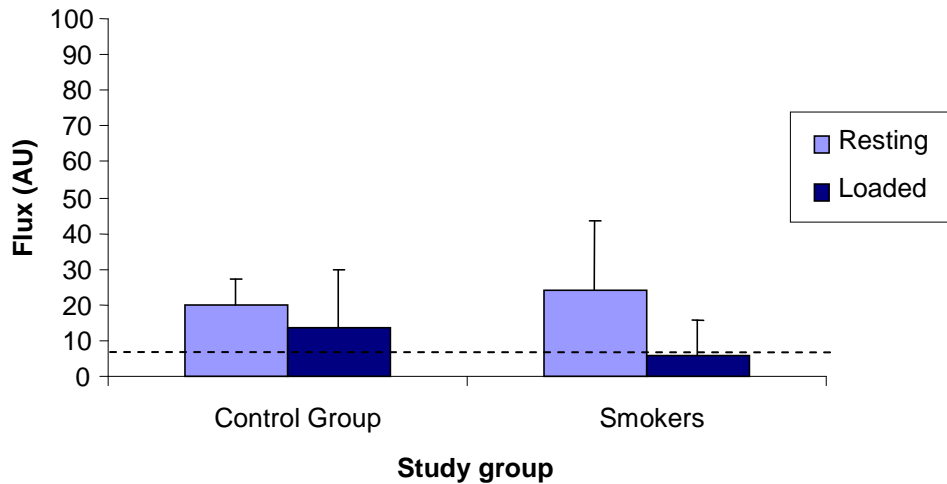


**Figure 3.3** A bar graph of resting flux and loaded flux at the forearm of the heavy smokers and the matched non-smokers (n=8). The data are median + IQR. There was a significant fall in flux with loading when tested using the Wilcoxon paired test, where  $p < 0.05$ , in both the control group and smokers. The BZ (dotted line on the graphs) measured in a group of 7 participants was calculated as  $5.8 \pm 2.6$  AU (median  $\pm$  IQR) (*Chapter 2, Section 2.2.2*).

### ***Resting flux***

The resting flux was  $19.8 \pm 7.4$  and  $23.9 \pm 19.4$  AU in the non-smokers and heavy smokers respectively (median  $\pm$  IQR). There was no significant difference between the groups; this was tested using the MWU test.

### ***Loaded flux***

In 94% of participants studied (15 out of 16 participants), loading caused a reduction in skin blood flux, but the magnitude of this effect was highly variable. The loaded flux fell to or below the BZ in only 2 out of 8 control group participants and 4 out of 8 smokers. This suggests that the load was not causing complete occlusion of blood vessels at the loaded site in most participants at the forearm. The loaded flux was measured as  $13.6 \pm 16.3$  and  $5.6 \pm 10.3$  AU in the non-smokers and smokers respectively (median  $\pm$  IQR). There was no significant difference between the groups and considerable variability present (MWU test,  $p = 0.234$ ). The heavy smokers tended to have reduced flux during loading.

### ***Body mass index and loaded flux***

The effect of BMI on percentage fall in flux with loading in the non-smokers considered alone, showed a significant correlation, where  $p=0.047$  (Figure 3.4); the higher the BMI, the greater the fall in flux during loading with 2500g.

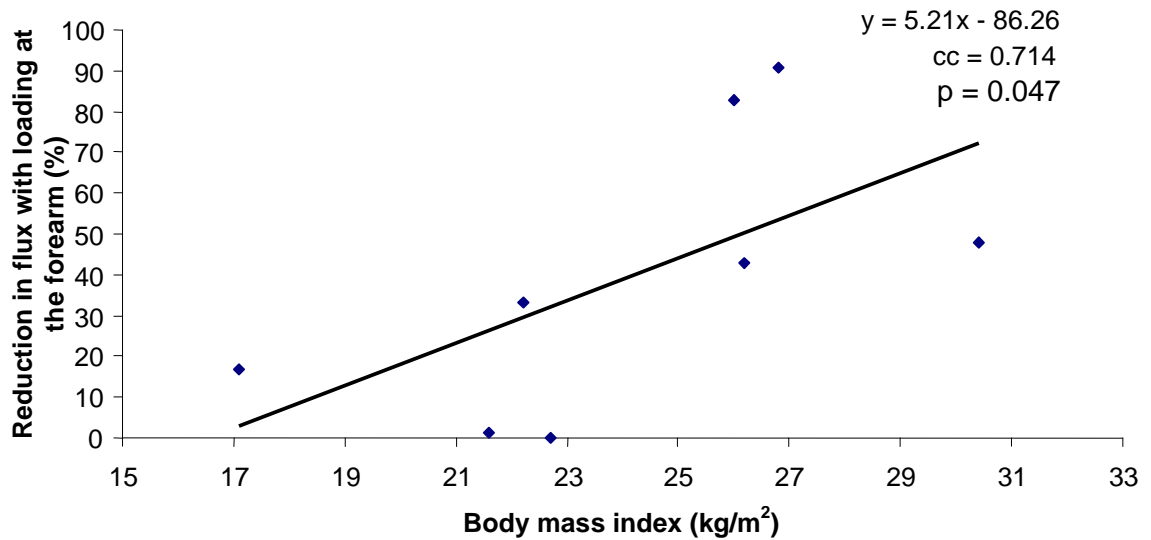


**Figure 3.4** A scatter graph to show the correlation between BMI and % fall in flux with loading of 2500g in 8 non-smokers measured at the forearm site. The correlation was significant, as tested by Spearman's rho, where  $p=0.047$ .

There was no significant difference in the RH response following removal of the load between the heavy smokers and their matched control participants measured at the forearm site.

### ***Maximum reactive hyperaemic response***

The maximum hyperaemic response was measured as  $95.2 \pm 67.1$  and  $80.8 \pm 117.2$  AU in the non-smokers and heavy smokers respectively (median  $\pm$  IQR). There was no significant difference between the groups (MWU test,  $p=0.918$ ).

### ***Total AUC to 90% recovery***

The area under the RH curve to 90% recovery was measured as  $2846.5 \pm 2341.8$  and  $4367.1 \pm 6169.8$  AU.sec in the non-smokers and heavy smokers respectively (median  $\pm$  IQR). There was no significant difference between the groups (MWU test,  $p=0.094$ ). The heavy smokers tended to have an increased RH compared to the non-smokers.

### ***BMI and reactive hyperaemic response***

The BMI of the participants, including both the heavy smokers and non-smokers, was shown to correlate significantly with the RH response, as measured using Spearman's Rho, where  $p=0.015$  (Figure 3.5).

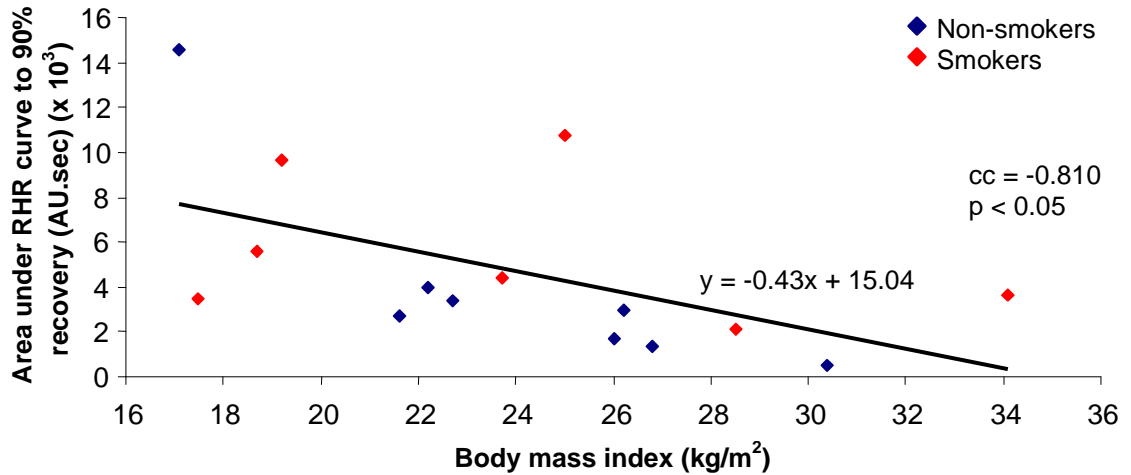


**Figure 3.5** A scatter graph to show the correlation between BMI and AUC of the RH curve to 90% recovery of resting flux in 8 heavy smokers and 8 non-smokers measured at the forearm site. The correlation was significant, as tested by Spearman's rho, where  $p < 0.05$ .

### ***Oscillations in the LDF flux during the reactive hyperaemic response***

The oscillations within the LDF signal before, during the loading and following removal of the load were not investigated using spectral analysis due to difficulties with the gradual loading protocol and the steep transient increase in flux following removal of the load. Both of these introduced a very low frequency to the signal which would distort the remaining frequencies. A change in the pattern of the oscillations in the signal could be observed in the signal from before to after removal of the load (Figure 3.6).

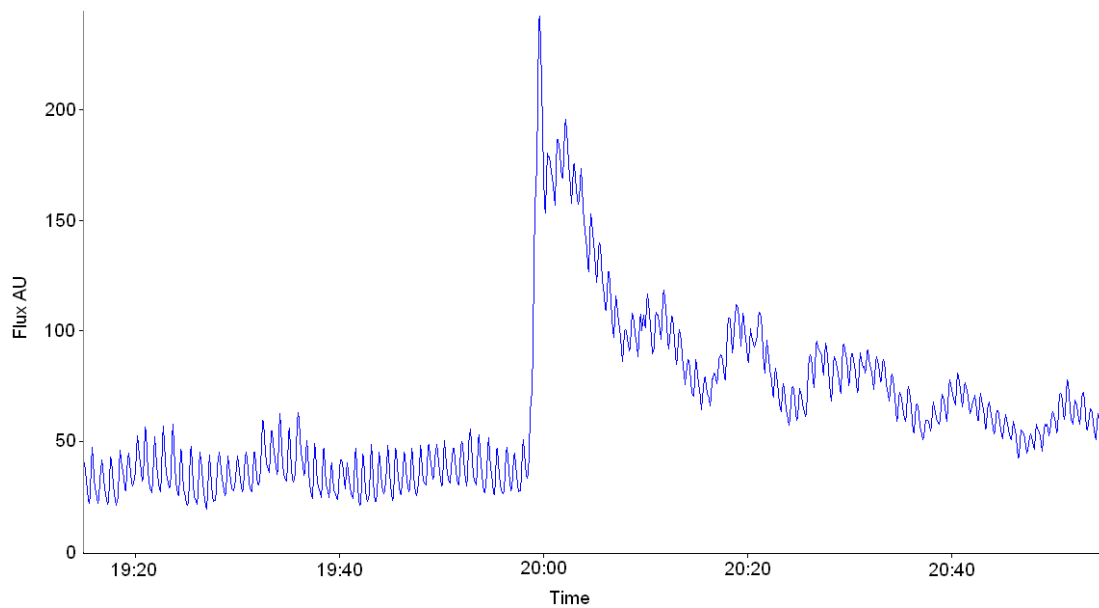


**Figure 3.6** An LDF trace showing approximately 50 seconds before removal of load and 50 seconds following load removal and the oscillations within the LDF signal from a non-smoking control participant.

### 3.5.3 Pressure loading at the sacrum of heavy smokers and matched non-smokers

The results measured during the loading challenge and the off-loading at the sacrum showed similar trends to the results at the forearm. The resting and loaded flux in the non-smokers and heavy smokers at the sacrum are represented in *Figure 3.7*.

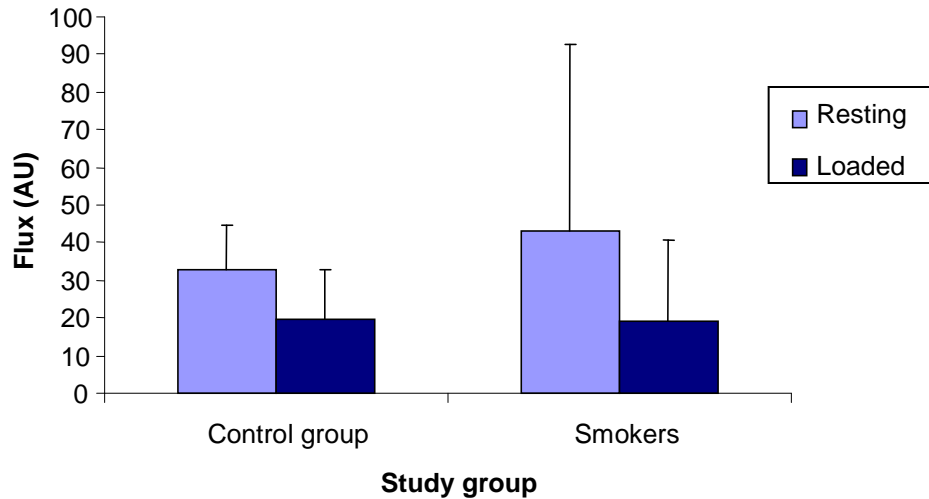


**Figure 3.7** The figure shows a bar chart of resting flux and loaded flux at the sacrum of the heavy smokers and the matched control participants (n=8). The data are median  $\pm$  IQR. There was a significant fall in flux with loading when tested using the Wilcoxon paired test, where  $p < 0.05$ , in both the non-smoker control group and heavy smokers.

#### ***Resting flux***

The resting flux measured at the sacrum was  $32.7 \pm 12.1$  and  $43.2 \pm 49.5$  AU in the non-smokers and heavy smokers respectively (median  $\pm$  IQR). There was no significant difference between the non-smokers and the heavy smokers.

#### ***Loaded flux***

The loaded flux with 2500g applied to the sacrum was  $19.3 \pm 13.4$  and  $19.0 \pm 21.9$  AU in the non-smokers and heavy smokers respectively (median  $\pm$  IQR). There was no significant difference between the loaded flux of the non-smokers and the heavy smokers.

### ***Body mass index and loaded flux***

The effect of BMI on the percentage fall in flux with loading in the non-smokers considered alone, showed a significant correlation, where  $p < 0.05$  (Figure 3.8); the results at the sacrum were the opposite to those at the forearm site. As the participants BMI increased, the fall in flux decreased, suggesting reduced occlusion of the blood vessels.

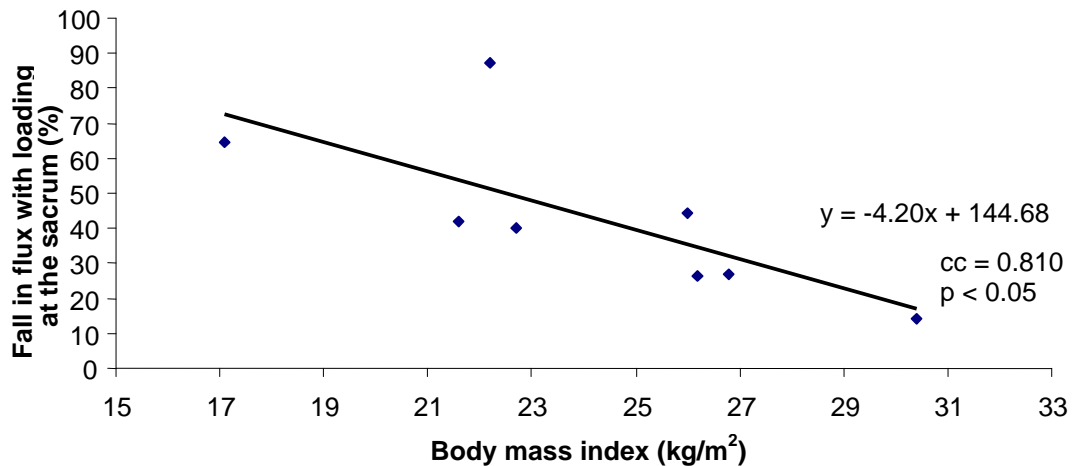


**Figure 3.8** A scatter graph to show the correlation between BMI and percentage fall in flux with loading of 2500g in 8 non-smokers measured at the sacrum site. The correlation was significant, as tested by Spearman's rho, where  $p = 0.015$ .

### ***Maximum reactive hyperaemic response***

The maximum RH response measured at the sacrum site was  $62.7 \pm 74.5$  and  $58.9 \pm 109.2$  AU in the non-smokers and heavy smokers respectively (median  $\pm$  IQR). There was no significant difference between the non-smokers and the heavy smokers (MWU test).

### ***Area under reactive hyperaemic response curve to 90% recovery at the sacrum***

The AUC of the RH curve to 90% recovery was measured as  $1078.3 \pm 8692.3$  and  $1046.1 \pm 1621.1$  AU/sec in the non-smokers and heavy smokers respectively. There was no significant difference between the non-smokers and the heavy smokers (MWU test).

### ***Body mass index and reactive hyperaemic response***

The BMI of the 16 participants (8 non-smokers/8 heavy smokers) showed a significant correlation with the RH response at the sacrum as measured as the area under the curve to 90% recovery (Figure 3.9). The trend followed that the higher the body mass index, the lower the RH following off-loading.

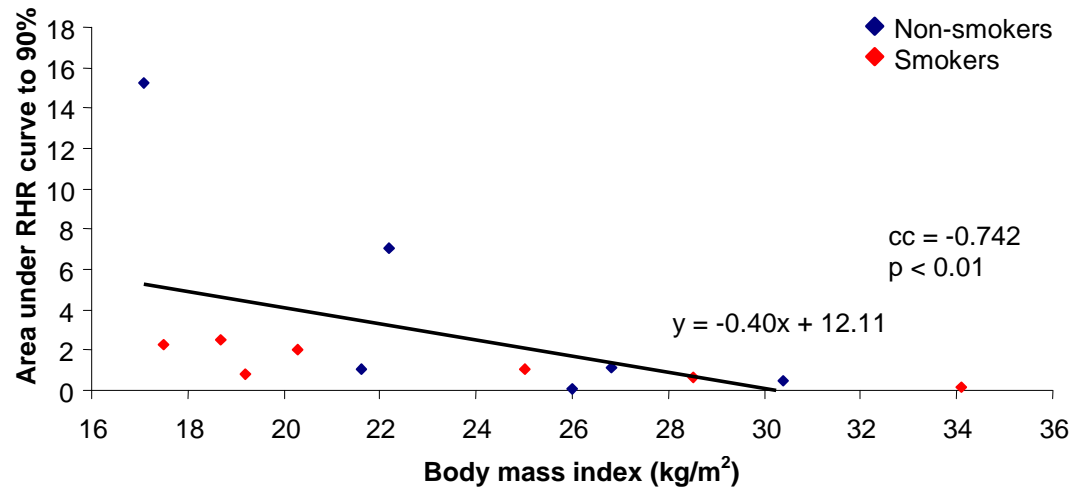


**Figure 3.9** A scatter graph to show the correlation between BMI and AUC of the RH curve to 90% recovery in 8 non-smoking participants and 8 heavy smokers measured at the sacrum. The correlation at the sacrum is significant, as tested by Spearman's rho, where  $p < 0.01$ .

#### ***Key findings from the chapter***

- The reactive hyperaemia response to the loading stimulus was highly variable in magnitude at both the forearm and sacrum in both the smoker and non-smoker participants.
- The participants in each group had widely varying BMI's, which probably contributed to the observed inter-subject variations.
- The artifact on the LDF signal caused by the loading and movement by participants also made measurements difficult to compare and analyse and subsequently difficult to interpret.

### **3.6 Discussion**

There has been much focus in recent years on the measurement of altered skin blood flux responses using LDF as an early indicator of the cardiovascular disease. As well as a potential non-invasive tool for this purpose, adequate skin blood flow and the appropriate regulation and control of the microcirculation is vital to the maintenance of healthy skin. Thus measurement of skin blood flow has the potential to provide important information about the health of the skin itself.

The resting cutaneous flux measured using LDF is generally known to be variable due to the architecture of the skin microcirculation, thus it is important to build in a provocation alongside

LDF measurements. The studies in this chapter are based on the skin blood flux response to the application and removal of a 2500g load. This enables the consideration of the ability of the cutaneous microcirculation to withstand external pressure and also increase blood flow on removal of the load.

The results presented in this chapter show the resting flux, loaded flux and RH response to removal of a 2500g load in a heterogeneous group of 8 heavy smokers and matched non-smoking control participants. The apparatus used was the same as a previous study in light smokers (Noble et al., 2003) where the RH response was measured at the sacrum of light smokers and matched non-smoking control participants.

The resting flux at both the forearm and the sacrum sites was not significantly different in the smokers compared to the non-smokers. It was observed that resting flux was higher at the sacrum compared to the forearm, but this was not formally tested. The forearm resting LDF flux was similar to some studies (Hagisawa et al., 1994), but higher than in others (Tee et al., 2004). The sacrum resting LDF flux was higher than has been previously found in other studies at the sacrum (Schubert and Fagrell., 1989; 1991). The indenter may have been applying a small amount of pressure during resting flux, when the probe within the indenter was placed on the skin with no load applied, causing changes in the resting flux.

The gradual loading of the skin (500g every 2 minutes) up to 2500g (~94mmHg) resulted in a reduction in flow in most participants at the sacrum and forearm, but to varying degrees. At the forearm, the blood flux decreased by  $38 \pm 69\%$  and  $58 \pm 59\%$  in the control and heavy smokers respectively (median  $\pm$  IQR). At the sacrum, the fall was  $41 \pm 33\%$  and  $57 \pm 52\%$  in the non-smokers and smokers respectively (median  $\pm$  IQR). A study has shown that pressures on the trochanter from lying on a standard hospital mattress are around 83mmHg, reducing to between 37 and 55mmHg on a pressure reducing mattress (Thompson-Bishop and Mottola, 1992). A more recent study showed the maximum contact pressure on the sacrum was 40mmHg and 26mmHg in subjects lying on 3-cell and 2-cell alternating pressure mattresses, respectively (Rithalia and Gonsalkorale, 2000). The magnitude of the load applied to the skin in the studies in this chapter potentially reflects the load on the skin from a standard hospital mattress, but only reflect this pressure applied over a short period of time.

Several other studies have found similar decreases in blood flux with similar levels of external pressure applied as was used in the studies in this chapter. In a study, progressive increases in pressure up to 110mmHg at the sacrum site, caused a 43% reduction in blood flux (Schubert and Fagrell, 1989). Another study measuring effects of gradual loading at the sacrum using LDF and transcutaneous oxygen (tcPO<sub>2</sub>), found that LDF was at a minimum (37% of initial value) when external pressure was 90mmHg, and tcPO<sub>2</sub> was at its minimum when external pressure was 100mmHg (Colin and Saumet, 1996). However, the pressures documented to cause occlusion of blood flow in the literature vary tremendously. One study applied progressive loads to the sacrum until complete occlusion occurred and showed that pressures up to 380mmHg were required in some participants (Schubert and Fagrell, 1991). In another study, where transcutaneous oxygen was being measured at the sacrum, it was shown that interface pressures ranging between 27 – 108mmHg were needed to reduced transcutaneous oxygen to a level that related to blood flow occlusion (20mmHg) (Bader and Gant, 1988).

The data in the studies in this chapter demonstrated high variability in the effect of loading in both heavy smokers and non-smokers at the forearm and sacrum site. There are various potential reasons for this variability. The requirement to manually apply and remove the weights from the loading pan, meant that there was potential for slight changes in angle or position of the indenter which could also change the amount of pressure applied to the tissue. It is also possible that slight movement could cause a change in the blood vessels over which the probe is measuring.

In some of the participants, there was an initial increase in blood flow with loading, and in at least one participant, this remained throughout the loading period, so that the final loaded flux was higher than resting flux. This could suggest the presence of pressure induced vasodilation (PIV) (Fromy et al., 2000); this may have been occurring in the participants in the studies in this chapter to varying degrees. A previous study demonstrated the presence of PIV when pressure was applied to the skin of the hand up to 25mmHg of pressure, and then blood flow reduction (Fromy et al., 2000). In a further study, a computer controlled indenter was used to apply pressure from 0-60mmHg to the sacrum of participants in 5mmHg steps, with the pressure constant for 3 minutes at each level. It was found that blood flow decreased when pressure was increased from 0-15mmHg, remained relatively constant between 15 and 30mmHg and then increased as pressure increased from 35 to 60mmHg (Brienza et al., 2005). This would suggest that not only the intensity of the load, but also the pattern of the loading applied to the skin, are important in determining whether PIV will occur.

Many studies, including the studies in this chapter, use progressive application of pressure to the skin to consider effects of loading on skin blood flow. In a study comparing constant loading and progressive loading, it was shown that constant loading of 30mmHg caused a reduction in skin blood flow, however, the progressive loading pattern caused an increase in blood flow up to 65mmHg of pressure (Jan et al., 2008). The gradual loading protocol used in the studies in this chapter may allow the skin to recover at each stage of loading, thus reducing the total impact of the load.

The participant's BMI would also be expected to affect the level of pressure that would cause occlusion of blood flow in the skin microcirculation. The literature suggests that the amount of external pressure applied to the skin is not the only factor that is important to the maintenance of blood flow to the tissues and that the interface pressure at the skin surface does not necessarily relate to the interstitial stress within the tissues (Bader and White, 1998) and the maintenance of tissue blood flow. The participants in both the smoking and non-smoking control groups were a convenience sample and although matched between the groups, they had a wide range of BMI's (BMI range = 17.1 - 30.4kg/m<sup>2</sup> in control group and 17.5 - 34.1kg/m<sup>2</sup> in the heavy smokers).

Interestingly, the forearm and sacrum sites showed different effects of BMI on loading in the non-smoker group (*Figure 3.4* and *Figure 3.8*). At the sacrum, as would be expected, the greater the participants BMI, the smaller the fall in flux with loading (significant correlation). Conversely, at the forearm, the greater the participant's BMI, the greater the fall in flux with loading. It would be expected that participants with a higher BMI would have more soft tissue to support the load, resulting in a reduced occlusion of blood flow, and a lower impact of loading. However, the volar forearm site is a narrow site and can accommodate the 5cm diameter indenter onto which the load was applied; however, in those participants with a higher BMI the indenter was able to be applied more centrally to the forearm. This may have resulted in increased effect of pressure.

In terms of pressure ulcer development, studies have shown that patients with lower BMI's or decreased body weight have a significantly increased prevalence of pressure ulcers (Allman et al., 1995; Compher et al., 2007; VanGilder et al., 2009). Although, studies also suggest that high BMI can increase the risk of pressure ulceration, a further study showed that hospitalized elderly patients with extra body fat (severe obesity) were at a reduced risk of pressure ulcer development (Compher et al., 2007). This is thought to be due to the protective effect of the soft tissues in supporting the external load. The increased risk of pressure damage in obese patients may be due to effects of obesity on the microcirculation and skin blood flow directly.

There was no significant difference in the effect of loading between the heavy smokers and non-smokers at either the forearm or sacrum site. Several studies have considered the effect of smoking on the skin structure and have found reduced skin collagen synthesis, both *in vitro* and *in vivo* (Yin et al., 2000; Knuutinen et al., 2002). The synthesis of type I and III collagen was found to be reduced by 18 and 22% respectively in smokers compared to non-smokers, and this is thought to be due to an increase in levels of MMPs in the skin, which degrade collagen (Knuutinen et al., 2002). Thus, reduced ability to support the load would be expected to result in increased blood flow occlusion with external loading in the smokers, but this was not demonstrated. Other studies have shown differences in the effect of loading in patient groups; Schubert and Fagrell (1991) found that a significantly lower pressure was needed to occlude blood flow over the sacrum compared to the gluteus muscle in an elderly group, but this difference was not present in the younger group.

The RH response followed the removal of the load from the loading pan above the LDF probe. The magnitude of the RH response was variable, and did not correlate significantly with the effect of loading; the highest reduction in flow during loading did not result in a greater RH response. The participant's BMI significantly correlated with the area under the response curve, so that with increasing BMI there was a reducing area under the curve, at both the forearm and sacrum sites. A previous study found variable responses to pressure loading over the trochanter and suggested that there are a range of physiological responses to external pressure (Frantz and Xakellis, 1989).

There was no significant difference in the response in the heavy smokers compared to the non-smokers. A previous study using the same apparatus in a group of light smokers and matched controls demonstrated significant attenuation of the response in the light smokers (Noble et al., 2003) (*Figure 3.10*). In the light smokers there was less variability in the RH response and BMI within the groups compared to the heavy smokers involved in this study. Other studies have shown smokers to have reduced RH responses to occlusion of flow to the finger (Carlsson and Wennmalm, 1983; Hashimoto, 1994). However, comparisons with studies involving post-occlusion reactive hyperaemia should be done with caution as the responses are considered to be different. The local pressure induced occlusion produces a prolonged hyperaemia, compared to the hyperaemia induced by proximal occlusion (Rendell and Wells, 1998; Capp et al., 2004). Several studies have also shown smokers to have chronically impaired vasodilation responses to both ACh and SNP (Pellaton et al., 2002; Edvinsson et al., 2008).

Other studies have shown the RH response to an external load to be different in different patient groups. The RH response was significantly reduced in elderly patients compared to a younger group (Schubert and Fagrell., 1991; Hagiwara et al., 1991) and also in patients with hypotension

(Schubert, 1991). Patients with recent SCI have also been shown to have a different reactive hyperaemic response following 2 hours of pressure loading at the sacrum compared to patients with acute orthopaedic trauma and healthy participants. The RH response on release of the load in these patients was shown to have a shorter time to increase blood flow and a steeper slope. The authors suggest this reveals an impaired response and the presence of microvascular dysfunction (Sae-Sia et al., 2007).

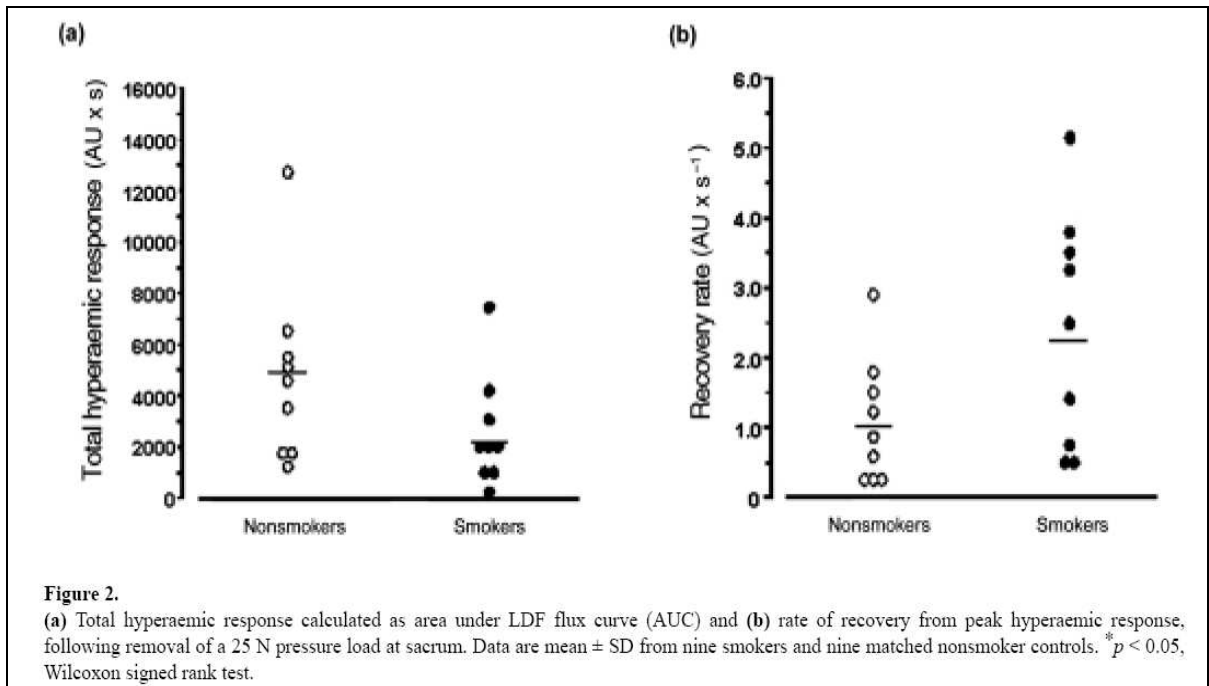


**Figure 3.10** A figure showing the parameters of the reactive hyperaemic response following removal of a pressure load in 9 light smokers and matched non-smokers. This figure is extracted from: Noble, M., Voegeli, D and Clough, G (2003) A comparison of cutaneous vascular responses to transient pressure loading in smoking and non-smokers. *Journal of Rehabilitation Research and Development*. 40, (3) 283-288.

It may have been expected that the increased intensity and length of the smoking habit in this group of heavy smokers would cause an enhanced attenuation in responses and that it would be a more pronounced difference than that seen in the previous study involving light smokers (Noble et al., 2003) (*Figure 3.10*). Alternatively, it may also have been expected that there would be compensation mechanisms functioning, which restricted the effects of smoking on the skin blood flow responses.

It was observed in the studies in this chapter that there was a reduced RH response at the sacrum compared to the forearm in both the heavy smokers and non-smokers. The variations in loading made this difficult to investigate further and thus statistics tests were not completed.

The oscillations within the LDF traces before, during and after RH could not be analysed using spectral analysis of the signal. Due to the step-wise loading pattern, the sections of LDF trace were too short to provide accurate results when completing spectral analysis. Also, the steep transient in the skin blood flux, when the load is removed from the skin, would appear in the spectral analysis as a very slow frequency and thus dominate the PSD. However, it could be observed from the traces that the frequency and amplitude of oscillations dominating the signal changed during the RH response (*Figure 3.6*).

The analysis of oscillations within the LDF trace during loading has been completed in a study using an animal model. In this study the loading duration was increased to 6hr/day for 4 days and the devices used to apply and remove the loads were optimized, so reducing artifact on the LDF probe (Li et al., 2006b). The length of LDF data collected during the loading period was significantly longer than in the studies in this chapter, so spectral analysis could be used to analyse the traces in that study. They found that loading of the skin caused a reduction in the oscillations in the LDF signal around 0.01Hz, suggesting that prolonged loading induces endothelial damage (Li et al., 2006b).

In a study involving human participants, it was observed that the ‘slow waves’ in the LDF signal decreased when 10mmHg was applied to the skin, suggesting early effects on the regulation of the microcirculation during external loading, but this was not analysed further (Colin and Saumet, 1996). In a further study where the effects of loading on the sacrum on the oscillations in the skin blood flux were investigated using Wavelet analysis of the signal, the myogenic mechanisms were the main mechanisms involved in the RH response following removal of the load (Brienza et al., 2005). They also found that there was only a minor role for metabolic control, suggesting that the effect of shear stress on the endothelium causing NO release is minimal during the RH response (Brienza et al., 2005).

### ***Limitations of the study***

Although there were no significant differences found between the heavy smokers and non-smokers in the experiments presented in this chapter, the study groups may be underpowered. The high variation in responses in both the heavy smokers and non-smokers at the sacrum and forearm meant that an increased sample size would be needed to be able to determine any potential

significant differences between the groups. Also, several participants were excluded due to movement artifact on the LDF traces.

The LDF method of measuring skin blood flow has been used in many studies and has many benefits associated with its use. However, due to the variation in the architecture of the skin microcirculation (Braverman et al., 1990) and the small size of the LDF probe, there is the potential for high variation in readings and poor reproducibility. The LDF probe is also susceptible to movement artifact. The loading apparatus potentially caused increased movement artifact on the LDF probe and thus on the resultant trace, during application and removal of external loads in an older group of participants. The fixation of the laser Doppler probe within the indenter also caused artifact to be present during resting flux. The previous study by Noble et al. (2003) using the same apparatus for the load application was not subject to as much artifact on the LDF trace. All the participants in this study were significantly older and thus found it more uncomfortable to remain in the positions required for the study, particularly the prone position for the studies at the sacrum site. The heavy smokers also found it more difficult to abstain from smoking before the studies and so there may be some acute effects of smoking in the results.

The measurement of skin blood flow during loading also has difficulties. When the skin blood flow is reduced under the external load, the random part of the LDF signal becomes a larger proportion of the signal and thus there is more error in the signal (Sacks et al., 1985).

Although direct pressure to skin is the major cause of pressure damage, there has been increased focus on the effects of the reperfusion on the skin tissue. Studies have investigated the effects of ischaemia and reperfusion; the injury caused by ischaemia reperfusion is known to be different from that caused by a single ischaemic insult (Peirce et al., 2000; Houwing et al., 2000). In fact, it has been shown in a rodent model, that repeated I/R injuries are more damaging to the tissue than a prolonged ischaemic insult (Peirce et al., 2000). The reperfusion of blood to a previously ischaemic tissue causes cellular injury, which is thought to be partly due to the higher levels of oxygen free radicals.

Since completing this part of my research, more sophisticated devices (Brienza et al., 2005; Jan et al., 2008) and protocols have been developed to simulate the external pressure loading environment. Sae-Sia et al. (2007) considered the effect of 2 hours local pressure at the sacrum of patients with a recent SCI. They showed a greater relative decrease in flux in the SCI patients compared to controls and a reduced RH following release of load. Studies have also considered the effect of alternating pressure loading to validate the use of alternating pressure mattresses for at-

risk patients in hospital. Jan et al. (2008) used a computer-controlled indenter to apply both alternating pressure levels and constant levels to the skin at the sacrum.

With the development of improved loading equipment there is scope for future work in considering the effects of loading in different patient groups, to improve the knowledge base regarding risk factors for skin damage. There is also scope to provide further evidence regarding the process of cycles of ischaemia and reperfusion on skin blood flow control mechanisms.

### ***Final Summary***

For the purposes of the studies in this chapter it was hypothesized that heavy smoking would result in significantly attenuated reactive hyperaemic response in the skin microcirculation following removal of an external load. However, the results demonstrate no significant differences in the responses in the heavy smokers compared with the non-smokers at either the sacrum or forearm sites. The loading stimuli resulted in highly variable changes in blood flow and RH response. This may be due to the loading apparatus; since completing these studies more sophisticated devices are being used. Therefore, loading of the skin using this apparatus will not be used as the stimulus alongside LDF to assess skin blood flow in the subsequent chapters in this thesis.

The studies in this chapter have highlighted the difficulties for participants and thus potentially patients of remaining very still in the prone position for prolonged periods of time. This is an important aspect that needs to be considered when studying skin blood flow as a potential tool for assessment of risk of pressure ulcer development. In the next chapter, the skin blood flow responses will be compared at the sacrum and forearm sites, the latter representing a more accessible location for skin-related studies.

The application of a local heating stimulus to the skin is a well-established stimulus that has been used in many studies. The local heating stimulus has already been shown to be more sensitive in detecting alterations in the microcirculation and risk of foot ulcer development compared to baseline blood flow measurements (Timar-Banu et al., 2001). The skin heating protocol can be completed with no interference to the probe, so reduces the problem of movement artefact. It also lends itself to further spectral analysis to investigate the oscillations in the signal and thus the local mechanisms mediating the responses of the skin microcirculation. The prolonged plateau vasodilatation induced by local heating has been shown, using spectral analysis, to have a strong endothelium dependent component (Brienza et al., 2005), which is thought to be one of the aspects of regulation directly effected by smoking. In the studies in this chapter, the sacrum (an area at risk of pressure ulcers) and the forearm (not at risk) were both investigated. The potential differences

between the sacrum and forearm sites, as well as the effects of smoking on blood flow control will be investigated further in this thesis using the local heating stimulus.



## **Chapter 4**

**Investigation into vasoreactivity of different skin sites: the local heating response at the sacrum and forearm**

## 4.1 Introduction

In the studies in chapter 3, the effects of loading the skin surface on skin blood flow and then the RH response to removal of the load were investigated. The studies demonstrated considerable variability in both the loading and the RH response to the removal of the load. The skin loading protocol meant there were difficulties in further analysing the LDF signal using spectral analysis to consider the mechanisms regulating the skin blood flow during resting and vasodilation responses. Therefore, a different stimulus – the local heating stimulus – will be used in all the remaining studies in this thesis.

The appropriate regulation of skin blood flow both during steady state and the ability for blood vessels to dilate and constrict appropriately in response to certain stimuli is vital to the health of the skin. Although the loading protocol directly considers the skin microcirculation, factors such as cushioning of the load by the tissue and PIV affect the skin blood flow response. The vascular responsiveness of the skin microcirculation has been investigated in studies using a variety of different stimuli, including blood flow occlusion and release using a cuff, skin cooling or heating and iontophoresis of ACh or SNP (Minson et al., 2001; IJzerman et al., 2003b). However, it is suggested that the local heating response may be an optimal tool to assess both endothelial and microvascular function than reactive hyperaemia, due to the 2-phase response (Minson and Wong, 2004).

The local heating of the skin has been used in many studies in the last decade and has been shown to rely mainly on NO produced by the endothelium to maintain the vasodilation during the prolonged plateau phase (Minson et al., 2001). Studies using spectral analysis of the LDF signal have demonstrated that the local heating response is dominated by endothelium-dependent mechanisms (Brienza et al., 2005). The function of the endothelium is vital to the production of appropriate vasodilation responses and dysfunctional endothelium has even been considered as a risk factor for pressure ulcer development due to its importance in blood flow control (Struck and Wright, 2007). Therefore, the skin blood flow response to local heating will be considered in the studies in the remainder of the thesis.

The local heating of the skin in combination with LDF has been used in recent literature to consider these responses in different patient groups (Geyer et al., 2004; Brienza et al., 2005; Jan et al., 2009). A local non-painful heating challenge to the skin of a high enough magnitude results in a 2-phase vasodilation response in the skin microcirculation as measured using LDF. It involves an initial rapid increase in skin blood flow, followed by a brief nadir and then a further rise to a

plateau. The initial rise has been shown to be mainly axon reflex dependent and the prolonged plateau is mainly NO-mediated (Minson et al., 2001; Kellogg et al., 1999). A study has shown that 42°C local heating for around 30 minutes evokes maximal vasodilatation (Kellogg et al., 1999; Gooding et al., 2006). Studies have also shown that a rapid rise in temperature can alter the 2-phase heating response, so that it is difficult to separate the axon-reflex and NO-mediated vasodilatation (Minson et al., 2001). Thus a progressive heating stimulus will be used in the studies in this thesis.

The local heating stimulus in combination with LDF provides information about the ability of the skin blood vessels to dilate to a given stimulus. There is also the potential for investigation of the regulation of skin blood flow using spectral analysis of the LDF signal. Historically studies have observed and also shown by analysis that there are oscillations at different frequencies in the LDF signal (Wilkin, 1986; Kastrup et al., 1989). More recently, spectral analysis has been used to show that the oscillation frequencies within the LDF signal relate to certain systemic and local aspects of blood flow regulation (*Chapter 1, section 1.5.3*)

The LDF signal contains oscillations that relate to systemic control of skin blood flow. The oscillations in the signal at a frequency around 1Hz (one per second) originate from the cardiac beat (Bracic and Stefanovska, 1999) and those around 0.4Hz originates from respiratory function (Bollinger et al., 1993). The local control mechanisms are revealed in the signal at around 0.1Hz, 0.04Hz and 0.01Hz and relate to myogenic, neurogenic and metabolic/endothelium mechanisms respectively (Akselrod et al., 1981; Soderstrom et al., 2003; Stewart et al., 2007) (*Chapter 1, section 1.5.3*)

The local control mechanisms result in the skin blood vessels undergoing vasomotion; the rhythmic constriction and dilation of blood vessels. The vasomotion may be beneficial to blood flow; studies have shown that vessels that oscillate have greater flow than a vessel with a constant diameter, but the same average width (Meyer et al., 2002). It may also improve oxygenation of tissues (Tsai and Intaglietta, 1993). In particular, the function of the endothelium in the control of skin blood flow has been the focus of much attention. Although this has been mainly in the field of cardiovascular medicine, more recently its importance in skin health has been suggested (Struck and Wright, 2007). The endothelium, and specifically the NO produced by the endothelium, has an important role in vasodilation of blood vessels and enables rapid increases in skin blood flow when required by the skin tissues.

The most common body site for pressure ulcer development is the sacrum. In a published summary of nine international pressure ulcer prevalence surveys (between 1989 and 2005), the most

common site of the body for pressure damage was found to be the sacrum (28%) (Vangilder et al., 2008). This is mainly due to the presence of a bony prominence; the pressure within the tissues during sitting and lying is centred most in these areas (Defloor, 2000).

The sacrum has been investigated in previous studies measuring skin blood flow control (Geyer et al., 2004; Jan et al., 2009). In a study using LDI to measure blood flow at the sacrum as well as the gluteus maximus, lower back, hand and fingers, the average skin blood flow at the sacrum was significantly greater than the other sites (Mayrovitz et al., 2002). Other studies have considered the anatomy of the sacral microcirculation to determine whether inherent differences in the skin microcirculation structure are the cause for increased incidence of pressure ulcers. Using light and scanning electron microscopy of human tissue samples excised post mortem, the sacrum was shown to have a higher density of capillary loops underneath the dermal papillae compared to skin tissues overlying the ischial tuberosity and the gluteus maximus (Hagisawa et al., 2001). They suggest that this could be due to the frequent loading of the sacrum site during lying and sitting which could cause the development of capillary loops (Hagisawa et al., 2001).

The sacrum is a body site that is at risk of pressure ulcer development. Although there have been some studies to consider the anatomy of the microcirculation and resting flux at the sacrum compared to other sites, there remains a need for more information regarding the skin blood flow at the sacrum. In particular, the regulation of skin blood flow at the sacrum and the ability of the microcirculation to respond to external stimuli compared to the forearm, as a reference site. Many studies, including some contained in this thesis, use the volar forearm site as a site to investigate blood flow responses. It is important to ascertain whether responses at the forearm can be related to the 'at risk' sacrum.

## **4.2 Hypothesis**

The magnitude of the skin blood flow responses to a local heating stimulus will be altered at a site at risk of pressure damage, the sacrum, compared to the forearm skin site.

### 4.3 Objectives

- To compare skin blood flow responses to a local heating stimulus at the sacrum and the forearm in healthy participants.
- To complete spectral analysis on the LDF signal during resting and local heating to consider the effect of the heating response on the regulation of skin blood flow at the forearm and sacrum sites.
- To examine whether there are correlations in blood flow responses between the sacrum and the forearm, to determine whether the forearm has potential for use as a reference site for skin blood flow testing.

### 4.4 Methods

#### 4.4.1 Participants

Nine, healthy, non-smoker participants involved in the studies considering responses to 20 minutes skin heating at the forearm found in *Chapter 5* were also studied at the sacrum body site (*Table 4.1*). The heating responses at the forearm were compared with responses at the sacrum in these participants, and the results from this are shown in this chapter.

<b>Parameter</b>	<b>Participants (n=9)</b>
<b>Age (yrs)</b>	24.3 ± 4.5 (19 – 32)
<b>Sex</b>	7 females / 2 males
<b>Body mass index (kg/m<sup>2</sup>)</b>	20.9 ± 3.3 (17.3 – 26.7)
<b>Mean arterial pressure (mmHg)</b>	78.3 ± 3.5 (73.3 – 83.3)

**Table 4.1** The table shows the age, sex, BMI and MAP of a group of healthy, non-smokers (n=9). The table shows data as mean ± standard deviation (range). The BMI was calculated as [weight (kg)/(height (m))<sup>2</sup>]. The mean arterial pressure was calculated as [(2\*diastolic BP) + systolic BP]/3.

#### 4.4.2 Study Protocol

The full protocol for the skin heating studies can be found in *Chapter 2, section 2.4*. The specific protocol for the heating studies is as follows (*Figure 4.1*):

The studies were completed in the temperature controlled environment of the WTCRF. The participants gave their written informed consent to take part in the study. The participants were made comfortable on a hospital mattress, with their arm maintained at heart level on a pillow. They acclimatised to room temperature for 10 - 15 minutes before the skin blood flow measurements began. The participants were asked to keep their arm as still as possible for the duration of the forearm section of the study.

The measurements were first completed at the forearm site. The LDF pinhead probe was positioned within a skin heater which was mounted within a plastic ring which was then attached to the skin using a sticky O-ring (*Chapter 2, section 2.4*). This was placed on the volar surface of the forearm midway between the wrist and elbow away from visible blood vessels. The skin blood flow was measured before, during and after a local heating stimulus of 43°C for 20 minutes. The participant was then made comfortable in a prone position for another period of 10-15 minutes acclimatisation, before the same measurements were completed at the sacrum site. The data was then saved on the laptop for processing.

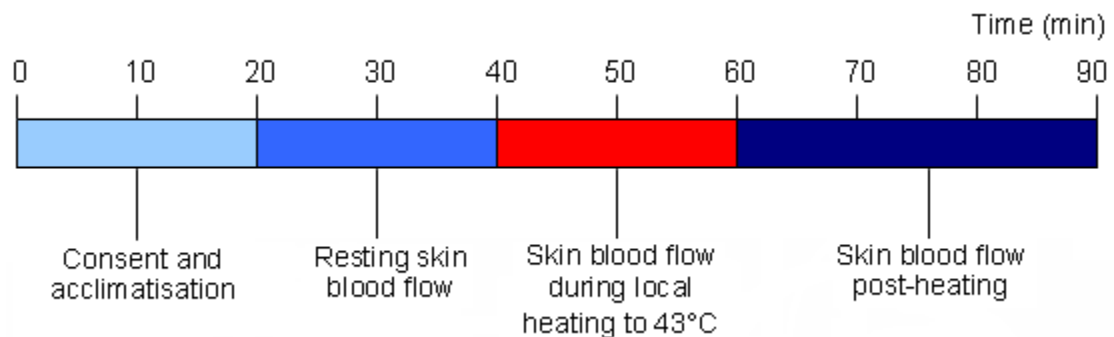


**Figure 4.1** A diagram to show the timeline of events occurring within the heating study protocol

#### 4.4.3 Spectral Analysis Methods

The FFT algorithm was used to determine the underlying frequencies within the LDF signal. The FFT makes the assumption that the waveform is discrete and periodic; that the signal is composed

of the same waveforms repeated. The FFT converts the time series in its frequency components by an algorithm called the Fourier Transform.

### ***Data collection and processing***

The skin blood flow was measured at the forearm and sacrum using LDF during 20 minutes resting and then 20 minutes local heating. The LDF trace was saved as two text files; 20 minutes resting flux and 20 minutes local heating flux. The sampling frequency was 40Hz, to ensure compliance with sampling theorem (*Chapter 2, Section 2.5.1*). The text files were then saved as Excel<sup>®</sup> files. The initial 100 seconds recording was removed from the heated flux to remove the steep gradient that occurred at the start of heating. The initial 100 seconds recording was also removed from the resting flux recording to ensure equal data length. The data was then saved into Matlab<sup>®</sup> workspace, where the remaining analysis was completed (*Figure 4.2*).

Matlab<sup>®</sup> is a software tool for studying digital signal processing. With the support of ISVR and particularly Dr David Simpson, Matlab<sup>®</sup> programs were written for the computation of FFT's from the LDF data. The Matlab<sup>®</sup> programs used in the spectral analysis in this chapter can be found in *Appendix 3*.

The trend was removed from the LDF traces using a Matlab<sup>®</sup> program; when the trend was not removed it featured as very low frequency power and distorted all the other frequencies within the signal. A program was then run in Matlab<sup>®</sup> to calculate the PSD of the resting flux and the flux during heating from 0 to 2 Hz (*Appendix 3*). The power was calculated as area under the PSD curve using integration and the trapezoidal method; the total power between 0 and 2Hz was calculated and also the power within each frequency band (*Figure 4.2*).

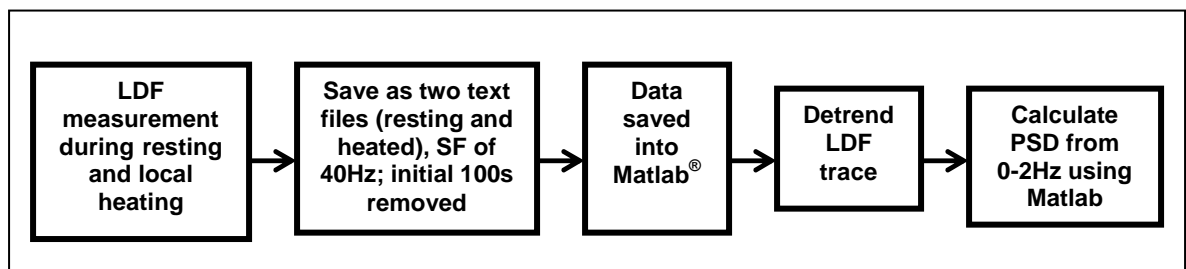


**Figure 4.2** A flowchart to summarise the pathway of data processing for the spectral analysis using Matlab<sup>®</sup> statistical package used for the data measured at the forearm and the sacrum.

#### 4.4.4 Statistics

The data for the studies in this chapter is treated as non-normal. The data is represented as median and error is shown by the IQR. All data is shown to 1 decimal place. The sacrum and forearm data is treated as paired data, so the Wilcoxon signed ranks test is used throughout this chapter to test for any significant differences. The data is presented graphically throughout this chapter using bar graphs. The line graphs to show the power in the LDF flux in the frequency range 0 to 2Hz generated using Matlab<sup>®</sup> are called periodograms.

##### *Measurement of the LDF signal in the time domain*

Various parameters of the heating response were measured from the LDF trace and these can be found in *Figure 2.6 (Chapter 2, Section 2.4.3)*.

##### *Measurement of LDF signal in the spectral domain*

The following measurements were taken from the LDF signal in the spectral domain:

**Absolute power between 0 and 2 Hz** – the area under the PSD curve between 0 and 2Hz measured using integration by the trapezoidal method.

**Absolute power between 0 and 0.2Hz** – the area under the PSD curve between 0 and 0.2Hz measured using integration by the trapezoidal method.

##### **Total power of each frequency band:**

**0.01Hz (0.008-0.02Hz)** – area under the PSD curve between 0.008-0.02Hz

**0.04Hz (0.02-0.05Hz)** – area under the PSD curve between 0.02-0.05Hz

**0.1Hz (0.05-0.15Hz)** – area under the PSD curve between 0.05-0.15Hz

**0.4Hz (0.15-0.4Hz)** – area under the PSD curve between 0.15-0.4Hz

**1Hz (0.4-2.0Hz)** – area under the PSD curve between 0.4-2.0Hz

**Relative power of each of the frequency bands** – absolute power of the band interval divided by the absolute power (either 0-2Hz or 0-0.2Hz)

## 4.5 Results

The local heating stimulus at the forearm and the sacrum provoked an increase in blood flow in all participants. An example of the LDF flux trace and the temperature of the heating block during the local heating response at the forearm and sacrum can be found in *Figure 4.3*

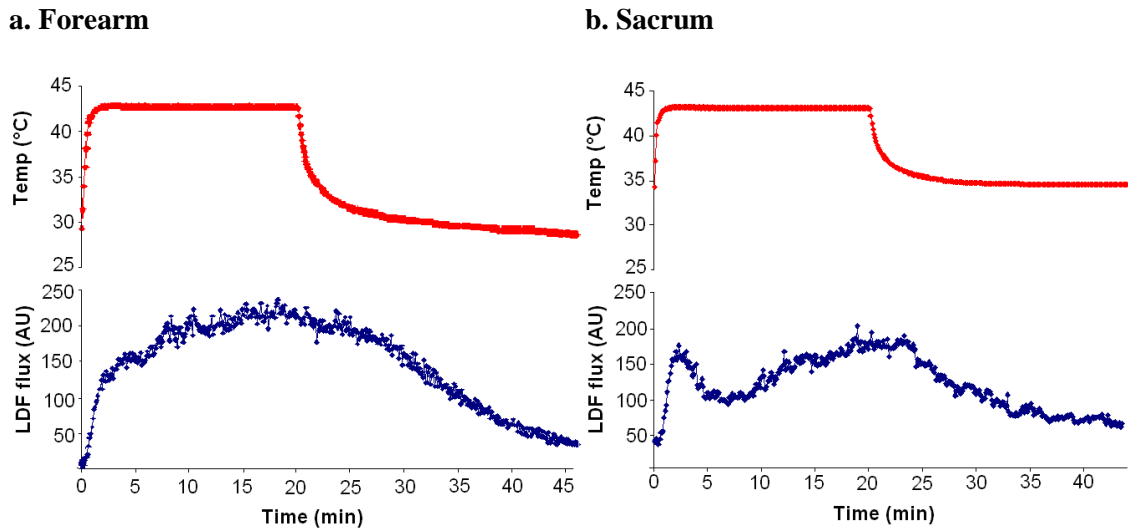


**Figure 4.3** The figure shows an example of a LDF trace at the **a.** forearm and **b.** sacrum of a healthy female control participant. The LDF flux graphs show flux during 20 minute local heating to 43 °C and flux measured for 20 minutes after switching off heater. The temperature graphs represent the change in temperature of the heater block during the course of the study.

### 4.5.1 Summary of the results

The skin blood flux was measured at the forearm and sacrum of 9 healthy participants before, during and after a local heating stimulus to 43°C using LDF. The skin blood flux measured during resting was significantly greater at the sacrum compared to the forearm. However, the hyperaemic response to the local heating stimulus was significantly smaller at the sacrum compared to the forearm.

Although the local heating responses at the forearm and sacrum were significantly different, the results from this chapter show that there was a significant correlation between the AUC of the local heating response at the forearm and the sacrum skin sites. The participants with greater vasodilation responses at the forearm also tended to have the greater responses at the sacrum.

The spectral analysis of the LDF signal during resting and heating at the forearm and sacrum allowed further investigation of the regulation of skin blood flow. The initial spectral analysis considered the frequencies associated with both local and systemic skin blood flow control mechanisms. In the resting flux, there was a significantly higher absolute power 0-0.2Hz in the LDF signal at the sacrum compared to the forearm, and the power of each of the frequency bands were also higher. However, the relative power of the bands showed that the low frequency bands (0.01Hz (endothelial control), 0.04Hz (neurogenic control), 0.1Hz (myogenic control)) were significantly higher at the forearm and there was no significant difference between the sites in the relative power of the frequency bands related to cardiac rhythm and respiratory function. The results showed that at both, the forearm and sacrum sites, the increase in absolute power 0-2Hz during local heating was mainly due to an increase in the 1Hz frequency which originates from cardiac rhythm.

The spectral analysis considering only the local mechanisms up to a maximum frequency of 0.2Hz, showed that the absolute power between 0 and 0.2Hz was significantly lower at the forearm compared to the sacrum. There was no significant difference in the relative power of the frequency bands at the sacrum compared to the forearm

#### 4.5.2 Time domain analysis: Resting and heating flux at the forearm and sacrum

All the participants showed a significant hyperaemic response to a 43 °C heating stimulus at both the forearm and the sacrum site (*Figure 4.4*).

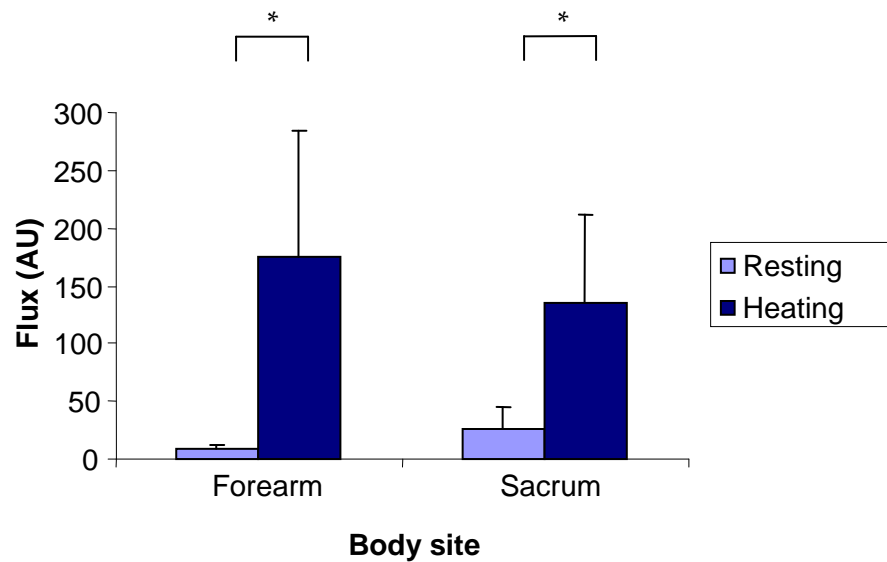


**Figure 4.4** A bar graph to show the resting flux measured for 20 minutes and the flux during 20 minute heating to 43 °C at the forearm and sacrum body sites. The data represent median  $\pm$  IQR range for non-smoker participants (n=9). The difference between resting and heated flux was significant at the both the forearm and sacrum ( $p < 0.05$ ) and is shown on the graph by \*.

### ***Resting flux***

The resting flux over 20 minutes was  $8.9 \pm 2.0$ AU and  $26.7 \pm 15.7$ AU at the forearm and sacrum respectively (median  $\pm$  IQR) (*Figure 4.5*). There was a significantly higher resting flux at the sacrum compared to the forearm, where  $p=0.012$  (Wilcoxon signed ranks test).

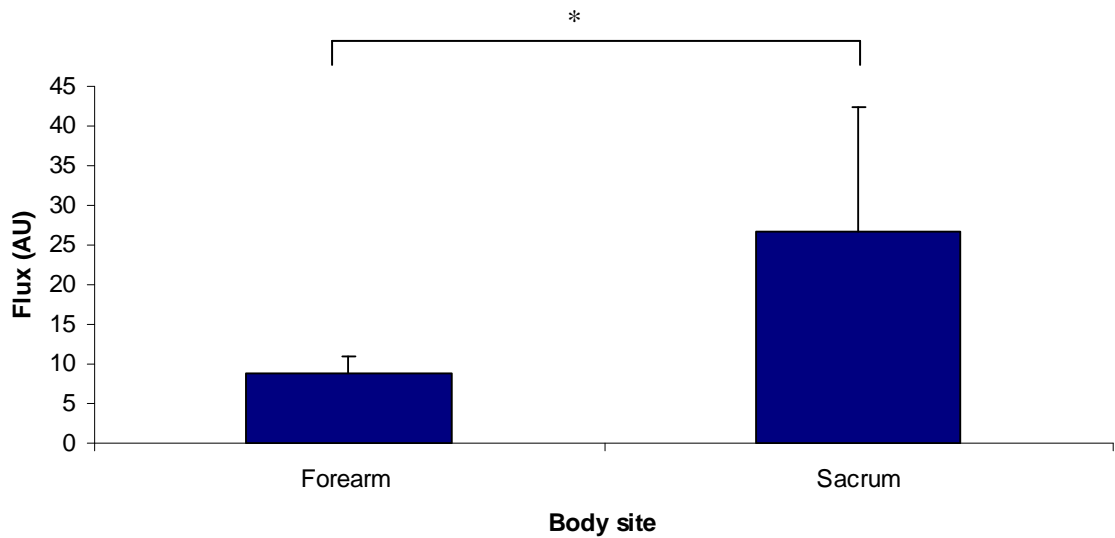


**Figure 4.5** A bar graph to show resting flux measured at the forearm and the sacrum of 9 healthy participants over a 20 minute period (n=9). The bars represent the median and the error bars represent the IQR.\* represents a significantly higher resting flux at the sacrum compared to the forearm, where  $p < 0.05$ , tested using the Wilcoxon signed ranks test.

### ***Maximum hyperaemia***

The maximum hyperaemic flux was  $230.4 \pm 102.6$  and  $175.9 \pm 70.3$ AU at the forearm and sacrum respectively. The maximum hyperaemic flux was significantly greater at the forearm compared to the sacrum, where  $p=0.011$  (Wilcoxon signed ranks test). However, the increase in flux from the resting flux is considered to be a more accurate measure.

***Increase in flux from resting to maximum hyperaemia***

The forearm and sacrum showed an increase in flux from resting to maximum hyperaemia of  $221.9 \pm 80.4$  AU and  $144.8 \pm 62.6$  AU (median  $\pm$  IQR), respectively (*Figure 4.6*). The increase in flux to maximum hyperaemia was significantly greater at the forearm compared to the sacrum, where  $p=0.017$  (Wilcoxon signed ranks test).

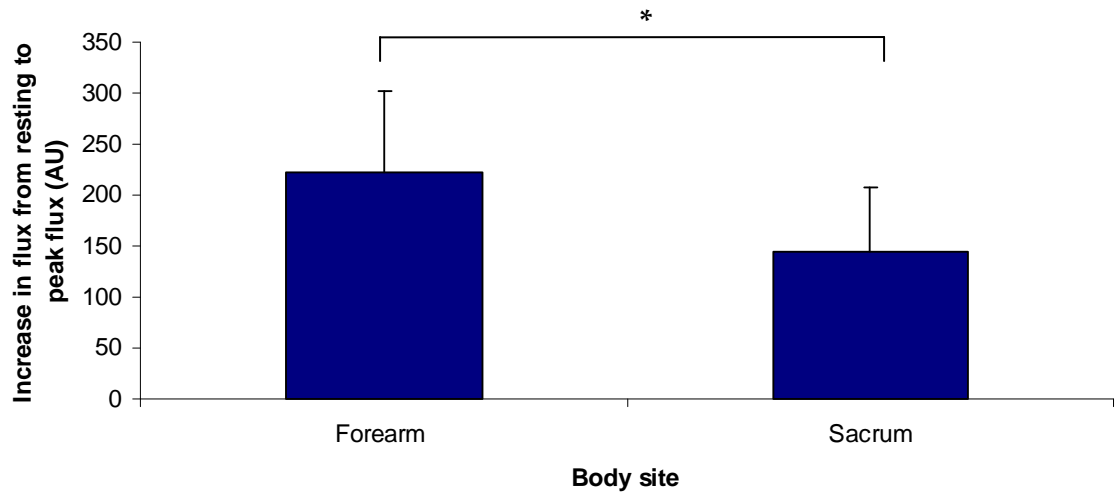


***Figure 4.6*** A bar graph to show increase in flux from resting to maximum hyperaemia measured at the forearm and the sacrum of 9 healthy participants as a result of a 20 minute heating stimulus (n=9). The bars represent the median and the error bars represent the IQR.. \* represents a significantly smaller increase in flux from resting to local heating flux at the sacrum compared to the forearm, where  $p < 0.05$  (Wilcoxon signed ranks test).

***Area under the curve during 20 minute local heating***

The area under the hyperaemia curve during the 20 minute heating was  $21.0 \pm 7.6 \times 10^4$  AU.sec and  $16.2 \pm 3.5 \times 10^4$  AU.sec at the forearm and sacrum respectively (median  $\pm$  IQR) (Figure 4.7). The AUC was significantly smaller at the sacrum compared to the forearm where  $p=0.011$  (Wilcoxon signed ranks test).

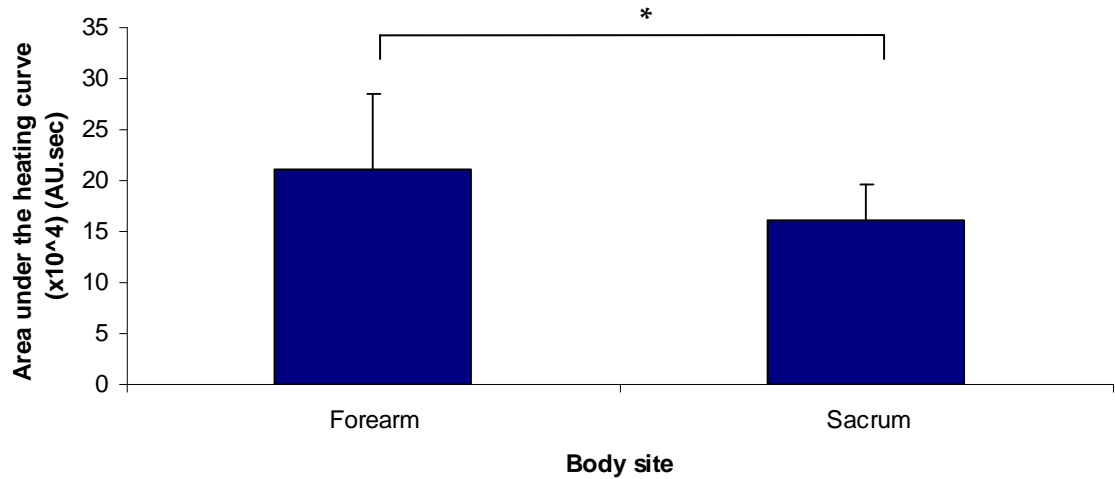


***Figure 4.7*** A bar graph to show area under the hyperaemia curve induced by local heating to 43°C for 20 minutes at the forearm and sacrum sites in 9 healthy control participants. The bars represent the median and the error bars represent the IQR. The area under the curve during the 20 minute heating was significantly smaller at the sacrum compared to the forearm analysed by the Wilcoxon signed ranks test ( $p<0.05$ ); this is shown on the graph by \*

### ***Time to 50% recovery***

The time taken for the skin blood flux to recover from heating was measured from the end of the heating period until blood flow had reduced towards resting flux by 50% at the forearm and sacrum (*Figure 4.8*). The time to 50% recovery at the forearm was  $825.9 \pm 559.9$  seconds compared to  $545.2 \pm 262.9$  seconds at the sacrum (median  $\pm$  IQR). The time taken for the skin blood flux to recover by 50% was significantly smaller in the responses at the sacrum site where  $p=0.012$  (Wilcoxon signed ranks test).

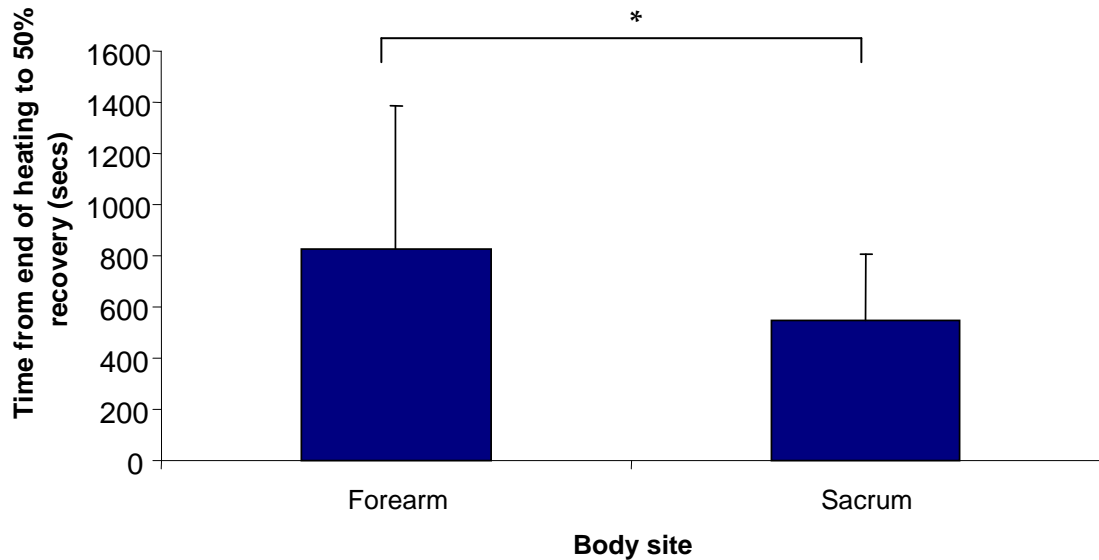


**Figure 4.8** A bar graph to show the time from the end of local heating to 50% recovery towards resting flux in 9 healthy participants at the forearm and sacrum ( $n=9$ ). The bars represent the median and the error bars represent the IQR. The time taken to reach 50% recovery was significantly shorter at the sacrum compared to the forearm, ( $p<0.05$ ), analysed using the Wilcoxon signed ranks test, and this is shown on the graph by \*.

### **4.5.3 Correlations between heating responses at the skin of the forearm and sacrum**

The forearm is an accessible location for the evaluation of skin blood flow responses, however it is important to consider whether the responses at the forearm can provide information regarding the microvasculature at a remote ‘at risk’ site, such as the sacrum.

The studies exploring any correlations between the forearm and sacrum sites were completed in the group of 9 healthy, non smoker participants. The initial analysis showed that there was not a significant correlation between the resting flux at the forearm and sacrum sites.

***Area under the hyperaemia curve during 20 minutes heating***

The AUC during the 20 minute heating period was analysed using Spearman's rho correlation test to consider whether there was a significant correlation between the forearm and sacrum site (*Figure 4.9*). The correlation between the forearm and sacrum total heating response was significant where  $p=0.01$ . This showed that the participants with a greater hyperaemic response at the forearm tended to have a greater response at the sacrum also.

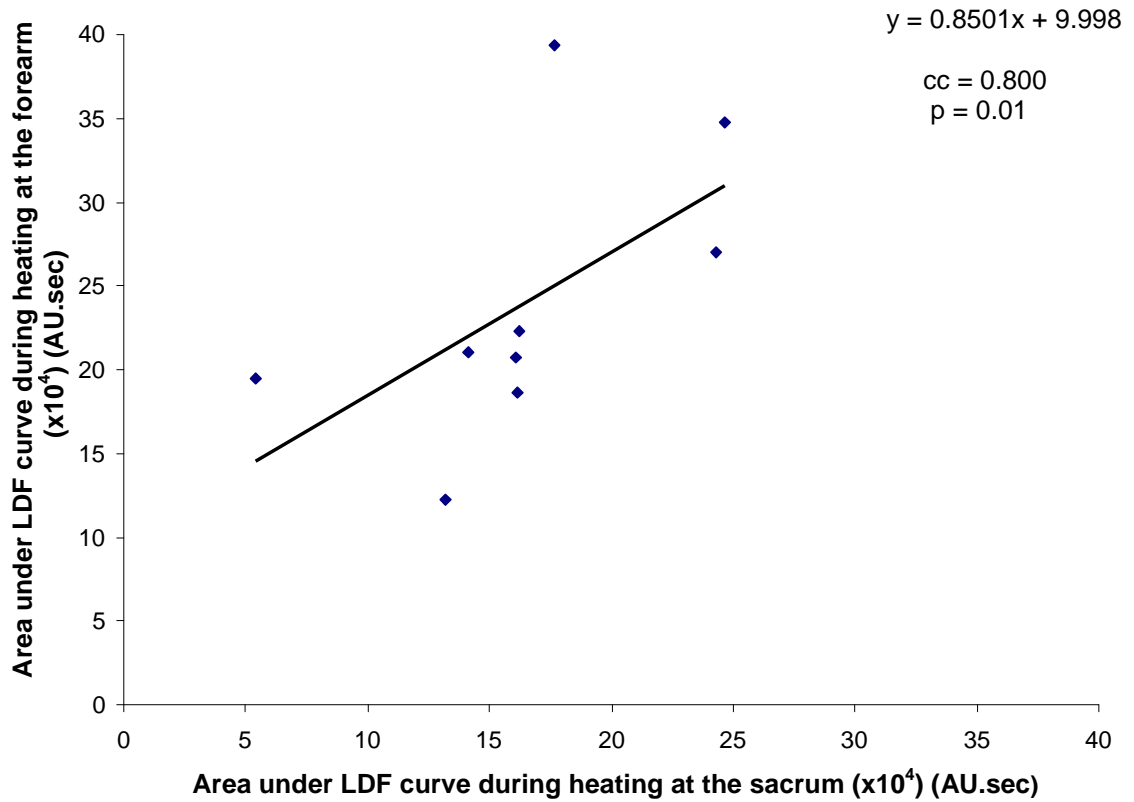


***Figure 4.9*** A scatter graph to show the correlation between the total heating responses as measured by AUC of the hyperaemia curve at the forearm and sacrum sites in the group of 9 healthy control participants. The correlation is significant where  $p<0.05$ , when analysed using Spearman's rho non-parametric correlation test. The Spearman's rho correlation coefficient (CC) = 0.800, significance = 0.01. The correlation shows that those with a higher AUC during heating at the sacrum tend to also showed a higher AUC during heating at the forearm.

### ***Maximum hyperaemia at the forearm and sacrum***

There was no significant correlation between increase from resting to maximum hyperaemia at the forearm and sacrum and only a weak correlation when considering the maximum hyperaemic response at the forearm and sacrum sites, which nearly reached significance, where the correlation coefficient = 0.650 and  $p=0.058$  (Spearman's Rho test).

### **4.5.4 Spectral domain analysis: Spectral analysis of the resting and local heating responses at forearm and sacrum between 0 and 2Hz.**

Spectral analysis was completed on the LDF traces from the participants involved in the previous sections of this chapter, using a FFT. The power was estimated for the frequency range 0 to 2Hz, which is thought to originate from both systemic and local mechanisms of blood flow control.

### ***Resting flux***

The absolute power between 0 and 2 Hz in the resting flux of the sacrum was significantly higher than in the resting flux of the forearm, where  $p=0.021$  (Wilcoxon signed ranks test) (*Figure 4.10*)

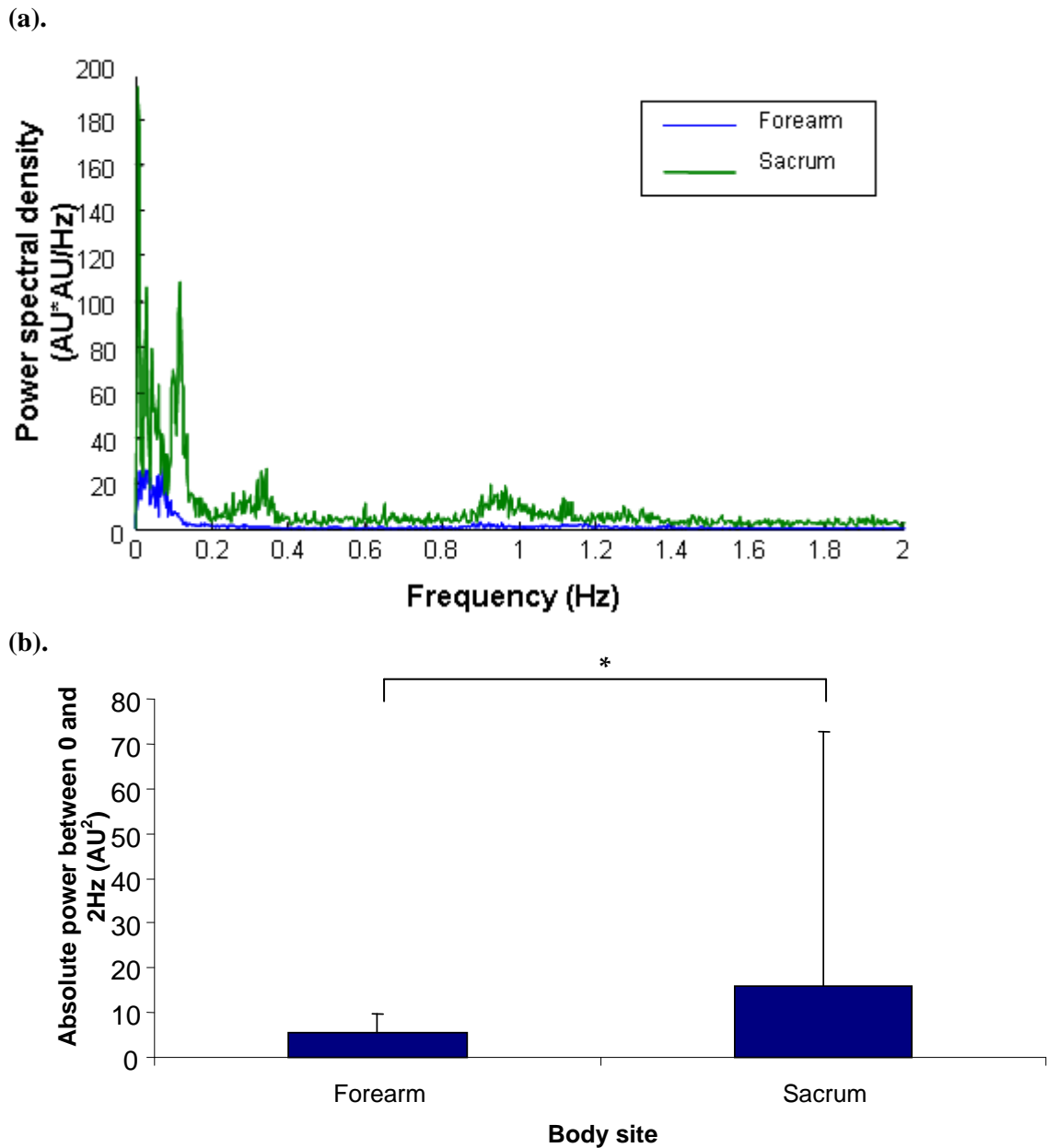


**Figure 4.10** Graphs to represent the absolute PSD between 0 and 2Hz in the resting flux of 9 healthy participants at the forearm and sacrum. **(a)**. A spectrum to show the median PSD of the LDF resting flux measured using Matlab<sup>®</sup> software; PSD is expressed as AU<sup>2</sup>/Hz. **(b)**. A bar chart to show the absolute power between 0 and 2Hz, expressed as AU<sup>2</sup>, of the resting flux at the forearm and sacrum; the data are median +IQR. The absolute power between 0 and 2Hz was significantly higher in the resting LDF at the sacrum compared to the forearm, where  $p=0.021$  (\*) (Wilcoxon signed ranks test).

The absolute power of the individual bands was lower in the resting flux at the forearm compared to the sacrum and this attained significance for the bands around 0.1Hz, 0.4Hz and 1Hz. However, when the power in each band was considered relative to the absolute power, the forearm had a significantly greater relative power in the bands around 0.01Hz, 0.04Hz and 0.1Hz compared to the sacrum (*Figure 4.11*)

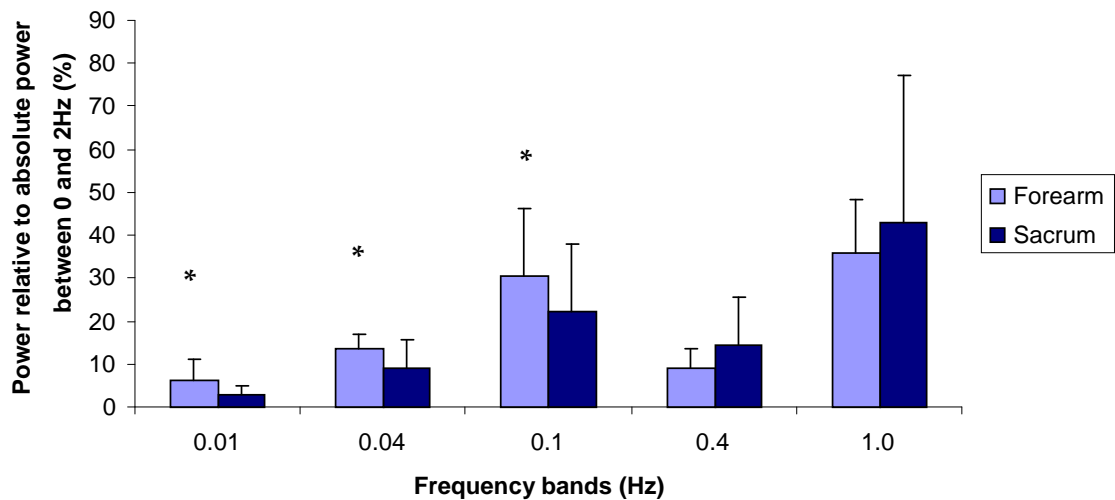
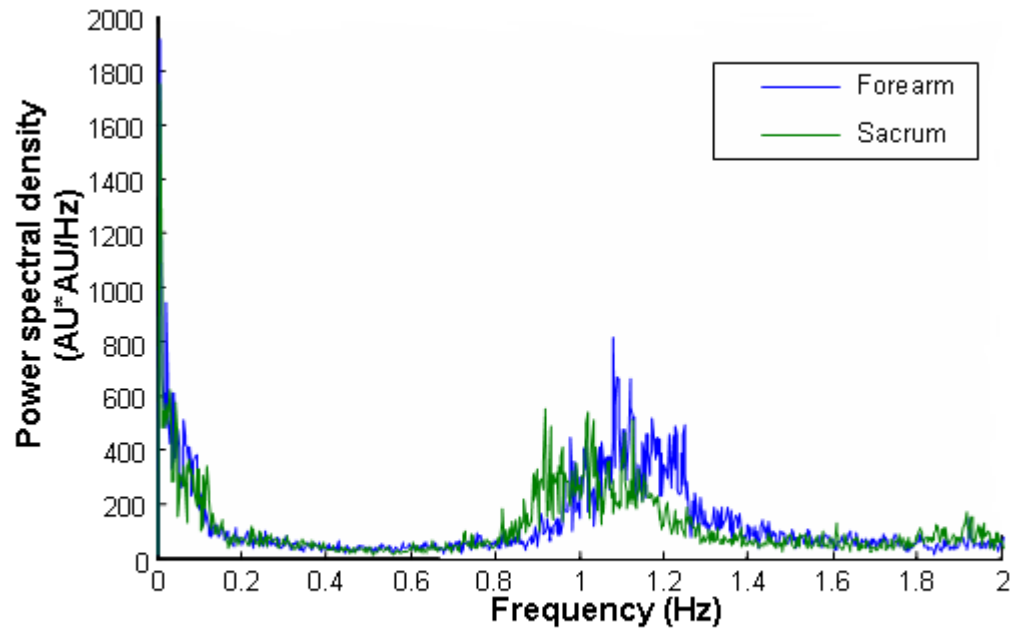


**Figure 4.11** A bar graph to show the relative power for each of the 5 frequency bands within the frequency range 0-2Hz measured in the resting LDF traces from 9 healthy participants at the forearm and the sacrum. The bars represent the median +IQR. The relative power in the frequency bands ~0.01Hz (0.008-0.02Hz), ~0.04Hz (0.02-0.05Hz) and ~0.1Hz (0.05-0.15Hz) in the LDF signal were significantly higher at the forearm compared to the sacrum where  $p=0.03$ ,  $0.04$  and  $0.04$ , respectively (Wilcoxon signed ranks test). This is shown on the graph by \*. The relative power of the frequency bands ~0.4 (0.15-0.4Hz) and ~1Hz (0.4-2Hz) were higher in the flux traces from the sacrum, but this did not reach significance

### **Heating Flux**

The spectral analysis was performed on the LDF trace during local heating. There was no significant difference in the absolute power between 0 and 2Hz or the relative power of the 5 frequency bands when comparing the forearm and the sacrum (*Figure 4.12*).

(a).



(b).

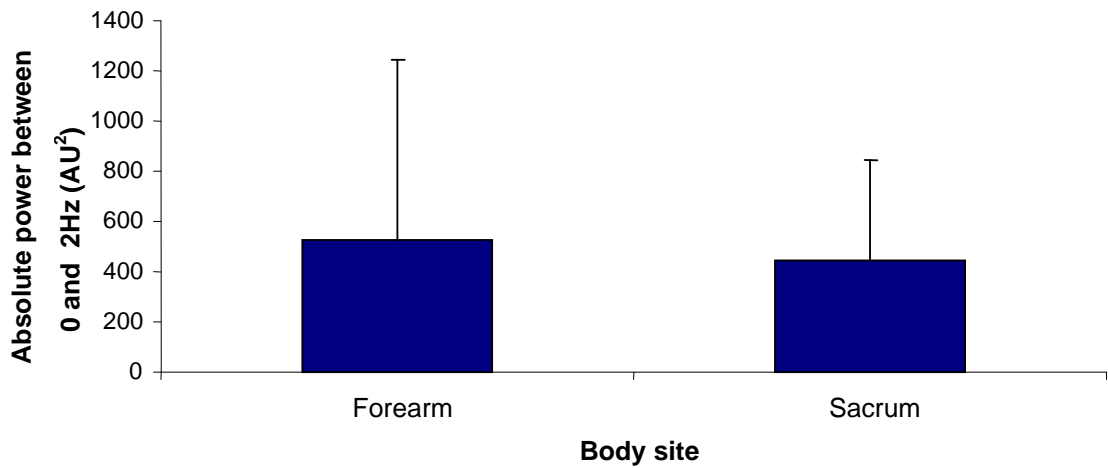


**Figure 4.12** Graphs to represent the absolute PSD between 0 and 2Hz of the flux during 20 minutes local heating to 43°C from 9 healthy participants at the forearm and sacrum. (a). A line graph to show the median PSD of the LDF heated flux (AU<sup>2</sup>/Hz). (b). A bar chart to show the power of the heated flux between 0 and 2Hz at the forearm and sacrum; the bars represent the median and the error bars represent the IQR. There was no significant difference in the absolute power between the heated flux traces from the forearm and the sacrum

### ***Changes in relative power of the frequency bands from resting to heated flux***

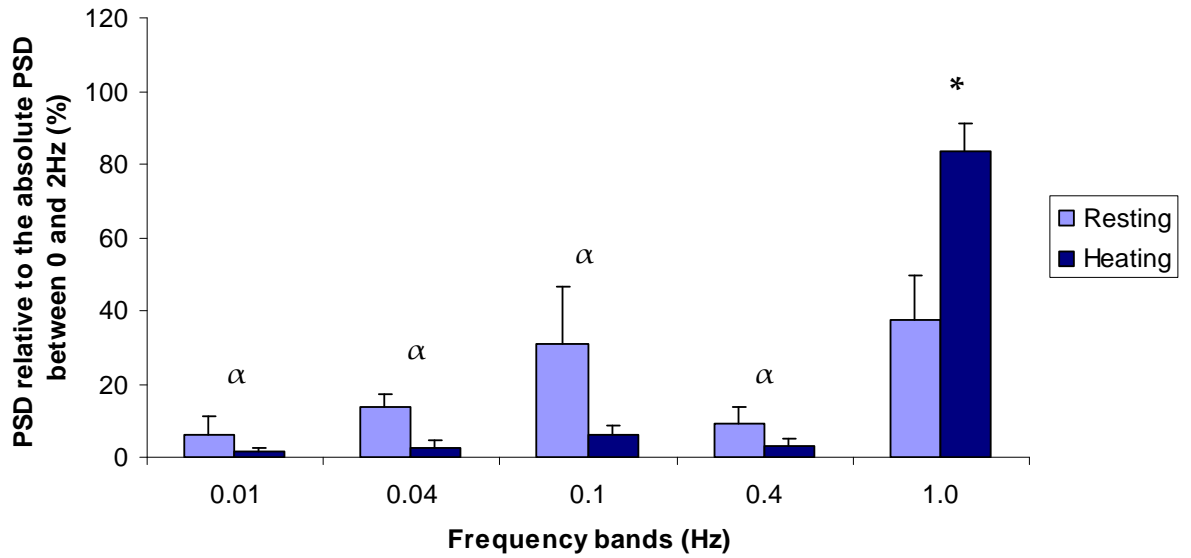
The local heating stimulus caused an increase in flux in all participants and this also resulted in an increased absolute power between 0 and 2. The power between 0 and 2Hz and also within each of the 5 frequency bands was significantly greater during heating compared to resting flux at both sites.

The relative power of each of the bands (power of the band divided by absolute power between 0 and 2Hz) revealed that the contribution of the 1Hz frequency within the signal, corresponding to the cardiac signal increased significantly during the heating stimulus at both the sacrum and forearm. This suggests that the cardiac component of skin blood flow control has an important role in increasing skin blood flow during local heating at the skin.

At the forearm, the relative power (relative to absolute power between 0 and 2Hz) of the frequency ~1Hz which originates from the cardiac rhythm increases significantly from  $37.4 \pm 12.4\%$  (median  $\pm$  IQR) during resting to  $83.6 \pm 7.3\%$  during heating (*Figure 4.13A*). At the sacrum, the relative power of the frequency band ~1Hz increased significantly from  $43.0 \pm 34.2\%$  during resting to  $86.1 \pm 14.8\%$  during heating (*Figure 4.13 B*).

The relative power of the frequency bands ~0.01Hz, ~0.04Hz, ~0.1Hz and ~0.4Hz, which relate to endothelium, neurogenic, myogenic and respiratory mechanisms of skin blood flow control respectively, were significantly lower during heating compared to resting at both the forearm and sacrum sites (*Figure 4.13*).

a.



b.

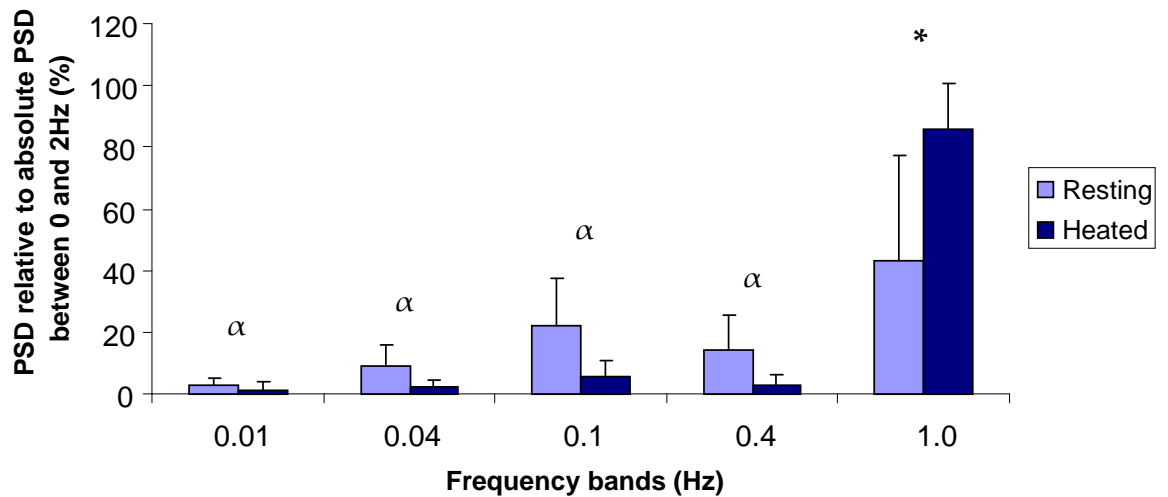


**Figure 4.13** A bar graph to show the relative power (power of band divided by absolute power between 0 and 2Hz) of the frequency bands ~0.01Hz (endothelium), ~0.04Hz (neurogenic), ~0.1Hz (myogenic), ~0.4Hz (respiratory) and ~1Hz (cardiac) of LDF flux during resting and heating at the (a) forearm and the (b) sacrum.

\* represents significant differences where heated > resting

$\alpha$  represents significant differences where heated < resting ( $p < 0.05$ ).

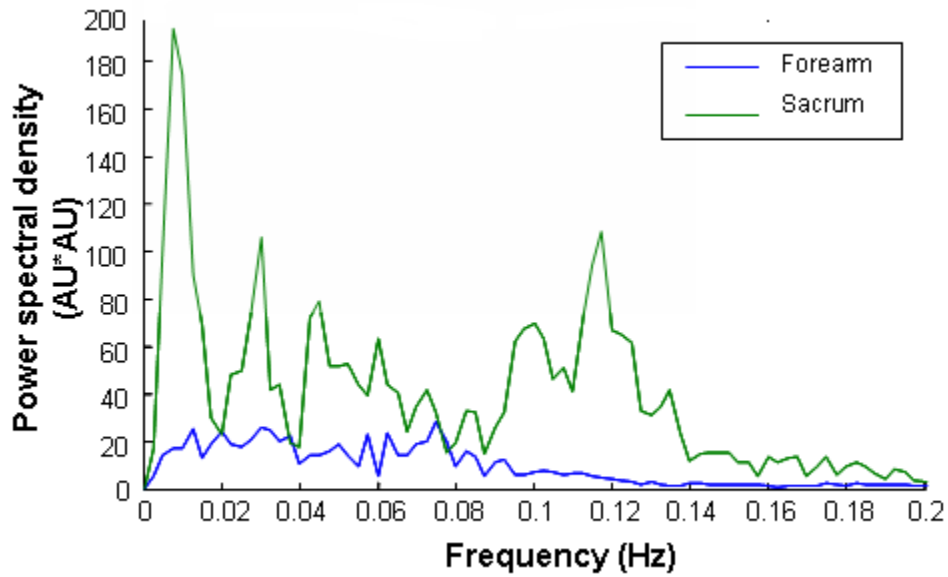
As the local, rather than systemic (respiratory and cardiac) mechanisms of skin blood flow control are the focus of this thesis, spectral analysis will be limited to the lower frequency components (endothelium, neurogenic and myogenic).

#### **4.5.5 Spectral domain analysis: Spectral analysis of the resting and heating flux between 0 - 0.2Hz (local control mechanisms)**

##### ***Resting***

The absolute power between 0 and 0.2Hz, including the frequencies relating to local control mechanisms only, was significantly higher in the resting flux at the sacrum compared to the forearm, where  $p=0.038$ , using Wilcoxon signed ranks test (*Figure 4.14*).

(a).



(b).

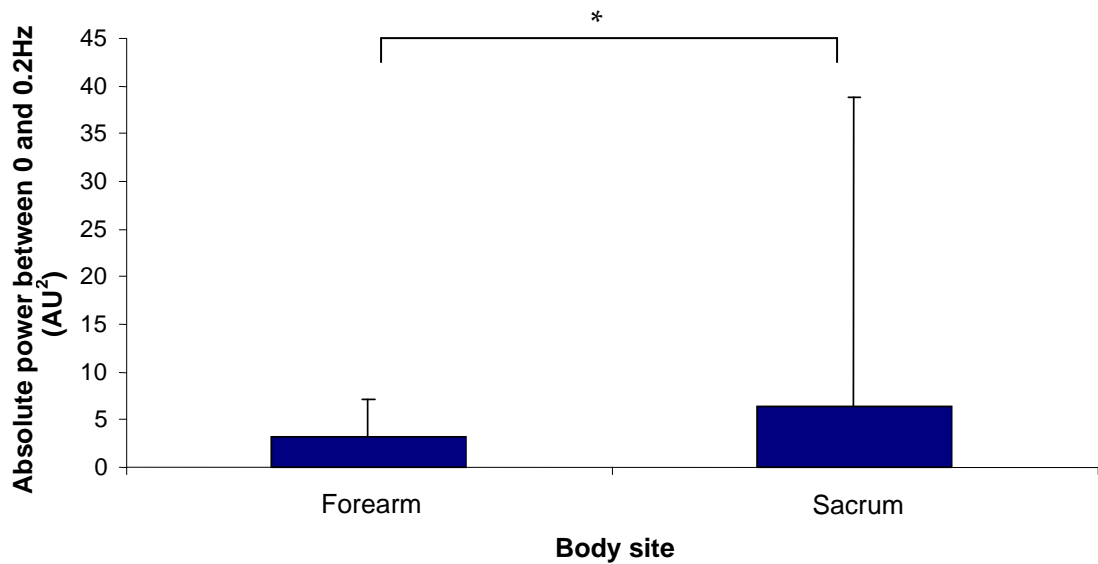


**Figure 4.14** Graphs to represent the PSD between 0 and 0.2Hz in 20 minutes of resting from 9 healthy participants at the forearm and sacrum. **(a)**. A line graph to show the median PSD of the LDF resting flux measured using Matlab<sup>®</sup> software; PSD is expressed as AU\*AU/Hz. **(b)**. A bar chart to show the absolute power of the resting flux at the forearm and sacrum between 0 and 0.2Hz; the bars represent the median and the error bars the IQR. The absolute power was significantly higher in the resting LDF at the sacrum compared to the forearm, where  $p=0.038$  (Wilcoxon signed ranks test) (\*).

The absolute power of the 3 low frequency bands around 0.01Hz, 0.04Hz and 0.1Hz (relative to the absolute power between 0-0.2Hz) was calculated (*Figure 4.15*). There was no significant difference found in the relative power of the frequency bands; the relative power of the band ~0.01Hz was lower at the sacrum than the forearm, and almost reached significance ( $p=0.051$ ).

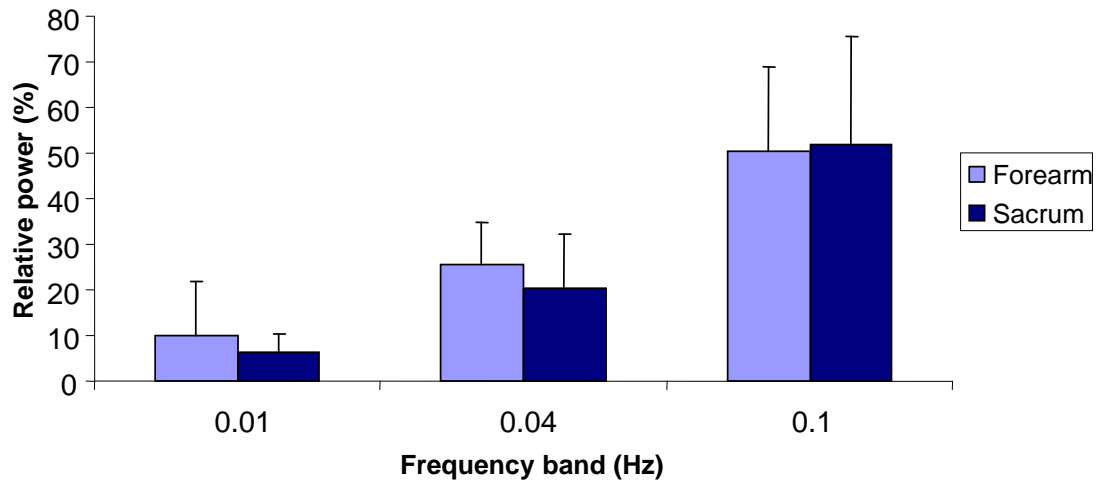
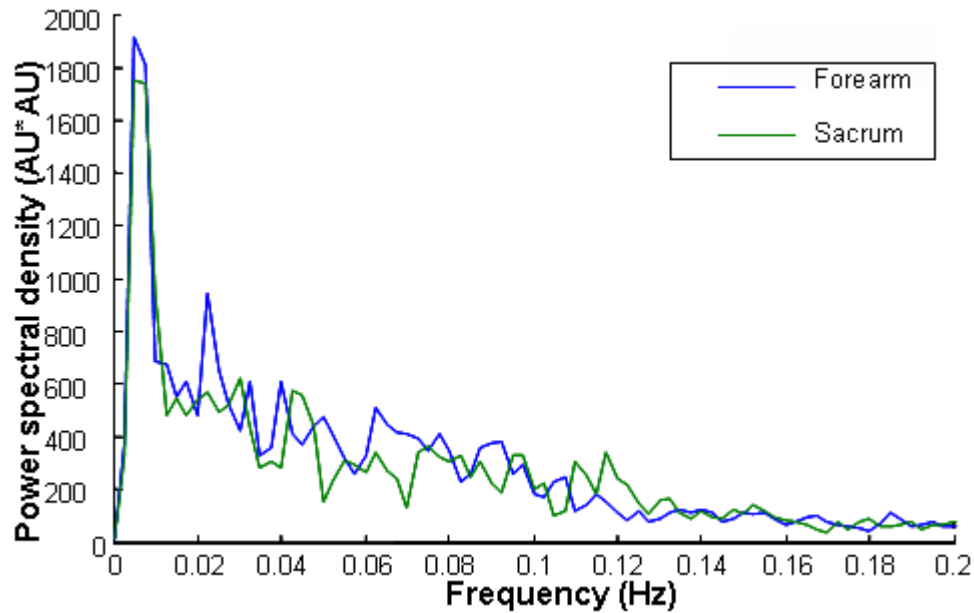


**Figure 4.15** A bar graph to show the relative power of the frequency bands around 0.01Hz, 0.04Hz and 0.1Hz at the forearm and sacrum in 9 healthy participants from 20 minutes of resting flux ( $n=9$ ). The bars represent the median and the error bars are the IQR. There was no significant difference in the relative power in the frequency bands between the resting flux at the forearm and sacrum (Wilcoxon signed ranks test). The relative power at the frequency around 0.01Hz was higher at the forearm, but does not reach significance:  $p=0.051$  (Wilcoxon signed ranks test)

### **Heating**

There was no significant difference in the absolute power between 0 and 0.2Hz or the relative power of the 3 frequency bands measured in the heated flux at the sacrum compared to the forearm, using Wilcoxon signed ranks test (*Figure 4.16*).

(a).



(b).

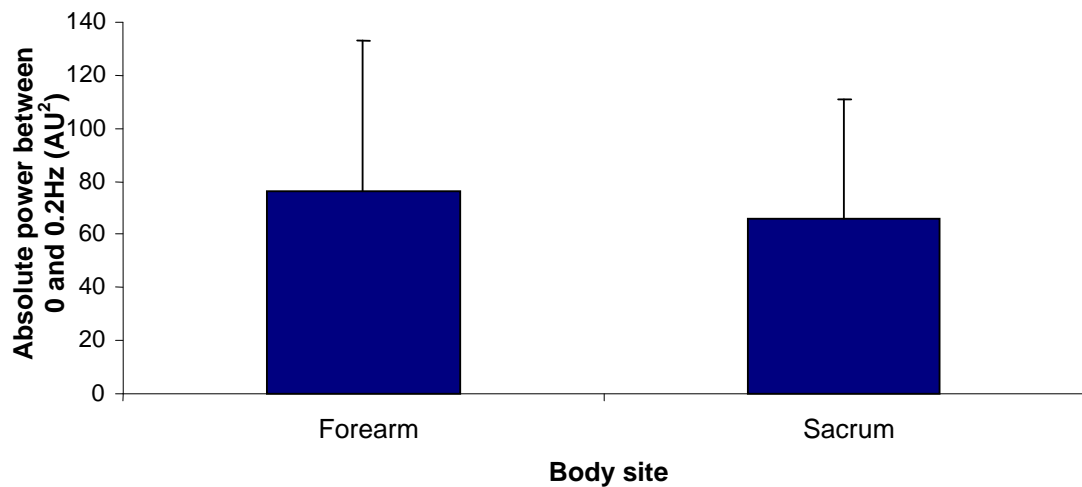


**Figure 4.16** Graphs to represent the absolute PSD between 0 and 0.2Hz in 20 minutes of heated flux (43°C) from 9 healthy participants at the forearm and sacrum. **(a)**. A line graph to show the median PSD of the LDF heated flux measured using Matlab<sup>®</sup> software; PSD is expressed as AU\*AU/Hz. **(b)**. A bar chart to show the power of the heated flux at the forearm and sacrum (AU<sup>2</sup>); the bars represent the median and the error bars represent the IQR. There was no significant difference in the absolute power in the heated LDF trace at the sacrum compared to the forearm (Wilcoxon signed ranks test).

### ***Change in relative power from resting to heating***

At both the forearm and sacrum, the absolute power 0-0.2Hz and the absolute power of each of the bands increased significantly during the heating response compared to at rest. However, the relative power of each frequency band during resting and heating were not significantly different either at the forearm site or the sacrum site.

In the heated flux at the sacrum, the relative power of the band ~0.1Hz (myogenic) to the absolute power between 0-0.2Hz was smaller during heating compared with at rest, but this did not quite reach significance ( $p=0.051$ ) (*Figure 4.17*).

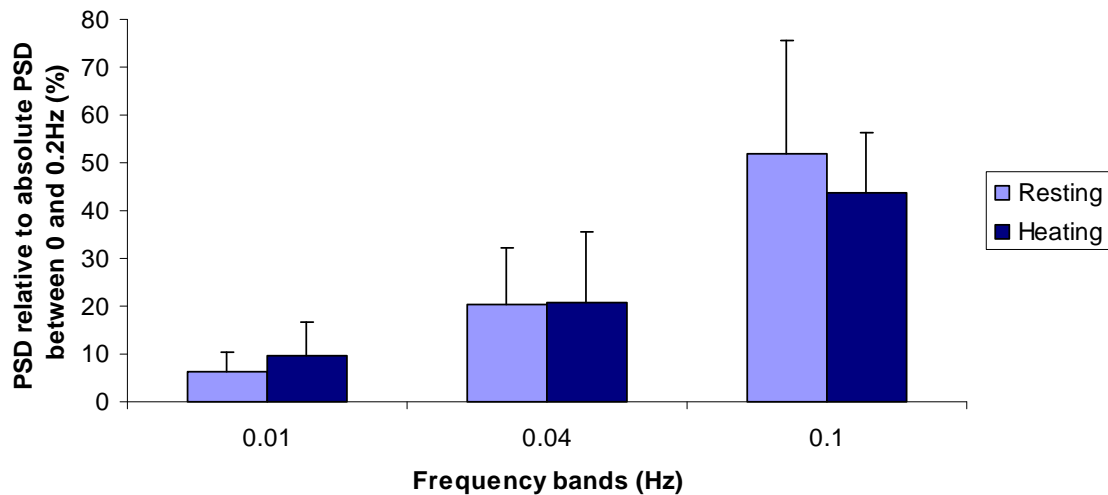


**Figure 4.17** A bar graph to show the relative power of the frequency bands around 0.01, 0.04 and 0.1Hz from the 20 minutes resting flux and 20 minutes heating flux at the sacrum of 9 healthy participants; the relative power is calculated by absolute power of band divided by absolute power between 0 and 0.2Hz, expressed as %. The bars represent median and the error bars represent the IQR. There was no significant difference between the groups as tested by the Wilcoxon signed ranks test.

### ***Summary of key findings***

- The sacrum has a significantly higher resting skin blood flow and a significantly smaller vasodilation response to local heating compared to the forearm skin site.
- The spectral analysis of the resting LDF signal showed a significantly higher power in the LDF signal at the sacrum, but the relative power of the bands around 0.01Hz (endothelial control), 0.04Hz (neurogenic control), 0.1Hz (myogenic control) were significantly higher at the forearm.

- There were no site differences in the spectral analysis of the local heating response.

#### **4.6 Discussion**

The sacrum is a body site known to be at risk of pressure ulcer development. Although this is considered to be due to the presence of a bony prominence, the regulation of the skin microcirculation may also be important due to its significant role in maintaining skin health. Studies have shown there to be a difference in the architecture of the skin microcirculation at the sacrum compared to other body sites. The local heating stimulus was used in the studies in this chapter to in order to consider vascular responsiveness and skin blood flow regulation at the sacrum site and a reference site, the forearm.

The median resting skin blood flux measured at the sacrum of participants was approximately 3 fold greater than the resting skin blood flux at the volar surface of the forearm. In another study, blood flow over the sacrum, posterior sites such as lower back and also remote sites such as hands and fingers were measured using LDI. They showed the sacrum to have a greater resting flux compared to the other sites (Mayrovitz et al., 2002). They found sacral skin blood flow to be 13.7% greater than gluteal flow and 21.3% greater than lower back skin blood flow (Mayrovitz et al., 2002). There has been a suggestion that as the skin tissue at the sacrum is used to higher levels of perfusion, any reduction or occlusion in flow could be potentially more damaging as the tissue relies on higher levels of skin blood flow relative to other sites (Mayrovitz et al., 2002)

The structure of the skin microvasculature at the sacrum may be a reason for the higher resting flux. In a study to consider the structure of skin tissue excised post-mortem from different body sites, it was found that sacral skin had more numerous blood capillary loops than other sites, such as gluteal skin and ischeal skin (Hagisawa et al., 2001). Thus the higher density of capillaries may mean that there is also a higher density of red cells flowing and thus LDF measurements are greater. It was also found that the temperature measured by the heater block at the end of the resting period was higher at the sacrum compared to the forearm. As far back as 1975, a study was completed using thermal imaging to measure temperature at many anatomical sites and particularly at sites at high risk of pressure ulcer development. They found that these high risk sites, including the sacrum, had significantly higher resting temperature (Trandel et al., 1975). However, another study, using LDI to measure skin blood flow found that although the sacrum had greater resting blood flow, it also had a lower skin temperature than the other sites measured (Mayrovitz et al., 2002).

The skin blood flow at the forearm and sacrum sites increased significantly with the local heating stimulus. The skin blood flow increased from resting flux  $24.9 \pm 12.6$  fold at the forearm and  $6.9 \pm 6.8$  fold at the sacrum. The increase in skin blood flux during local heating and the area under the curve of the local heating response, which represents the total response, were significantly smaller at the sacrum compared to the forearm. The time taken for the flux to recover by 50% from maximum hyperaemia was also significantly reduced at the sacrum.

There are many studies that have considered the hyperaemic response to local heating in different participants groups using LDF (Nicotra et al., 2004; Minson et al., 2002). However, the studies have differences in study design including length of heating, local temperature applied, gradual or step-wise heating and also differences in the measurements of the response. A study considered the maximum response, measured as the maximum at the initial peak vasodilation, at the hand and foot of participants as a result of local heat to  $44^{\circ}\text{C}$  applied to the skin for 15 minutes. The maximum flux of the initial peak was  $259 \pm 73\text{AU}$  and  $205 \pm 92\text{AU}$  at the hand and foot, respectively. These findings are similar to those in the studies in this chapter, although the maximum flux was not always in the initial peak in the measurements in this chapter; the maximum flux at the forearm was  $230.4 \pm 102.6$  and at the sacrum  $175.9 \pm 70.3\text{AU}$ .

The results from the studies in this chapter showed that the skin microcirculation at the sacrum had a smaller capacity to vasodilate and maintain that vasodilation compared to the forearm site. The increased subcutaneous fat at the sacrum, as well as higher density of collagen and elastin (Hwang et al., 2001) could mean that that the heating had a reduced effect on skin blood flow. The higher temperature of the local heater at the start of heating at the sacrum also meant that the increase in temperature was smaller at the sacrum and thus the time to reach the  $43^{\circ}\text{C}$  was on average 17 seconds faster; this was 78 seconds at the sacrum and 95 seconds at the forearm site. The median rate of increase in block temperature from start of heating was 0.15 degrees/sec and 0.12 degrees/sec at the forearm and sacrum respectively (*Chapter 2, Section 2.4.1*).

A potentially important difference between the forearm and sacrum skin sites is the amount of stress in terms of loading and unloading that the sites endure. The sacrum undergoes repeated loading and unloading during the daily events of sitting and lying. Other animal studies have shown reduced vasodilation responses at sites where there had previously been prolonged periods of ischaemia (Herrman et al., 1999). The structure of the skin tissue and the microcirculation at the sacrum may be altered due to the increased stress on the skin at that site.

The total response at the sacrum site measured by the area under the hyperaemia curve correlates significantly with the forearm site. Although the responses were significantly different at the sites, the responses correlated in their intensity in the participants. Thus, the assessment of forearm cutaneous vasoreactivity may reflect the skin microcirculation at other body sites. As with the emerging use of skin blood flow responses as a possible marker for other organ damage (Rossi et al., 2006a), potentially measurement of skin blood flow responses at an accessible site could provide information regarding all skin sites. Although Li et al. (2006a) found that there were differences in the density of capillaries at different body sites, they found that consistently at all 4 body sites (crow's feet, dorsum of hand, volar forearm and forehead) the skin blood flow increased with ageing. They also found that the skin blood flow at the sun-exposed sites had significantly higher skin blood flow than the photo-protected volar forearm. In this study, the two sites investigated, the forearm and sacrum, are both photo-protected, so neither have the additional effect of sun exposure to effect the findings.

The mechanisms of the regulation of skin blood flow were investigated in the resting and heated flux at the forearm and sacrum using spectral analysis. In the resting flux, the absolute power both 0-2Hz and 0-0.2Hz was significantly higher at the sacrum compared to the forearm. This follows the significantly higher flux present during rest at the sacrum. The relative power of the individual frequency bands in the resting flux showed that there was significantly greater relative power in the frequencies related to the endothelium, neurogenic and myogenic control of skin blood flow at the forearm compared to the sacrum.

Although the vasodilation responses to the local heating stimulus at the sacrum were significantly reduced compared to the forearm, spectral analysis did not provide any further information regarding the mechanism of this. There were no significant differences in the absolute power, the absolute power of the individual frequencies, or the relative power of the frequencies during the local heating induced hyperaemia at the forearm and the sacrum sites. It may be that there are no differences in the skin blood flow control mechanisms as the vasoreactivity is adequate for that particular skin tissue.

The local heating of the skin resulted in vasodilation and thus increased absolute power in the heated LDF signal compared to the resting LDF signal. The spectral analysis showed the increase in flux during heating to mainly due to a significant increase in the relative power at 1Hz related to cardiac rhythm. As the microcirculatory flow into capillaries via arterioles is driven by the force of the heartbeat (Hsiu et al., 2008), the dilation of the vessels in the microcirculation may cause this

propelling force to be more evident in the LDF signal during local heating. This then increases the power of the 1Hz frequency during local heating in the LDF signal.

The forearm skin site showed no patterns when comparing the change in regulation of skin blood flow from resting to heating. However, at the sacrum, there was an increase in endothelium frequency and decrease in myogenic frequency compared to resting flux but this did not reach significance. This shows a similar pattern to some other studies. Other studies considering spectral analysis of the local heating response have found the relative contribution of the frequency band around 0.01Hz (related to the endothelium) to be increased with heating at the sacrum (Geyer et al., 2004). The endothelium related frequency has also been shown to be significantly more dominant than the frequency around 0.1Hz related to the myogenic control during heating (Jan et al., 2009) and more dominant during heating induced vasodilation compared to loading induced vasodilation (Brienza et al., 2005). However, these studies used Wavelet analysis to complete the spectral analysis, so in that way differ from the use of FFT in the studies in this thesis. Only the study by Jan et al. (2009), used a heating pattern similar to this study which resulted in a bi-phasic heating response; the studies by Geyer et al. (2004) and Brienza et al. (2005) both used a significantly slower gradual application of the heating stimulus which did not result in the 2 phase response. The pattern of the application of the heating stimulus is considered to effect the regulation of the local heating induced vasodilation.

### ***Limitations***

The sample size for the studies in this chapter was appropriately powered for the time domain analysis. However, the smaller differences and higher variation in the spectral analysis might have required larger sample to be able to determine any differences between the forearm and the sacrum.

The skin blood flow measurements were always completed at the forearm prior to the sacrum. It was important that there was a period of acclimatisation with the participants in a prone position; however, the prolonged studies at the forearm site may have affected the sacral studies. Also, at both skin sites, the local heating probe was switched off during resting flux, but its presence meant that the skin heated up under the probe. This resulted in a significantly higher temperature at the sacrum compared to the forearm at the end of the resting period. It may be important to fix the temperature of the probe during resting measurements in future studies. There was huge variability in the resting flux at the sacrum, which could be due to variations in the thickness of the skin or distribution of fat tissue at the sacrum in the participants involved.

It is important to acknowledge the potential limitations of the spectral analysis used to estimate the power of the oscillations within the LDF signal. The different frequency components in the cutaneous microvasculature are considered to be non-constant and they vary with time (Smith, 1997). The LDF signal is a non-stationary signal and any change in time in the signal is spread over the entire frequency interval. In the studies in this chapter the steep increase in flux at the start of heating was removed and the resting flux and heating flux were analysed separately, to avoid any spread over the frequencies. Also, the LDF signal was detrended before analysis occurred. Finally, it has also been suggested that the bandwidths used to determine the different frequencies may be changed by the local heating stimulus, so the assumption has to be made that the bands used are reflective of the mechanisms expected.

### ***Final summary***

The studies in this chapter have shown that the forearm and sacrum skin sites exhibit a different magnitude of resting skin blood flow and also respond differently to a local heating stimulus. The sacrum site had a higher resting flux and smaller response to local heating compared to the forearm site. These differences may be a factor in increasing the risk of developing pressure ulcers at the sacrum site. The results showed that the local heat-induced hyperaemic response at the forearm did correlate significantly with the responses at the sacrum in the individual participants. However, the correlation must be interpreted with caution due to the small number of participants.

This thesis is focusing on the potential development of an objective measure of the skin microcirculation and its control mechanism as a way to determine risk of pressure damage. Although this chapter has demonstrated differences between the forearm and an at risk site, the sacrum, it is important to consider that alterations in the control mechanisms of skin blood flow have the potential to be detected at any skin site measured. For example, the effects of smoking on the endothelium control of skin blood flow can potentially be measured using spectral analysis in the LDF signal of the skin microcirculation, at any skin site in the smoker participants. The forearm is a more accessible site for further studies and also a more acceptable site when considering the development of an objective measure for risk assessment for potential use on patients in hospital. Thus, the remaining studies in this thesis will use the forearm as the site for analysis.

## **Chapter 5**

### **The cutaneous vascular response to local heating in heavy smokers and light/moderate smokers**

## 5.1 Introduction

Skin blood flow is essential for the maintenance of cutaneous viability and health. Tissue breakdown, specifically pressure ulcer development, results from an inadequate cutaneous vascular perfusion, known to be caused by external forces such as pressure, friction and shear. The risk of developing a pressure ulcer may be increased by factors, such as smoking and ageing which alter the vascular responsiveness and the mechanisms regulating the control of skin blood flow. Thus the measurement of vascular responsiveness and its control mechanisms could be a potential objective measurement of pressure ulcer risk.

The studies in this chapter will investigate the skin blood flow response to a local heating stimulus in a group of heavy smokers and their matched non-smoking controls and light/moderate (LM) smokers and their matched non-smoking controls. The studies will be completed at the forearm site in all participants. The studies in chapter 4 demonstrated the heterogeneity of the skin microvasculature; the resting skin blood flow and skin blood flow response to local heating was different at the sacrum, a site at risk for pressure ulcer development, compared to the forearm. However, the magnitude of the local heating induced vasodilation did correlate between the sacrum and forearm skin sites. The participants that showed a smaller response to local heating at the skin of the sacrum also showed a smaller response at the skin of the volar forearm. This would suggest that the volar surface of the forearm is a relevant skin site at which to complete further studies. It is important to be able to use an accessible skin site such as the volar forearm, particularly if studies are to be completed in elderly patients, but also a site where the results are relevant for other potentially at-risk skin sites.

The local heating stimulus used within the studies in this chapter has been shown to be composed of a prolonged plateau vasodilation which is mainly NO, and thus endothelium, dependent. The endothelium lining the blood vessels is important in the regulation of blood flow, particularly in its role in vasodilation of the blood vessels. It also has vital roles in angiogenesis, anti-inflammatory and anti-thrombotic mechanisms. It has been suggested that malfunctioning of these roles are hypothesised to be involved in the pathogenesis of pressure ulceration (Struck and Wright, 2007). The local heating response allows consideration of vasodilation of the skin blood vessels that is known to be endothelium-dependent.

Smoking has been shown to affect the vasoreactivity of the skin microcirculation, potentially due to effects of the products of smoking directly on the endothelium lining of blood vessels. Studies have shown lower level of NO in blood and this is thought to be due to the actions of ROS and also

reduced circulating levels of antioxidants. Thus, the consideration of effects of smoking on the microcirculation enables investigation of a group of participants with potentially altered microcirculation and thus a potentially increased risk of pressure ulcers.

It may be that changes to cutaneous vascular responses can occur early in smoking history. It has been shown that heavy and light smokers have similar resting blood flow (Midttun et al., 2006). A pilot study measuring the skin blood flow response to loading in a group of light smokers demonstrated that changes in vascular responses are present in a people that have been smoking for only a short period (Noble et al., 2003). Barua et al. (2002) also found that heavy and light smoking had similar detrimental effects on endothelial dependent vasodilation and the NO pathway in particular, by investigating flow and nitroglycerin-mediated reactivity of the brachial artery. The effect of 'light' cigarettes, which contain low-nicotine and low-tar, on the coronary microcirculation has also been investigated; the 'light' cigarettes were found to be as hazardous as normal cigarettes (Gullu et al., 2007). This would suggest that smoking has a detrimental effect on the microcirculation.

As well as smoking, ageing is known to have a detrimental effect on the skin and the skin microvasculature. There have been studies in recent years to show that ageing has a detrimental effect on the functioning of the endothelium. A recent study in rats showed that co-factors of NO, such as BH<sub>4</sub>, are reduced with age and this may be the cause of altered NO-mediated microvasculature function (Delp et al., 2008). Thus, both smoking and aging could affect the vasoreactivity of the skin microcirculation through effects on the endothelium, which may result in increased risk of pressure ulcer development.

## **5.2 Hypothesis**

The skin blood flow response to a local heating stimulus is significantly attenuated in both heavy and light smokers compared to their matched controls. In addition it is proposed that the response is further attenuated with advancing age and increasing smoking habit.

### 5.3 Objectives

- To measure the resting skin blood flux and vascular response to a local heating stimulus at the forearm skin site in heavy smokers and compare the responses to matched non-smoking control participants.
- To measure the responses to a local heating stimulus in a younger group of light / moderate (LM) smokers and their non-smoking matched control participants.
- To consider the effects of magnitude of smoking history and age on the responses to the skin heating challenge by comparing the results from the older heavy smokers and younger light smokers.

### 5.4 Methods

#### 5.4.1 Participants

##### *Heavy smoker study*

The heavy smoker participants had smoked cigarettes for longer than 15 years and for more than 10 pack years. They smoked an average of  $18.75 \pm 3.5$  (mean  $\pm$  SD) cigarettes per day and had smoked between 12.5 – 42 packyears (range).

The study was performed on a group of eight healthy smokers and eight healthy matched control subjects. The study was completed at the volar surface of the forearm in each volunteer. The baseline parameters are shown in *Table 5.1*. There were no significant differences between the two groups.

<b>Parameter</b>	<b>Control group (n=8)</b>	<b>Smokers (n=8)</b>
<b>Age (yrs)</b>	46.0 ± 12.9 (34 – 67)	49.6 ± 12.7 (28 – 63)
<b>Sex</b>	5 females / 3 males	5 females / 3 males
<b>Body Mass Index (kg/m<sup>2</sup>)</b>	25.3 ± 3.2 (20.3 – 30)	28.6 ± 6.7 (19.3 – 39.8)
<b>Mean Arterial Pressure (mmHg)</b>	76.8 ± 11.4 (73 – 90)	88.4 ± 11.1 (77 – 110)

**Table 5.1** A table to show the baseline parameters of the control group and heavy smokers in the skin heating study (n=8), including age, sex, BMI and MAP. The data are mean ± standard deviation (range). There were no significant differences between the control group and the smokers ( $p < 0.05$ ) in the parameters. The BMI is calculated as  $[\text{weight (kg)} / (\text{height (m)}^2)]$ . The mean arterial pressure was calculated as  $[(2 * \text{diastolic BP}) + \text{systolic BP}] / 3$ . (note that data for MAP was missing for 3 participants in the control group, thus  $n = 5$  for this parameter).

The heavy smoker and their matched non-smoking controls were studied initially. The experimental protocol was then altered following the data analysis to aim to improve the accuracy of the spectral analysis by increasing the data length and thus resolution of the analysis. The length of data collection was increased for the LM smoker studies.

***Light / moderate smoking participants***

The light/moderate (LM) smokers had smoked for less than 15 years and they had all smoked for less than 10 packyears. They smoked an average of  $10.8 \pm 3.8$  (mean ± SD) cigarettes per day for between 2 and 15 years (range), and between 1.5 and 10 packyears (range).

This study was performed on a group of 20 LM smokers and 20 matched non-smoking control participants. The groups were comprised of 5 males and 15 females. The study was completed at the volar surface of the forearm of each participant. In some of these participants the study was also completed at the sacrum (*results in Chapter 3*). The baseline parameters are shown in *Table 5.2*. There were no significant differences between the two groups.

<b>Parameter</b>	<b>Control group (n=20)</b>	<b>Smokers (n=20)</b>
<b>Age (yrs)</b>	24.7 ± 4.9 (19 – 35)	23.4 ± 3.9 (18 – 32)
<b>Sex</b>	15 females / 5 males	15 females / 5 males
<b>Body Mass Index (kg/m<sup>2</sup>)</b>	21.6 ± 2.9 (17.3 – 26.7)	24.2 ± 4.4 (19.3 – 34.4)
<b>Mean Arterial Pressure (mmHg)</b>	81.0 ± 6.1 (73 – 96)	83.2 ± 5.7 (73 – 97)

**Table 5.2** A table to show the baseline parameters of the control group and LM smokers in the skin heating study (n=20), including age, sex, BMI and MAP. The data are mean ± standard deviation (range). There were no significant differences between the control group and the LM smokers (p<0.05) in the parameters. The BMI is calculated as [weight (kg)/(height (m))<sup>2</sup>]. The mean arterial pressure was calculated as [(2\*diastolic BP) + systolic BP]/3.

#### **5.4.2 Participant smoking history**

Smoking history was gained from the heavy and LM smokers by self-report; in the heavy smokers this was also confirmed by urine cotinine measurement (Accutest<sup>®</sup> Nicometer<sup>®</sup> strips). All the smokers were asked to abstain from smoking for at least 1 hour, but compliance was not measured by blood carbon monoxide levels, and was potentially variable in the heavy smokers.

#### **5.4.3 Protocol**

The full protocol for the skin heating studies can be found in the *Chapter 2, Section 2.4*. The specific protocol for the heating studies is as follows:

The studies were completed in the temperature controlled environment of the WTCRF. The participants gave their written informed consent to take part in the study. The participants were made comfortable on a hospital mattress, with their arm maintained at heart level on a pillow. They acclimatised to room temperature for 10 - 15 minutes before the skin blood flow measurements began. The participants were asked to keep their arm as still as possible for the duration of the study.

The LDF pinhead probe was positioned within a skin heater which was mounted within a plastic ring which was then attached to the skin using a sticky O-ring (*Chapter 2, Section 2.4*). This was

placed on the volar surface of the forearm midway between the wrist and elbow away from visible blood vessels. The skin blood flow was measured before, during and after a local heating stimulus of 43°C for 10 minutes in the heavy smokers and this was increased to 20 minutes in the light smokers. The data was then saved on a computer laptop for processing.

***Heavy smokers’ protocol***

The specific protocol for the study involving the heavy smoker participants and their matched controls can be found in *Figure 5.1*.

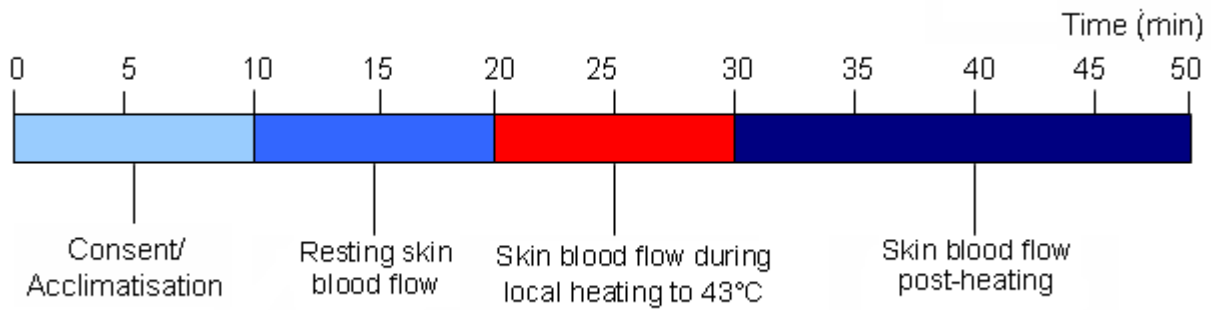


***Figure 5.1*** The time scale for the process through each of the skin heating studies, completed at the volar surface of the forearm in 8 heavy smokers and 8 matched non-smoking control participants.

***Light / moderate smokers’ protocol***

The specific protocol for the study involving the light smoker participants and their matched controls can be found in *Figure 4.1 (Chapter 4, Section 4.3.2)*.

**5.4.4 Statistical analysis**

A detailed summary of the statistical analysis for this study can be found in *Chapter 2, Section 2.6*. A definition of how each of the parameters of the skin blood flow during resting and heating were measured can be found in *Chapter 2, Section 2.4.3*.

The statistical tests used on the data contained in this chapter and the graphical presentation of the data is detailed below:

***Heavy smoker study***

The sample size was small, so a normal population was not assumed and non-parametric statistics were used. The data is presented as median and IQR quoted to 1 decimal place. The MWU

statistical test is used to compare the response parameters in the heavy smokers to the matched non-smoking participants. The data is presented graphically in the form of bar graphs.

#### ***Light/moderate smoker study***

The SWILK test of normality showed that the results were also non-normal, so non-parametric statistics were used. The data is presented as median and IQR to 1 decimal place. The MWU test is used to compare the response parameters in the LM smokers to the matched non-smoker participants. The data is presented graphically in the form of bar graphs.

#### ***Heavy and light/moderate smoker comparisons***

There were different lengths of sampling and application of the local heating in the studies involving the heavy and LM smokers, so the results could not be compared directly as they are. In order to consider the heavy and LM smokers and the matched non-smokers in a group as a whole, the initial 10 minutes of the resting flux and heating stimulus application was extracted from the light smoker results for the comparisons with the heavy smokers. The results were compared using non-parametric statistics, as the assumptions that both populations have a normal distribution cannot be made.

#### ***Median regression analysis***

The median regression analysis was completed using the statistical package Stata (version 9.0) and the guidance of Dr Peter Nicholls. It uses the 50 quantile to estimate, so it is median regression analysis and used a 95% Confidence Interval.

Describing the results:

**For continuous variables (eg. age):** for every one unit increase in the independent variable the predicted value of the absolute power between 0-0.2Hz increases by the value of the coefficient.

**For binary variables (smokers and non-smokers)** – the coefficient is the difference in medians between the 2 groups.

## **5.5 Results**

The results from the studies involving the heavy smokers and matched controls are outlined first (n=8 pairs), followed by the results from the studies involving the longer data collection protocol in the LM smokers and matched controls (n=20 pairs). The results from the first 10 minutes heating are then combined for the heavy smokers and LM smokers to form a ‘smokers group’ and these are compared with all the matched controls (n=28 pairs). Finally, median regression analysis was

completed for all participants studied in this chapter to consider effect of age and smoking intensity on the magnitude of the local heating response.

### **5.5.1 Summary of results**

Although the resting flux was similar in the heavy smokers and the matched non-smoking participants, the skin blood flow response to the local heating stimulus was significantly attenuated in the heavy smokers. The increase in flux, maximum hyperaemia and total response measured by area under the hyperaemia curve in response to local heating were significantly smaller in the heavy smokers compared to the matched non-smoking controls.

The data collection period was increased to 20 minutes for the studies in the LM smokers. The LM smokers showed no difference in resting flux compared to the matched non-smoking controls and there was no significant difference in the parameters of the local heating response. When considering all the participants together in the median regression analysis, packyears was found to be significantly predictive, so that with increasing packyears, there was reduced mean heated flux and total hyperaemic response. However, the results showed no significantly predictive effects of increasing age on the parameters of the local heating response.

### **5.5.2 Heavy smoker study**

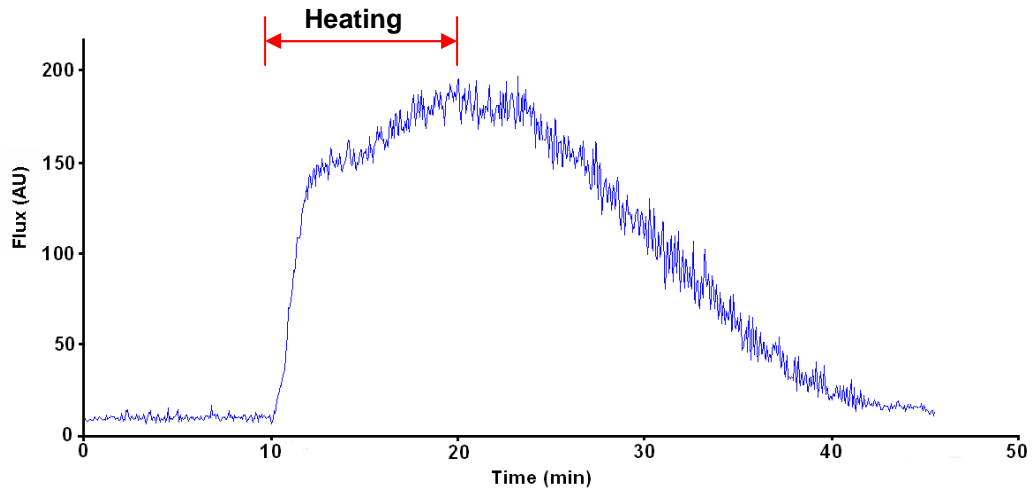
#### ***Smoking history***

The heavy smokers had cotinine levels between 3 and 6, which correlates to a cotinine range of 1,000ng/ml and above. The non-smokers had cotinine level of 0, which correlates to a cotinine range of 0-100ng/ml; non-smoker levels (*Table 2.1*).

#### ***Local heat-induced hyperaemia***

A local-heat induced hyperaemic response was evident in all of the heavy smokers and non-smoking controls tested (n=8 pairs). An example of the LDF trace of the resting flux followed by the local heating response can be found in *Figure 5.2*. The responses showed 2-phases, but the initial peak and plateau were not always easy to separate from each other and tended to merge directly into each other (*Figure 5.2*).

(a).



(b).

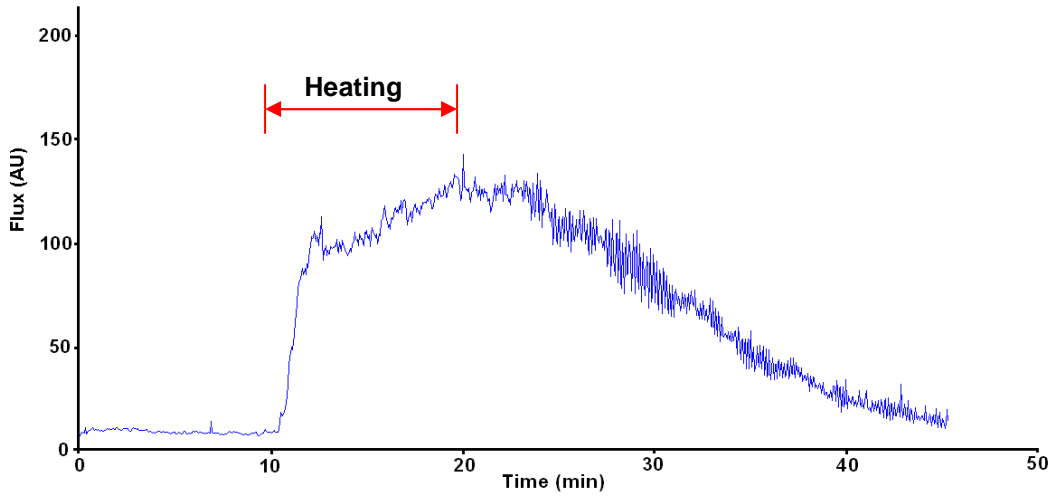


**Figure 5.2** An LDF trace of resting flux followed by heat-induced hyperaemia from: (a) a non-smoker participant and a matched (b) heavy smoker participant. The traces from each participant show the flux during 10 minutes resting flux, 10 minutes heating to 43°C and then post-heating for a further 20 - 30 minutes.

### ***Resting flux and local heat-induced hyperaemic response***

The average resting skin blood flux was  $11.2 \pm 2.0$ AU and  $9.9 \pm 7.0$ AU (median  $\pm$  IQR) in the non-smokers and heavy smokers respectively (Figure 5.3). There was no significant difference between the 2 groups, where  $p=0.721$ , as tested using the MWU test.

In both heavy smokers and non-smokers, the skin blood flow increased significantly during local heating (Figure 5.3). However, the average heat-induced hyperaemic response was significantly higher in the non-smokers compared to the smokers ( $p=0.05$ ); the average heated flux was  $91.9 \pm 59.9$ AU and  $56.8 \pm 32.5$ AU (median  $\pm$  IQR) in the non-smoking controls and smokers, respectively (n=8).

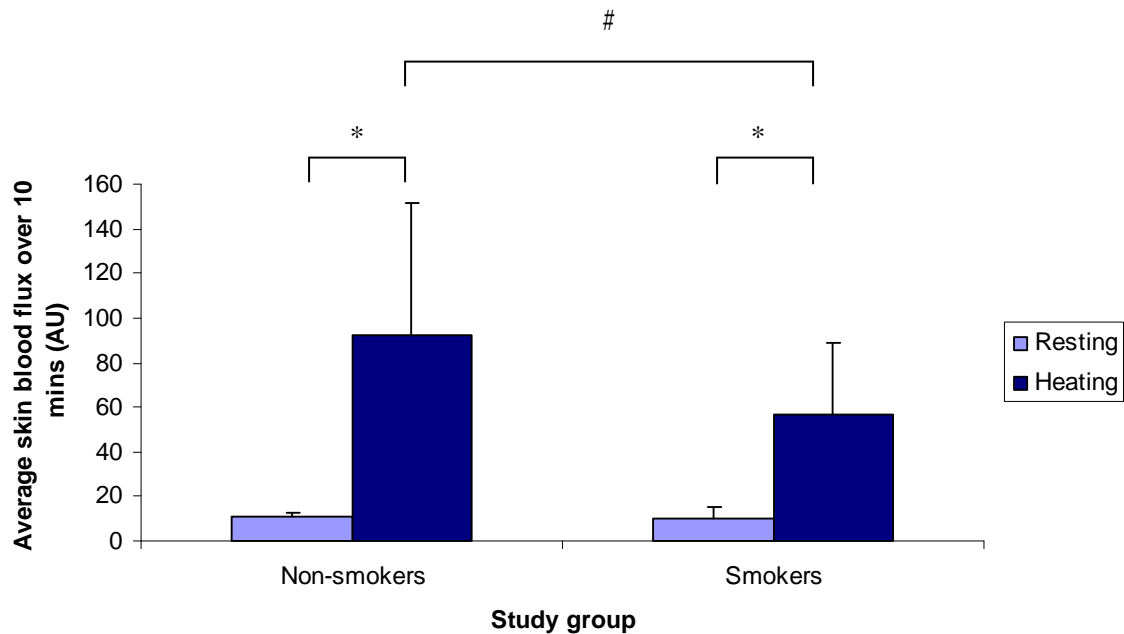


**Figure 5.3** A bar graph to show the average resting forearm skin blood flux measured continuously over a 10 minute period and the average hyperaemic response during 10 minutes local heating to 43°C. The bars represent median and the error bars represent the IQR from 8 non-smoking controls and 8 heavy smokers. The difference in flux between resting and heated flux was tested using the non-parametric Wilcoxon paired test and \* shows significance difference where  $p<0.05$ . The difference between non-smokers and heavy smokers was tested using the MWU test and # shows significant difference where  $p<0.05$ .

### ***Peak skin blood flux above resting***

The peak skin blood flux was also significantly lower in the heavy smokers compared to the non-smokers when corrected for the resting variation. The corrected peak skin blood flux was  $130.0 \pm 63.3$  AU and  $71.8 \pm 45.8$  AU in the non-smoking controls and smokers, respectively (*Figure 5.4*). The difference was significant where  $p=0.007$ , as tested using the MWU test.

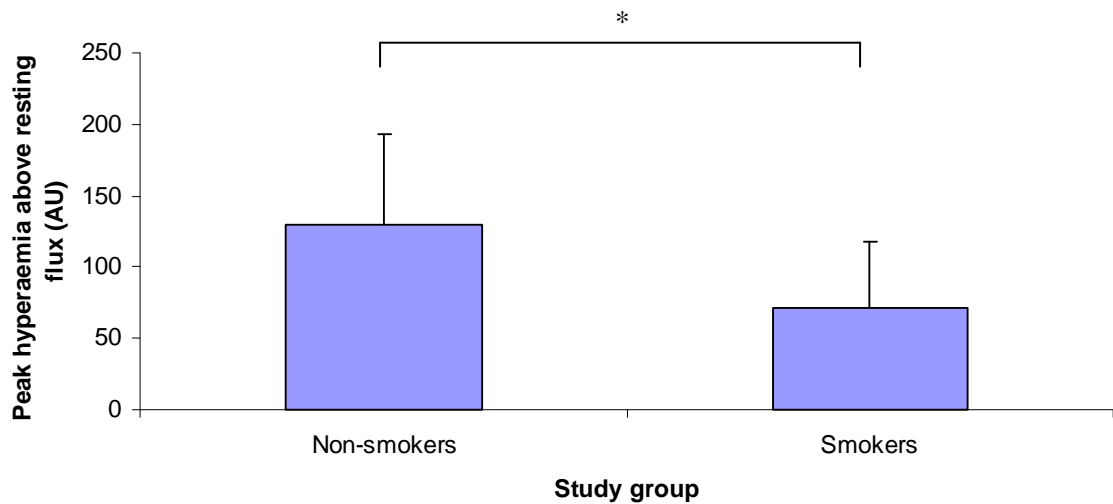


***Figure 5.4*** A bar graph to show the peak heat-induced hyperaemic flux corrected for resting variation measured at the volar forearm of 8 non-smokers and 8 heavy smokers. The bars on the graph represent the median and the error bars represent the IQR. The difference between the smokers and non-smokers was tested using the MWU test and \* shows significant difference, where  $p=0.007$ .

In 3 non-smokers and 2 smokers, the peak flux was reached after the heating stimulus had been switched off. The time taken to reach the peak flux from the beginning of heating was  $583.9 \pm 357.7$  and  $392.6 \pm 410.10$  seconds in the non-smoking controls and smokers, respectively. In order to represent the vasodilation occurring during the 10 minutes that the heating stimulus was applied at  $43^{\circ}\text{C}$ , the mean flux during heating was also calculated.

***Average heat-induced hyperaemia measured above resting skin blood flux***

The average heat-induced hyperaemic flux was measured over the 10 minute heating period and was corrected for resting variation. The average heated flux corrected for resting flux was  $77.7 \pm 59.7$  and  $45.4 \pm 36.4$  AU in the non-smoking controls and the smokers, respectively and this was a significant difference ( $p < 0.05$ ) (Figure 5.5).

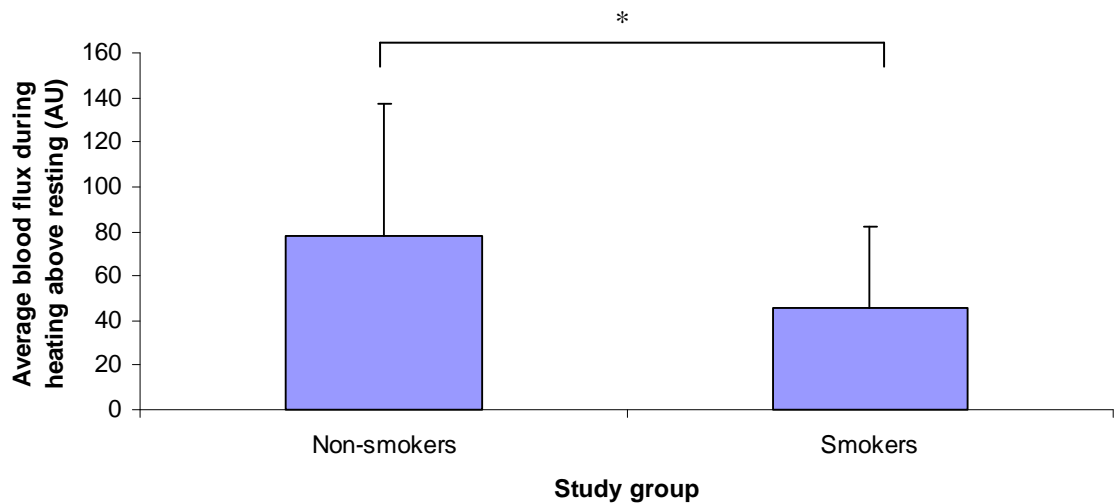


**Figure 5.5** A bar graph to show the average skin blood flux during heating corrected for the resting flux measured over 10 minutes at the volar surface of the forearm of 8 non-smokers and 8 smokers. The bars represent the median and the error bars represent IQR. The difference between the non-smoking controls and smokers was tested using MWU test; \* shows a significant difference where  $p < 0.05$ .

### ***Total response to local heating***

The total response to local heating measured by AUC during the 10 minute heating period was significantly lower in the smokers compared to the non-smokers ( $p < 0.05$ ). The area under the local heating response curve during 10 minutes heating was  $55.2 \pm 36.0$  and  $34.1 \pm 19.5$  ( $\times 10^3$ ) AU in the non-smoking controls and heavy smokers, respectively (*Figure 5.6*).

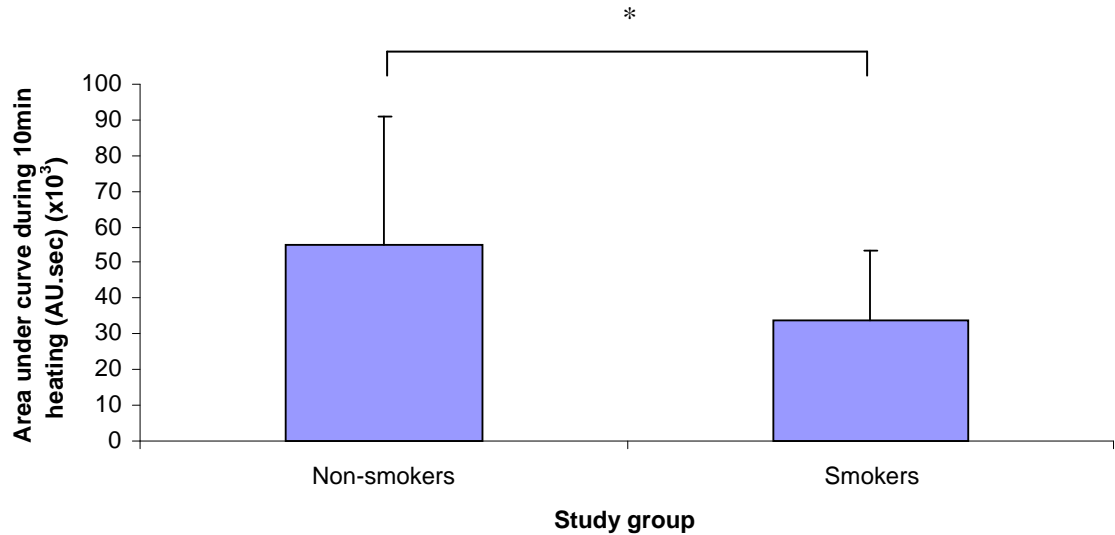


**Figure 5.6** A bar graph to show the total response to local heating measured as area under the LDF curve during 10 minutes heating at the volar forearm of 8 non-smokers and 8 heavy smokers. The graphs represent the median and the error bars represent the IQR. The difference between the non-smokers and heavy smokers was tested using the MWU test (\* shows significant difference where  $p = 0.05$ )

### **5.5.3 Light/Moderate smoker study**

An example of an LDF trace from a LM smoker and matched non-smoker, including 1 minute of the resting flux, the 20 minute heating period and a further 30 minutes recovery can be found in *Figure 5.7*

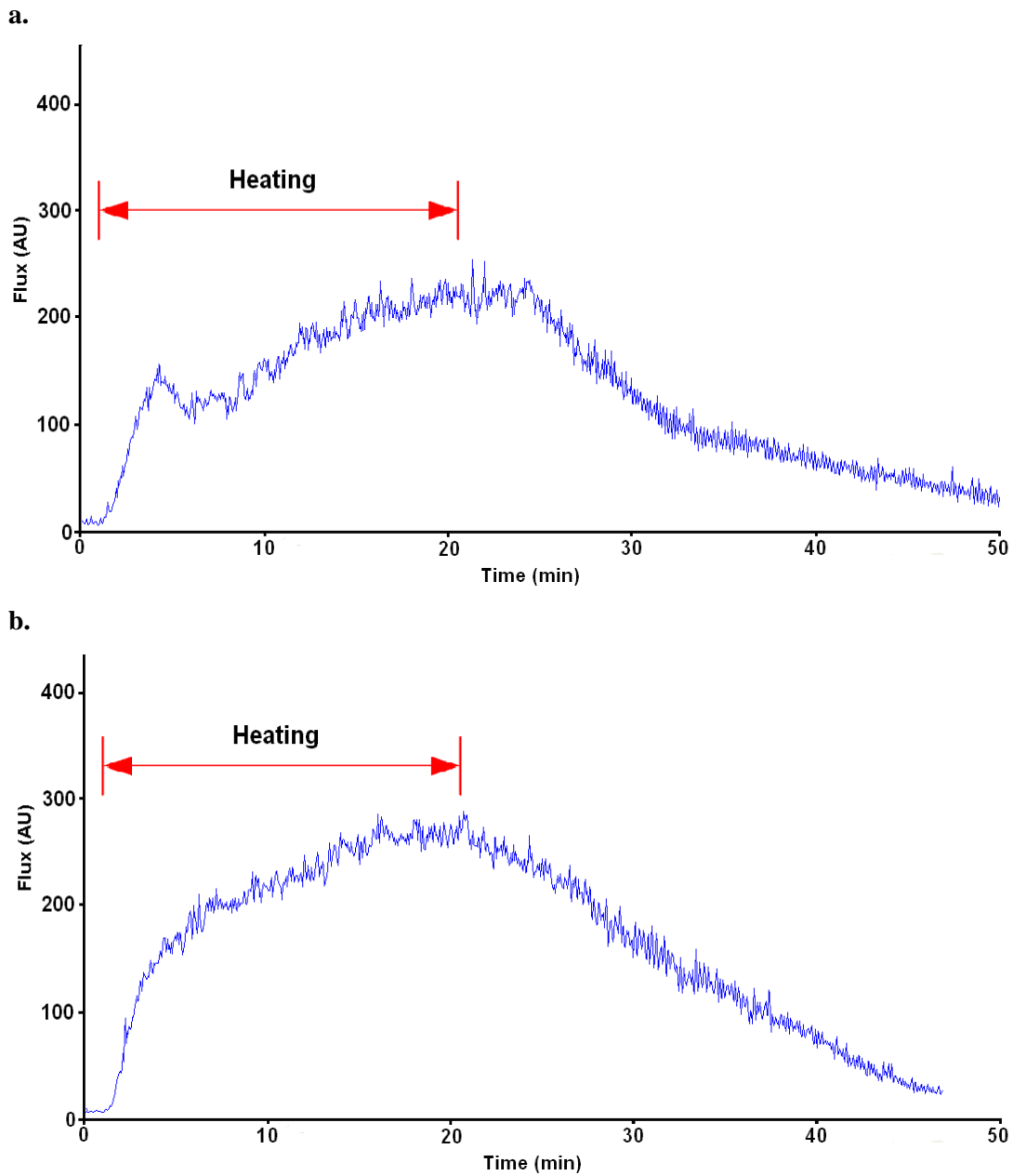


**Figure 5.7** An LDF trace of the last minute of resting flux followed by 20 minutes local heat-induced hyperaemia and then 30 minutes recovery from: (a) a non-smoker participant and a matched (b) LM smoker participant. The traces from each participant show the flux during the final 1 minute of the 20 minute resting flux, 20 minutes heating to 43°C and then post-heating for a further 20 - 30 minutes.

***Average resting and heating flux in non-smokers and smokers***

There was no significant difference in resting flux between the non-smokers and LM smokers, measured over 20 minutes. The resting flux was  $10.1 \pm 2.7$ AU and  $11.8 \pm 8.7$ AU in the non-smokers and smokers respectively (median  $\pm$  IQR). Both the non-smokers and LM smokers showed a significant increase in average flux with heating (analysed using Wilcoxon test,  $p < 0.05$ ) (Figure 5.8).

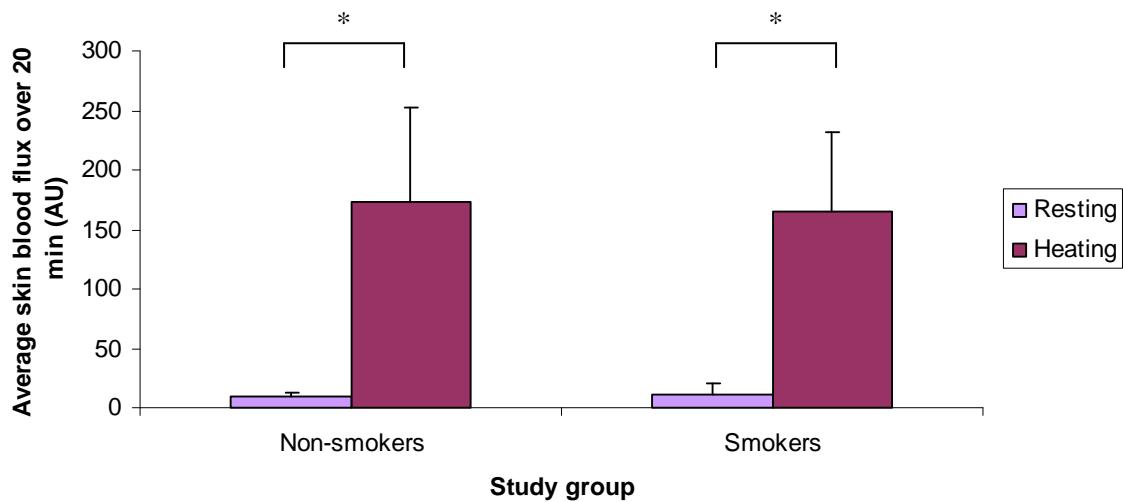


**Figure 5.8** A bar graph to show the average resting skin blood flux measured over 20 minutes and the average flux during 20 minutes local heating to 43 °C at the forearm skin site. The bars represent the median and the error bars represent the IQR from 20 non-smokers and 20 LM smokers. The differences between resting and heated flux were tested using the Wilcoxon paired test (\*  $p < 0.05$ ;  $p = 0.000$ ) and the difference between non-smokers and LM smokers was tested using the MWU test. The difference between the non-smokers and the LM smokers showed no significant difference, where  $p = 0.192$ .

***Peak skin blood flux above resting***

There was no significant difference in the peak skin blood flux above resting flux in the LM smokers compared to the non-smokers, as measured using the MWU test. The corrected peak skin blood flux was  $213.4 \pm 100.6\text{AU}$  and  $207.6 \pm 56.1\text{AU}$  in the non-smoking controls and LM smokers, respectively (*Figure 5.9*).

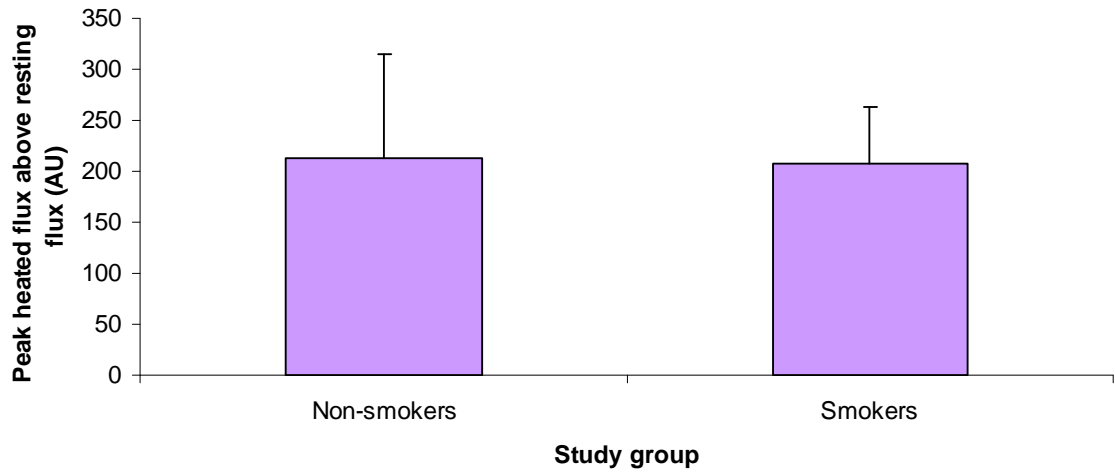


***Figure 5.9*** A bar graph to show the peak heat-induced hyperaemic flux corrected for resting variation measured at the volar forearm of 20 non-smokers and 20 matched LM smokers. The bars represent the median and the error bars represent the IQR. The difference between the LM smokers and non-smokers was tested using the MWU test and there was no significant difference.

***Average heated flux above resting skin blood flux***

The average skin blood flux during heating, when corrected for the variation of the resting skin blood flux showed no significant difference between the LM smokers compared to the non-smokers (MWU;  $p=0.156$ ). The average heated flux above resting flux was  $163.4 \pm 75.2$ AU and  $152.7 \pm 54.3$ AU in the non-smoking controls and LM smokers, respectively (median  $\pm$  IQR) (Figure 5.10).

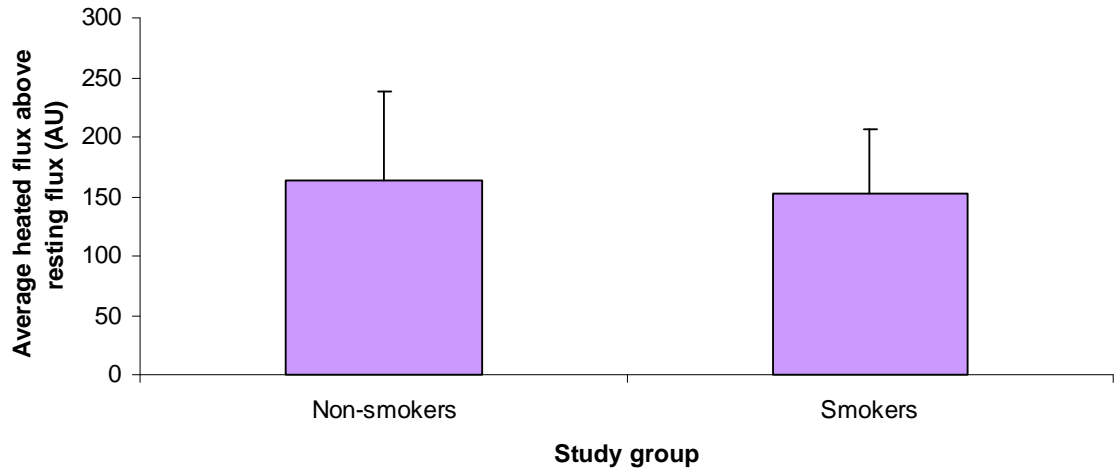


***Figure 5.10*** A bar graph to show the average heated skin blood flux above the resting flux, during 20 minutes local skin heating to 43°C, in 20 non-smokers and 20 LM smokers measured at the forearm. The bars represent median and the error bars represent the IQR. The difference between the non-smokers and the LM smokers was not significantly different; analysis completed using the MWU test ( $p=0.156$ ).

### ***Total response to local heating stimulus***

The total response to the local heating stimulus, as measured by area under the LDF curve during 20 minutes heating showed no significant difference between the LM smokers compared to the non-smokers (MWU;  $p=0.192$ ). The area under the curve was  $20.9 \pm 9.4$  ( $\times 10^4$ ) AU.sec and  $19.8 \pm 8.0$  ( $\times 10^4$ ) AU.sec in the non-smoking controls and LM smokers, respectively (median  $\pm$  IQR) (Figure 5.11).

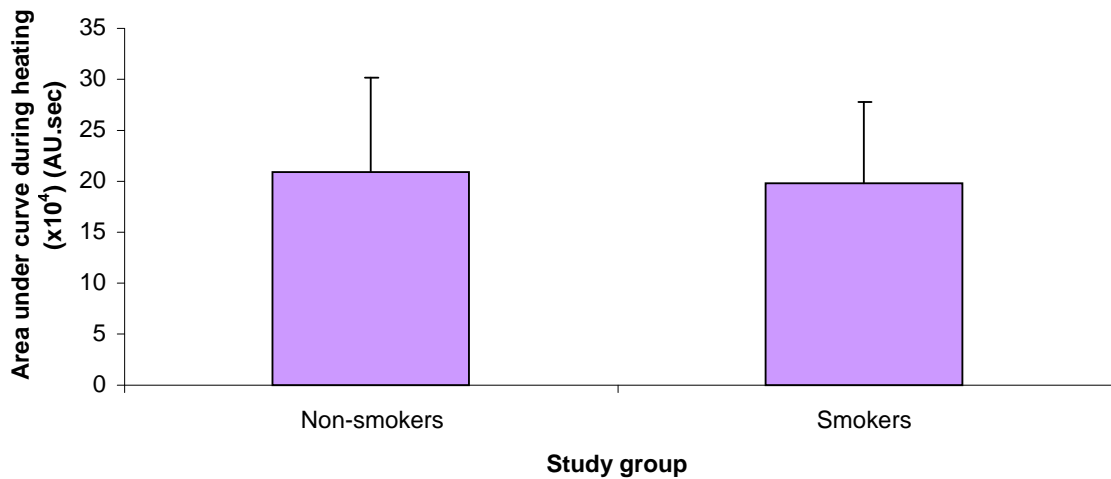


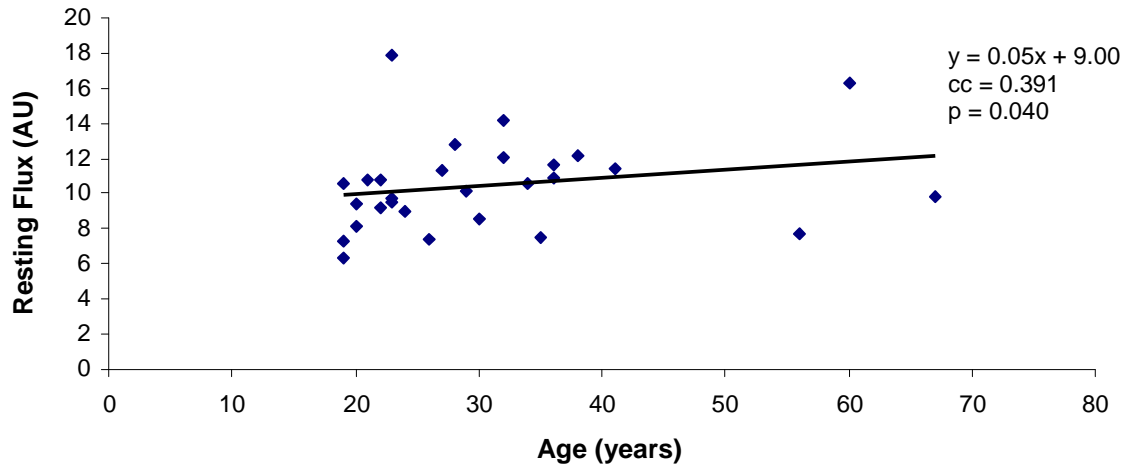
**Figure 5.11** A bar graph to show the total response to heating measured as the area under the curve during 20 minutes heating at the forearm of 20 non-smokers and 20 LM smokers. The bars represent the median and the error bars represent the IQR. The difference between the non-smokers and LM smokers was tested using the MWU test. There was no significant difference between the non-smoking controls and the LM smokers ( $p=0.192$ ).

#### **5.5.4 Analysis of all control participants only**

Analysis was completed in the control group only ( $n=28$ ) to determine whether there was any effect of the baseline parameters on the magnitude of the local heating induced hyperaemia in the controls alone. The effects of age, sex, MAP and BMI were considered. The Spearman's Rho test was used to analyse the effects of age, MAP and BMI on the results and differences between males ( $n=8$ ) and females ( $n=20$ ) were tested using the MWU test.

There was no significant difference between males and females and no significant correlations of either BMI or MAP with the resting flux or any of the parameters of the local heating response. However, age was shown to be significantly correlated with BMI ( $p=0.022$ ) and resting flux ( $p=0.04$ ). The correlations showed that with increasing age, the participants showed significantly increased BMI and also resting flux (Figure 5.12).

a.



b.

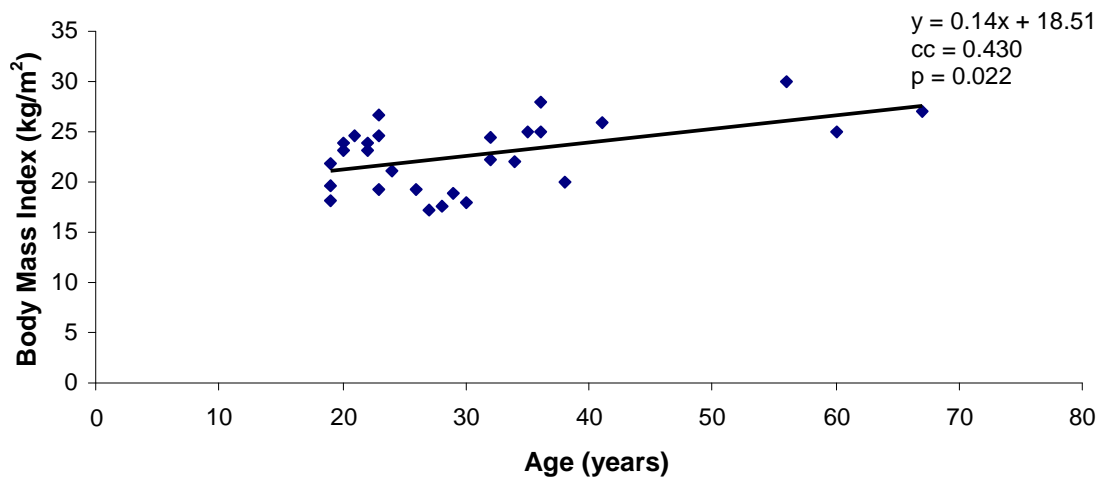


**Figure 5.12** Graphs to show the effect of age on 10 minutes measurement of a. resting flux and b. BMI (kg/m<sup>2</sup>) in 28 control non-smoker participants. The correlations were significant where  $p=0.040$  (resting flux) and  $p=0.022$  (BMI) as tested using the Spearman's Rho test.

### 5.5.5 All smokers (heavy and light/moderate) compared to all controls

The total local heating response in all smokers combined was compared with the response in all non-smokers involved in the studies in this chapter.

#### ***Total response: Area under the local heating response (initial 10 minutes)***

The total response to the local heating stimulus as measured by AUC of the LDF trace during 10 minutes heating in the smokers (heavy and LM) was  $6.8 \pm 4.1$  ( $\times 10^4$ ) AU.sec and in the non-smokers  $8.2 \pm 4.4$  ( $\times 10^4$ ) AU.sec (*Figure 5.13*). When tested using the MWU test, the difference was not significant where  $p=0.082$

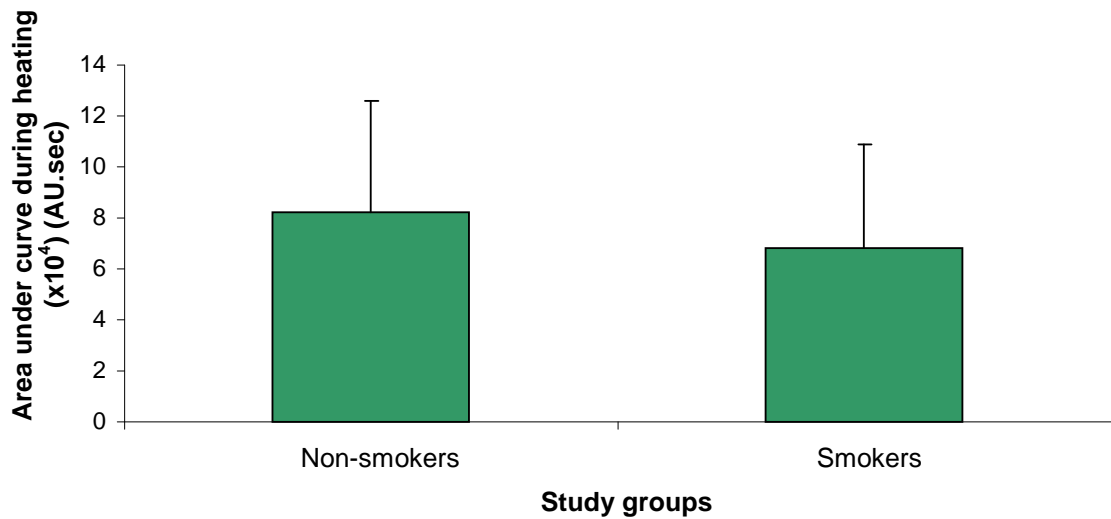


**Figure 5.13** A bar graph to show the total response to heating measured as the area under the curve during 10 minutes heating at the forearm of 28 smokers (heavy/moderate/light) and 28 matched non-smokers. The bars on the graph represent median and the error bars represent +IQR.

#### ***Median regression analysis in heavy and light/moderate smokers and non-smokers***

The longevity and intensity of the smoking habit (measured as Packyears) and age, sex, BMI and MAP were used in the median regression analysis to determine whether there were any predictive variables for the outcome measures: Mean Heated Flux and Area Under the local heating response Curve.

### **Outcome measure: Mean heated flux**

The predictive value of each independent variable individually (as *univariates*) on the mean heated flux was initially calculated using median regression analysis (Stata version 9.0). The results are shown in *Table 5.3*. Only smoking status in terms of packyears was significantly predictive for the dependent variable mean heated flux, where  $p=0.006$ .

#### ***Univariate analysis table***

<b>Independent variables</b>	<b>Coefficient</b>	<b>t-value</b>	<b>P&gt; t </b>	<b>[95% Conf. Interval</b>
Age	-.7487179	-0.91	0.365	-2.392111 .894675
Sex	13.89999	0.54	0.591	-37.60228 65.40227
BMI	-2.81538	-1.19	0.239	-7.555219 1.924451
MAP	-0.7799999	-0.79	0.433	-2.763724 1.203724
Smoking status packyears	-2.065217	-2.84	<b>0.006</b>	-3.52298 -.6074546

**Table 5.3** A table to show the *univariate* analysis, assessing the predictive value of age, sex, BMI, MAP and smoking status (defined as packyears) for the dependent variable mean heated flux in a group of 56 participants, including heavy smokers, LM smokers and non-smokers. The analysis showed that only smoking status in terms of packyears was significantly predictive, where  $p=0.006$ . The Pseudo  $R^2$  value for the analysis was 0.1338.

The predictive value of the independent variables considered together in a model as a *multivariate* analysis was then completed using median regression analysis. The results are shown in *Table 5.4*. The smoking status measured by packyears was significantly predictive, where  $p=0.047$ .

#### ***Multivariate analysis table***

<b>Independent variables</b>	<b>Coefficient</b>	<b>t-value</b>	<b>P&gt; t </b>	<b>[95% Conf. Interval</b>
Age	.4887929	0.54	0.590	-1.324759 2.302344
Sex	26.02446	1.14	0.258	-19.7399 71.78882
BMI	-.4373641	-0.18	0.855	-5.235074 4.360346
MAP	.2569367	0.17	0.864	-2.737393 3.251266
Smoking status packyears	-2.29906	-2.04	<b>0.047</b>	-4.565269 -.0328518

**Table 5.4** A table to show the *multivariate* analysis, assessing the predictive value of age, sex, BMI, MAP and smoking status (defined as packyears) for the dependent variable mean heated flux in a group of 56 participants, including heavy smokers, LM smokers and non-smokers. The analysis showed that packyears was significantly predictive for mean heated flux, where  $p=0.047$ . The Pseudo  $R^2$  value for the analysis was 0.1847.

The results of the median regression analysis show that for every one unit increase in packyears, the predicted value of the mean heated flux was reduced by 2.30AU. The age of the participant was not significantly predictive for the dependent variable mean heated flux either in the univariate analysis or when considered within a model as a multivariate analysis.

**Outcome measure: Area under response curve**

The predictive value of each independent variable individually (as *univariates*) on the area under the response curve was initially calculated using median regression analysis (Stata version 9.0). The results are shown in *Table 5.5*. Only smoking status in terms of packyears was significantly predictive for the dependent variable mean heated flux, where  $p=0.001$ .

***Univariate analysis table***

<b>Independent variables</b>	<b>Coefficient</b>	<b>t-value</b>	<b>P&gt; t </b>	<b>[95% Conf. Interval</b>
Age	-847.5662	-1.78	0.081	-1802.388 107.255
Sex	6100.711	0.40	0.692	-24649.67 36851.09
BMI	-1501.589	-1.18	0.244	-4057.279 1054.101
MAP	-386.6823	-0.50	0.619	-1937.556 1164.192
Smoking status packyears	-1471.35	-3.36	<b>0.001</b>	-2349.39 -593.3105

**Table 5.5** A table to show the *univariate* analysis, assessing the predictive value of age, sex, BMI, MAP and smoking status (defined as packyears) for the dependent variable area under local heating response curve during 10min heating in a group of 56 participants, including heavy smokers, LM smokers and non-smokers. The analysis showed that packyears was significantly predictive, where  $p=0.001$ , with the Pseudo  $R^2$  value for the analysis = 0.1603.

The predictive value of the independent variables considered together in a model as *multivariate* analysis was then completed using median regression analysis. The results are shown in *Table 5.6*. The smoking status measured by packyears was significantly predictive, where  $p=0.007$ .

### *Multivariate analysis table*

Independent variables	Coefficient	t-value	P> t	[95% Conf. Interval
Age	84.665	0.20	0.845	-779.6939 949.0239
Sex	7569.552	0.65	0.517	-15753.93 30893.04
BMI	-188.0115	-0.16	0.877	-2614.181 2238.158
MAP	145.0177	0.22	0.831	-1212.116 1502.151
Smoking status packyears	-1559.56	-2.85	<b>0.007</b>	-2661.877 -457.2437

**Table 5.6** A table to show the *multivariate* analysis, assessing the predictive value of age, BMI, sex, MAP and smoking status (defined as packyears) for the dependent variable area under local heating response curve during 10min heating in a group of 56 participants, including heavy smokers, LM smokers and non-smokers. The analysis showed that packyears was significantly predictive, where  $p=0.007$ . The Pseudo  $R^2$  value for the analysis was 0.1892.

The results of the *multivariate* median regression analysis show that for every one unit increase in packyears, the predicted value of the area under the hyperaemia curve was reduced by 1559.6AU.sec.

The results suggest that smoking status through the range of non-smokers through to heavy smokers is predictive for the time domain local heating induced vasodilator responses. Although further median regression analysis was completed to consider whether smoking (yes/no) as a categorical variable was predictive for the vasodilator responses to local heating. However, smoking (yes/no) as a *univariate* was not significantly predictive for the mean heated flux ( $p=0.544$ ) or area under the local heating response curve ( $p=0.132$ ) and there were no significantly predictive independent variables when considering smoking (yes/no) in a *multivariate* analysis including age, sex, BMI and MAP.

### *Summary of key findings*

- All of the participants showed a significant hyperaemic response to the local heating challenge of 43°C at the forearm site.
- The magnitude of this local heat-induced response was significantly attenuated in the heavy smokers compared to the matched controls
- In the LM smokers there was a trend towards a reduced response to local heating compared to the matched non-smokers, but this did not reach significance.

- When considering all the participants together there was a significant relationship between increasing packyears and reduced mean heated flux and total hyperaemic response.
- There was no significant relationship with ageing and the parameters of the local heating induced hyperaemic response.
- When considering the control participants alone, with increasing age the participants showed significantly increased BMI and also resting flux.

## 5.6 Discussion

The local heating response was measured in a group of heavy smokers and their matched controls and in LM smokers and their matched controls. In previous studies, the local heating response has been well-validated; it is composed of an initial axon reflex mediated peak, a nadir and then a plateau vasodilatation, which is thought to be mainly NO mediated (Minson et al., 2001; Kellogg et al., 1999). In this study, this observable pattern was present in most participants, but to differing degrees. The initial peak was more defined in some participants than others and the nadir between the phases was more pronounced in some participant than others. This was spread between the groups of participants studied and did not differ in the smokers and non-smokers.

Studies considering acute effects of cigarette smoking have generally shown that smoking a cigarette significantly reduces resting skin blood flow (Monfrecola et al., 1998; Richardson, 1987). However, when considering the effects after a period of abstinence in this study, there was no significant difference in resting flux between smokers and non-smokers, whether in the heavy smoker studies or the light smoker studies. This has been shown in a recent study using LDF to measure forearm skin blood flow in smokers and non-smokers (Edvinsson et al., 2008). The values for resting flux for the control participants in this study are similar to those found in control participants in recent studies using LDF (Rossi et al., 2008; Edvinsson et al., 2008).

However, other studies have shown differences in resting flux between smokers and non-smoking controls. A recent study by Midttun et al. (2006), found the baseline capillary blood flow rate for light and heavy smokers, as measured by <sup>133</sup>Xenon washout, was higher than their published work on non-smokers; these smokers had abstained from smoking for 6-8 hours. They suggest that this is due to degeneration of elastic fibres in arteriole walls, so that the arterioles become distended and

peripheral resistance is reduced. The blood flow rate in AVA's, measured by the heat washout method was also around 10% higher in smokers than in non-smokers.

The differences in the results from these studies may be due to the different methods of skin blood flow measurement. The method of LDF has much inter-site variability due to the small diameter of the LDF probe and the varied architecture of the skin microcirculation (Braverman, 2000); thus differences in resting flux are difficult to detect. The variability in the resting flux value as a measure of skin blood flow has been well-documented (Tenland et al., 1983). It has been shown that the LDF probe can be lying between arterioles and AV shunts or directly over them and thus give different values. The variability in the resting flux means it is very difficult for differences between study groups to be found. Therefore it is important to focus attention on the effect of a stimulus on skin blood flow and changes from resting blood flow when using LDF to measure skin blood flow.

The application of local heat to 43°C for 10 minutes at the volar forearm caused a non-painful vasodilation in all subjects. The local heating of the skin to 43°C is usually not associated with pain (Gooding et al., 2006). The local heating stimulus showed a significant hyperaemia in all participants studied, which has been found previously (Wardell, 1994). However, there is variability in the literature concerning the temperature or duration of local heating required to cause maximal hyperaemia. It is therefore difficult to ascertain whether the peak hyperaemia measured in the studies in this chapter can be defined as maximum hyperaemia and thus the capacity for skin blood vessels to dilate. A research group found that 42°C of local heating for 30 minutes produces a vasodilation that cannot be further enhanced by SNP, so suggested that this was a maximal response (Kellogg et al., 1999).

It is also important to consider that the measurements of local temperature directly underneath the probe are approximately 2°C lower than that of the probe temperature itself (Minson et al., 2001). This would mean that the skin temperature produced in this study was nearer 41°C; thus the local heating protocol in this study is likely to have produced a sub-maximal hyperaemia, and the results do not reflect the capacity of the skin microvasculature. The findings from this study are related to the ability of the skin microvasculature directly underneath the LDF probe to vasodilate to a given stimulus.

It was also found that in some participants the peak blood flow occurred after the heating stimulus had finished, especially in the heavy smokers study with the 10 minute heating protocol. This was also found in a previous study in which the mean blood flow during the post-heating period was

higher than during the 45°C heat application, which they also suggested caused maximal thermal stress in their study (Geyer et al., 2004). In this study this was suggested to be due to nitric oxide production which maintained the vasodilatation for a while during the post-heating period. Therefore, measurements during the heated period alone may miss some important parameters of the response that occur after the period of direct heating. The peak flux was measured in this study as the total response during local heating may not fully encompass the response as a whole.

The average heated flux and peak flux, corrected for resting flux, as well as the total response during local heating were significantly reduced in the heavy smokers compared to the controls. Other studies have shown reduced cutaneous hyperaemia responses in long-term smokers in response to local heating to 44°C (Edvinsson et al., 2008), iontophoresis of both ACh and SNP (Pellaton et al., 2002), pressure loading of the patellar tendon (Sprigle et al., 2002) and forearm cuff occlusion (Rossi et al., 2007). The attenuated total vasodilation in the smokers compared to control participants implies a reduced ability to vasodilate in response to external damaging stimuli

There are various possible explanations for this. The damage to the endothelium of blood vessels by the products of smoking may result in impaired production of vasoactive mediators (Anggard, 1994). Nitric oxide is a significant vasoactive mediator that has the potential to be affected by smoking, and studies have shown a reduction in the circulating levels in smokers (Heitzer et al., 1996, 2000; Barua et al., 2001; Node et al., 1997; Tsuchiya et al., 2002), and thus reduced NO bioavailability. Smokers have been shown to have increased levels of ROS and lower antioxidant levels. This causes an inhibition of endothelial nitric oxide synthase (eNOS), reduces the bioactivity of NO and impairs endothelium dependent vasodilatation (Heitzer et al., 1996; Barua et al., 2001). Alternatively, reduced shear stress in the smokers due to a lower level initial increase in flux, may result in reduced production of NO, and thus reduced plateau vasodilation.

In terms of consideration of the mechanisms of skin blood flow control affected by smoking, a study was conducted to measure the brachial artery vasodilation in response to ACh (endothelium-dependent) and SNP (endothelium independent). They showed that smokers had significantly reduced response to ACh and not SNP, suggesting that this demonstrates a loss or impairment in endothelial function. However, this study was considering the larger arteries in the circulation, whereas another more recent study has demonstrated reduced responses in smokers to the iontophoresis of ACh, SNP and also local heating using LDF to measure skin blood flow, suggesting that the changes in microvascular reactivity in smokers are not solely endothelium related (Edvinsson et al., 2008). Interestingly, a study was completed to specifically consider the effects of nicotine on the skin blood flow of smokers and showed that nicotine nasal spray caused

an increase in the axon reflex part of the response, but an attenuation of the prolonged plateau phase (Warner et al., 2004).

There was no significant difference found in the response to local heating in the LM smokers compared to the matched controls, although the responses were decreased and the differences were borderline significance. A previous study has shown that even light smoking affects the vasoreactivity of blood vessels although the study did consider the effects on a larger artery, the brachial artery, and not specifically the microcirculation, as in the studies in this chapter. In the study, they measured endothelium-dependent vasodilation in the brachial artery, and also the effect of the sera from light smokers (smoked a pack per week or less) and heavy smokers (smoked a pack per day or more) on Human Umbilical Vein Endothelial Cells (HUVEC) on NO and eNOS production and eNOS activity (Barua et al., 2002). They found that all of these parameters measured were significantly reduced in both groups of smokers to the same extent, compared to the controls. This suggests that even light smoking has detrimental effects on NO concentration. Interestingly, the LM smokers in the studies in this chapter smoked at a higher intensity compared to those in this paper and the differences did not reach significance. This may be due to differences in measuring responses in the brachial artery compared to the microcirculation.

When considering the heavy and LM smokers and matched controls together, median regression analysis showed that packyears was a significant predictor for the magnitude of the response, so that increasing smoking intensity/longevity meant reducing vasodilation response to local heating. It was also found that when considered as one group with an age range of 18 -67 years, ageing was not a significant independent variable for the response as might be expected due to the finding of diminished responses in elderly participants in previous studies (Minson et al., 2002; Hagiwara et al., 1991). In the studies in this chapter, the calculation of predictive value of both age and smoking intensity (packyears) must be considered with caution due to the uneven distribution of age through the range 18-67 years and pack years through the range 1.5-42 packyears (*Table 5.7*). The potential acute effects of smoking in the heavy smokers due to difficulties with abstinence from smoking in this group must also be considered.

a.

Age band (years)	Number of Participants
18 – 20	10
21 – 30	26
31 – 40	9
41 – 50	4
51 – 60	4
61 – 70	3

b.

Smoking intensity (Packyears)	Number of Participants
1 – 5	14
6 – 10	6
11 – 20	2
21 – 30	2
31 – 40	3
41 – 50	1

**Table 5.7** Two tables to show the a. age distribution and b. smoking intensity distribution of participants in the study including all 56 participants.

Also, a recent study has shown that the local heating response was maintained in elderly sedentary subjects, even though there was a decline in the NO contribution of the response. This suggests that although there may be a decline in the NO mediated response, there are other compensatory mechanisms that preserve the overall response in elderly participants. It was also found that the NO function in both heating and acetylcholine induced vasodilation was significantly greater in older fit participants compared to older sedentary participants (Black et al., 2008). This shows that there may be a number of variables within the elderly group, such as exercise, that can affect the response and so disguise the effects of age.

It must also be considered that the oldest participant in this study (67 years) was still younger than the patients in groups termed ‘elderly’ in previous studies and this may be a further explanation for the lack of correlation with ageing. Although increasing age has been shown to be negatively correlated with capillary density in the skin (Li et al., 2006a) so that there is a gradual loss of capillary density between 20 and 70 years of age, the skin blood flow was found to be significantly increased with age potentially due to the expanded parallel vasculature in the deeper dermis (Li et al., 2006a). This would suggest that the picture regarding skin blood flow and skin blood flow responses with ageing is not clear.

### **Limitations**

It is important to consider the findings in this chapter in the light of any study limitations. The LDF in combination with the skin heater does not require interference by the experimenter during the course of the study protocol, so the artifact from this is no longer present. However, movement by the participant causes artifact on the trace. Efforts were made to keep this to a minimum by ensuring the participants comfort at the beginning of the studies and explaining the need to remain still throughout the procedure.

A further limitation is the lack of compliance of the heavy smokers. Many of the heavy smokers were in the habit of smoking at least a pack a day, so in some cases struggled to comply with the requirement to abstain for the 1 hour prior to experimentation. Although the cotinine levels were measured, this does not give an indication of compliance to abstinence from cigarette smoking. A measure of exhaled carbon monoxide would have been a useful indicator of compliance as levels remain increased for at least one hour after cigarette smoking (Van der Vaart et al., 2005). The LM smokers tended to have smoked their last cigarette a longer period before the study began. When considering the results it must be acknowledged that there may be some acute effects of smoking in the results, particularly in the heavy smokers.

Ideally, the participants would have been asked to refrain from smoking for longer than 1 hour, as Goodfield et al. (1990) observed that blood flow changes following cigarette smoking persisted for at least 3 hours in some subjects. However, other studies have shown the acute effects of smoking to have reached pre-smoking levels within 40-50 minutes of smoking (Sorenson et al., 2009). Others have found that the hypoxia (Jenson et al., 1991) and endothelial dysfunction (Lekakis et al., 1998) following cigarette smoking lasts around 1 hour.

It is also clear that the vasodilatation measured from the local heating stimulus cannot be considered to be a measure of capacity of the microcirculation to vasodilate, but as ability for the microcirculation to respond to a given stimulus.

The median regression analysis has enabled the consideration of whether independent variables can be extracted from the data that are predictive of the mechanisms involved in the heating response. The median regression analysis showed evidence of predictive value of smoking status, measured as packyears, for the vasoreactive response to local heating. However, a limitation of this finding is that there is increased numbers of LM smokers and their controls in my sample compared to the heavy smokers and their older controls. Thus, the findings may be skewed in the direction of the young and the light smoker intensity. It is also the case that the R-squared values are generally low and this suggests that other factors not included in the analysis also have an effect. This finding is not unexpected due to many factors that impact on skin blood flow and unfortunately could not be controlled for in this study. This includes factors such as antioxidant intake in the diet (Chavez et al., 2007) and variability of position of probe (Bravermann, 2000).

### ***Final Summary***

All the participants studied in this chapter showed a significant vasodilation response to the local heating stimulus. The heavy smokers had significantly attenuated responses to the local heating

stimulus compared to the matched non-smokers, although it must be considered that there may be more acute effects of smoking in this group. The responses in the LM smokers had a trend towards reduced responses compared to the non-smokers, but this was not a significant finding. When considering the participants together in median regression analysis, the results showed that packyears was significantly predictive for the vasodilation response, so that with increasing packyears the response reduced. Although ageing was not shown to be significantly predictive, the increasing longevity/intensity of smoking, as measured by packyears, was shown to result in altered vascular reactivity, and the extent of this alteration depends on intensity/duration of smoking history as defined by number of packyears.

The mechanisms of blood flow control affected by smoking can be investigated using spectral analysis of the LDF signal. The following chapter shows the spectral analysis of the local heating induced vasodilation responses from the participants in this chapter. The measurement of skin blood flow responses using LDF in combination with spectral analysis to pinpoint mechanisms of blood flow control may provide an objective measure which could be used to define risk of pressure damage.



## **Chapter 6**

### **Mechanisms underlying altered vasoreactivity in heavy and light/moderate smokers: Spectral analysis**

## 6.1 Introduction

The studies in the previous chapter have shown attenuated vasoreactivity in a group of heavy smokers and a small, but not significant, difference in the responses in LM smokers compared to non-smoking control participants. These findings in themselves do not provide specific information regarding the particular mechanisms that are being adversely affected in the heavy smokers. The spectral analysis in this chapter will aim to provide insight into the pathway of dysfunction in the heavy smokers and any potential changes in blood flow control in the LM smokers. The effect of age on the control of the microcirculation will also be investigated. Altered function of the skin microcirculation could increase the risk of a patient developing a pressure ulcer.

In the studies in chapter 5, the median regression analysis showed that packyears was a significant independent variable. The effect of age was also investigated as there was a broad range of age between the groups, with the light smokers being significantly younger. The effect of age was not found to be a significant independent variable for the hyperaemic responses to local heating measured as mean heated flux and area under the hyperaemia curve.

The LDF signal of skin blood flow is composed of oscillations in flow with different times of repetition or frequencies (*Chapter 2, section 2.5*). The LDF signal can be analysed using spectral analysis to determine the power of the frequencies contained within it. In recent years, spectral analysis of the LDF signal has advanced rapidly with either FFTs or Wavelet Analysis being used for the process. Several studies from the late 90's revealed 5 different oscillation frequencies to be present in the LDF signal and these were related to certain mechanisms of microvascular control and regulation (Kvermmo et al., 1999) (*Chapter 1, Section 1.5.3, Table 1.1*).

The LDF signal contains oscillations that relate to systemic control of skin blood flow. The oscillations in the signal at a frequency around 1Hz (one per second) originate from the cardiac beat (Bracic and Stefanovska, 1999) and those around 0.4Hz originates from respiratory function (Bollinger et al., 1993). The local control mechanisms are revealed in the signal at around 0.1Hz, 0.04Hz and 0.01Hz and relate to myogenic, neurogenic and metabolic/endothelium mechanisms respectively (Akselrod et al., 1981; Soderstrom et al., 2003; Stewart et al., 2007) (*Chapter 1, Section 1.5.3, Table 1.1*). The benefits of oscillatory skin blood flow termed flowmotion, which results partly from vasomotion (constriction and dilation of blood vessels), have been discussed previously (*Chapter 1, Section 1.2.4*)

In this decade, there have been several patient studies where this method of analysis has been used to detect a dysfunctional microcirculation as a non-invasive indicator for the development of disease (Rossi et al., 2008; Bernjak et al., 2008); the main focus of this being cardiovascular disease. These studies have focused on changes in the mechanisms of blood flow control in the skin microcirculation as an indicator for disease in macrocirculation and other organs. The specific mechanism of blood flow control that is considered of particular importance is the function of the endothelium; the endothelium is important in the hemodynamics of the microcirculation.

There is some evidence that smoking can cause dysfunction of the endothelium through the effects of reactive oxygen species on the bioavailability of NO. This has been shown in *in vitro* studies and also through measurement of plasma levels of NO, markers of oxidative stress, such as malondialdehyde (MDA) and plasma levels of anti-oxidants (Rocchi et al., 2007). Although there are conflicting studies, smokers have generally been shown to have reduced levels of NO (Node et al., 1997; Tsuchiya et al., 2002) and antioxidants (Tousoulis et al., 2003) and raised levels of markers of oxidative stress (Smith and Fischer., 2001). This has substantiated the link between smoking, oxidative stress and reduced bioavailability of NO. However, these studies are often invasive and measurement of both NO and markers of oxidative stress have issues of reliability due to their short half-life and also the numerous factors that can alter the levels of them.

The functioning of the skin microcirculation is important in maintaining the health of the skin. There are a number of mechanisms involved in the control of the skin blood flow that enable the metabolic demands of the tissues to be met and homeostasis to be maintained. The use of LDF and spectral analysis enables a consideration of these mechanisms. Patients with a cutaneous microcirculation that has altered vasoreactivity, potentially due to a dysfunctional endothelium, may be at risk for pressure ulcer development.

## **6.2 Hypothesis**

The reduced hyperaemic responses to local heating in the heavy smokers is potentially due to altered endothelial function which will be shown by reductions in the power of the frequency around 0.01Hz using spectral analysis; the light smokers will also show some attenuation at this frequency.

### 6.3 Objectives

- To investigate the mechanisms underlying the reduced vasoreactivity in the heavy smokers by using FFT spectral analysis on the LDF traces of resting and local heating induced hyperaemic flux in the heavy smokers and their matched control participants.
- To determine whether there are any alterations in blood flow control in LM smokers compared to their matched control participants using spectral analysis of the LDF signal.
- To seek any evidence of the independent effects of age and smoking status on the skin microcirculation by performing statistical median regression analysis on the spectral analysis from the LDF signal during local skin heating

### 6.4 Methods

#### *Participants*

Spectral analysis was completed on the resting and local heating LDF signal in the 8 heavy smokers and 8 matched controls (*Table 5.1*) and the 20 LM smokers and 20 matched controls (*Table 5.2*) from the studies described in chapter 5 (*Chapter 5, Section 5.3*).

#### *Spectral analysis*

In *Chapter 2, Section 2.5* there can be found a detailed description of the methods used for the spectral analysis in this chapter. The FFT algorithm was used to determine the underlying frequencies within the LDF signal. The FFT converts the time series in its frequency components by an algorithm called the Fourier Transform.

Matlab is a software tool for studying digital signal processing. With the support of ISVR (Dr D. Simpson), several Matlab<sup>®</sup> programs and functions were written for the computation of FFT's from the LDF data. The programs used in the spectral analysis in this chapter can be found in *Appendix 3*.

#### *The spectral analysis process for the LDF data from the heavy smokers*

The resting and heating flux was measured over a period of 10 minutes in the heavy smokers and their matched non-smoking controls; the resting flux signal and the heating flux signal were 600

seconds or 24001 data points in length. The data sections were loaded into Matlab<sup>®</sup> version 7, student version, with additional signal processing toolbox. The mean value was then removed from the signal, so that the mean of the signal was equal to zero. The initial 100 seconds of data was removed from both the resting and heating Flux signals and the signals were detrended to a power of 10 to remove the sharp increase in flux at the onset of heating and the general trend in the signals. Thus, the length of the files analysed in the heavy smoker study were 500 seconds or 20001 data points.

The PSD of the LDF signal in the heavy smokers was estimated using the Welch method. The 500 seconds of data or 20001 data points was separated into windows of length 250 seconds (10001 data points) and overlap 50%. The Hanning window was used for the calculations. The number of windows in this analysis was 5. The frequency resolution of the signal is 0.004Hz, which is sufficient to measure the power of the low frequencies around 0.01Hz.

The PSD was calculated over the frequencies 0 - 2Hz. The maximum frequency present in the signal is equal to half the sampling rate, 20Hz. The program for calculation of the PSD and the function required for that program can be found in *Appendix 3*. The estimated PSD could be saved as an image (*Appendix 3*) and as text, in excel format (*Appendix 3*). The power can be calculated from the PSD using the area under the curve; this is approximated by integration using the trapezoidal method.

#### ***The spectral analysis process for the LDF data from the light/moderate smokers***

In the studies involving the LM smokers and their matched controls, the skin blood flow was continuously recorded using LDF for 20 minutes at rest and the local heating stimulus to 43°C was applied for 20 minutes. The length of data collection was increased to reduce the random error and the bias error within the PSD estimate. As with the heavy smoker study, the initial 100 seconds was removed from the resting and heated Flux data to give 1100 second lengths of data and 44001 data points. The 1100 seconds or 44001 data points (N) was separated into windows of length 400 seconds (M) and overlap 50%. The Hanning window was used for the calculations. The number of windows using the Welch method for PSD estimation was 6, so that there were more windows to reduce the random error. The frequency resolution was 0.0025Hz, so improved resolution to reduce bias error.

*Specific definitions for this chapter:*

**Resting flux used for spectral analysis** – the LDF signal measured continuously for 10 minutes (heavy smokers) or 20 minutes (LM smokers) during rest; there was no heat applied to the skin during this measurement. The resting flux is the LDF signal that was measured in the studies excluding the initial 100 seconds of recording.

**Heated flux used for spectral analysis** - the LDF signal measured continuously for 10 minutes (heavy smokers) or 20 minutes (LM smokers) during heating of the skin to 43°C. The heated flux is the LDF signal that was in the studies during heating excluding the initial 100 seconds of recording.

**Absolute power (AU<sup>2</sup>)** – the area under the PSD curve for the frequency range specified; either over the low frequency range (0-0.2Hz) or the frequency band intervals (0.008-0.02Hz, 0.02-0.05Hz and 0.05-0.15Hz)

**Relative power (%)** – the absolute power of the frequency band interval divided by the absolute power over the low frequency range (0-0.2Hz), then multiplied by 100 and given as a percentage.

All the Matlab<sup>®</sup> functions used to estimate the PSD in this chapter can be found in *Appendix 3*.

***Neurogenic mechanisms considered***

The method used in the study to improve the accuracy of the spectral analysis by making the signal more stationary involved removing the initial 100 seconds of the data from the start of heating. This is thought to be mainly axon reflex related, so would be shown around 0.04Hz in the LDF signal. A small study was completed in a group of 6 non-smoking participants (*Appendix 4*) to consider whether a change in the neurogenic mechanisms of blood flow control induced by application of EMLA to the skin could be detected in the plateau vasodilation of the local heating response using spectral analysis.

The studies showed that the EMLA caused a reduction of skin blood flux during the plateau vasodilation in response to a local heating stimulus. The studies showed that there was a significant reduction in the relative contribution of the frequency ~0.04Hz at the EMLA treated site during the plateau section of the local heating response compared to the contribution in the resting flux at the site prior to EMLA application. There was no such difference in the control site or in the

frequencies around 0.01Hz and 0.1Hz. This would suggest that the spectral analysis methods used in this chapter may be sensitive enough to measure changes in neurogenic mechanisms of skin blood flow control in the plateau section of the local heating response.

***Repeatability and coefficient of variance of spectral analysis***

The site-to-site CV was calculated from resting LDF measurements (500 seconds) taken at two different sites on the volar forearm of a group of 17 non-smoking control participants involved in some of the studies and this data is found in the methods chapter section. The site-to-site CV was also calculated from the spectral analysis of the resting flux from these participants. The results can be seen in *Table 6.1*.

<b>Frequency band (Hz)</b>	<b>0 – 0.2Hz</b>	<b>0.01Hz (0.008-0.02)</b>	<b>0.04Hz (0.02-0.05)</b>	<b>0.1Hz (0.05-0.15)</b>
<b><i>CV of Absolute power</i></b>	0.66	0.62	0.74	0.59
<b><i>CV of Relative power</i></b>		0.18	0.15	0.15

**Table 6.1** A table to show the CV measured from the spectral analysis of 500 second resting skin blood flow at 2 sites on the volar surface of the forearm. The data are taken from 17 non-smoking participants. The CV is measured by the standard deviation (of the 2 PSD measurements)/mean (of the 2 PSD measurements).

The site-to-site variation in resting flux is known to be high, as evidenced by these data, but the relative values are much reduced suggesting reduced variation with site.

**6.5 Results**

**6.5.1 Summary of results**

The results have shown attenuated absolute power of the heating flux between 0 and 0.2Hz in the heavy smokers compared to the matched non-smoking controls, but not in the LM smokers. The relative power of the frequency around 0.01Hz was significantly increased during heating compared to resting in the non-smokers, but this was absent in the heavy smokers. The absolute power of the LDF signal between 0 and 0.2Hz was not attenuated during heating in LM smokers compared to the non-smokers. The LM smokers had a reduced power around 0.1Hz during heated flux compared to the matched non-smokers; the difference almost reached significance.

The analysis including all 56 participants together showed that the change in the relative power around 0.01Hz (related to the endothelium) from resting to heating was significantly different in the smokers compared to the non-smoking group. The non-smokers showed an increase in the relative power around 0.01Hz with heating and the smokers showed a fall in the median relative power around 0.01Hz frequency.

### **6.5.2 Spectral analysis in heavy smokers and matched controls**

Spectral analysis using an FFT was completed on the LDF signal to determine the absolute power of the LDF signal, through the frequency range 0 - 2Hz, during resting and heating in the heavy smokers and their respective non-smoking control participants.

#### ***Spectral analysis of LDF measured between 0 and 2Hz***

The absolute power of the LDF signal measured between 0 and 2Hz was significantly increased during heating when compared to resting in both the heavy smokers and the non-smokers, where  $p < 0.05$ . The absolute power between 0 and 2Hz was  $4.9 \pm 3.7 \text{ AU}^2$  and  $271.8 \pm 302.0 \text{ AU}^2$  (median  $\pm$  IQR) in the non-smokers, during resting and heating flux respectively. The absolute power between 0 and 2Hz was  $4.4 \pm 7.0 \text{ AU}^2$  and  $88.0 \pm 84.5 \text{ AU}^2$  (median  $\pm$  IQR) in the heavy smokers during resting and heating flux, respectively.

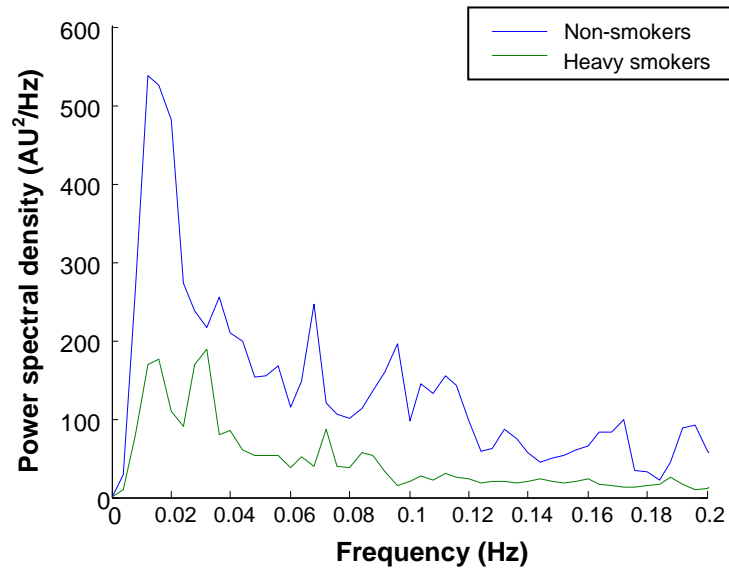
The contribution of this frequency band increased from  $30.2 \pm 13.9\%$  to  $80.5 \pm 25.2\%$  in the non-smokers and from  $39.8 \pm 14.8\%$  to  $78.8 \pm 12.3\%$  in the heavy smokers (median  $\pm$  IQR). The results showed that in both the heavy smokers and their matched non-smoking controls, increase in flux during heating is mainly due to an increase in contribution of the power of the frequency around 1Hz, which originates from the cardiac rhythm.

The main aim of this work is to consider the local mechanisms of skin blood flow control. The low frequency bands contained between 0 - 0.2Hz will be the focus of the remainder of the spectral analysis. The analysis will consider the power of the heated signal as well as the change in power from resting to heated flux.

#### ***Power of LDF signal during the local heating stimulus***

The power between 0 and 0.2Hz of the heated LDF flux was significantly lower in the heavy smokers compared to the matched non-smokers (*Figure 6.1*). The absolute power between 0 and 0.2Hz was  $29.6 \pm 16.7$  and  $8.8 \pm 14.6 \text{ AU}^2$  in the non-smokers and heavy smokers, respectively (median  $\pm$  IQR).

(a).



(b).

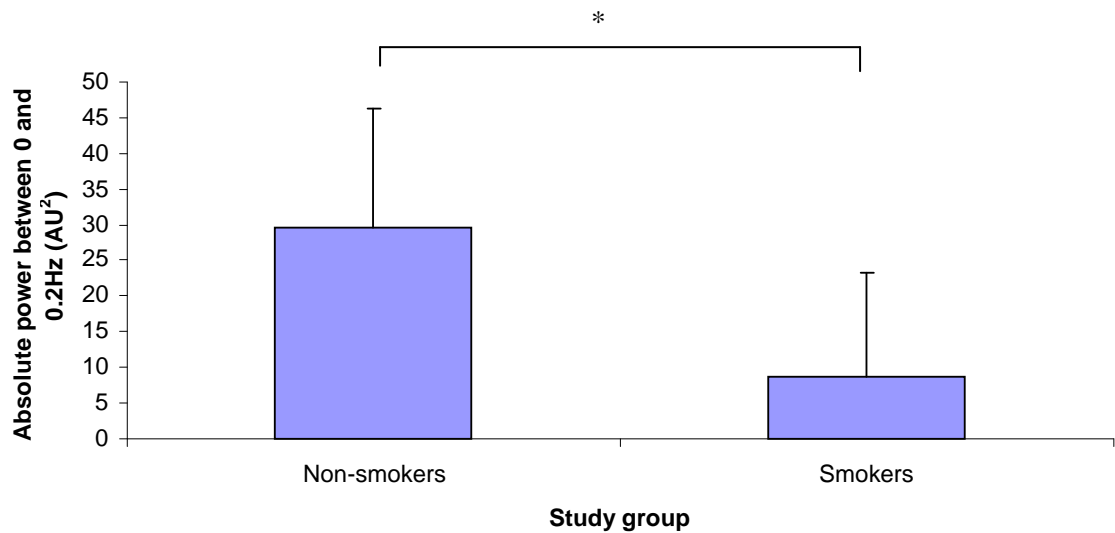


**Figure 6.1** Graphs to show the power between 0 and 0.2Hz of local heated flux measured over 500 seconds at the forearm of 8 non-smokers and 8 heavy smokers. **(a)** represents the median PSD between 0 and 0.2Hz for the non smokers and heavy smokers (AU<sup>2</sup>/Hz) and **b.** represents the power between 0 and 0.2Hz (median +IQR) (AU<sup>2</sup>) for the non-smokers and heavy smokers. The absolute power shown in graph **(b)** is measured as area under the PSD curve **(a)**. The difference was tested using the MWU test (\*p<0.05) and was significant where p=0.012

The absolute power measured between 0 and 0.2Hz of all 16 participants (8 heavy smokers and 8 non-smokers) showed a significant positive correlation with the total hyperaemic response measured by area under the curve. The correlation was tested using the non-parametric Spearman's rho test; the correlation coefficient = 0.647 and the correlation was significant where  $p=0.007$  (Figure 6.2)

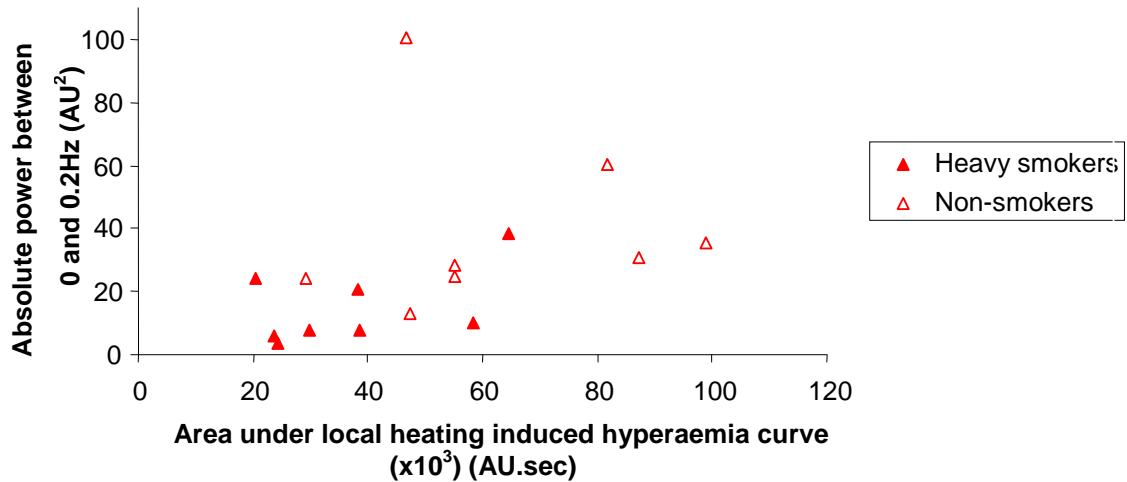


**Figure 6.2** A scatter graph to show the correlation between the absolute local heating response (AUC) and the absolute power of the LDF signal between 0 and 0.2Hz, from 8 heavy smokers and 8 non-smokers. The correlation was significant where  $p=0.007$  (Spearman's Rho test) and the correlation coefficient = 0.647. The graph shows that the heavy smokers had the smaller absolute power of the LDF signal and smaller local heating AUC.

### *Absolute power of frequency bands*

During the local heating stimulus, the absolute power of the frequency band around 0.01Hz (0.008-0.02Hz) and 0.1Hz (0.05-0.15Hz) was significantly smaller in the heavy smokers compared to the control participants (*Figure 6.3*). The absolute power of the frequency band around 0.01Hz, originating from the endothelium, was  $5.2 \pm 5.0$  and  $2.1 \pm 1.0$  AU<sup>2</sup> in the non-smokers and heavy smokers, respectively (median  $\pm$  IQR). The absolute power of the frequency band around 0.1Hz, originating from myogenic microvascular control, was  $12.9 \pm 7.6$  and  $3.8 \pm 7.2$  AU<sup>2</sup> in the non-smokers and heavy smokers, respectively (median  $\pm$  IQR).

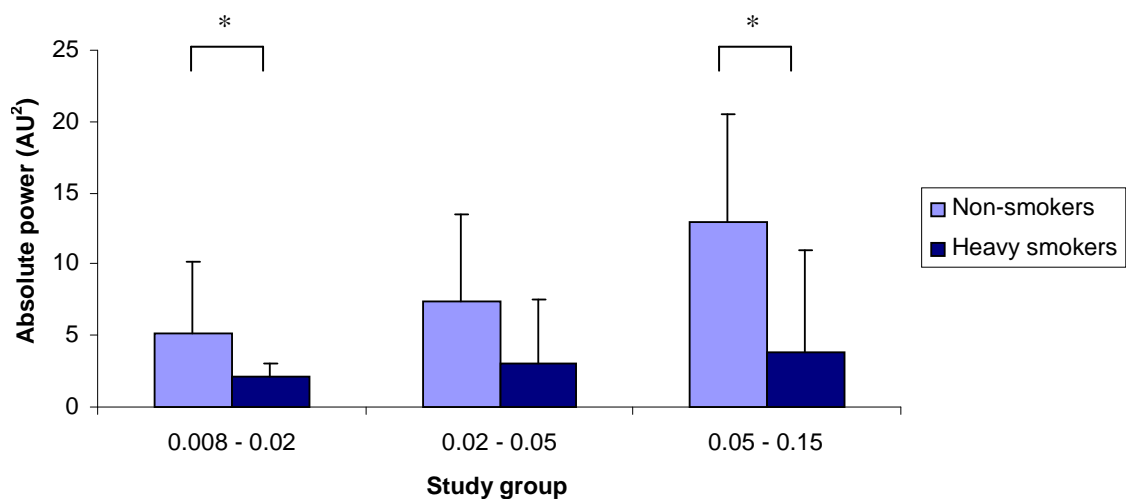


**Figure 6.3** A bar graph to show the absolute power of the frequency band intervals around 0.01Hz (0.008-0.02Hz), 0.04Hz (0.02-0.05Hz) and 0.1Hz (0.05-0.15Hz) during 500 seconds skin heating measured at the forearm of 8 non-smokers and 8 heavy smokers. The data represents median +IQR and the difference between the groups was analysed using the MWU test (\*p<0.05)

The relative power of each of the frequency bands was measured in the LDF signal during the local heating stimulus. The relative power of the band around 0.04Hz (0.02-0.05Hz) was significantly higher in the heavy smokers compared to the matched non-smoking control participants. The relative power was  $23.2 \pm 6.0$  and  $34.3 \pm 10.6\%$  (median  $\pm$  IQR) in the non-smokers and heavy smokers, respectively (*Figure 6.4*)

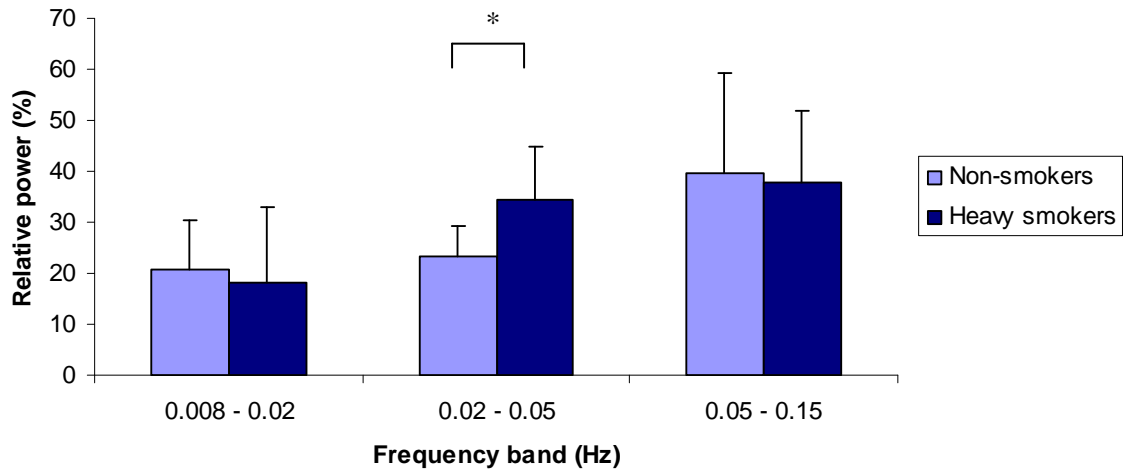


**Figure 6.4** A bar graph to show the relative power of the 3 low frequency bands expressed as a percentage of the absolute power between 0 and 0.2Hz. The bars represent median and the error bars represent IQR for 8 non-smokers and 8 heavy smokers measured during local heating at the forearm. The difference between the groups was tested using the MWU test (\* $p < 0.05$ ).

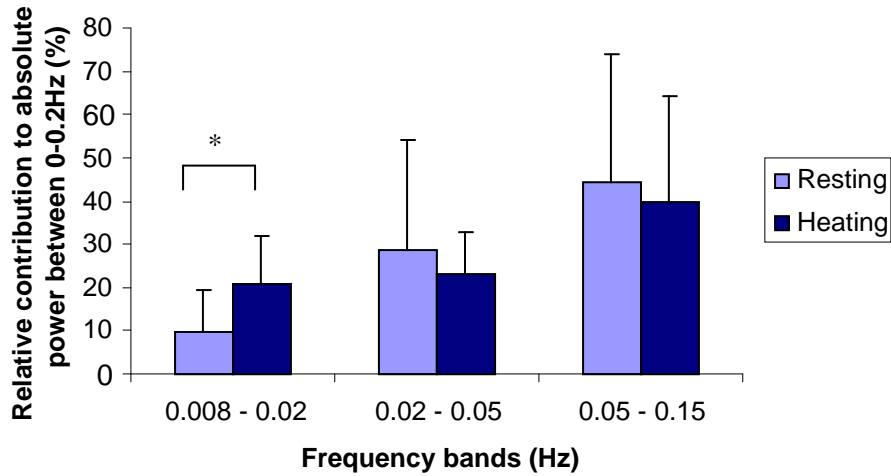
***The change in power of LDF signal from resting flux to local heating flux***

The absolute power between 0 and 0.2Hz and also each of the individual frequency bands around 0.01Hz, 0.04Hz and 0.1Hz were increased in the LDF signal during the local heating response in both the heavy smokers and non-smoker groups.

In the non-smokers, the relative power of the band interval around 0.01Hz (0.008-0.02) increased significantly from resting to heating flux. The relative power of the band interval around 0.01Hz was  $9.5 \pm 9.9$  and  $20.9 \pm 11.0\%$  at rest and during heating, respectively (*Figure 6.5*). This showed more than a 2 fold increase in the contribution of the 0.01Hz frequency band to the absolute power between 0 and 0.2Hz.

In the heavy smokers, there was no significant difference in the relative power of the band interval around 0.01Hz from resting to heating flux. The relative power was  $14.9 \pm 8.1$  and  $18.2 \pm 17.0\%$  at rest and during heating, respectively (*Figure 6.5*).

(a)



(b)

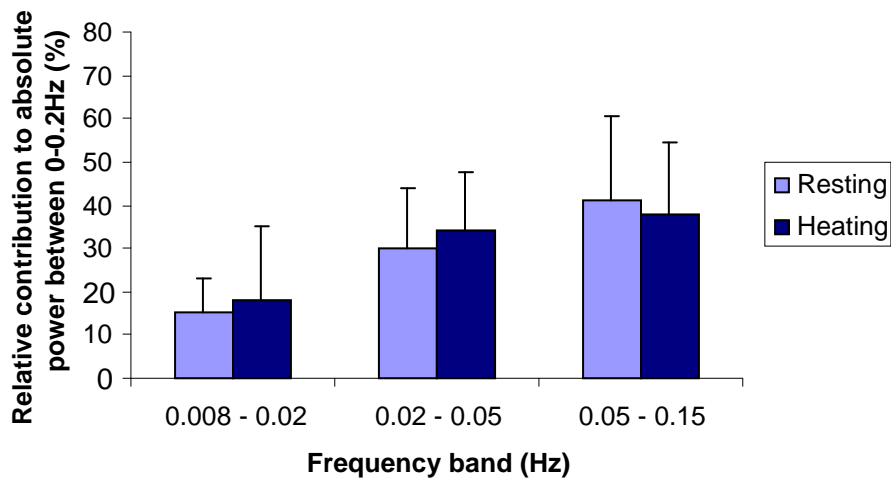


**Figure 6.5** Bar graphs to show the change in the relative contribution of the low frequency bands to the absolute LDF signal power during heated flux compared to resting skin blood flux in the (a) non-smokers and (b) the heavy smokers. The bars represent the median and the error bars represent the IQR. The relative contribution of the frequency around 0.01Hz (endothelium) is significantly increased in the non-smokers during heating compared to resting, when tested using the Wilcoxon paired test (\* $p < 0.05$ ).

### **6.5.3 Spectral analysis in light/moderate smokers and matched controls**

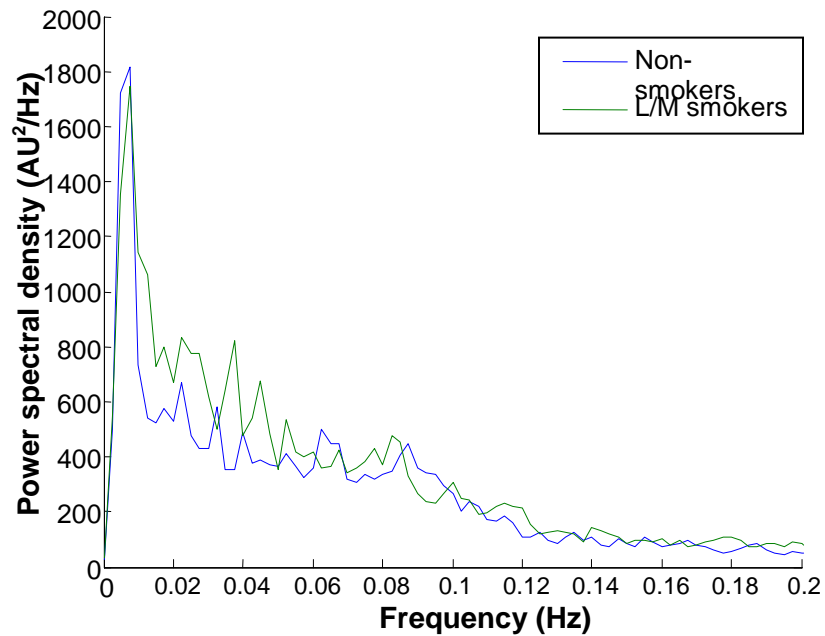
The spectral analysis using an FFT was completed on 20 minutes of resting and heating flux in the LM smokers and matched non-smoking controls.

The spectral analysis to include frequencies up to 2Hz showed identical themes in the LM smokers as has already been described in the heavy smokers. The major contribution to the heating response were the frequencies around 1Hz relating to cardiac control mechanisms. As the main aim was to consider local skin microvasculature control mechanisms, only the low frequency bands up to 0.2Hz are considered in detail in the LM smokers.

#### ***The power of the LDF signal during the local heating stimulus***

The heating stimulus significantly increased the absolute power of the LDF signal between 0 and 0.2Hz. The absolute power of heated skin blood flux was  $71.0 \pm 48.5$  and  $77.4 \pm 84.1$  AU<sup>2</sup> (median  $\pm$  IQR) in the non-smokers and LM smokers, respectively (*Figure 6.6*). There was no significant difference, measured using the MWU test.

(a)



(b)

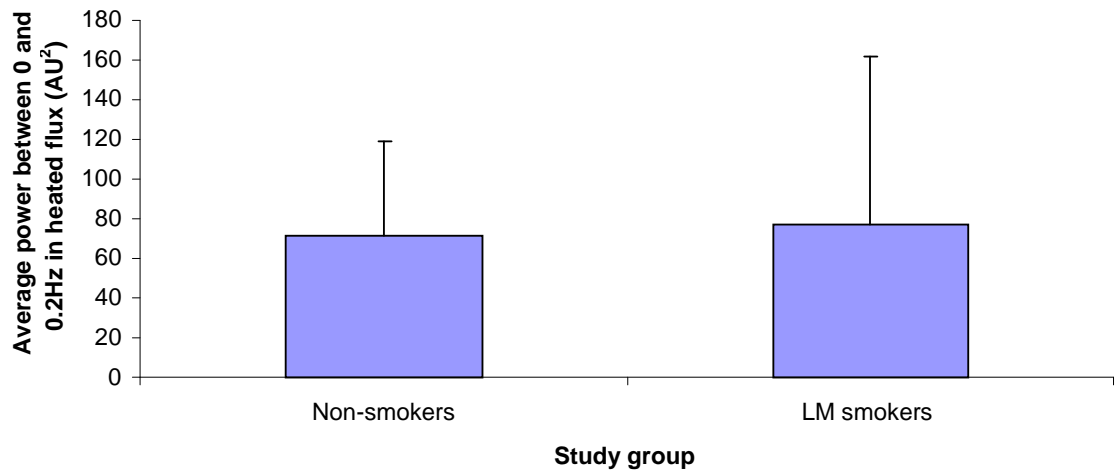


**Figure 6.6** Graphs to show the power of the LDF signal of heated skin blood flux measured between 0 and 0.2Hz over 1100 seconds **(a)** using the Matlab<sup>®</sup> program as a spectrum showing PSD (AU<sup>2</sup>/Hz) and **(b)** represented as a bar graph of the power of the signal (median +IQR) (AU<sup>2</sup>), measured as AUC of the spectrum shown in **(a)**. The data was analysed using the MWU test and the difference between the LM smokers and non-smokers was not significant, where  $p=0.465$ .

### ***Absolute power of LDF signal and the AUC of the local heat induced hyperaemia curve***

The absolute power of the LDF signal and the area under the hyperaemia curve (measured in the time domain) (Figure 6.7) were not significantly correlated in the LM smokers, where the correlation coefficient = 0.334 and  $p = 0.150$ . However, in the LM smoker controls there was a significant correlation, where  $cc = 0.580$  and  $p = 0.007$  (Spearman's Rho test)

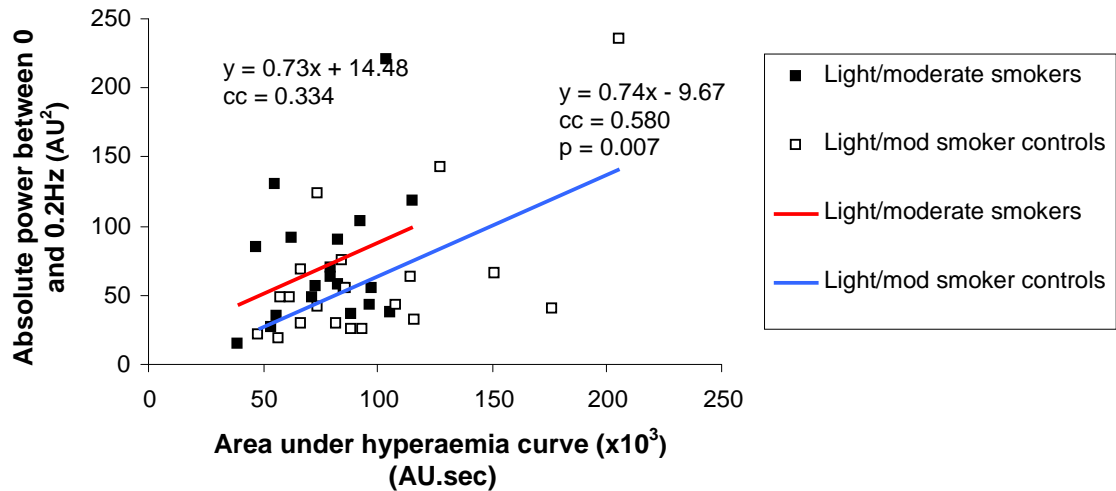


**Figure 6.7** A scatter graph to show the total local heating response (area under response curve) and the absolute power of the LDF signal between 0 and 0.2Hz from 20 LM smokers and 20 matched non-smokers. The correlation was not significant as measured by the Spearman Rho test, where  $p=0.102$

The heating stimulus significantly increased the absolute power in each of the 3 low frequency band intervals. There was no significant difference between the non-smokers and LM smokers in the absolute power of the frequency band intervals around 0.01Hz, 0.04Hz and 0.1Hz measured in the LDF signal during local heating.

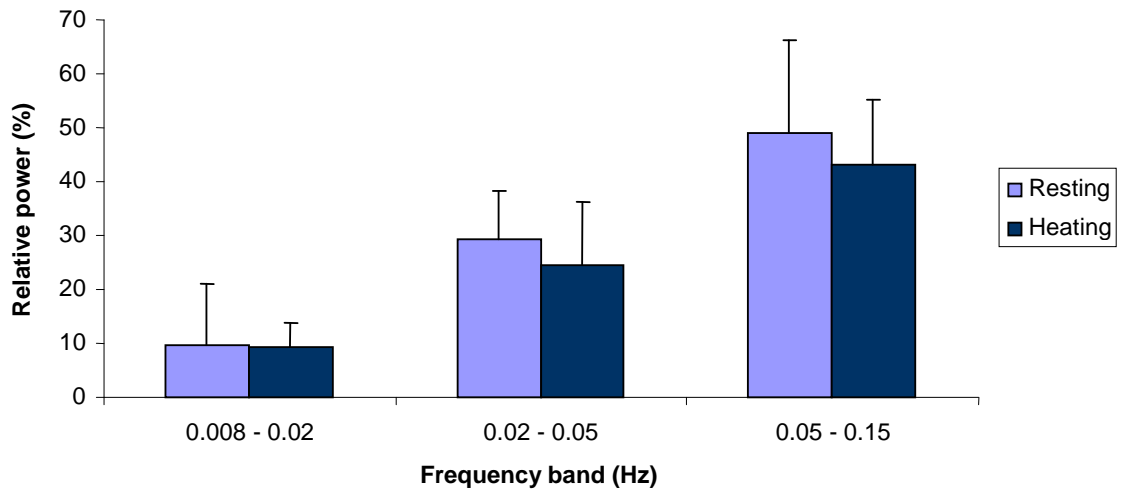
The relative power of each of the low frequency band intervals in the LDF signal during local heating was not significantly different between the non-smokers and LM smokers. The trend was for the relative power of the frequency band around 0.01Hz to be higher in the LM smokers than the non-smokers, but this did not reach significance when analysed using the MWU test ( $p=0.137$ ). The relative power, measured in the heated flux, for the frequency band around 0.1Hz was  $43.0 \pm 11.5$  and  $37.8 \pm 14.9\%$  in the non-smokers and LM smokers, respectively. When analysed using the MWU test, the difference did not reach significance ( $p=0.079$ )

***The effect of the local heating on the relative power of the LDF signal***

The change in the relative power of each of the frequency bands from resting to heating was considered in the non-smokers and the LM smokers. The relative power of each of the low frequency bands measured during heating flux was not significantly different to the relative power measured at rest in either the non-smokers or the LM smokers.

In the non-smokers, the relative power of the 0.01Hz frequency band interval was  $9.5 \pm 11.3$  and  $9.2 \pm 4.6\%$  at rest and during heating respectively (*Figure 6.14*). However, in the LM smokers the trend was for the relative PSD of the frequency band interval around 0.01Hz to be lower in the heated flux compared to the resting flux. The relative PSD was  $14.2 \pm 6.2\%$  in the resting flux and  $10.8 \pm 4.3\%$  in the heating flux, but the difference was not significant, when analysed using the Wilcoxon paired test ( $p=0.057$ ) (*Figure 6.8*).

**(a) Non-smokers**



**(b) LM smokers**

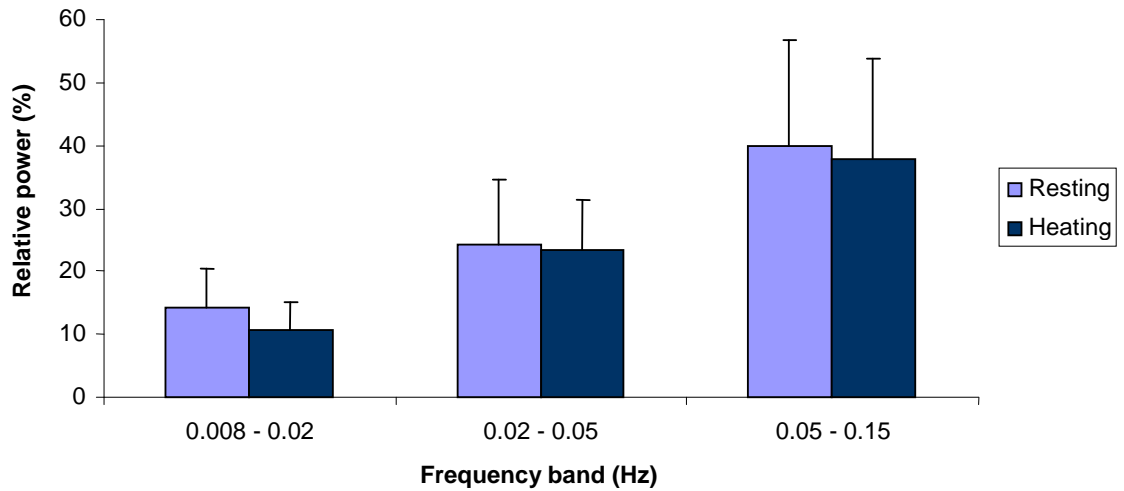


**Figure 6.8** Bar graphs to show the change in the relative contribution of the low frequency bands within the absolute power of the LDF signal between 0 and 0.2Hz, during local heating compared to resting in (a) 20 non-smokers and the (b) 20 LM smokers. Data are expressed as median +IQR. The change in relative power between resting and heated flux was analysed using the Wilcoxon paired test; there was no significant differences in either the non-smokers or the LM smokers ( $p < 0.05$ ).

#### 6.5.4 All smokers (heavy/moderate/light) and matched non-smoker controls

When considering the responses from all 56 participants involved in the studies (10 minute data in both heavy and light smoker groups), a scatter plot shows that there is a positive significant correlation between the magnitude of the local heating measured in the time domain as the area under the response curve and the absolute power between 0 and 0.2Hz of the LDF signal during the heating response. When analysed using the Spearman's Rho correlation test, there is a significant correlation where  $p < 0.0001$  and the correlation coefficient = 0.515. The highest values for both absolute power and the area under the response curve in the LM non-smoking controls and the lowest values are in the heavy smokers (*Figure 6.9*).

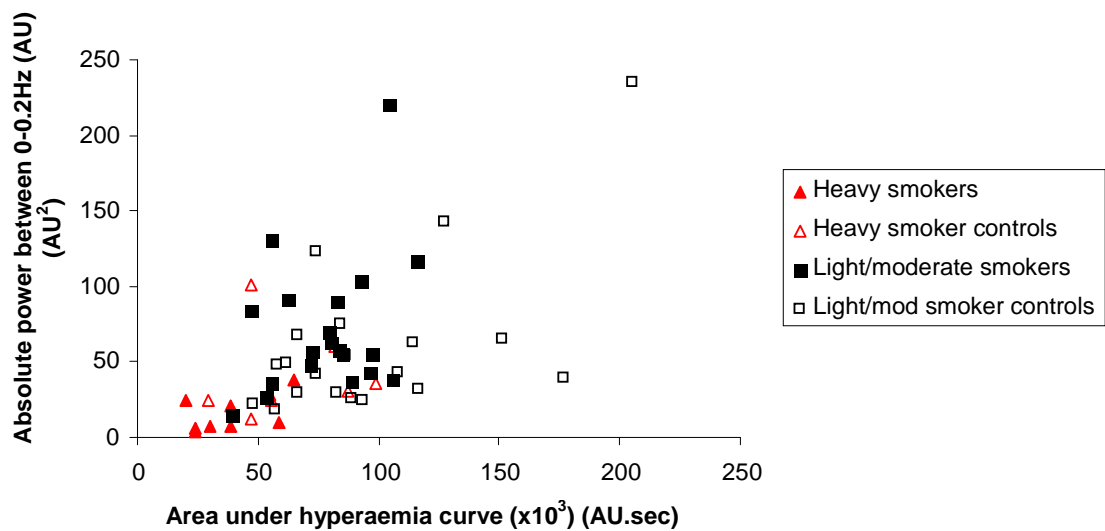


**Figure 6.9** A scatter plot to show the area under the hyperaemia curve plotted against the absolute power between 0 and 0.2Hz of the heated flux in all 56 participants in the studies. The 4 groups involved in the studies can be identified using the key; heavy smokers and matched controls (n=8 pairs) and the light smokers and their matched controls (n=20 pairs). There is a significant correlation between absolute power 0-0.2Hz and the area under the curve, where  $p < 0.0001$  and the correlation coefficient = 0.515, analysed using Spearman's rho test for correlation.

When considering the 10 minute data of each of the participant groups individually (heavy smokers, heavy smoker controls, light/moderate smokers and light/moderate smoker controls), there were no significant correlations between absolute power 0-0.2Hz and the area under the curve.

When considering the absolute power 0-0.2Hz of the local heating response and the absolute power of the low frequency bands, there was no significant differences between the smokers and non-smokers. The change in relative power of the frequency bands around 0.01Hz, 0.04Hz and 0.1Hz in the LDF signal during local heating compared to the resting was analysed in all smokers studied in this chapter (n=28) and compared to all the matched non-smokers (n=28). The results showed that the median change in relative power around 0.01Hz from resting to heating was an increase of  $5.5 \pm 11.9\%$  in the non-smokers, but a decrease of  $1.7 \pm 14.0\%$  in the heavy/moderate/light smokers (median  $\pm$  IQR). The difference was significant where  $p=0.036$  (MWU test) (*Figure 6.10*)

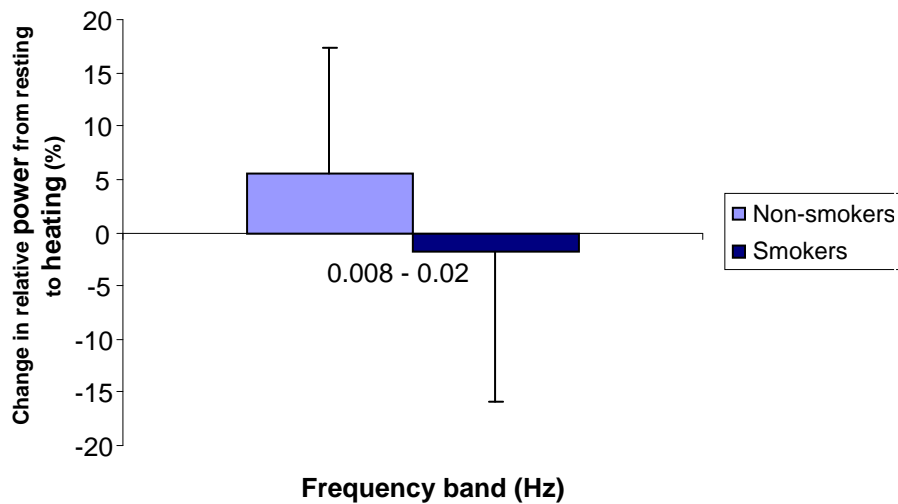


**Figure 6.10** A bar graph to show the change in relative power of the frequency band ~0.01Hz in the heating flux signal compared to the resting flux signal in 28 non-smokers and 28 smokers (light, moderate and heavy). The bars represent the median change and the error bars show minus IQR in the smokers and plus IQR in the non-smokers. The difference between the non-smokers and smokers is significant, where  $p=0.036$  as tested using the MWU test.

There was no significant difference in the change from resting to local heating in the relative power of the 0.04Hz or 0.1Hz frequencies between the smokers and the non-smokers. In the non-smokers, the trend was for a reduced relative power of both the 0.04Hz and the 0.1Hz frequencies. In the smokers, the trend was for an increase in the 0.04Hz frequency, but a slight reduction in the 0.1Hz frequency in the local heating flux compared to resting flux.

### ***Median regression analysis***

Median regression analysis was completed on the results of the spectral analysis. The results were variable and there were some significant correlations, however there is caution in considering these results due to the potential for over-analysis of the LDF signal by completing median regression analysis on the spectral analysis data. Thus, these results have not been included in this thesis.

### ***Summary of key findings***

- The heavy smokers showed reduced absolute power of all 3 low frequency bands compared to the matched non-smoker group, and this reached significance for the frequency bands around 0.01Hz and 0.1Hz.
- A significant increase in the power ~0.01Hz with heating was present in the older non-smokers, but not in the matched heavy smokers.
- There was no significant difference in the absolute power of the LDF signal during the local heating stimulus in the LM smokers compared to the matched controls and also no differences in the change in relative power from resting to heating.
- When considering the 56 participants combined, whereas the non-smokers showed an increase in the relative contribution of the 0.01Hz band with heating, the smokers showed a decrease in this parameter. The difference between these subject groups was significant.

## **6.6 Discussion**

In this chapter, the mechanisms underlying the vasoreactivity of the cutaneous microcirculation to a local heating stimulus at the forearm in heavy and LM smokers and their matched controls has been investigated using spectral analysis of the LDF signal. The results from chapter 4 have shown that the frequency related to cardiac rhythm (~1Hz) dominates the LDF signal during the local heating response. The aim of this thesis is to investigate the vasoreactivity and the local control of skin blood flow, which originate from the low frequency oscillations in the LDF signal. The focus of the analysis in this chapter has been on the power of the low frequency section of the LDF signal between 0 and 0.2Hz. Although the absolute power is described in the results section; the relative power and the change in relative power during heating compared to resting is also given as it

provides information about the contribution of the specific frequency bands to the absolute power between 0 and 0.2Hz.

### ***Heavy smokers***

The absolute power between 0 and 0.2Hz measured in the LDF signal during the local heating response was significantly lower in the heavy smokers compared to the matched controls. This was an expected finding as the total local heating response, measured by AUC was significantly smaller in the smokers, and further analysis of the data has shown that the absolute power correlates significantly with this response parameter. The results showed that the reduced absolute power between 0 and 0.2Hz in the heavy smokers was due to a reduced absolute power in all three low frequency bands, but only significantly in the bands around 0.01Hz (endothelium) and 0.1Hz (myogenic).

When the absolute power of the frequency bands was calculated relative to the absolute power between 0 and 0.2Hz there was no significant difference in any of the frequency bands between heavy smokers and non-smokers. When considering post-ischaemic changes in skin blood flow in smokers, the smokers were shown to have an absent post-ischaemic increase in skin blood flow and this was particularly related to the frequency components originating from endothelium and myogenic control (Rossi et al., 2007). The post-ischaemic hyperaemia results in a different response to that produced by local heating response, but is considered to involve shear-induced vasodilation (Rubanyi et al., 1986), as well as accumulation of metabolic vasodilators and the myogenic response (Rasool et al., 2009). Although studies have shown there to be a role for NO in the post-ischaemic response (Tagawa et al., 1994), others have shown little effect of NO in the response following more prolonged ischaemia (Cankar et al., 2009).

The initial 100 seconds of LDF trace immediately after the beginning of the local heating stimulus was removed from the spectral analysis because the sharp upward rise in skin blood flux during this period is shown in the spectral analysis as a very low frequency itself. The aim of this work is to consider the oscillation frequencies within the LDF signal itself. This means that the section of flux that would be expected to include significant neurogenic control (Minson et al., 2001) was removed from the analysis. The plateau section of the local heating response has been shown to be mainly NO-dependent (Minson et al., 2001).

When making direct comparisons between the heavy smoker group and the matched non-smokers, the only significant difference in the relative power during heating was in the band around 0.04Hz. The relative power around 0.04Hz was significantly higher in the heavy smokers during heating.

The neurogenic mechanisms of blood flow control have been shown to have only a minimal contribution to the plateau phase of the local heating response (Minson et al., 2001). However, a small study (Appendix 4) completed during the thesis, showed that the effect of EMLA (block axon reflex) at the site of heating in 6 participants, was a reduction in the plateau heating response and a significant reduction in the relative power around 0.04Hz compared to the resting flux prior to EMLA application. This suggests that changes in neurogenic control in the frequency around 0.04Hz can be measured in the spectral analysis of the plateau phase of the heating response using the methods in this study. It maybe that in the heavy smokers the balance in the control of skin blood flow is altered; the myogenic and neurogenic contribution to the absolute power was similar. Although there is some evidence to suggest that cigarette smoking increases sympathetic activity in the skin (Narkiewicz et al., 1998), this is shown to be an acute effect.

The change in the relative power of each band from resting flux to heated flux was also analysed in the LDF trace. The non-smoking controls showed a significant increase in the absolute power around 0.01Hz with heating. Studies have shown that the local heating response is mainly caused by an increase in blood flow control related to the endothelium, and that this is more influential in the heating response than myogenic mechanisms (Brienza et al., 2005). Others have found that although the endothelium band was increased with maximum thermally induced hyperaemia, the myogenic band was decreased (Jan et al., 2005). Geyer et al. (2004) showed, using Wavelet analysis of the heating response, that endothelium related mechanisms are responsible for local heat induced blood flow regulation. The lack of an increased contribution of endothelium-related control in the heavy smokers may be due to the effects of smoking on the endothelium.

It is important to consider that direct comparison of the results in this study with other studies are difficult due to the varying methods used for completing spectral analysis (mainly Wavelet and FFT) and the way the data is described. For example, although in this chapter the absolute power of the individual frequency bands was normalised to the absolute power in the whole frequency range being considered, either 0-0.2Hz or 0-2Hz, others normalise the results to the resting power (Jan et al., 2009; Brienza et al., 2005) or quote the mean amplitude of the PSD curve (Azman-Juvan et al., 2008).

### ***Light/moderate smokers***

In order to reduce the random error and the bias error within the PSD estimate (methods section 2.5), the resting and heating data were collected for longer in the light smokers; the resting flux was measured continuously for 20 minutes and the local heating was applied for 20 minutes.

The results showed high variability, both in the LM smokers and the non-smokers, and particularly when analysing the local heating flux. This can be illustrated by considering the range of results; the range of absolute power in the heating flux of the non-smokers and LM smokers was 25.2-254.6 and 29.5-448.0 AU<sup>2</sup>, respectively. There were no significant differences in absolute power or the relative power of the frequency bands between the LM smokers and non-smokers.

The change in relative power from resting to heating showed no significant differences. Interestingly, there was no observed increase in the relative power around 0.01Hz in the non-smokers or the LM smokers during the heated flux when compared to the resting flux. It may be that a compensation mechanism to increase the capillary flow during resting in LM smokers may mean the contribution does not increase more during heating.

The variability in the spectral analysis of the LDF signal in the LM smokers and matched controls may be due to the range of age and smoking status within this group. The participants were aged between 18 and 35, and the smokers had smoked for between 2 and 15 years (1.5-10 packyears). It may be that the participants had differing degrees of altered endothelial function and also compensation mechanisms. It is also possible that due to the longer data collection (20 minutes) to reduce the random and bias error in the measurements, the stationarity of the data was affected.

#### ***All participants considered together***

The spectral analysis of the local heating response for all 56 participants was considered as one group including 28 non-smokers and 28 smokers (light, moderate and heavy). The median regression analysis was completed on these results, however, there was caution as to the interpretation of these results and these have not been included in this thesis.

When considered as one group, the results showed that there was an increase in the median relative power around 0.01Hz in the heating flux compared to the resting flux in the non-smokers, but a small decrease in the smokers, and this difference was significant. It would have been expected that the frequency around 0.01Hz related to endothelium and specifically endothelial NO activity would have been reduced in the smokers. Many studies have shown reduced vasoreactivity and endothelial dysfunction with smoking, but there have also been studies to show an increase in NO in smokers (Chavez et al., 2007), and also increased anti-oxidant levels in smokers (Chavez et al., 2007). Although studies have shown endothelium mechanisms to be dominant in the local heating response (Jan et al., 2009; Brienza et al., 2005; Geyer et al., 2004), there is general acknowledgement that the skin blood flow response to local heating is controlled by different mechanisms to differing degrees (Jan et al., 2009).

### *Limitations*

There are limitations to the findings in this chapter. The smoking status of the smoker participants relies on cotinine levels (heavy smokers only) and /or self-report and therefore there is no biological reference for time since last cigarette. The 1 hour abstinence from cigarette smoking may mean that there are some acute effects of cigarette smoking present in the results of the spectral analysis and that some of the effects on the underlying mechanisms found in the smokers are acute effects. As the heavy smokers tended to have smoked more recently than the light smokers, and have difficulty with compliance, the acute effects may differ between the 2 groups.

The spectral analysis is derived from a LDF signal, the limitations of which have been discussed in the previous chapters. The artefact inherent in LDF recordings can affect the spectral analysis, although efforts were made to limit the artefact on the signal in this study. The PSD is also only an estimate of the distribution of signal power over the frequency bands in the signal. The PSD of a random, non-stationary signal, such as a biomedical signal, can only ever be an estimate. The different frequency components in the cutaneous microvasculature are non-constant and they vary with time (Smith, 1997). The resting and heating flux was analysed separately as any change in time in the signal is spread over the entire frequency interval. There is much debate over the techniques used for spectral analysis and much of the work completed in this area has used Wavelets rather than FFT's.

In this study, the spectral analysis during heating relied on adequate detrending of the heating response flux signal in order to remove the very low frequency increase in flux at the commencement of heating. This would otherwise dominate the PSD at the very low frequencies, but the detrend may also effect the lowest frequency band. The effect of the detrend on the power around 0.01Hz was checked to consider the effect of different levels of detrend (methods), but this need for manipulation of the data in this way must be considered a limitation. It is possible that although the method of detrend was the same in each participant, the higher increases in blood flow were not detrended as efficiently as the lower increases; this is because each response was different, but the detrend system was always the same. This could mean that there remain higher very low frequency in some individuals that could effect the power of the band around 0.01Hz (0.008-0.02Hz) and/or the absolute power 0-0.2Hz.

The initial 100 seconds was also removed from the heating analysis to aid in the process of detrending and this removes the initial, axon-reflex controlling rise in flux caused by heating. Thus, findings relating to the neurogenic mechanisms of blood flow control must be treated with caution as important information regarding these mechanisms has been removed. It is also important to

acknowledge that the frequency band around 0.01Hz involves one oscillation per 100s, so the analysis is involving only 5 cycles in the heavy smoker study.

Although the CV for the site to site and day-to-day measurements of the spectral analysis showed that the relative power had much reduced CV compared to the absolute values, the relative values may contain some error. The relative power is measured as the contribution of the band to the absolute power 0-0.2Hz; this included frequency range above and below the bands being focussed on. It is also important to consider that the bandwidths used to determine the different frequencies may be changed by the local heating stimulus (comment by Simpson, DS), so the assumption has to be made that the bands used are reflective of the mechanisms expected. The studies that have explored the bandwidths and the mechanisms of skin blood flow control they relate to were mainly done using Wavelet analysis.

After completion of the spectral analysis as shown in this chapter, further work was done on the data and refinements to the process of the spectral analysis by Dr David Simpson. There was an additional step introduced so that the sections of LDF signal to be analysed were first decimated to a 1 Hz sampling rate, and then high-pass filtered (3<sup>rd</sup> order Butterworth filter, cut-off frequency of 0.005 Hz). Spectral analysis was then carried out only on the last 350 seconds of the resting and heating data, to avoid the sudden changes in flux during heating. The results from this analysis had similarities to those in this chapter.

### ***Final Summary***

In order to maintain cutaneous viability and health, an appropriate cutaneous blood flow is essential. When pressure, friction and/or shear are applied to the skin, then inadequate cutaneous blood flow can result and eventually pressure ulcer development. The risk of developing a pressure ulcer can be increased by factors which alter the cutaneous microcirculation, such as smoking and ageing.

So far in this thesis it has been shown that heavy smokers have a significantly attenuated response to a local heating stimulus applied to their skin and there was a trend towards reduced responses in LM smokers. Increasing smoking longevity/intensity, as measured by packyears, was significantly predictive for a reduced response to local heating.

In this chapter, the spectral analysis of the LDF signal has shown that the absolute power of the LDF signal between 0 and 0.2Hz during heating is significantly lower in the heavy smokers. It has also been shown that the significantly increased contribution of the 0.01Hz frequency from resting

to heating flux in the heavy smoker controls, was absent in the heavy smokers. This may suggest an altered endothelial function as the cause for the reduced vasoreactivity in the heavy smokers. However, no differences could be seen in the LM smokers compared to the controls, and there was no increase in the relative power of the 0.01Hz frequency band in either the LM smokers or their controls.

When considering all the participants together, the non-smokers showed an increase in the relative power around 0.01Hz in the heating flux compared to the resting flux, and the smokers showed a decrease, and the difference between the groups was significant. This suggests that the attenuated responses to local heating with smoking may be due to a reduced relative contribution of the frequency related to endothelial control of the cutaneous microcirculation. The measurement of skin blood flow responses to local heating using LDF with further analysis using FFT can provide evidence of changes in the control of the microcirculation and thus potentially demonstrate increased risk of pressure ulcer development.



## **Chapter 7**

### **General Discussion**

## 7.1 The concept of the thesis

This thesis set out to investigate the impact of smoking on cutaneous vasoreactivity and its effects on microvascular control mechanisms. Any attenuation in cutaneous vasoreactivity in the smokers and verification that there are changes in blood flow control mechanisms in this group, would provide evidence for a potential increased risk of pressure ulcer damage in smokers, and may be a method for skin assessment and risk determination in vulnerable patient groups.

The regulation of the skin microcirculation by endothelial, smooth muscle and neurogenic mechanisms results in an oscillatory blood flow; this is in part related to the rhythmical contraction and relaxation of the arterioles in the skin, which is termed vasomotion. This vasomotion is thought to benefit the tissues, due to its ability to increase flow and oxygenation to the tissues (Tsai and Intaglietta, 1993; Ursino et al., 1996). The appropriate regulation of skin blood flow is important in order to meet the metabolic demands of the tissue and maintain tissue homeostasis, but it is also important that the skin microcirculation have the capacity to respond appropriately to external stimuli.

There is evidence that direct pressure on the skin surface, as well as friction and shear forces are important causal factors in the development of pressure ulcers. The effect of these forces is directly on the skin microcirculation and can result in blood flow occlusion and ischaemia, impaired interstitial fluid flow and lymphatic drainage and clot formation. There is also the suggestion that the reperfusion that follows the relief of the pressure loading on the skin causes additional damage due to the influx of reactive oxygen species into the area.

Smoking is a recognised risk factor for cardiovascular disease; it is also a potential risk factor for pressure ulcer development. It is thought that smoking can increase the risk of developing a pressure ulcer through modulating cutaneous vascular control, potentially through its effects on endothelial function. The endothelial lining of the blood vessels is not simply a barrier between the blood flow and interstitial compartment, but is important in regulating changes in blood flow, angiogenesis and metabolic, anti-inflammatory and antithrombogenic processes (O’Riordan et al., 2005). Thus, normal endothelial function is important in regulation of skin blood flow and changes in endothelial function may be a factor on which to determine pressure ulcer risk (Struck and Wright, 2007).

## 7.2 Summary of findings

Initially the impact of smoking on vascular responsiveness was measured using the application and removal of a loading stimulus in heavy smokers and matched non-smokers (*Chapter 3*). The results demonstrate no attenuation in the RH in the heavy smokers compared with the non-smokers. The loading stimuli resulted in highly variable changes in blood flow and reactive hyperaemic response. It could be seen by observing the LDF trace during loading and following removal of the load that the oscillations within the signal changed during reactive hyperaemia. This could not be accurately explored in the participants in this study due to the steep transient increase in blood flow after removal of the load, which was non-stationary.

The local heating stimulus in combination with LDF was used in the remaining studies in the thesis, due to its relevance in terms of measuring the vasoreactivity of the skin and also so that the mechanisms of regulation of skin blood flow could be investigated using spectral analysis. Initially, the local heating response at the sacrum (a site at risk for pressure damage) was compared to the responses at the forearm (*Chapter 4*). The sacrum had a significantly greater resting skin blood flow and reduced responses to the local heating challenge. Assessment of the mechanisms of skin blood flow control using spectral analysis (FFT) showed that although the resting SBF was higher at the sacrum, the relative contribution of the frequency around 0.01Hz (endothelium) was borderline significantly ( $p=0.051$ ) lower. There was no significant difference in the mechanisms controlling the heating response at the sacrum compared to the forearm. The studies showed there to be significant correlation in the hyperaemia responses to local heating between the forearm and sacrum sites.

The skin blood flow response to a local heating stimulus was measured in a group of heavy smokers and LM smokers, and their respective matched control participants at the forearm (*Chapter 5*). The local heating induced hyperaemia (43°C for 10 minutes) was significantly attenuated in the heavy smokers compared to the control participants. In the LM smokers, there was also a trend for reduced vasoreactivity to the local heating stimulus compared to the control participants. When considering heavy and LM participants together, the median regression analysis showed that smoking status measured in packyears was significantly predictive, so that with increasing packyears, there was a predictive fall in mean blood flux during heating.

The underlying mechanisms for the significantly attenuated responses in the heavy smokers and the reduced response in the LM smokers were investigated using spectral analysis (FFT) of the LDF

signal (*Chapter 6*). The LDF signal in the heavy smokers had a significantly reduced absolute power in the low frequency range (0-0.2Hz) and in the absolute power of the frequency bands related to endothelial (0.01Hz) and myogenic (0.1Hz) mechanisms. However, the relative contribution showed no differences between the heavy smokers and non-smokers.

The heating response in the non-smokers caused a significant increase in the contribution of the frequency band related to the endothelium (0.01Hz), but this was not present in the heavy smokers. This would suggest that the reduced responses in the heavy smokers were due to a dysfunctional endothelium. There was no significant difference in the spectral analysis of the LDF signal in the LM smokers compared to the controls. The increased contribution of the 0.01Hz frequency during the heating response in the heavy smoker controls was not found in either the LM smokers or their matched control participants.

When considering all the participants together, the non-smokers showed an increase in the relative power around 0.01Hz in the heating flux compared to the resting flux, and the smokers showed a decrease, and the difference between the groups was significant. This suggests that the attenuated responses to local heating with smoking may be due to altered endothelial control of the cutaneous microcirculation.

### **7.3 Implications of the findings**

In the past, patients and their relative accepted the development of a pressure ulcer as an inevitable result of the disease process and incapacity of the patient concerned. They are now considered as the result of below standard patient care and legal action can be brought against those who were responsible for the care of the patient (Dimond, 2003). Alongside the increased awareness regarding pressure ulcers in the general public, there is also a lack of rigorous research to support the clinical management of pressure ulcers (NICE, 2001).

There are several reasons for this lack of research. The most important ones relate to the ethical difficulties in conducting human studies to sample and biopsy pressure ulcer tissue at different stages of development. Much research is completed in vitro or in animal models, but these results are limited in their application to the human body (Edsberg, 2007). The appropriate assessment of a patient's risk of developing a pressure ulcer is also an area that has a lack of research. Few of the risk factors contained on risk assessment tools are based on rigorous research evidence.

In this past few years, work has been focused on creating systems in hospitals and the community, where patients at risk of pressure damage are seen by an appropriate specialist as quickly as possible. For example, Choromanski et al. (2008) and Cho et al. (2008) and others have looked at creating a database of 'at risk' patients, which automatically alert pressure ulcer specialists about these patients. This seems an obvious direction to go in given the leaps in technology used in many walks of life. However, these systems require an appropriate determination of pressure ulcer risk, otherwise patients will be overlooked or there will be large resource implications of pressure ulcer prevention strategies enforced in patients that don't require them.

The studies in this thesis highlight two main aspects about risk assessment for pressure ulcer development. Firstly, although smoking is considered to be a risk factor for many diseases, it is not considered on all pressure ulcer risk assessment scales. The findings from the studies in this thesis have shown that heavy smokers have an attenuated vasoreactive response to a local heating challenge to the skin. Other studies have shown reduced cutaneous hyperaemia responses in long-term smokers (Pellaton et al., 2002; Sprigle et al., 2002; Rossi et al., 2007; Edvinsson et al., 2008). However, in this study, there were also reduced responses in the LM smokers (borderline significance), and across all the participants, a general significant trend where increased packyears, result in a reduced skin blood flow response to local heating. Although further studies are needed to clarify the link between reduced vasoreactivity and increased incidence of pressure ulcers, the results provide potential evidence that smoking should be considered as a risk factor for pressure damage.

Secondly, the studies in this thesis consider the potential to use spectral analysis to investigate the mechanisms involved in the control of skin blood flow, and in particular the function of the endothelium. Although the findings of the thesis showed there to be potential alterations in endothelial function in an older group of heavy smokers compared to non-smokers, there were no differences in LM smokers. Altered endothelial function has been shown to be present in smokers (Celermajer et al., 1993) and this may be due to the degradation of NO by increased levels of ROS as a result of smoking or direct endothelial cell damage (Radi et al., 1991). The findings of this thesis, using LDF in combination with spectral analysis, show that this can be detected non-invasively and locally in the skin tissue. However, as there were no differences in the spectral analysis of the mechanisms of blood flow control in the LM smokers, it would suggest that either the LM smokers do not show early changes or that the methods used in this thesis are not accurate enough to detect them.

Although the heavy smokers showed attenuated vasoreactivity in response to local heating and the LM smokers also showed a trend towards attenuated responses (borderline significance), there were not similar patterns shown by the spectral analysis in terms of effects on blood flow control mechanisms. It may be that the LM smokers and heavy smokers would need to be considered as separate populations due to different effects on skin blood flow mechanisms. It has been shown that when light smokers smoked a cigarette, the skin blood flow of the thumb decreased, but returned to baseline levels immediately after the end of smoking a cigarette. In the heavy smokers, the skin blood flow remained unchanged before, during and after smoking a cigarette. The authors suggest that the heavy smokers have a severely disturbed microcirculation (Midttun et al., 2006). Another study showed similar results when measuring forehead skin blood flow in light and heavy smokers, during cigarette smoking and suggest that there is potential tolerance in heavy smokers (Meekin, et al., 2000). It is possible that the LM smokers have some chronic effects from the cigarette smoke on their cutaneous microcirculation, but that compensation mechanisms overcome these effects. In the heavy smokers, these mechanisms can no longer cope and dysfunctional responses are present. It may also be due to a combination of acute and chronic effects of smoking in the heavy smoker group.

In the literature, there are differences in findings related to skin blood flow in smokers and the mechanisms of blood flow control that may be affected by smoking. Although some studies show reduced resting skin blood flow in smokers, more recently there has been shown to be elevated resting flow and reduced forearm vascular resistance in smokers (Mitchell et al., 2005) and others have shown neovascularisation in response to nicotine is actually enhanced with increasing age (Suner et al., 2004), so that heavy smokers may have increased baseline flow. In terms of skin microvascular reactivity, although studies have shown reduced responses in smokers (Rossi et al., 2007a; Edvinsson et al., 2008), there has not been consensus regarding reduced endothelium-dependent vasodilation specifically. Although, Celermajer et al. (1993) showed reduced endothelium-dependent vasodilation and not endothelial-independent vasodilation in smokers, this study involved measurement of flow-mediated brachial artery vasodilation; this was not confirmed when considering the microcirculation (Edvinsson et al., 2008). These results suggest that the attenuated responses in smokers are not solely the result of endothelial dysfunction.

Since the completion of the studies contained in this thesis, other groups have used LDF with spectral analysis to aid in the development of pressure ulcer prevention strategies, including specialized mattresses. These mattresses work to certain timing schedules and patterns, so that different sections of the mattress inflate and deflate in order to relieve pressure regularly. In a recent study there has been consideration of the effects of different timings of pressure on skin

vascular responses and the control of skin blood flow (Jan et al., 2008). It is thought that a more detailed understanding of the evident vascular control mechanisms in certain patient groups have the possibility of determining the patients need for a mattress and/or the particular timing regime for the mattress (Jan et al., 2008).

Although the studies in this thesis has focussed on measurement of vasoreactivity and mechanisms of blood flow control in smokers in relation to their skin health and potential increased risk of skin tissue damage. Much of the recent literature has considered similar investigation of the skin microcirculation as a non-invasive method to assess general endothelial function in the vasculature and have shown that changes in the skin microcirculation can be an early sign of vascular disease in other organs. It is argued that the skin microcirculation mirrors the microcirculation in other organs and has the benefit of allowing non-invasive study.

In particular, there has been much attention on cardiovascular disease and recognition of early changes in the skin microcirculation occurring even before changes in the macrocirculation. It has been shown in several studies that early changes can be detected using spectral analysis of LDF during a vasodilation response (Rossi et al., 2006b; Rossi et al., 2009). For example, skin vasodilator responses to ACh in patients with hypercholesterolemia with and without manifest coronary artery disease showed blunted responses in patients with Coronary Artery Disease (CAD), but normal skin vasoreactivity to ACh in the patients with hypercholesterolaemia without CAD (Khan et al., 1999). A further study has shown a similar maintenance of microvascular reactivity to ischaemia and heating in patients with hypercholesterolemia and no CAD (Stulc et al., 2003).

More recently, Rossi et al. (2009) completed a study in which they measured the vasoreactivity response in the skin to ACh and SNP in patients with hypercholesterolaemia and no manifest arterial disease and matched controls. The resultant signal was then analysed further using a FFT algorithm to determine the power of the LDF signal. They found that although there were no differences in the hyperaemic response to ACh and SNP in the patients compared to controls, the hypercholesterolaemia patients showed a smaller increase in absolute power between 0.01-1.6Hz and smaller increase in endothelium-dependent interval and respiration interval and this was statistically significant (Rossi et al., 2009). This study demonstrates the potential of spectral analysis of the LDF signal of skin blood flow to be more sensitive than the measurement of vasoreactivity alone to assess early changes in skin blood flow regulation

In a study considering patients with stage II peripheral arterial obstructive disease (PAOD), the patients were found to have a normal baseline leg skin perfusion (Del Guercio et al., 1986).

However, spectral analysis of the skin tracing showed abnormal flow pattern in these patients, with abnormally increased amplitude of the low frequency flowmotion waves relating to endothelial function, neurogenic and myogenic activity. It is suggested that there may be compensatory mechanisms to maintain normal perfusion in these patients. The post-ischaemic hyperaemia was blunted in these patients, and the waves related to endothelial, neurogenic and myogenic regulation of skin blood flow did not increase during the hyperaemia, suggested that the compensatory mechanisms are exhausted (Rossi and Carpi, 2004). Changes in the mechanisms of skin blood flow regulation have also been demonstrated in patients with long-standing essential hypertension (EHT) and newly diagnosed EHT (Rossi et al., 2006b). The magnitude of the increase in blood flow at the forearm following ischaemia was not significantly different in the controls, newly diagnosed or longstanding hypertension. However, the longstanding hypertensive patients showed an absence of increase in total power and the frequencies (apart from myogenic) compared to the controls and newly diagnosed EHT patients.

Finally, a further study has shown an association between risk of coronary heart disease and microvascular function (IJzerman et al., 2003a). In this study, they used LDF in combination with ACh and SNP and capillary microscopy to observe nailfold capillaries at the finger. They assessed the Coronary Heart Disease (CHD) risk according to the Framingham Heart study and none of the participants had cardiovascular disease. They found that an increased risk for CHD was associated with lower endothelium dependent vasodilation and capillary recruitment and this finding was independent of age.

If we consider that changes in skin vasoreactivity and changes in mechanisms of regulation of blood flow have the potential to increase risk of pressure ulcer development, then the current plethora of research using the skin microcirculation as a tool to study vascular diseases has much relevance. If changes to the skin microcirculation are an early indicator of cardiovascular disease, then they also occur before the patient is potentially aware of the disease and thus may be a hidden risk factor for pressure ulcer development.

The method of skin blood flow assessment using LDF and a challenge is simple and non-invasive and can be used at many sites in the human body. The studies in this thesis have demonstrated the potential for LDF in combination with a challenge to the skin to be used in different potentially at risk patient groups. Furthermore, the potential for the LDF signal to be analysed using spectral

analysis to consider the control mechanisms of the skin microcirculation, should have huge implications for the field of pressure ulcer risk and prevention. An appropriate functioning skin microcirculation, and in particular the endothelium, is vital to the health of the skin and an increased knowledge of blood flow control mechanisms in different patient groups and disease states should provide vital evidence regarding risk.

#### **7.4 Implications of the findings for clinical practice – LDF research equipment or clinical tool?**

The health of the skin is dependent on adequate skin blood flow and vasoreactivity of the skin microcirculation, due to the need to provide for the metabolic needs of the tissue and maintain homeostasis within the tissue.

The studies in this thesis used the non-invasive technique of LDF to measure the vasoreactive responses to a loading and heating stimulus in smokers and matched non-smokers. Although the findings demonstrated difficulties with the loading study and interpretation of the results due to problems with artifact on the LDF trace, more recent advances in technology to apply a load make this a relevant and useful stimulus for future studies to consider cutaneous vasoreactivity.

The majority of this thesis focused on the cutaneous microvascular response to a local heating stimulus in a group of smokers. The studies demonstrated significant differences in the response in heavy smokers and this was dependent on intensity/longevity of smoking habit. These patients may be at increased risk of damage to the skin and pressure ulcer development, due to attenuation of the blood supply needed to maintain the metabolic needs of the skin tissue and reduced ability to respond to the increased needs of the tissues. Therefore smoking should be considered as a potential risk factor for pressure ulcer development.

At the moment, the use of the LDF to measure vasoreactive responses in the skin microcirculation is purely scientific to aid in the development of knowledge regarding the skin blood flow and vasoreactivity in certain patient groups. This scientific study regarding skin blood flow can develop knowledge regarding which factors indicate increased risk of pressure ulcers; consensus on these factors is currently lacking (Gould et al., 2002).

With developments in technology such as specialist beds to reduce the risk of pressure ulceration in ‘at risk’ patients, there is a need for developments in risk assessment, so that the correct patients are given the technology. Although LDF is a non-invasive tool, there would need to be improved

technology to make it accessible to use on patients and to ensure that artifact on the signal produced is considerably reduced. The use of LDF in combination with spectral analysis also has the potential to provide information about mechanisms of blood flow control, but developments in technology to produce this information at the bedside would be needed. At the moment, LDF with spectral analysis is a useful research tool, but needs more research and development before it could be a clinical tool for pressure ulcer risk assessment.

There has been much development in the clinical use of the LDI particularly in its potential to indicate whether burn wounds are likely to heal, and to help determine the potential necessity for surgery (Moor Instruments, 2011a). Although the LDI is easier to use clinically, the LDF has also been used clinically in skin flap monitoring applications (Moor Instruments, 2011b). Further development of the LDF and software relating to spectral analysis of the signal is needed for progress in the field of pressure ulcer risk assessment.

## **7.5 Future work**

### **7.5.1 Nitric oxide and microdialysis studies**

The results from the studies in this thesis have demonstrated that there is attenuated cutaneous microcirculation vasoreactivity in heavy smokers. It also reveals that an increase in cigarette smoking duration and/or intensity measured by packyears, significantly predicts reducing local-heating induced hyperaemic responses. Although the difficulties with abstinence in the heavy smokers may mean that acute effects of smoking must be considered too. Using LDF in combination with spectral analysis, there is evidence that the attenuated vasoreactivity in the heavy smokers may be due to endothelial dysfunction. In order to investigate this further, the sampling of the specific local factor NO associated with endothelial function within the tissue will be completed. The plateau section of the local heating response has been shown to be mainly NO-dependent (Kellogg et al., 1999), and thus regulated by the endothelium. Several studies have shown that smoking effects the plasma levels of NO, further confirming that a reduction in the NO produced by the endothelium, may be responsible for the attenuated vascular responses to local heating in the smokers. The technique of microdialysis has the potential to allow measurement of the local levels of NO in the extracellular space as opposed to systemic plasma levels, and thus may provide more information on local endothelium function in the skin microcirculation. A pilot study has been completed and this can be found in *Appendix 5*.

### **7.5.2 Stage 1 pressure ulcers**

The analysis and sampling of the skin tissue during the stages of pressure ulcer development has been problematic due to the ethical issues of sampling damaged skin in humans (Edsberg et al., 2007). LDF as a non-invasive method of skin blood flow assessment has the potential to be used at the early stages of pressure ulcer development in intact skin, to measure skin blood flux. At the initial stage of pressure ulcer development (stage I), the pressure ulcer is defined by the National Pressure Ulcer Advisory Panel (NPUAP, 2007) as intact skin with non-blanchable redness of a localised area usually over a bony prominence. Therefore, future studies could involve measurement of resting flux over the stage 1 pressure ulcer and also at adjacent sites. The spectral analysis of the signal would provide evidence of changes in blood flow control mechanisms in skin that goes on to develop into a full pressure sore. This is a potential future work which has been recently suggested by Jan et al. (2008).

### **7.5.3 Smoking cessation and health promotion**

The effects of smoking on cutaneous microvascular function have been clearly demonstrated in this thesis. There is potential for further work to consider the effect of smoking cessation on the function of the skin microcirculation and to determine whether abstinence can improve microvascular function and health. This research could also provide a useful tool in the encouragement of individuals to stop smoking, and aid health promotion campaigns. It could also contribute to advice given to patients prior to admission in hospital.



## **Appendix 1**

### **Detail of parameter calculations**

### **A1.1 Area Under Curve Analysis During Heating**

The following is the process by which the area under the local heating curve for the LDF traces at the sacrum and the forearm was calculated:

1. For each LDF trace, data saved as text file at sampling frequency of 40Hz and then transferred to excel format.
2. The excel spreadsheet contains all the data for the LDF trace including time in hours, minutes seconds, flux, concentration, speed, temperature.
3. The section of flux data from the start of heating (ie. 10 minutes into the recording), to the end of heating (total 10 minutes / 600 seconds) highlighted and copied onto new spreadsheet into column B.
4. The time in seconds is in column A of the new spreadsheet ie. 0, 0.025, 0.05, 0.075, 0.1.....
5. The area under the curve (AUC) is then calculated in column C by the following formula:  
$$0.025*((B1+B2)/2)$$

The sum of this column is the AUC.
6. This was completed for each of the traces at the sacrum and forearm in the smokers and non-smokers

### **A1.2 Maximum Hyperaemia during heating**

The following is the process by which the maximum hyperaemia during local heating for the LDF traces at the sacrum and the forearm was calculated:

1. For each LDF trace, data saved as text file at sampling frequency of 20Hz and then transferred to excel format.
2. The excel spreadsheet contains all the data for the LDF trace including time in hours, minutes seconds, flux, concentration, speed, temperature.

3. The section of flux data from the **start** of heating (ie. 10 minutes into the recording), to the **end** of recording was highlighted and copied onto new spreadsheet into column B. This is because the maximum hyperaemia wasn't always during the heating itself, but was sometimes after the heating had been switched off.
4. The time in seconds was in column A of the new spreadsheet ie. 0, 0.025, 0.05, 0.075, 0.1.....
5. The mean flux of each 30second period from the start of heating onwards was calculated in column C and the maximum value in column C was called the maximum hyperaemia.

### **A1.3. Mean flux during heating**

The following is the process by which the mean flux during heating for the LDF traces at the sacrum and the forearm was calculated:

1. For each LDF trace, data saved as text file at sampling frequency of 20Hz and then transferred to excel format.
2. The excel spreadsheet contains all the data for the LDF trace including time in hours, minutes seconds, flux, concentration, speed, temperature.
3. The mean of the whole section from the start of the local heating stimulus application to the end of the heating was calculated and this is the mean flux during heating.



## **Appendix 2**

### **List of Materials**

## List of Materials

**DRT4 LDF monitor** (*Moor Instruments Ltd, Axminster, Devon*)

**SHO2™ Skin heating unit** (*Moor Instruments Ltd, Axminster, Devon*)

**SHP1 Heater probe** (*Moor Instruments Ltd, Axminster, Devon*)

**LDF pinhead probes with skin heater (VP12)** (*Moor Instruments Ltd, Axminster, Devon*)

**Loading apparatus** – loan from Salisbury group

**Matlab and Simulink release 14 (student version) with added signal processing toolbox**  
(*The MathWorks, Inc*)

**SPSS statistics package version 14.0**

**Stata statistics package version 9.0**

**NOA-280 Nitric Oxide Analyser** (*Sievers*)

**Ethylene oxide sterilization** (*Sterile Services International Ltd., 9 Columbus Walk, Brigantine Place, Cardiff CF10 4YY, UK*).

**Cyanoacrylate glue 4061** (*Loctite (Ireland) Ltd*)

**Portex tubing ((0.28 mm (ID), 0.61 mm (OD); 0.58mm(ID)/1.02mm(OD))**(*Portex Ltd*)

**Cuprophane dialysis membranes (5kDa cutoff, 216µm diameter)** (*Focus 90H Hemophan Hollow Fibre Dialyser, National Medical Care, Rockleigh, USA*)

**Epidural connector**

**Stainless steel AISI 302 wire** (*Goodfellow Cambridge Ltd, Huntingdon, Cambs., UK*).

**Sterile Ringer's solution** (*Fresenius Kabi Ltd, Warrington UK*)

**EMLA (Lidocaine 25mg and Prilocaine 25mg/gram)** (*AstraZeneca*)

**Microinfusion pump** (*CMA400; Biotech Instruments Ltd*)

**Anti-fungal cleaner** (*Mikrozyd AF, Schulke & Mayr*)

**Melonin dressing**

**Sodium Iodide**

**Sodium Nitrite**

**Distilled water**

**Acetic Acid**

**Eppendorfs**

## **Appendix 3**

### **Matlab functions**

### A3.1 Detrend program

This function removes the general trend from the LDF trace, which would affect analysis of the frequencies within the signal itself.

```
D=name of file;           insert name of file and renames it D  
t=D(:,1);                denotes that t (time) is in the first column of D  
y=D(:,2);                denotes that y (signal for processing) is in column 2  
fs=1/mean(diff(t));      calculates the sampling frequency and names it fs  
[y1_detrend,a_est,T]=poly_detrend1(y,10);  
y1_est=T*a_est;  
figure  
plot(t,y,t,y1_est,'r');  
xlabel ('time from start of heating (seconds)');  
ylabel('skin blood flux (AU)');  
figure  
plot(t,y1_detrend)  
xlabel ('time from start of heating (seconds)');  
ylabel('detrended skin blood flux (AU)');
```

### A3.2 Poly detrend function

```
function [z,a,X]=poly_detrend(y,order);  
N=length(y);  
y=y(:);  
x=[0:N-1]'/N;  
X=ones(N,1);  
for n=1:order  
    X=[X,x.^n];  
end  
a=inv(X'*X)*(X'*y);  
z=y-X*a;
```

### A3.3 Spectrogram function

```
function [P,f]=spec1(x>window,overlap,fs);
% Estimate the PSD for the signal x, using FFTs of length(window), and the overlap (0-1)
% fs is the sampling rate.
Nfft=length(window);
N=length(x);
x=reshape(x,N,1);
window=reshape(window,Nfft,1);
P=nan;
f=nan;
shift=round((1-overlap)*Nfft);
if (shift>0) & (Nfft<N)
    y=[];
    weight=[];
    weight0=sum(window.^2);
    weight1=sum(window.^2);
    i_start=1;
    i_end=Nfft;
    no_windows=0;
    while i_end<=N
        x_temp=x(i_start:i_end).*window;
        weight=[weight,weight0];
        y=[y,x_temp];
        no_windows=no_windows+1;
        i_start=i_start+shift;
        i_end=i_end+shift;
    end
    Y=fft(y)';
    Y2=abs(Y).^2;
    if no_windows>1
        P=mean(Y2);
    else
        P=Y2;
    end
    P=P/weight0/fs;
```

```

if mod(Nfft,2)==0
    P(2:Nfft/2+1)=P(2:Nfft/2+1)+P(Nfft:-1:Nfft/2+1);
    P=P(1:Nfft/2+1);
else
    P(2:(Nfft-1)/2+1)=P(2:(Nfft+1)/2)+P(Nfft:-1:(Nfft+1)/2+1);
    P=P(1:(Nfft+1)/2);
end
P(1)=2*P(1);
f=[0:length(P)-1]/Nfft*fs;
end
% keyboard

```

### **A3.4 Power Spectral Density Estimation Program**

This function is used to estimate the PSD:

```

D=name of file;
t=D(:,1);
y=D(:,2);
Tw=250;
overlap=0.5;
fs=1/mean(diff(t));
[y1_detrend,a_est,T]=poly_detrend1(y,10);
  

w=hanning(round(Tw*fs));
[Pa1,f]=spec2(y1_detrend,w,overlap,fs);

```

### **A3.5 Saving PSD as a text file**

This function allows the PSD to be saved as a text file:

```

D=name of file;
t=D(:,1);
y=D(:,2);

```

```

Tw=250;
overlap=0.5;
fs=1/mean(diff(t));
fc=.5;

[y1_detrend,a_est,T]=poly_detrend1(y,10);

w=hanning(round(Tw*fs));
[Pa1,f]=spec2(y1_detrend,w,overlap,fs);

result=[Pa1' Pa2' Pa3' Pa4' Pa5' Pa6' Pa7' Pa8' Pa9' Pa10' Pa11' Pa12' Pa13' Pa14' Pa15'
Pa16' f'];
save result.PSD result -ASCII;

```

### **A3.6 Image of median PSD and all PSD on a graph**

This function enables production of a graph showing the median PSD and also all of the individual PSD's on one graph:

```

D=name of file;
t=D(:,1);
y=D(:,2);
Tw=250;
overlap=0.5;
fs=1/mean(diff(t));
fc=.5;
[y1_detrend,a_est,T]=poly_detrend1(y,10);

w=hanning(round(Tw*fs));
[Pa1,f]=spec2(y1_detrend,w,overlap,fs);

B=[Pa1 ;Pa2 ;Pa3 ;Pa4 ;Pa5 ;Pa6 ;Pa7 ;Pa8 ];
C=[Pa9 ;Pa10 ;Pa11 ;Pa12 ;Pa13 ;Pa14 ;Pa15 ;Pa16]
m_B=median(B);
m_C=median(C);

```

```

figure
for i=1:8
    plot(f,B(i,:))
    hold on
end
xlabel('Frequency (Hz)');
ylabel('Power Spectral Density (AU2/Hz)');
title('Non-smokers');
figure
for i=1:8
    plot(f,C(i,:))
    hold on
end
xlabel('Frequency (Hz)');
ylabel('Power Spectral Density (AU2/Hz)');
title('Smokers');
figure
plot(f,m_B,f,m_C);
legend('Non-smokers','Smokers');
xlabel('Frequency (Hz)');
ylabel('Power Spectral Density (AU2/Hz)');

```

## **Appendix 4**

**A pilot study to consider the neurogenic  
mechanisms in local heating**

#### **A4.1 Introduction**

In the local heating response, the main contribution of the neurogenic component is the axon reflex mediated initial peak at the beginning of the local heating response. The initial rise in flux due to local heating was removed from the LDF trace before the spectral analysis was completed, so the main part of the initial section was removed from the analysis. The spectral analysis concentrates on the absolute power and then the relative power around 0.01Hz, 0.04Hz and 0.1Hz, however, the expected contribution of the frequency band around 0.04Hz would be expected to be minimal in the plateau. A recent study has shown that the application of EMLA to the skin for 60 minutes decreases the initial peak of a local heating response that is applied immediately following the removal of the EMLA, but had no effect on the plateau vasodilation (Cracowski et al., 2007). This confirms other studies that have shown that the axon reflex has its main role in the initial peak response to local heating and only a minimal role in the plateau vasodilation (Kellogg et al., 1999).

In the studies in this thesis, the spectral analysis is completed on the plateau section of the local heating response and thus the contribution of the 0.04Hz frequency in the signal would be expected to be minimal. This small pilot study aims to measure whether changes in the 0.04Hz frequency related to neurogenic control of skin blood flow could be detected in the heating response over an EMLA treated site compared to a control site. This would determine whether this frequency has any significant impact on the plateau response to a local heating stimulus.

#### **A4.2 Methods**

##### ***Participants***

The study involved 6 non-smoking participants; the baseline parameters of the group can be found in *Table A4.1*

<b>Parameter</b>	<b>Participants (n=6)</b>
<b>Age (yrs)</b>	25.8 ± 6.3 (20 – 35 )
<b>Sex</b>	4 females / 2 males
<b>Body mass index (kg/m<sup>2</sup>)</b>	23.8 ± 1.0 (22.3 – 25.0)

**Table A4.1.** The table shows the age, sex and BMI of a group of healthy, non-smokers (n=6). The table shows data as mean ± standard deviation (range). The body mass index was calculated as [weight (kg)/(height (m))<sup>2</sup>].

### ***Study protocol***

The participants were made comfortable in a semi-recumbent position on a hospital mattress and allowed to acclimatise to room temperature for 15 minutes. Skin blood flow was measured for 20 minutes at 2 sites at least 5 cm apart on the volar surface of the forearm (pre-baseline measurements). The position of the sites was marked for reference and EMLA (2.5g) was applied to one of the sites under an occlusive dressing for 60 minutes. The EMLA was then cleaned from the skin surface and the prick test was completed to ensure that the axon reflex was blocked by the EMLA. The LDF probes were then replaced in the same positions as pre-baseline recording and a further 20 minutes baseline measurements were recorded at both sites (baseline measurements). The skin was then heated at both sites to 43°C for 20 minutes. The heater was then switched off and measurements continued for a further 20 minutes.

### ***Spectral Analysis Information***

The spectral analysis was completed on the LDF traces using Matlab®. The data was saved at a sampling frequency of 40Hz in an excel spreadsheet. The initial 100 seconds was removed from the baseline and heated data and the data was detrended to the power of 10. The PSD was estimated using the Welch method:

- Data length = 1100 seconds
- Window length = 400 seconds
- Window type = Hanning
- Overlap = 50%
- Frequency resolution = 0.0025Hz

The absolute power was measured by the area under the power spectral density graph between 0-0.2Hz. The power of the frequency bands were calculated as follows:

~0.01Hz: power between 0.008-0.02Hz - endothelium

~0.04Hz: power between 0.02-0.05Hz - neurogenic

~0.1Hz: power between 0.05-0.15Hz - myogenic

The power of each band was measured relative to the absolute power as a percentage.

### A4.3 Results

An example of the LDF traces produced at the control site and EMLA site can be found in *Figure A4.1*. The EMLA caused the local heating response to be attenuated to varied degrees in 5 out of 6 of the participants. In one of the participants the response to local heating was increased at the EMLA site compared to the control site.

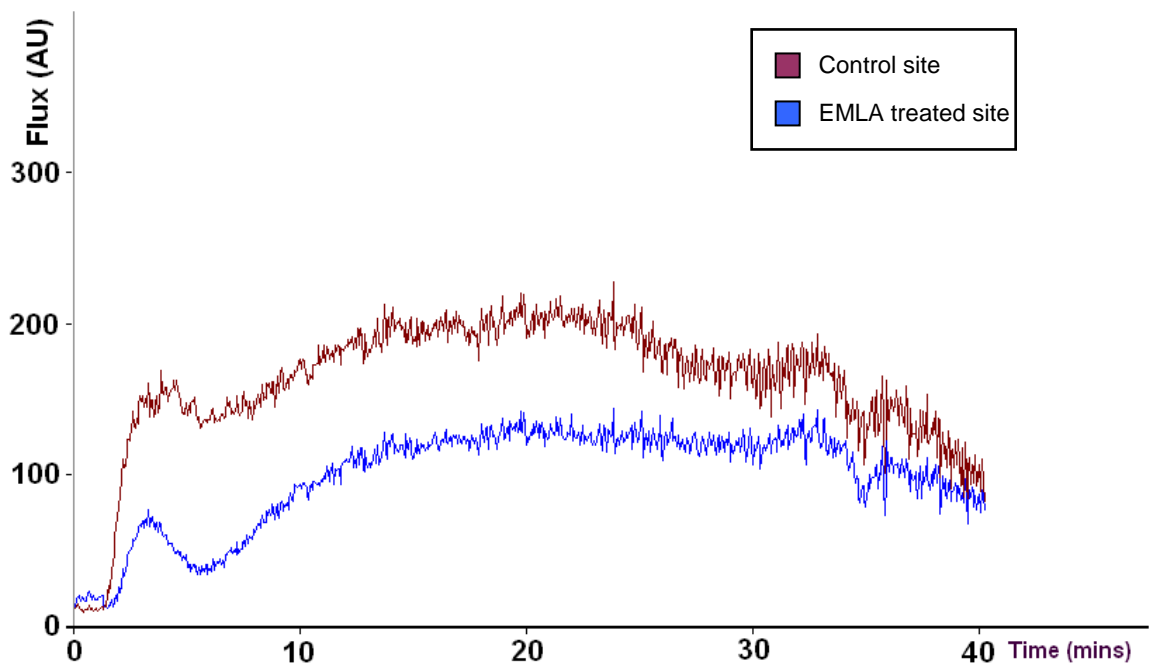


*Figure A4.1.* The LDF traces in a participant involved in the study to consider effects of EMLA on the response to local heating. The protocol for the measurements on the graph was resting flux for 1 minute, followed by local heating to 43°C for 20 minutes and approximately 20 minutes recovery. The red line shows the LDF signal from the protocol completed at the control site and the blue line shows the same protocol, at the volar surface of the same forearm in the same individual, but at a site that has been treated with EMLA to block the neurogenic responses.

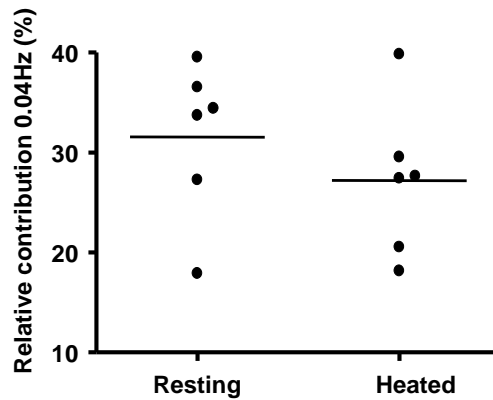
The results showed that there were no changes to the resting flux with the application of EMLA to the skin, however, the local heating response as measured by area under the curve during heating at the EMLA site was approximately  $63.4 \pm 52.5\%$  (median  $\pm$  IQR) of the responses at control site. When the initial 100 seconds was removed, which is the section considered to be mainly under neurogenic control, and the mean heated flux measured for the remainder of the heating response, the flux at the EMLA site was still found to be approximately  $64.2 \pm 53.5\%$  (median  $\pm$  IQR) of the heating response at the control site.

***The effects of EMLA on the responses to local heating assessed using spectral analysis***

Spectral analysis was completed on the LDF signal to consider whether any changes in the neurogenic contribution to skin blood flow control could be detected in the LDF signal during EMLA application compared to the control site. When comparing pre-EMLA resting to EMLA resting flux, although there was a small reduction in flux with EMLA, the results did not reach significance.

When comparing the pre-EMLA resting flux, with the local heating flux (minus initial 100secs) in the EMLA site, the contribution of the oscillations around 0.04Hz (associated with neurogenic control of the vasculature) was significantly reduced. There were no differences in the spectral analysis at the control site (*Figure A4.2*). There were no such differences in the relative contribution of the frequencies around 0.01Hz or 0.1Hz.

**a. Control site**



**b. EMLA site**

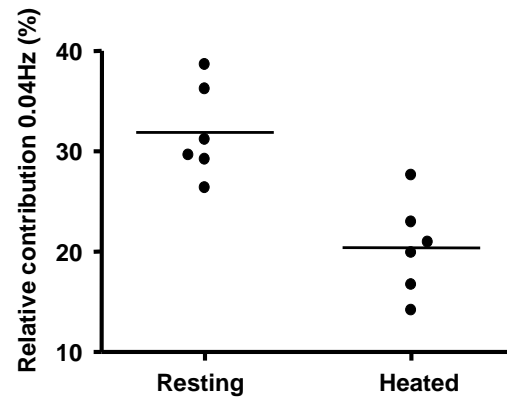


**Figure A4.2.** Graphs to show the relative contribution of the frequency around 0.04Hz to the total signal during resting flux prior to application of EMLA/control and during local heating. The graphs show the results at the control site (a) and the EMLA site (b) in 6 non-smoking participants measured at the volar surface of the forearm.

**Summary**

This small study suggests that neurogenic mechanisms related to local heating may be involved in the plateau response in the local heating response. A previous study has shown reduced maximal vasodilation responses to iontophoresis of SNP and local warming to 40°C and 42°C, but not 44°C in subjects following the application of EMLA local anaesthetic cream (Caselli et al., 2003). This provides further evidence that stimulation of nerve fibres is involved in the local heat induced vasodilation response, but the vasoconstrictor effect of the EMLA may also have counteracted some of the vasodilation as well (Caselli et al., 2003).

The study also showed that the method used for spectral analysis in these participants is able to detect changes at the 0.04Hz frequency during the heating response. It is not possible, using the spectral analysis program used in this study, to measure the total spectral power of the initial peak in this study, because the length of data would be too small. It is also important to consider that studies have shown that EMLA may have other vasoconstrictive effects on the skin blood vessels (Wiles et al., 2008).

## **Appendix 5**

# **Cutaneous microdialysis for the measurement of nitric oxide**

## **A5.1 Introduction**

The previous chapters have shown that the LDF measurement of the skin blood flow response to a local heating stimulus of 43°C is significantly attenuated in older heavy smokers compared to matched non-smokers. The study protocol was optimised by increasing the length of the heating challenge to 20 minutes and further studies were completed comparing LM smokers to matched non-smoking controls. This study showed a trend towards reduced local heat-induced vasodilation responses in the LM smokers compared to the controls, but the data was found to be highly variable in this group, and any differences were not significant.

In the heavy smokers, spectral analysis using a FFT of the LDF heating signal found that the heavy smoker group had reduced absolute low frequency power in the LDF signal during heating and this was due in particular to reduced power at the frequencies related to endothelium and myogenic vascular control. The contribution of each of the frequency bands to the absolute low frequency power (relative PSD) was calculated. The change in relative PSD of each of the frequency bands from resting to heated flux showed that the frequency interval originating from the endothelium was significantly increased in the non-smokers, but not in the heavy smokers. Although this would suggest that the attenuated heating response was mainly due to reduced endothelium dependent vasodilation in the heavy smokers, the same trends were not present in the younger group of light/moderate smokers and their matched controls. There were no significant changes in the relative PSD of the frequency band associated with the endothelium control of blood vessels from resting to heating flux in either the LM smokers or the non-smokers in this group. When considering the heavy and LM smokers together compared to the non-smokers, the relative power of the frequency related to the endothelium increased in the non-smokers, but decreased in the smokers, suggesting altered endothelial function in the smokers.

The effects of smoking on the endothelium will be further explored in this chapter. We have shown evidence that there is attenuated vasoreactivity in the heavy smokers and that this may be due to endothelial dysfunction in this 'at risk' group. In order to further investigate this, the sampling of the specific local factor NO associated with endothelial function within the tissue will be completed.

### ***Nitric oxide***

The plateau section of the local heating response has been shown to be mainly NO-dependent (Kellogg et al., 1999), and thus regulated by the endothelium. This is the component of the LDF

signal attenuated in the heavy smokers, as assessed by the spectral analysis. NO has been shown to be an important element in vascular control, causing vasodilation of blood vessels by stimulation of soluble guanylyl cyclase and also by increasing cyclic guanosine monophosphate (cGMP) in smooth muscle cells (Forstermann and Munzel, 2006).

Several studies have shown that smoking effects the plasma levels of NO, further confirming that a reduction in the NO produced by the endothelium, may be responsible for the attenuated vascular responses to local heating in the smokers. However, at present the picture regarding NO in smokers is conflicting: some studies have shown lower levels of NO in the plasma of smokers (Barua et al., 2001; Node et al., 1997; Tsuchiya et al., 2002) and another has shown raised levels (Chavez et al., 2007). The technique of microdialysis, used for the purposes of the studies in this chapter, has the potential to show local levels of NO in the extracellular space rather than systemic plasma levels, which may give more information on local endothelium function in the skin microcirculation.

## **A5.2 Objective**

To determine whether differences in the concentration of NO can be detected in the skin extracellular tissues of smokers compared to non-smokers. This would provide further and different evidence regarding local endothelial function in this group.

## **A5.3 Methods**

### **A5.3.1 Participants**

The study was performed on a group of seven LM smokers and seven healthy matched control subjects. Each group was comprised of two males and five females. The study was completed at the volar surface of the forearm in each volunteer. The baseline parameters are shown in *Table 6.1*. There was no significant difference between the two groups.

<b>Variable</b>	<b>Statistical Measurements</b>	<b>Control Group</b>	<b>Smokers</b>
<b>Age (years)</b>	Median	23.0	22.0
	IQR	6.0	9.0
<b>Body Mass Index (kg/m<sup>2</sup>)</b>	Median	21.5	23.9
	IQR	4.5	4.7

**Table A5.1** A table to show the age and BMI of 7 non-smoking controls and 7 LM smokers used in the microdialysis studies to measure NO.

### **A5.3.2 Participant smoking history**

Smoking history was gained from the light/moderate smokers by self-report. All the smokers were asked to abstain from smoking for at least 1 hour before the study.

### **A5.3.3 Microdialysis**

#### ***Microdialysis background***

Microdialysis is a well-established technique for the sampling of the extracellular fluid space. It has been used in many organs in the human body, initially in the brain, but there have now been many studies using microdialysis in the skin (Petersen et al., 2009; Angst et al., 2008).

During microdialysis a hollow semi-permeable membrane is implanted within the tissue space, the skin in this study, and is continuously perfused with a physiological solution (Clough, 1999; Muller, 2002). The physiological solution has the same osmotic concentration and composition as blood serum. As the physiological solution is slowly perfusing, molecules move into and out of probe through the semi-permeable membrane. The direction and speed of the flux from the extracellular space into the microdialysis probe through the permeable membrane depends on the concentration gradient for each particular molecule. The outflow from the probe, the dialysate, is collected and assayed for the particular molecule(s) being investigated. The concentration gradient allowing exchange across the membrane will depend on the absolute levels of solute within the fluid section of the tissue space.

The process of solute exchange across the dialysis can be described by the Fick equation (*Equation A5.1*):

$$J = -DA \frac{dC}{dx}$$

*Equation A5.1* The solute flux across the membrane  $J$ , is proportional to the diffusion coefficient of the solute,  $D$ , the area of diffusion,  $A$  and the concentration gradient  $dC/dx$ .

### ***Construction of microdialysis probes***

The microdialysis fibres used for the collection of nitric oxide had a 5 kDa molecular mass cut off and external diameter of 216 $\mu$ m and were constructed from cuprophane membranes extracted from a renal dialysis capsule (Focus 90H Hemophane Hollow Fibre Dialyser, National Medical Care, Rockleigh, USA).

For the construction of each of the probes, a length of the dialysis membrane measuring approximately 5cm was cut from the renal dialysis capsule and was strengthened using a length of stainless steel wire (Stainless steel AISI 302 wire, diameter 0.1 mm, Goodfellow Cambridge Ltd, Huntingdon, Cambs., UK). The membrane was then glued into a pre-cut 15 cm length of fine bore polythene tubing (Portex Ltd.: 0.28 mm id, 0.61 mm od) using cyanoacrylate glue (Loctite (Ireland) Ltd). The dialysis membrane was inserted into the tubing for about 15mm and sealed in by allowing the glue to flow by capillarity down the tube. The microdialysis probes were left to dry for approximately 24 hours and then packaged and sent for ethylene oxide sterilization (Sterile Services International Ltd., 9 Columbus Walk, Brigantine Place, Cardiff CF10 4YY, UK).

### ***Microdialysis study protocol***

The study was approved by the Southampton and South West Hampshire Joint Research Ethics Committee, approval number 138/01. The volunteers gave their written informed consent to take part in the study. Their age, sex, height and weight were then recorded and smoking history taken. The studies were completed in the temperature controlled environment of the WTCRF. The participants had their non-dominant forearm positioned on a cushion at heart level for the duration of the studies. An area of skin was selected on the distal portion of the volar surface of the forearm at least 5cm from the wrist, away from observable large blood vessels.

The local anaesthetic EMLA (2.5mg) was applied to an area of the skin approximately 2cmx3cm, and an occlusive dressing applied to cover the area for 2 hours prior to the insertion of the microdialysis probes. The dressing and EMLA was then removed and the site cleaned with water to

ensure complete removal of the EMLA cream. The area was also checked for adequate anaesthesia using the prick test at the edges of the site.

The equipment needed for the insertion of the probes was prepared beforehand to ensure the sterile nature and efficiency of the insertion procedure. The surface of a table at the bed side in the clinical room (WTCRF) was cleaned, using an anti-fungal cleaner (Mikrozid AF, Schulke & Mayr) and a sterile field was prepared using a sterile paper dressing onto the table surface. The equipment needed for the insertion procedure was placed on the sterile field. This included green (21G) and blue needles (23G), 20ml syringe, 1ml syringes, sterile giving tubing, microdialysis probes and blue epidural connectors. The Ringers solution was drawn into the 1 ml syringe, removing all the air bubbles, and the sterile giving tubing was attached. The 1ml syringe was then clamped onto the CMA400 pump. The giving tubing was primed with the Ringer's solution, the 5kDa microdialysis probe was attached into the end of the primed giving tube and the Ringers solution was allowed to flush through probe onto the sterile paper as a test of the probe to ensure no leakage prior to insertion. Each of the collection eppendorfs to be used for the study was labeled with the sample number, weighed and this was documented.

### ***Insertion of microdialysis probes***

The process of insertion of the microdialysis probes began once the area of skin to be used was checked for adequate anaesthetization. A length of 20mm was then marked on the participants arm with a pen to ensure that the microdialysis probes were inserted under the skin for the correct distance. A 23G blue needle was then inserted under the skin into the dermis, approximately 0.6 – 0.8 mm beneath the surface, for the length marked with the pen (ensuring that the needle was not inserted through the pen marks). The 5kDa microdialysis probe was inserted through the needle and then the needle was removed, leaving the probe in the skin. The probe is anchored to ensure that it remains in position using a small piece of micropore tape. When more than one probe was applied, there was a gap of greater than 2cm between the probes.

The microdialysis probes were immediately perfused at 3 $\mu$ L/min for 15 minutes to flush away any molecules that had entered the probe using a microinfusion pump (CMA400; Biotech Instruments Ltd). The sample (1) contained in the collection eppendorf was immediately placed in an ice bath for later re-weighing and storage at -80°C. The probe was then taped securely in place and covered by a Melonin<sup>®</sup> dressing a bandage, and was left for 1.5 hours to allow the skin to settle down after the trauma of probe insertion. The insertion procedure increases local blood flow and this would effect the concentrations of molecules within the extracellular tissue space. A study has shown

using microdialysis in the skin of rats, that insertion caused an increase in blood flow and histamine release. They suggested a minimum equilibrium period of 30 minutes between insertion and sample collection to allow the trauma to subside (Groth et al., 1998).

At the end of the 1.5 hour gap in experimentation to allow the microdialysis probe(s) and extracellular tissue space to settle, the dressings were removed and the probe(s) were reconnected to the primed giving tubing and the perfusion at 3 $\mu$ L/min was restarted.

#### ***Protocol for collection of samples for measurement of nitric oxide (NO)***

For the measurement of NO in the tissue space, the microdialysis probes (5 kDa cut off) were inserted and perfused at a rate of 3 $\mu$ L/min. The samples were collected in the following protocol into pre-weighed and labelled eppendorf containers:

- **Sample 1:** A collection for 15 minutes immediately following insertion of fibres
- **Stop perfusing for 90 minutes for microdialysis probes to settle**
- **Samples 2 – 7:** Collections taken at 5 minute intervals (0-5min, 5-10min, 10-15min, 15-20min, 20-25min and 25-30min).
- **Stop perfusing for 30 minutes in order to measure build up of NO over time**
- **Samples 8-19:** Collections taken at 5 minute intervals (0-5min, 5-10min, 10-15min, 15-20min, 20-25min and 25-30min, 30-35min, 35-40min, 40-45min, 45-50min, 50-55min, 55-60min)
- **All samples re-weighed and stored in freezer at -80°C**

#### **A5.3.4 Measurement of NO from microdialysate**

The Sievers NOA-280 Nitric Oxide Analyser was used to measure the concentration of NO in the microdialysate samples. The concentration of NO can be determined using a chemiluminescent reaction, which involves ozone. A sample containing nitric oxide is mixed with a large quantity of ozone. The nitric oxide reacts with the ozone to produce oxygen and nitrogen dioxide and this reaction produces light, which can be measured with a photodetector. The amount of light produced is proportional to the amount of NO in the sample.

To measure the concentration of NO in the microdialysate samples, the Sievers NOA-280 was set-up according to the manufacturer's instructions. A Hamilton syringe was used to add the Ringer and the microdialysate samples for analysis. The calibration curve was created, so that the concentration in the samples could be calculated from this calibration curve. The software

connected to the Sievers NOA-280 meter calculates the AUC of the peaks and then gives an indication of the concentration of NO using the loaded calibration curve.

The calibration curve was created using dilutions of sodium nitrate in distilled water. A 100mM solution was initially made up using 345mg sodium nitrate in 50ml distilled water. The following dilutions of the sodium nitrate solution were done using Ringer's solution for the calibration curve:

1 in 100 dilution (50 $\mu$ l in 4950 $\mu$ l) = 1mM.

1 in 100 dilution (50 $\mu$ l in 4950 $\mu$ l) = 10 $\mu$ M

1 in 2 dilution (1ml in 2ml) = 5 $\mu$ M

1 in 2 dilution (1ml in 2ml) = 2.5 $\mu$ M

1 in 2 dilution (1ml in 2ml) = 1.25 $\mu$ M

1 in 2 dilution (1ml in 2ml) = 0.625 $\mu$ M

The calibration curve was generated by injecting 3 x 10 $\mu$ l injections of Ringer's solution and then 3 of each of the different concentrations. A calibration curve was created for each session of sample analysis. These calibration curves were then compiled to form the final calibration curve (*Figure A5.1*).

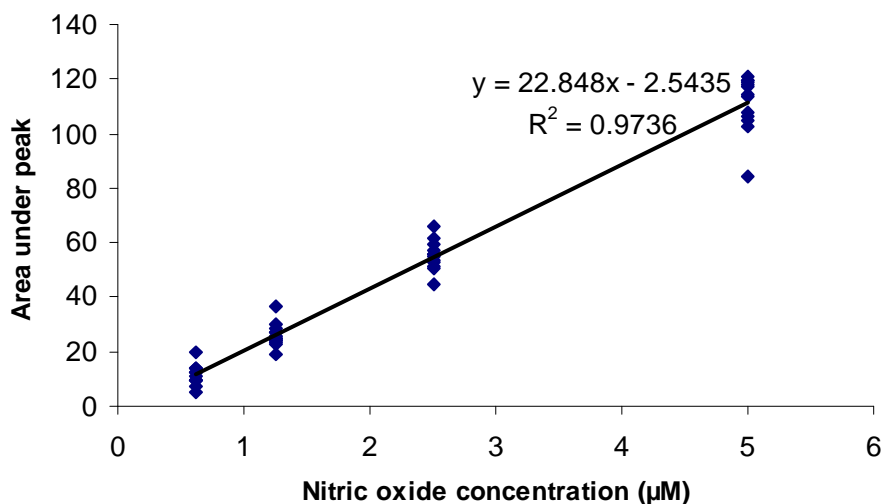


*Figure A5.1* A graph to show the combined calibration curve used to estimate the concentration of NO in microdialysis samples from 7 LM smokers and 7 matched non-smokers.

## **A5.4 Results**

The recovery concentrations quoted in the results section refers to the relative recovery, as it is not expected that at the flow rate used the probe dialysate would reach equilibrium with the extracellular space. Therefore, the concentrations are not considered to be equivalent to the tissue level.

### **A5.4.1 Measurement of basal [NO] in the skin of smokers and matched controls**

The [NO] in the first 5 minute dialysate collection was  $4.2 \pm 3.5\mu\text{M}$  and  $2.4 \pm 1.7\mu\text{M}$  (median  $\pm$  IQR) in the control group and LM smokers, respectively. There was no significant difference between the groups in the first collection, as measured by the MWU test ( $P < 0.05$ ), although the analysis was borderline ( $p = 0.062$ ), with the trend being lower levels in the LM smokers (*Figure A5.2*).

The LM smoker group showed lower mean dialysate [NO] compared to the non-smoking control group throughout most of the initial 30 minute collection period. The [NO] was significantly lower ( $p = 0.028$ ) in the light/moderate smokers in the sample collected at the 10 minute time point (5-10 minute sample). The [NO] at that time point was  $1.7 \pm 0.7\mu\text{M}$  and  $1.2 \pm 0.5\mu\text{M}$  in the control group and LM smokers respectively (median  $\pm$  IQR) (*Figure A5.2*).

However, by the end of this period, the [NO] in the 25-30 minute collection was almost exactly the same in both groups; the relative [NO] was  $1.0 \pm 0.4\mu\text{M}$  and  $0.9 \pm 0.5\mu\text{M}$  in the control group and LM smokers respectively (median  $\pm$  IQR).

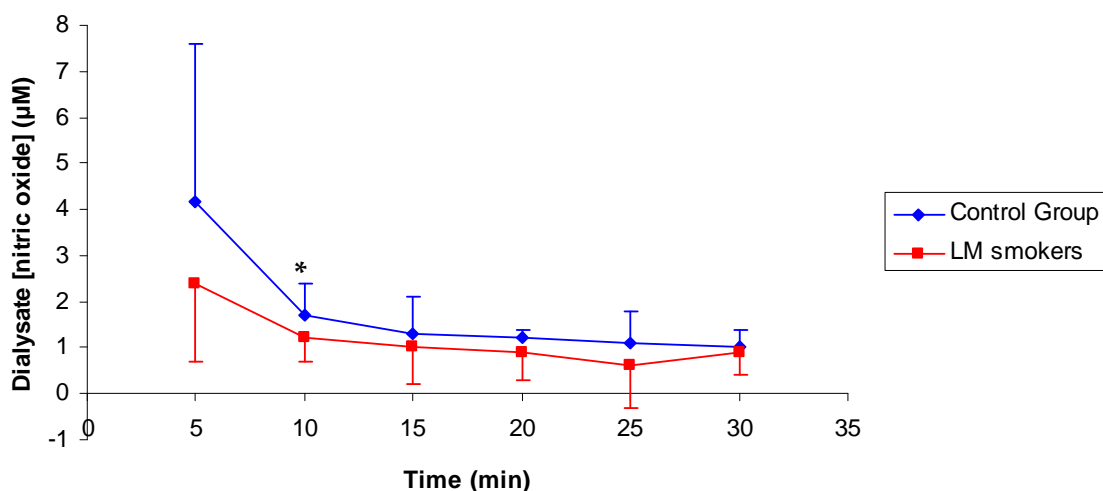


**Figure A5.2** A line graph to show the microdialysate [NO] (median  $\pm$  IQR) measured in the skin of 7 light smokers and 7 matched non-smoking controls. The microdialysis probes inserted in the volar surface of the forearm had a 5KDa cut off and were perfused with Ringers solution at a rate of 3 $\mu$ L/min. The samples were collected every 5 minutes for 30 minutes. The [NO] in the dialysate was measured using a chemiluminescence reactions (Sievers NOA-280). The LM smoker group showed a significantly lower level of NO at the 10 minute collection compared to the control group (\*) measured using the MWU test, where  $p=0.028$ .

### *Steady state*

The sample at which the [NO] was considered to have reached steady state levels for the purposes of this thesis was at the sample where the group showed no significant difference between that and the previous sample [NO], as analysed by the Wilcoxon paired test.

In the non-smoker group, there was a significant difference between the samples collected at 5 min compared to 10 min ( $p=0.046$ ) and between the 10 min and 15 min samples ( $p=0.042$ ), but from 15 min onwards, there was no change and the levels of [NO] were at steady state. In the LM smoker group, there was a significant difference between the samples collected at 5 min compared to 10 min ( $p=0.027$ ), but then steady state from 10 min onwards.

### *Area under the NO curve between 5 - 30 minutes*

The area under the NO curve against time was measured in the LM smokers and the control group, to consider the collection of NO over the 30 minute time period. The area under the NO curve between 5 and 30 minutes was  $39.5 \pm 19.8$  and  $31.0 \pm 21.5$   $\mu$ M.min in the control group and

light/moderate smokers respectively (*Figure A5.3*). The difference between the groups was not significant when analysed using the MWU test.

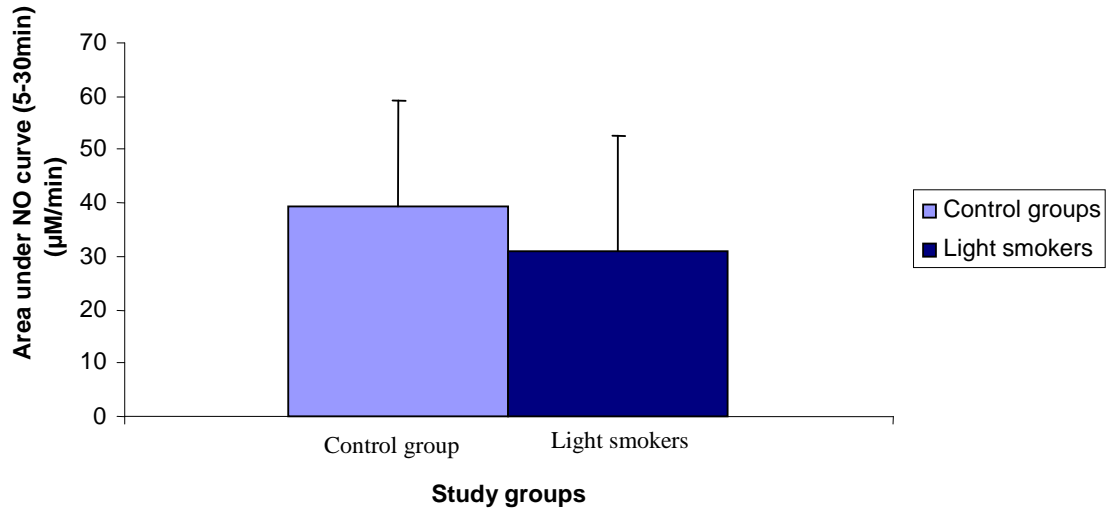


**Figure A5.3** A column graph to show area under the dialysate [NO] over time curve from 5 minutes to 30 minutes in 7 light smokers and 7 matched non-smoking controls. The data are median and the error bars represent the IQR and the difference was tested using the MWU test. There was no significant difference between the groups, where  $p=0.142$ .

***Area under NO curve between 5 - 15 minutes (before steady state)***

The area under the NO curve between 5 and 15 minutes was  $23.5 \pm 8.8$  and  $15.5 \pm 5.0$   $\mu\text{M}\cdot\text{min}$  in the control group and light/moderate smokers respectively. The difference between the groups was significant as measured using the MWU test, where  $p=0.047$ .

#### A5.4.2 Measurement of build-up of [NO] over 30 minutes

After the initial 30 minutes dialysis, the perfusion of the probes was stopped for 30 minutes, and then restarted. The [NO] of this subsequent dialysate sample was highly variable in both the non-smokers and the LM smokers, measuring  $7.8 \pm 7.3\mu\text{M}$  and  $2.6 \pm 11.7\mu\text{M}$  (median  $\pm$  IQR) in the control group and LM smokers, respectively (*Figure A5.4*). There were no significant differences between the groups, measured using the MWU test.

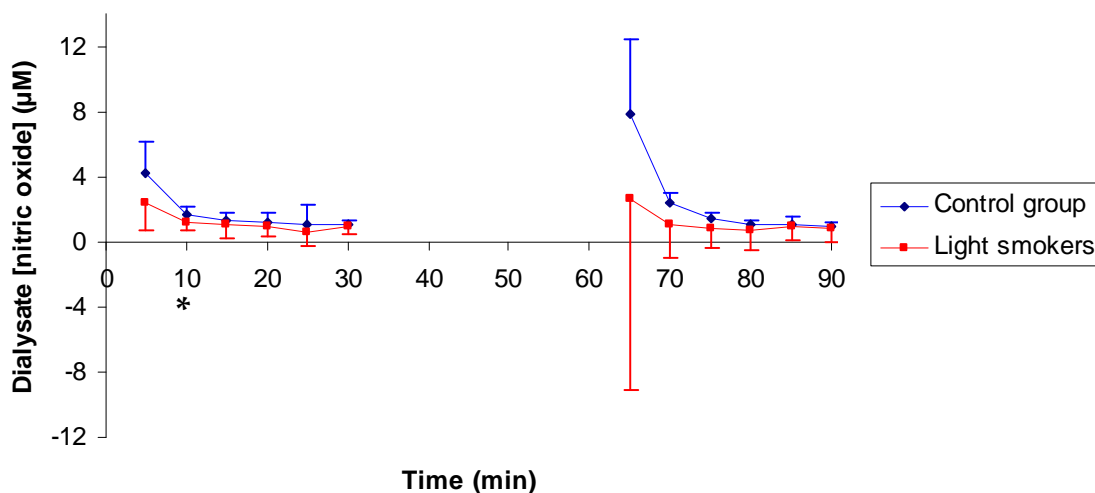


**Figure A5.4** A line graph to show the microdialysate NO levels measured in the skin of 7 LM smokers and 7 matched non-smoking controls (median  $\pm$  IQR). The microdialysis probes inserted in the volar surface of the forearm of the participants had a 5KDa cut off and were perfused with Ringers solution at a rate of  $3\mu\text{L}/\text{min}$ . The samples were collected every 5 minutes for 30minutes, the perfusion of the probes was stopped for 30min and then collections were taken every 5 minutes for a further 30 – 60 minutes. The [NO] in the dialysate was measured using a chemiluminescence reaction.

There was high variability in the concentration of NO in the sample following the 30 minute stop in perfusion. The increase in nitric oxide from the steady state level measured in the sample immediately prior to the stop in perfusion was  $6.2 \pm 6.9$  and  $1.1 \pm 10.9\mu\text{M}$  (median  $\pm$  IQR) in the control group and LM smokers, respectively (*Figure A5.5*).

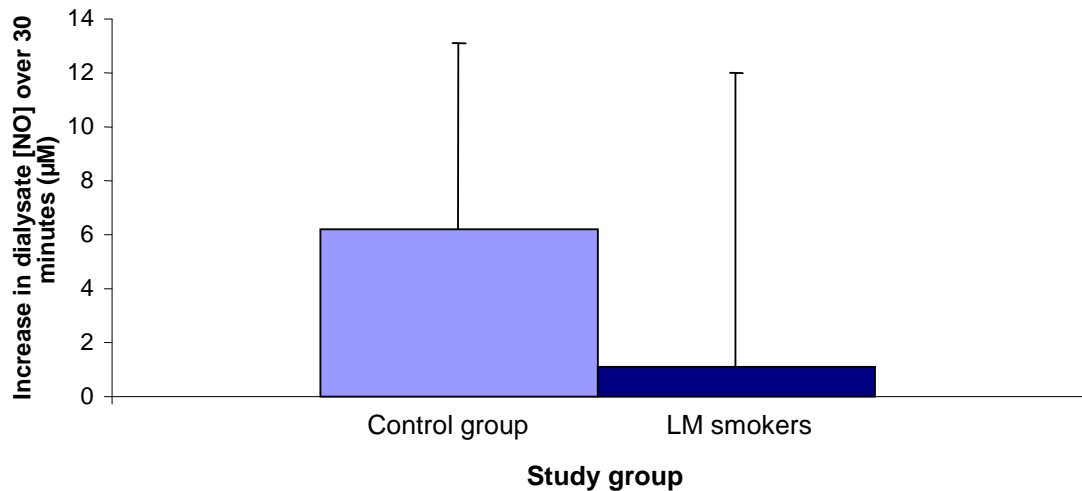


**Figure A5.5** A column graph to show the increase in dialysate [NO] over a 30 minute break in probe perfusion measured in 7 light smokers and 7 matched control participants (median + IQR). The measurements were taken as the dialysate concentration of the first collection following the re-start of perfusion minus the final dialysate collection before the 30 minute break. There was no significant difference between the smokers and control group, as measured by the MWU test ( $p < 0.05$ ).

The concentration of NO measured at steady state (30 minutes following the stop in perfusion) at 90 minutes in *Figure A5.4*, were  $0.9 \pm 0.5$  and  $0.8 \pm 0.8\mu\text{M}$  in control group and LM smokers, respectively. The concentration of NO at 90 minutes was similar to the level of NO measured at 30 minutes.

### **A5.5 Discussion**

In order to consider the factors that may be contributing to the differences in the local heating response, the measurement of NO in the skin using microdialysis was considered. The measurement of local mediators during the local heating response has difficulties due to the increased blood flow and thus short presence at the site. Many studies have used the method of blocking the action of certain prospective mediators, during the local heating response. The studies

in this chapter set out to measure the level of NO in the interstitial space of the skin in seven LM smokers and seven non-smoking controls, matched for age, sex and BMI.

There is much confusion in the literature regarding the effect of smoking on the levels of NO in the bloodstream, either measured in serum or plasma. Studies have shown that there is no significant difference in the serum NO of smokers and non-smokers (Barua et al., 2001) and others have shown the same in plasma measurements (Tsuchiya et al., 2002). However, others have found differences (Node et al., 1997). It has been suggested that the level of NO in the bloodstream is an unreliable measure of the nitric oxide produced by the endothelium. The [NO] in the bloodstream is effected by a number of factors including diet and renal function (Kelm et al., 1996).

In the study in this chapter, the microdialysis fibres were placed in the volar forearm and, after a 90 minute break to recover from the insertion trauma, they were perfused with Ringers solution at a rate of 3 $\mu$ L/min for 30 minutes. Samples were collected at 5 minute intervals throughout this period. The perfusion was then stopped for 30 minutes and then restarted for a second period of 30-60 minutes perfusion, with collections every 5 minutes again. The NO concentration in each of the samples was measured using a chemiluminescence reaction (Sievers NOA-280). This method has been used previously to measure [NO] from microdialysis of the skin in vivo (Katugampola et al., 2000, Rhodes et al., 2001; Crandall and MacLean, 2001; Boutsiouki et al., 2003).

The concentration of NO measured at 5 minute intervals in all of the participants involved showed high variability, so that in all subjects (n=14) the values ranged 0.4 – 7.6 $\mu$ M. The concentration of NO measured in the first 5 minute collection was the highest in most participants and the concentration fell as dialysis progressed. This fall in dialysate NO has previously been shown in a study by Clough (1999); demonstrating a gradual reduction in the concentration of dialysate NO over the first 30 minutes of perfusion and then no further fall. It is suggested that this is most likely to be due to the dialysis depleting the interstitial space of NO (Clough, 1999). The finding that after a 30 minute break in perfusion, the NO levels increased again (Clough, 1999), was also found in this study, and provides some confirmation for the depletion theory.

Interestingly, the analysis in this study showed that there was no further significant fall in dialysate [NO] after only 15 minutes of perfusion in the non-smokers and 10 minutes in the heavy smokers. The microdialysis membranes used in this study had a 5 kDa cut-off compared to 2 kDa cut-off fibres in the study by Clough (1999). The higher membrane cut-off may mean that the NO diffuses more readily into the microdialysis probe, depletes the tissue space of NO faster, so that a low steady state level of NO is reached more quickly. The slower perfusion rate in this study (3 $\mu$ L/min

compared to 5 $\mu$ L/min) has also the potential to cause faster uptake of NO into the microdialysis probe and thus faster tissue depletion. The recovery of a molecule from the tissues with a given probe increases when perfusion rates are kept low (Fox et al., 2002).

The results show that the interstitial space of the smokers was depleted of NO more quickly than the non-smokers. This may be due to a lower interstitial [NO] in the smokers or a reduced capacity to replace NO as it is removed from the interstitial space into the perfusate, causing depletion to occur more quickly. The area under the [NO] curve up to the 15 minute collection was significantly lower in the LM smokers compared to the non-smoking controls. The area under the curve up to the 30 minute time point were not significantly different between the groups and this was expected as the steady state levels of NO (from 10-15 minutes onwards) were similar in the two groups.

The median [NO] in the sample collected at 5 minutes was higher in the non-smokers compared to the smokers ( $4.2 \pm 3.5\mu\text{M}$  (smokers) and  $2.4 \pm 1.7\mu\text{M}$  (non-smokers)), but the difference did not reach significance ( $p=0.062$ ). The [NO] measured at the 10 minute time point was significantly lower in the light/moderate smokers compared to the non-smoking controls. After this, the samples collected up to the 30 minute time point were not significantly different and reached a similar steady state level.

The [NO] measured in this 5 minute sample can be compared directly to dialysate concentrations measured in a study by Clough (1999). They found the mean value of NO in the first 5 minute sample to be  $1.24 \pm 0.19 \mu\text{M}$ , using an amperometric NO sensor and the steady state level at the 30 minute time point was  $0.63 \pm 0.09 \mu\text{M}$ . The reasons for the higher [NO] in the first collection in this study are likely to be the higher membrane cut-off and lower flow rate used as already discussed or alternatively, the different method used to measure the [NO] (chemiluminescence reaction v amperometric sensor).

Although Kellogg et al. (2003) and Crandall and MacLean (2001) were both studying the effects of whole body heating on the [NO] in the skin, the studies involved measurement in the normothermic state prior to heating. Kellogg et al. (2003) used a selective membrane amperometric electrode placed under the skin to measure interstitial [NO] and found that over a 10 – 20 minute period in normothermic conditions the concentration of cutaneous interstitial [NO] was  $548 \pm 108\text{nM}$ . This method did not involve microdialysis and used a technique similar to Clough et al (1999) to measure the [NO]; thus the lower levels of NO measured in that study compared to the findings in my study may be due to these differences. Interestingly, the [NO] found by Kellogg et al. (2003) is more equivalent to the steady state levels found in this study.

Alternatively, Crandall and MacLean (2001) used microdialysis and then analysis by a chemiluminescence technique to study levels of NO in samples collected in each participant over 12 minutes, during normothermia. They found the mean interstitial concentration of NO to be nearly 8  $\mu\text{M}$  in 12 participants studied. These results are comparatively higher than the findings in the study in this chapter as well as the studies by Clough (1999) and Kellogg et al. (2003). It is clear that Crandall and MacLean (2001) used a flow rate of 2  $\mu\text{L}/\text{min}$  through the microdialysis probes in their study, which would potentially increase the recovery. However, the samples were collected over a 12 minute period and then divided up and analysed in triplicate. The concentration would be expected to be more similar to the median of the first 2 samples in the study in this chapter, which would be  $1.7 \pm 2.6$  and  $1.2 \pm 1.3$   $\mu\text{M}$  in the control group and LM smokers respectively. Thus the difference in [NO] between the studies is even more pronounced.

Although the studies discussed have shown that the levels of interstitial [NO] in the literature have been variable, the important aspect in this study is the relative differences between the non-smokers and the LM smokers. The lower levels of NO in the initial collections and the faster depletion of the interstitial space would support the hypothesis that cigarette smoking causes an increase in the activity of ROS, which causes a reduction in NO. Barua et al. (2001) found no significant differences in the [NO] of the blood serum in smokers, but when HUVECs were treated with the serum from smokers and non-smokers, there was a reduced basal NO production by the HUVECs treated with the smokers serum. This appeared not to be due to a reduced eNOS expression, as this was higher in the smokers, but due to a reduced eNOS activity in the smokers. The results from this study support these findings.

The [NO] in the samples following the 30 minute stop in perfusion were highly variable and it is difficult to form any conclusions from them because of this. Clough (1999) showed that after the stop and restart in perfusion, the [NO] were higher than steady state, but not as high as the first sample collected. This supports the depletion theory as the tissue space replenishes its [NO] over the 30 minute period, but the results of this study are too variable to support it.

### ***Limitations***

The results of this pilot study must be considered in the light of any limitations in the study. The *in vitro* studies completed previously to measure recovery of NO have shown a >80% recovery, but 2 kDa cut off microdialysis probes were used in that study and also a higher probe perfusion rate than in this study (Clough, 1999). It may be useful to complete *in vitro* studies using the exact set-up used in the participants in the studies in this chapter, in order to estimate the rate of recovery of

NO. However, the usefulness of *in vitro* studies has also been questioned previously. The rate of diffusion of a given molecule is reduced in complex spaces when compared to molecules in aqueous solutions (Benveniste et al., 1990). This means that *in vitro* experiments often do not mimic the conditions of the *in vivo* environment anyway and so must be considered with caution.

It is also known that NO is highly reactive and can be oxidised or complexed with other biomolecules, such as superoxide. NO has a short half-life of less than 4 seconds in biological solutions (Vallance and Chan, 2001). The short half-life may have implications for the results in this study. However, the samples were immediately placed in ice once collected and then frozen at -80°C. They were kept frozen for a maximum of 26 days between collection and analysis and there was no thawing and re-freezing of the samples. Finally, it must be considered that aspects of the microdialysis technique, such as insertion of the probe into the skin, may effect the concentration of NO in the tissues.

### ***Summary***

The benefits of microdialysis for this study relate to its ability to measure levels of NO in the local skin interstitial space, as well as the capacity of the microdialysis membrane to exclude large molecules that cause degradation of NO. This is also done so that there is minimal trauma to the tissues and the measurements can be taken continuously over a period of time. The studies have shown that in the LM smokers the interstitial space was depleted of NO faster than the non-smokers, but the steady state NO concentration was similar between the groups. The accumulation of NO during the 30 minute stop in perfusion was highly variable. The measurement of NO concentration in the tissue space in smokers and non-smokers using microdialysis has the potential to provide information regarding effects of NO by smoking. A larger study potentially involving heavy smokers is needed to further explore this.



## **Appendix 6**

### **List of Publications**

### List of Publications

Clough, G.F. and Noble, M. 2003. Microdialysis – A model for studying chronic wounds. *Lower Extremity Wounds.*, 2, (4) 233-239

Noble, M., Voegeli, D., & Clough, G.F. 2003. A comparison of cutaneous vascular responses to transient pressure loading in smokers and nonsmokers. *J.Rehabil.Res.Dev.*, 40, (3) 283-288

Avery, M., Voegeli, D. and Clough, G.F. 2004. Evidence for endothelial dysfunction in the skin microvasculature of long-term smokers. *Proceedings of The Physiological Society*. PC153A pp170P

Avery MR, Voegeli D & Clough GF. 2005, Endothelial dysfunction in long-term smokers. *Proceedings joint meeting Microcirc Inc and BMS, J Vasc Res ;12, 670.*

Avery MR , Voegeli D & Clough GF. 2005, Microdialysis recovery of fluid from chronic wounds. *Proceedings joint meeting Microcirc Inc and BMS, J Vasc Res 12; 674.*

Avery, M., Voegeli, D., Byrne, C., Simpson, D. and Clough, G. 2009. Age and cigarette smoking are independently associated with the cutaneous vascular response to local warming. *Microcirculation.*, 16, (8) 725-734

## **Reference List**

## List of References

- Abraham, P., Fromy, B., Merzeau, S., Jardel, A., & Saumet, J.L. 2001. Dynamics of local pressure-induced cutaneous vasodilation in the human hand. *Microvasc.Res.*, 61, (1) 122-129
- Ahlsten, G., Ewald, U., & Tuvemo, T. 1987. Impaired vascular reactivity in newborn infants of smoking mothers. *Acta Paediatr.Scand.*, 76, (2) 248-253
- Akselrod, S., Gordon, D., Ubel, F.A., Shannon, D.C., Berger, A.C., & Cohen, R.J. 1981. Power spectrum analysis of heart rate fluctuation: a quantitative probe of beat-to-beat cardiovascular control. *Science*, 213, (4504) 220-222
- Allender, S., Peto, V., Scarborough, P., Kaur, A., & Rayner, M. 2008, *Coronary heart disease statistics*, British Heart Foundation, London.
- Allman, R.M., Goode, P.S., Patrick, M.M., Burst, N., & Bartolucci, A.A. 1995. Pressure ulcer risk factors among hospitalized patients with activity limitation. *JAMA*, 273, (11) 865-870
- Anggard, E. 1994. Nitric oxide: mediator, murderer, and medicine. *Lancet*, 343, (8907) 1199-1206
- Angst, M.S., Clark, J.D., Carvalho, B., Tingle, M., Schmelz, M., & Yeomans, D.C. 2008. Cytokine profile in human skin in response to experimental inflammation, noxious stimulation, and administration of a COX-inhibitor: a microdialysis study. *Pain.*, 139, (1) 15-27
- Ankrom, M.A., Bennett, R.G., Sprigle, S., Langemo, D., Black, J.M., Berlowitz, D.R., & Lyder, C.H. 2005. Pressure-related deep tissue injury under intact skin and the current pressure ulcer staging systems. *Adv.Skin Wound.Care*, 18, (1) 35-42
- Asmussen, I. & Kjeldsen, K. 1975. Intimal ultrastructure of human umbilical arteries. Observations on arteries from newborn children of smoking and nonsmoking mothers. *Circ.Res.*, 36, (5) 579-589
- Azman-Juvan, K., Bernjak, A., Urbancic-Rovan, V., Stefanovska, A., & Stajer, D. 2008. Skin blood flow and its oscillatory components in patients with acute myocardial infarction. *J.Vasc.Res.*, 45, (2) 164-172

- Bader, D.L. & Gant, C.A. 1988. Changes in transcutaneous oxygen tension as a result of prolonged pressures at the sacrum. *Clin.Phys.Physiol Meas.*, 9, (1) 33-40
- Bader, D.L., & White, S.H. 1998. The viability of soft tissues in elderly subjects undergoing hip surgery. *Age and ageing*, 27, 217-221
- Bari, F., Toth-Szuki, V., Domoki, F., & Kalman, J. 2005. Flow motion pattern differences in the forehead and forearm skin: Age-dependent alterations are not specific for Alzheimer's disease. *Microvasc.Res.*, 70, (3) 121-128
- Barua, R.S., Ambrose, J.A., Eales-Reynolds, L.J., DeVoe, M.C., Zervas, J.G., & Saha, D.C. 2001. Dysfunctional endothelial nitric oxide biosynthesis in healthy smokers with impaired endothelium-dependent vasodilatation. *Circulation*, 104, (16) 1905-1910
- Barua, R.S., Ambrose, J.A., Eales-Reynolds, L.J., DeVoe, M.C., Zervas, J.G., & Saha, D.C. 2002. Heavy and light cigarette smokers have similar dysfunction of endothelial vasoregulatory activity: an in vivo and in vitro correlation. *J.Am.Coll.Cardiol.*, 39, (11) 1758-1763
- Bayliss, W.M. 1902. On the local reactions of the arterial wall to changes of internal pressure. *J.Physiol*, 28, (3) 220-231
- Bennett, G., Dealey, C., & Posnett, J. 2004. The cost of pressure ulcers in the UK. *Age Ageing*, 33, (3) 230-235
- Benveniste, H. & Huttemeier, P.C. 1990. Microdialysis--theory and application. *Prog.Neurobiol.*, 35, (3) 195-215
- Bergstrand, S., Lindberg, L.G., Ek, A.C., Linden, M., & Lindgren, M. 2009. Blood flow measurements at different depths using photoplethysmography and laser Doppler techniques. *Skin Res.Technol.*, 15, (2) 139-147
- Berne, R., Levy, M., Koepfen, B., & Stanuton, B. 1998. *Physiology*, 4th ed. London, Mosby.
- Bernjak, A., Clarkson, P.B., McClintock, P.V., & Stefanovska, A. 2008. Low-frequency blood flow oscillations in congestive heart failure and after beta1-blockade treatment. *Microvasc.Res.*, 76, (3) 224-232

- Binggeli, C., Spieker, L.E., Corti, R., Sudano, I., Stojanovic, V., Hayoz, D., Luscher, T.F., & Noll, G. 2003. Statins enhance postischemic hyperemia in the skin circulation of hypercholesterolemic patients: a monitoring test of endothelial dysfunction for clinical practice? *J.Am.Coll.Cardiol.*, 42, (1) 71-77
- Bircher, A., de Boer, E.M., Agner, T., Wahlberg, J.E., & Serup, J. 1994. Guidelines for measurement of cutaneous blood flow by laser Doppler flowmetry. A report from the Standardization Group of the European Society of Contact Dermatitis. *Contact Dermatitis*, 30, (2) 65-72
- Black, M.A., Green, D.J., & Cable, N.T. 2008. Exercise prevents age-related decline in nitric-oxide-mediated vasodilator function in cutaneous microvessels. *J.Physiol*, 586, (14) 3511-3524
- Bollinger, A., Yanar, A., Hoffmann, U., & Franzeck, U. K. 1993, "Is high-frequency flux motion due to respiration or to vasomotion activity?," *In Vasomotion and Flow Motion*, vol. 20 C. Allegra, M. Intaglietta, & K. Messmer, eds., Basel: Karger, pp. 52-58.
- Bongard, O. & Bounameaux, H. 1993. Clinical investigation of skin microcirculation. *Dermatology*, 186, (1) 6-11
- Bornmyr, S. & Svensson, H. 1991. Thermography and laser-Doppler flowmetry for monitoring changes in finger skin blood flow upon cigarette smoking. *Clin.Physiol*, 11, (2) 135-141
- Boutsiouki, P., Georgiou, S., & Clough, G. 2003. Recovery of nitric oxide from acetylcholine-mediated vasodilatation in human skin in vivo. *Microcirculation*, 11, (3) 249-259
- Bracic, M. & Stefanovska, A. 1999. Wavelet analysis in studying the dynamics of blood circulation. *Nonlinear phenomena in complex systems 2*, (1) 68-77
- Braverman, I.M. 1989. Ultrastructure and organization of the cutaneous microvasculature in normal and pathologic states. *J.Invest Dermatol.*, 93, (2 Suppl) 2S-9S
- Braverman, I.M., Keh, A., & Goldminz, D. 1990. Correlation of laser Doppler wave patterns with underlying microvascular anatomy. *J.Invest Dermatol.*, 95, (3) 283-286
- Braverman, I.M. 2000. The cutaneous microcirculation. *J.Investig.Dermatol.Symp.Proc.*, 5, (1) 3-9

- Breuls, R.G., Mol, A., Petterson, R., Oomens, C.W., Baaijens, F.P., & Bouten, C.V. 2003. Monitoring local cell viability in engineered tissues: a fast, quantitative, and nondestructive approach. *Tissue Eng*, 9, (2) 269-281
- Brienza, D.M., Geyer, M.J., & Jan, Y.K. 2005. A comparison of changes in rhythms of sacral skin blood flow in response to heating and indentation. *Arch.Phys.Med.Rehabil.*, 86, (6) 1245-1251
- Bulkley, G.B. 1987. Free radical-mediated reperfusion injury: a selective review. *Br.J.Cancer Suppl*, 8, 66-73
- Bungum, L., Kvernebo, K., Oian, P., & Maltau, J.M. 1996. Laser doppler-recorded reactive hyperaemia in the forearm skin during the menstrual cycle. *Br.J.Obstet.Gynaecol.*, 103, (1) 70-75
- Burrus, C.S., McClellan, J.H., Oppenheim, A.V., Parks, T.W., Schafer, R.W., & Schuessler, H.W. 1994. Computer-based exercises for signal processing using Matlab<sup>®</sup>. New Jersey: Prentice-Hall, Inc.
- Butler, R., Morris, A.D., & Struthers, A.D. 2001. Cigarette smoking in men and vascular responsiveness. *Br.J.Clin.Pharmacol.*, 52, (2) 145-149
- Cable, N.T. 2006. Unlocking the secrets of skin blood flow. *J.Physiol*, 572, (Pt 3) 613
- Cakmak, S.K., Gul, U., Ozer, S., Yigit, Z., & Gonu, M. 2009. Risk factors for pressure ulcers. *Adv.Skin Wound.Care*, 22, (9) 412-415
- Cankar, K., Finderle, Z., & Strucl, M. 2009. The effect of alpha-adrenoceptor agonists and L-NMMA on cutaneous postocclusive reactive hyperemia. *Microvasc.Res.*, 77, (2) 198-203
- Capp, C.L., Dorwart, W.C., Elias, N.T., Hillman, S.R., Lancaster, S.S., Nair, R.C., Ngo, B.T., Rendell, M.S., & Smith, D.M. 2004. Post pressure hyperemia in the rat. *Comp Biochem.Physiol A Mol.Integr.Physiol*, 137, (3) 533-546
- Carlson, B.E., Arciero, J.C. & Secomb, T.W. 2008. Theoretical model of blood flow autoregulation: roles of myogenic, shear-dependent, and metabolic responses. *Am.J.Physiol.*, 295, (4) H1572-H1579

Carlsson, I. & Wennmalm, A. 1983. Effect of cigarette smoking on reactive hyperaemia in the human finger. *Clin.Physiol*, 3, (5) 453-460

Caselli, A., Uccioli, L., Khaodhiar, L., & Veves, A. 2003. Local anesthesia reduces the maximal skin vasodilation during iontophoresis of sodium nitroprusside and heating. *Microvasc.Res.*, 66, (2) 134-139

Ceelen, K.K., Stekelenburg, A., Loerakker, S., Strijkers, G.J., Bader, D.L., Nicolay, K., Baaijens, F.P., & Oomens, C.W. 2008. Compression-induced damage and internal tissue strains are related. *J.Biomech.*, 41, (16) 3399-3404

Celermajer, D.S., Sorensen, K.E., Georgakopoulos, D., Bull, C., Thomas, O., Robinson, J., & Deanfield, J.E. 1993. Cigarette smoking is associated with dose-related and potentially reversible impairment of endothelium-dependent dilation in healthy young adults. *Circulation*, 88, (5 Pt 1) 2149-2155

Chao, C.Y. & Cheing, G.L. 2009. Microvascular dysfunction in diabetic foot disease and ulceration. *Diabetes Metab Res.Rev.*, 25, (7) 604-614

Charkoudian, N. 2003. Skin blood flow in adult human thermoregulation: how it works, when it does not, and why. *Mayo Clin.Proc.* , 78, (5) 603-612

Chavez, J., Cano, C., Souki, A., Bermudez, V., Medina, M., Ciszek, A., Amell, A., Vargas, M.E., Reyna, N., Toledo, A., Cano, R., Suarez, G., Contreras, F., Israili, Z.H., Hernandez-Hernandez, R., & Valasco, M. 2007. Effect of cigarette smoking on the oxidant/antioxidant balance in healthy subjects. *Am.J.Ther.*, 14, (2) 189-193

Cho, I., Park, S., & Jung, E. 2008. Availability of nursing data in an electronic medical record system for assessing the risk of pressure ulcers. *AMIA.Annu.Symp.Proc.* 905

Choromanski, L., Westra, B., Oancea, C., Savik, K., & Holmes, J.H. 2008. Predictive modeling for improving incontinence and pressure ulcers in homecare patients. *AMIA.Annu.Symp.Proc.* 908

Clark, M., & Watts, S. 1991. The incidence of pressure sores within a National Health Service Trust hospital during 1991. *J.Adv.Nurs.*, 20, 33-36

- Clough, G.F., Bennett, A.R., & Church, M.K. 1998. Effects of H1 antagonists on the cutaneous vascular response to histamine and bradykinin: a study using scanning laser Doppler imaging. *Br.J.Dermatol.*, 138, (5) 806-814
- Clough, G.F. 1999. Role of nitric oxide in the regulation of microvascular perfusion in human skin in vivo. *J.Physiol*, 516 ( Pt 2), 549-557
- Clough, G., Chipperfield, A., Byrne, C., de, M.F., & Gush, R. 2009. Evaluation of a new high power, wide separation laser Doppler probe: potential measurement of deeper tissue blood flow. *Microvasc.Res.*, 78, (2) 155-161
- Colin, D. & Saumet, J.L. 1996. Influence of external pressure on transcutaneous oxygen tension and laser Doppler flowmetry on sacral skin. *Clin.Physiol*, 16, (1) 61-72
- Compher, C., Kinosian, B.P., Ratcliffe, S.J., & Baumgarten, M. 2007. Obesity reduces the risk of pressure ulcers in elderly hospitalized patients. *J.Gerontol.A Biol.Sci.Med.Sci.*, 62, (11) 1310-1312
- Cooke, E.D. & Almond, N.E. 1990. Laser Doppler flowmetry. *J.Med.Eng Technol.*, 14, (5) 177
- Cracowski, J.L., Minson, C.T., Salvat-Melis, M., & Halliwill, J.R. 2006. Methodological issues in the assessment of skin microvascular endothelial function in humans. *Trends Pharmacol.Sci.*, 27, (9) 503-508
- Cracowski, J.L., Lorenzo, S., & Minson, C.T. 2007. Effects of local anaesthesia on subdermal needle insertion pain and subsequent tests of microvascular function in human. *Eur.J.Pharmacol.*, 559, (2-3) 150-154
- Crandall, C.G. & MacLean, D.A. 2001. Cutaneous interstitial nitric oxide concentration does not increase during heat stress in humans. *J.Appl.Physiol*, 90, (3) 1020-1024
- Csiszar, A., Podlutzky, A., Wolin, M.S., Losonczy, G., Pacher, P., & Ungvari, Z. 2009. Oxidative stress and accelerated vascular aging: implications for cigarette smoking. *Front Biosci.*, 14, 3128-3144
- Cui, J. & Sathishkumar, M. 2006. Spectral characteristics of skin sympathetic nerve activity in heat-stressed humans. *Am.J.Physiol.*, 290, H1601-H1609

- de Jongh, R.T., Clark, A.D., IJzerman, R.G., Serne, E.H., de, V.G., & Stehouwer, C.D. 2004. Physiological hyperinsulinaemia increases intramuscular microvascular reactive hyperaemia and vasomotion in healthy volunteers. *Diabetologia*, 47, (6) 978-986
- Debbabi, H., Bonnin, P., Ducluzeau, P.H., Leftheriotis, G., & Levy, B.I. 2010. Noninvasive Assessment of Endothelial Function in the Skin Microcirculation. *Am.J.Hypertens.*, 23, (5) 541-546
- Defloor, T. 2000. The effect of position and mattress on interface pressure. *Appl.Nurs.Res.*, 13, (1) 2-11
- del, G.R., Leonardo, G., & Arpaia, M.R. 1986. Evaluation of postischemic hyperemia on the skin using laser Doppler velocimetry: study on patients with claudicatio intermittens. *Microvasc.Res.*, 32, (3) 289-299
- Delp, M.D., Behnke, B.J., Spier, S.A., Wu, G., & Muller-Delp, J.M. 2008. Ageing diminishes endothelium-dependent vasodilatation and tetrahydrobiopterin content in rat skeletal muscle arterioles. *J.Physiol.*, 586, (4) 1161-168
- Dimond, B. 2003. Pressure ulcers and litigation. *Nurs.Times*, 99, (5) 61-63
- Dinsdale, S.M. 1974. Decubitus ulcers: role of pressure and friction in causation. *Arch.Phys.Med.Rehabil.*, 55, (4) 147-152
- Doll, R. & Hill, A.B. 1956. Lung cancer and other causes of death in relation to smoking; a second report on the mortality of British doctors. *Br.Med.J.*, 2, (5001) 1071-1081
- Doll, R., Peto, R., Boreham, J., & Sutherland, I. 2004. Mortality in relation to smoking: 50 years' observations on male British doctors. *BMJ*, 328, (7455) 1519-1527
- Dora, K.A., Hinton, J.M., Walker, S.D., & Garland, C.J. 2000. An indirect influence of phenylephrine on the release of endothelium-derived vasodilators in rat small mesenteric artery. *Br.J.Pharmacol.*, 129, (2) 381-387
- Edsberg, L.E. 2007. Pressure ulcer tissue histology: an appraisal of current knowledge. *Ostomy.Wound.Manage.*, 53, (10) 40-49

- Edvinsson, M.L., Andersson, S.E., Xu, C.B., & Edvinsson, L. 2008. Cigarette smoking leads to reduced relaxant responses of the cutaneous microcirculation. *Vasc.Health Risk Manag.*, 4, (3) 699-704
- Elliot, C., Voegeli, D., Church, M., & Clough, G. 1999. Circadian rhythms in the cutaneous response to histamine. *Immunology* 98 (Suppl), 79
- European Pressure Ulcer Advisory Panel & National Pressure Ulcer Advisory Panel. 2009. *Prevention and treatment of pressure ulcers: quick reference guide*. Washington DC, National Pressure Ulcer Advisory Panel.
- Forstermann, U., Closs, E.I., Pollock, J.S., Nakane, M., Schwarz, P., Gath, I., & Kleinert, H. 1994. Nitric oxide synthase isozymes. Characterization, purification, molecular cloning, and functions. *Hypertension*, 23, (6 Pt 2) 1121-1131
- Forstermann, U. & Munzel, T. 2006. Endothelial nitric oxide synthase in vascular disease: from marvel to menace. *Circulation*, 113, (13) 1708-1714
- Fox, E., Bungay, P.M., Bacher, J., McCully, C.L., Dedrick, R.L., & Balis, F.M. 2002. Zidovudine concentration in brain extracellular fluid measured by microdialysis: steady-state and transient results in rhesus monkey. *J.Pharmacol.Exp.Ther.*, 301, (3) 1003-1011
- Frantz, R.A. & Xakellis, G.C. 1989. Characteristics of skin blood flow over the trochanter under constant, prolonged pressure. *Am.J.Phys.Med.Rehabil.*, 68, (6) 272-276
- Fredriksson, I., Larsson, M., & Stromberg, T. 2009. Measurement depth and volume in laser Doppler flowmetry. *Microvasc.Res.*, 78, (1) 4-13
- Fromy, B., Abraham, P., & Saumet, J.L. 2000. Progressive calibrated pressure device to measure cutaneous blood flow changes to external pressure strain. *Brain Res.Brain Res.Protoc.*, 5, (2) 198-203
- Fromy, B., Abraham, P., Bouvet, C., Bouhanick, B., Fressinaud, P., & Saumet, J.L. 2002. Early decrease of skin blood flow in response to locally applied pressure in diabetic subjects. *Diabetes*, 51, (4) 1214-1217

- Furchgott, R.F. 1999. Endothelium-derived relaxing factor: discovery, early studies, and identification as nitric oxide. *Biosci.Rep.*, 19, (4) 235-251
- Gamble, J., Grewal, P.S., & Gartside, I.B. 2000. Vitamin C modifies the cardiovascular and microvascular responses to cigarette smoke inhalation in man. *Clin.Sci.(Lond)*, 98, (4) 455-460
- Geyer, M.J., Jan, Y.K., Brienza, D.M., & Boninger, M.L. 2004. Using wavelet analysis to characterize the thermoregulatory mechanisms of sacral skin blood flow. *J.Rehabil.Res.Dev.*, 41, (6A) 797-806
- Girouard, K., Harrison, M.B., & VanDenKerkof, E. 2008. The symptom of pain with pressure ulcers: a review of the literature. *Ostomy.Wound.Manage.*, 54, (5) 30-40, 42
- Goodfield, M.J., Hume, A., & Rowell, N.R. 1990. The acute effects of cigarette smoking on cutaneous blood flow in smoking and non-smoking subjects with and without Raynaud's phenomenon. *Br.J.Rheumatol.*, 29, (2) 89-91
- Gooding, K.M., Hannemann, M.M., Tooke, J.E., Clough, G.F., & Shore, A.C. 2006. Maximum skin hyperaemia induced by local heating: possible mechanisms. *J.Vasc.Res.*, 43, (3) 270-277
- Gorecki, C., Brown, J.M., Nelson, E.A., Briggs, M., Schoonhoven, L., Dealey, C., Defloor, T., & Nixon, J. 2009. Impact of pressure ulcers on quality of life in older patients: a systematic review. *J.Am.Geriatr.Soc.*, 57, (7) 1175-1183
- Gould, D., Goldstone, L., Gammon, J., Kelly, D., & Maidwell, A. 2002. Establishing the validity of pressure ulcer risk assessment scales: a novel approach using illustrated patient scenarios. *Int.J.Nurs.Stud.*, 39, (2) 215-228
- Griendling, K.K. & Harrison, D.G. 1999. Dual role of reactive oxygen species in vascular growth. *Circ.Res.*, 85, (6) 562-563
- Groth, L., Jorgensen, A., & Serup, J. 1998. Cutaneous microdialysis in the rat: insertion trauma and effect of anaesthesia studied by laser Doppler perfusion imaging and histamine release. *Skin.Pharmacol.Appl.Skin.Physiol.*, 11, (3) 125-132

- Gullu, H., Caliskan, M., Ciftci, O., Erdogan, D., Topcu, S., Yildirim, E., Yildirim, A., & Muderrisoglu, H. 2007. Light cigarette smoking impairs coronary microvascular functions as severely as smoking regular cigarettes. *Heart*, 93, (10) 1274-1277
- Gunes, U.Y. 2008. A descriptive study of pressure ulcer pain. *Ostomy.Wound.Manage.*, 54, (2) 56-61
- Guthikonda, S., Sinkey, C., Barenz, T., & Haynes, W.G. 2003. Xanthine oxidase inhibition reverses endothelial dysfunction in heavy smokers. *Circulation*, 107, (3) 416-421
- Haddock, R.E. & Hill, C.E. 2005. Rhythmicity in arterial smooth muscle. *J.Physiol*, 566, (Pt 3) 645-656
- Hagisawa, S., Barbenel, J.C., & Kenedi, R.M. 1991. Influence of age on postischaemic reactive hyperaemia. *Clin.Phys.Physiol Meas.*, 12, (3) 227-237
- Hagisawa, S., Ferguson-Pell, M., Cardi, M., & Miller, S.D. 1994. Assessment of skin blood content and oxygenation in spinal cord injured subjects during reactive hyperemia. *J.Rehabil.Res.Dev.*, 31, (1) 1-14
- Hagisawa, S., Shimada, T., Arao, H., & Asada, Y. 2001. Morphological architecture and distribution of blood capillaries and elastic fibres in the human skin. *Journal of Tissue Viability* 11(2), 59-63
- Hashimoto, H. 1994. Impaired microvascular vasodilator reserve in chronic cigarette smokers--a study of post-occlusive reactive hyperemia in the human finger. *Jpn.Circ.J.*, 58, (1) 29-33
- Heitzer, T., Just, H., & Munzel, T. 1996. Antioxidant vitamin C improves endothelial dysfunction in chronic smokers. *Circulation*, 94, (1) 6-9
- Heitzer, T., Brockhoff, C., Mayer, B., Warnholtz, A., Mollnau, H., Henne, S., Meinertz, T., & Munzel, T. 2000. Tetrahydrobiopterin improves endothelium-dependent vasodilation in chronic smokers : evidence for a dysfunctional nitric oxide synthase. *Circ.Res.*, 86, (2) E36-E41

- Helfrich, Y.R., Yu, L., Ofori, A., Hamilton, T.A., Lambert, J., King, A., Voorhees, J.J., & Kang, S. 2007. Effect of smoking on aging of photoprotected skin: evidence gathered using a new photonumeric scale. *Arch.Dermatol.*, 143, (3) 397-402
- Herrman, E.C., Knapp, C.F., Donofrio, J.C., Salcido, R. 1999. Skin perfusion responses to surface pressure-induced ischemia: implications for the developing pressure ulcer. *J.Rehab.Res.Dev.*, 36, (2) 109-120
- Hill, C.E., Eade, J., & Sandow, S.L. 1999. Mechanisms underlying spontaneous rhythmical contractions in irideal arterioles of the rat. *J.Physiol*, 521, (2) 507-516
- Holowatz, L.A., Thompson-Torgerson, C.S., & Kenney, W.L. 2008. The human cutaneous circulation as a model of generalized microvascular function. *J.Appl.Physiol.*, 105, 370-372
- Hopkins, A., Dealey, C., Bale, S., Defloor, T., & Warboys, F. 2006. Patient stories of living with a pressure ulcer. *Journal of Advanced Nursing*, 56, (4) 345-353
- Houghton, B.L., Meendering, J.R., Wong, B.J., & Minson, C.T. 2006. Nitric oxide and noradrenaline contribute to the temperature threshold of the axon reflex response to gradual local heating in human skin. *J.Physiol*, 572, (3) 811-820
- Houwing, R., Overgoor, M., Kon, M., Jansen, G., van Asbeck, B.S., & Haalboom, J.R. 2000. Pressure-induced skin lesions in pigs: reperfusion injury and the effects of vitamin E. *J.Wound.Care*, 9, (1) 36-40
- Hsiu, H., Hsu, C.L., Chiang, W.R., Chao, P.T., Hsu, T.L., Jan, M.Y., Wang, W.K., & Wang, Y.Y. 2008. Connection between RR-interval length and the pulsatile microcirculatory flow. *Physiol Meas.*, 29, (2) 245-254
- Huang, A., Sun, D., Koller, A., & Kaley, G. 1997. Gender difference in myogenic tone of rat arterioles is due to estrogen-induced, enhanced release of NO. *Am.J.Physiol*, 272, (4 Pt 2) H1804-H1809
- Hutchison, S.J., Sudhir, K., Sievers, R.E., Zhu, B.Q., Sun, Y.P., Chou, T.M., Chatterjee, K., Deedwania, P.C., Cooke, J.P., Glantz, S.A., & Parmley, W.W. 1999. Effects of L-arginine on atherogenesis and endothelial dysfunction due to secondhand smoke. *Hypertension*, 34, (1) 44-50

- Hwang, K., Kim, D.J., & Lee, I.J. 2001. An anatomic comparison of the skin of five donor sites for dermal fat graft. *Ann.Plast.Surg.*, 46, (3) 327-331
- Hyndman, B.W., Kitney, R.I., & Sayers, B.M. 1971. Spontaneous rhythms in physiological control systems. *Nature*, 233, (5318) 339-341
- IJzerman, R.G., de Jongh, R.T., Beijk, M.A., van Weissenbruch, M.M., Delemarre-van de Waal HA, Serne, E.H., & Stehouwer, C.D. 2003a. Individuals at increased coronary heart disease risk are characterized by an impaired microvascular function in skin. *Eur.J.Clin.Invest*, 33, (7) 536-542
- IJzerman, R.G., Serne, E.H., van Weissenbruch, M.M., de Jongh, R.T., & Stehouwer, C.D. 2003b. Cigarette smoking is associated with an acute impairment of microvascular function in humans. *Clin.Sci.(Lond)*, 104, (3) 247-252
- Jan, Y.K., Brienza, D.M., & Geyer, M.J. 2005. Analysis of week-to-week variability in skin blood flow measurements using wavelet transforms. *Clin.Physiol Funct.Imaging*, 25, (5) 253-262
- Jan, Y.K., Brienza, D.M., Geyer, M.J., & Karg, P. 2008. Wavelet-based spectrum analysis of sacral skin blood flow response to alternating pressure. *Arch.Phys.Med.Rehabil.*, 89, (1) 137-145
- Jan, Y.K., Struck, B.D., Foreman, R.D., & Robinson, C. 2009. Wavelet analysis of sacral skin blood flow oscillations to assess soft tissue viability in older adults. *Microvasc.Res.*, 78, (2) 162-168
- Jensen, J.A., Goodson, W.H., Hopf, H.W., & Hunt, T.K. 1991. Cigarette smoking decreases tissue oxygen. *Arch.Surg.*, 126, (9) 1131-1134
- Kastrup, J., Bulow, J., & Lassen, N.A. 1989. Vasomotion in human skin before and after local heating recorded with laser Doppler flowmetry. A method for induction of vasomotion. *Int.J.Microcirc.Clin.Exp.*, 8, (2) 205-215
- Katugampola, R., Church, M.K., & Clough, G.F. 2000. The neurogenic vasodilator response to endothelin-1: a study in human skin in vivo. *Exp.Physiol*, 85, (6) 839-846
- Kellogg, D.L., Jr., Liu, Y., Kosiba, I.F., & O'Donnell, D. 1999. Role of nitric oxide in the vascular effects of local warming of the skin in humans. *J.Appl.Physiol*, 86, (4) 1185-1190

- Kellogg, D.L., Jr., Zhao, J.L., Friel, C., & Roman, L.J. 2003. Nitric oxide concentration increases in the cutaneous interstitial space during heat stress in humans. *J.Appl.Physiol*, 94, (5) 1971-1977
- Kelm, M., Preik, M., Hafner, D.J., & Strauer, B.E. 1996. Evidence for a multifactorial process involved in the impaired flow response to nitric oxide in hypertensive patients with endothelial dysfunction. *Hypertension*, 27, (3 Pt 1) 346-353
- Kernick, D.P., Tooke, J.E., & Shore, A.C. 1999. The biological zero signal in laser Doppler fluximetry - origins and practical implications. *Pflugers Arch.*, 437, (4) 624-631
- Khan, F., Litchfield, S.J., Stonebridge, P.A., & Belch, J.J. 1999. Lipid-lowering and skin vascular responses in patients with hypercholesterolaemia and peripheral arterial obstructive disease. *Vasc.Med.*, 4, (4) 233-238
- Klede, M., Clough, G., Lischetzki, G., & Schmelz, M. 2003. The effect of the nitric oxide synthase inhibitor N-nitro-L-arginine-methyl ester on neuropeptide-induced vasodilation and protein extravasation in human skin. *J.Vasc.Res.*, 40, (2) 105-114
- Knight, S.L., Taylor, R.P., Polliack, A.A., & Bader, D.L. 2001. Establishing predictive indicators for the status of loaded soft tissues. *J.Appl.Physiol*, 90, (6) 2231-2237
- Knotzer, H., Maier, S., Dunser, M., Stadlbauer, K.H., Ulmer, H., Pajk, W., & Hasibeder, W.R. 2007. Oscillation frequency of skin microvascular blood flow is associated with mortality in critically ill patients. *Acta Anaesthesiol.Scand.*, 51, (6) 701-707
- Knuutinen, A., Kokkonen, N., Risteli, J., Vahakangas, K., Kallioinen, M., Salo, T., Sorsa, T., & Oikarinen, A. 2002. Smoking affects collagen synthesis and extracellular matrix turnover in human skin. *Br.J.Dermatol.*, 146, (4) 588-594
- Koenigsberger, M., Sauser, R., Beny, J.L., & Meister, J.J. 2006. Effects of arterial wall stress on vasomotion. *Biophys.J.*, 91, (5) 1663-1674
- Kosiak, M. 1959. Etiology and pathology of ischemic ulcers. *Arch.Phys.Med.Rehabil.*, 40, (2) 62-69
- Kosiak, M. 1961. Etiology of decubitus ulcers. *Arch.Phys.Med.Rehabil.*, 42, 19-29

Krouskop, T.A. 1983. A synthesis of the factors that contribute to pressure sore formation. *Med.Hypotheses*, 11, (2) 255-267

Kruger, A., Stewart, J., Sahityani, R., O'Riordan, E., Thompson, C., Adler, S., Garrick, R., Vallance, P., & Goligorsky, M.S. 2006. Laser Doppler flowmetry detection of endothelial dysfunction in end-stage renal disease patients: correlation with cardiovascular risk. *Kidney Int.*, 70, (1) 157-164

Kvandal, P., Stefanovska, A., Veber, M., Kvernmo, H.D., & Kirkeboen, K.A. 2003. Regulation of human cutaneous circulation evaluated by laser Doppler flowmetry, iontophoresis, and spectral analysis: importance of nitric oxide and prostaglandines. *Microvasc.Res.*, 65, (3) 160-171

Kvandal, P., Landsverk, S.A., Bernjak, A., Stefanovska, A., Kvernmo, H.D., & Kirkeboen, K.A. 2006. Low-frequency oscillations of the laser Doppler perfusion signal in human skin. *Microvasc.Res.*, 72, (3) 120-127

Kvernmo, H.D., Stefanovska, A., Kirkeboen, K.A., & Kvernebo, K. 1999. Oscillations in the human cutaneous blood perfusion signal modified by endothelium-dependent and endothelium-independent vasodilators. *Microvasc.Res.*, 57, (3) 298-309

Lagaud, G.J., Skarsgard, P.L., Laher, I., & van, B.C. 1999. Heterogeneity of endothelium-dependent vasodilation in pressurized cerebral and small mesenteric resistance arteries of the rat. *J.Pharmacol.Exp.Ther.*, 290, (2) 832-839

Larsson, M., Steenbergen, W., & Stromberg, T. 2002. Influence of optical properties and fiber separation on laser doppler flowmetry. *J.Biomed.Opt.*, 7, (2) 236-243

Leanderson, P. & Tagesson, C. 1992. Cigarette smoke-induced DNA damage in cultured human lung cells: role of hydroxyl radicals and endonuclease activation. *Chem.Biol.Interact.*, 81, (1-2) 197-208

Lefrandt, J.D., Bosma, E., Oomen, P.H., Hoeven, J.H., Roon, A.M., Smit, A.J., & Hoogenberg, K. 2003. Sympathetic mediated vasomotion and skin capillary permeability in diabetic patients with peripheral neuropathy. *Diabetologia*, 46, (1) 40-47

- Lehr, H.A., Kress, E., Menger, M.D., Friedl, H.P., Hubner, C., Arfors, K.E., & Messmer, K. 1993. Cigarette smoke elicits leukocyte adhesion to endothelium in hamsters: inhibition by CuZn-SOD. *Free Radic.Biol.Med.*, 14, (6) 573-581
- Lehr, H.A., Frei, B., & Arfors, K.E. 1994. Vitamin C prevents cigarette smoke-induced leukocyte aggregation and adhesion to endothelium in vivo. *Proc.Natl.Acad.Sci.U.S.A*, 91, (16) 7688-7692
- Lekakis, J., Papamichael, C., Vemmos, C., Stamatelopoulos, K., Voutsas, A., & Stamatelopoulos, S. 1998. Effects of acute cigarette smoking on endothelium-dependent arterial dilatation in normal subjects. *Am.J.Cardiol.*, 81, (10) 1225-1228
- Levy, M., Stanton, B., & Koeppen, B. 2006. *Principles of Physiology*, 4th ed. Elsevier, Mosby.
- Li, P.F., Dietz, R., & von, H.R. 1997. Differential effect of hydrogen peroxide and superoxide anion on apoptosis and proliferation of vascular smooth muscle cells. *Circulation*, 96, (10) 3602-3609
- Li, L., Mac-Mary, S., Sainthillier, J.M., Nouveau, S., de, L.O., & Humbert, P. 2006a. Age-related changes of the cutaneous microcirculation in vivo. *Gerontology*, 52, (3) 142-153
- Li, Z., Tam, E.W., Kwan, M.P., Mak, A.F., Lo, S.C., & Leung, M.C. 2006b. Effects of prolonged surface pressure on the skin blood flowmotions in anaesthetized rats--an assessment by spectral analysis of laser Doppler flowmetry signals. *Phys.Med.Biol.*, 51, (10) 2681-2694
- Lin, S.J., Hong, C.Y., Chang, M.S., Chiang, B.N., & Chien, S. 1992. Long-term nicotine exposure increases aortic endothelial cell death and enhances transendothelial macromolecular transport in rats. *Arterioscler.Thromb.*, 12, (11) 1305-1312
- Lindstedt, I.H., Edvinsson, M.L., & Edvinsson, L. 2006. Reduced responsiveness of cutaneous microcirculation in essential hypertension--a pilot study. *Blood Press*, 15, (5) 275-280
- Magerl, W. & Treede, R.D. 1996. Heat-evoked vasodilatation in human hairy skin: axon reflexes due to low-level activity of nociceptive afferents. *J.Physiol*, 497 ( Pt 3), 837-848

- Margolis, D.J., Bilker, W., Knauss, J., Baumgarten, M., & Strom, B.L. 2002. The incidence and prevalence of pressure ulcers among elderly patients in general medical practice. *Ann.Epidemiol.*, 12, (5) 321-325
- Martin, H.L., Loomis, J.L., & Kenney, W.L. 1995. Maximal skin vascular conductance in subjects aged 5-85 yr. *J.Appl.Physiol*, 79, (1) 297-301
- Mauban, J.R., Lamont, C., Balke, C.W., & Wier, W.G. 2001. Adrenergic stimulation of rat resistance arteries affects Ca(2+) sparks, Ca(2+) waves, and Ca(2+) oscillations. *Am.J.Physiol Heart Circ.Physiol*, 280, (5) H2399-H2405
- Mayhan, W.G. & Sharpe, G.M. 1998. Superoxide dismutase restores endothelium-dependent arteriolar dilatation during acute infusion of nicotine. *J.Appl.Physiol*, 85, (4) 1292-1298
- Mayhan, W.G. & Sharpe, G.M. 1999. Chronic exposure to nicotine alters endothelium-dependent arteriolar dilatation: effect of superoxide dismutase. *J.Appl.Physiol*, 86, (4) 1126-1134
- Mayrovitz, H.N., Smith, J., Delgado, M., & Regan, M.B. 1997. Heel blood perfusion responses to pressure loading and unloading in women. *Ostomy.Wound.Manage.*, 43, (7) 16-20, 22, 24
- Mayrovitz, H.N. & Smith, J. 1998. Heel-skin microvascular blood perfusion responses to sustained pressure loading and unloading. *Microcirculation.*, 5, (2-3) 227-233
- Mayrovitz, H.N., Macdonald, J., & Smith, J.R. 1999. Blood perfusion hyperaemia in response to graded loading of human heels assessed by laser-Doppler imaging. *Clin.Physiol*, 19, (5) 351-359
- Mayrovitz, H.N., Sims, N., & Taylor, M.C. 2002. Sacral skin blood perfusion: a factor in pressure ulcers? *Ostomy.Wound.Manage.*, 48, (6) 34-2
- Mazzoni, M.C., Borgstrom, P., Warnke, K.C., Skalak, T.C., Intaglietta, M., & Arfors, K.E. 1995. Mechanisms and implications of capillary endothelial swelling and luminal narrowing in low-flow ischemias. *Int.J.Microcirc.Clin.Exp.*, 15, (5) 265-270
- McCord, G.R., Cracowski, J.L., & Minson, C.T. 2006. Prostanoids contribute to cutaneous active vasodilation in humans. *Am.J.Physiol Regul.Integr.Comp Physiol*, 291, (3) R596-R602

McGeown, J.G. 2002. *Master medicine: Physiology - A clinical core text of human physiology with self-assessment*, 2nd ed. London, Churchill Livingstone.

Meekin, T.N., Wilson, R.F., Scott, D.A., Ide, M., & Palmer, R.M. 2000. Laser Doppler flowmeter measurement of relative gingival and forehead skin blood flow in light and heavy smokers during and after smoking. *J.Clin.Periodontol.*, 27, (4) 236-242

Meredith, I.T., Currie, K.E., Anderson, T.J., Roddy, M.A., Ganz, P., & Creager, M.A. 1996. Postischemic vasodilation in human forearm is dependent on endothelium-derived nitric oxide. *Am.J.Physiol*, 270, (4 Pt 2) H1435-H1440

Meyer, C. 2002. Letter to the editor. *J.Appl.Physiol.*, 92, 888-889.

Meyer, M.F., Rose, C.J., Hulsmann, J.O., Schatz, H., & Pfohl, M. 2003. Impaired 0.1-Hz vasomotion assessed by laser Doppler anemometry as an early index of peripheral sympathetic neuropathy in diabetes. *Microvasc.Res.*, 65, (2) 88-95

Midttun, M., Sejrnsen, P., & Paaske, W.P. 2006. Smokers have severely disturbed peripheral micro-circulation. *Int.Angiol.*, 25, (3) 293-296

Minson, C.T., Wladkowski, S.L., Cardell, A.F., Pawelczyk, J.A., & Kenney, W.L. 1998. Age alters the cardiovascular response to direct passive heating. *J.Appl.Physiol*, 84, (4) 1323-1332

Minson, C.T., Berry, L.T., & Joyner, M.J. 2001. Nitric oxide and neurally mediated regulation of skin blood flow during local heating. *J.Appl.Physiol*, 91, (4) 1619-1626

Minson, C.T., Holowatz, L.A., Wong, B.J., Kenney, W.L., & Wilkins, B.W. 2002. Decreased nitric oxide- and axon reflex-mediated cutaneous vasodilation with age during local heating. *J.Appl.Physiol*, 93, (5) 1644-1649

Minson, C.T. & Wong, B.J. 2004. Reactive hyperemia as a test of endothelial or microvascular function? *J.Am.Coll.Cardiol.*, 43, (11) 2147-2148

Mitchell, G.F., Vita, J.A., Larson, M.G., Parise, H., Keyes, M.J., Warner, E., Vasan, R.S.,

- Levy, D., & Benjamin, E.J. 2005. Cross-sectional relations of peripheral microvascular function, cardiovascular disease risk factors, and aortic stiffness: the Framingham Heart Study. *Circulation*, 112, (24) 3722-3728
- Monfrecola, G., Riccio, G., Savarese, C., Posteraro, G., & Procaccini, E.M. 1998. The acute effect of smoking on cutaneous microcirculation blood flow in habitual smokers and nonsmokers. *Dermatology*, 197, (2) 115-118
- Moor Instruments (a) 2011, Moor LDI2-BI Burn Assessment. <http://gb.moor.co.uk/product/moorldi2-bi-burn-assessment/9>, Accessed 31<sup>st</sup> March 2011
- Moor Instruments (b) 2011, Trend Flap Monitoring. <http://gb.moor.co.uk/product/trend-flap-monitoring/16>, Accessed 31<sup>st</sup> March 2011
- Moore, Z. & Cowman, S. 2008, *Risk assessment tools for the prevention of pressure ulcers (review)*. *The Cochrane Collaboration*, John Wiley and Sons, Ltd.
- Moore, Z. & Cowman, S. 2010, *Risk assessment tools for the prevention of pressure ulcers (review)*. *The Cochrane Collaboration*, John Wiley and Sons, Ltd.
- Morrow, J.D., Frei, B., Longmire, A.W., Gaziano, J.M., Lynch, S.M., Shyr, Y., Strauss, W.E., Oates, J.A., & Roberts, L.J. 1995. Increase in circulating products of lipid peroxidation (F<sub>2</sub>-isoprostanes) in smokers. Smoking as a cause of oxidative damage. *N.Engl.J.Med.*, 332, (18) 1198-1203
- Muller, M. 2002. Science, medicine, and the future: Microdialysis. *BMJ.*, 324, (7337) 588-591
- Murray, R.P., Connett, J.E., Lauger, G.G., & Voelker, H.T. 1993. Error in smoking measures: effects of intervention on relations of cotinine and carbon monoxide to self-reported smoking. The Lung Health Study Research Group. *Am.J.Public Health*, 83, (9) 1251-1257
- Murray, A.K., Moore, T.L., Manning, J.B., Taylor, C., Griffiths, C.E., & Herrick, A.L. 2009. Noninvasive imaging techniques in the assessment of scleroderma spectrum disorders. *Arthritis Rheum.*, 61, (8) 1103-1111

Narkiewicz, K., van de Borne, P.J., Hausberg, M., Cooley, R.L., Winniford, M.D., Davison, D.E., & Somers, V.K. 1998. Cigarette smoking increases sympathetic outflow in humans. *Circulation*, 98, (6) 528-534

National Institute for Health and Clinical Excellence 2001, *Inherited clinical guideline B. Pressure ulcer risk assessment and prevention*.

National Pressure Ulcer Advisory Panel 2007, Pressure ulcer stages revised by NPUAP. <http://www.npuap.org/pr2.htm>, Accessed 2<sup>nd</sup> April 2011

Neunteufl, T., Heher, S., Kostner, K., Mitulovic, G., Lehr, S., Khoschsorur, G., Schmid, R.W., Maurer, G., & Stefenelli, T. 2002. Contribution of nicotine to acute endothelial dysfunction in long-term smokers. *J.Am.Coll.Cardiol.*, 39, (2) 251-256

Nicotra, A., Asahina, M., & Mathias, C.J. 2004. Skin vasodilator response to local heating in human chronic spinal cord injury. *Eur.J.Neurol.*, 11, (12) 835-837

Nilsson, G.E., Tenland, T., & Oberg, P.A. 1980. Evaluation of a laser Doppler flowmeter for measurement of tissue blood flow. *IEEE Trans.Biomed.Eng.*, 27, (10) 597-604

Nilsson, H. & Aalkjaer, C. 2003. Vasomotion: mechanisms and physiological importance. *Mol.Interv.*, 3, (2) 79-89, 51

Noble, M., Voegeli, D., & Clough, G.F. 2003. A comparison of cutaneous vascular responses to transient pressure loading in smokers and nonsmokers. *J.Rehabil.Res.Dev.*, 40, (3) 283-288

Node, K., Kitakaze, M., Yoshikawa, H., Kosaka, H., & Hori, M. 1997. Reversible reduction in plasma concentration of nitric oxide induced by cigarette smoking in young adults. *Am.J.Cardiol.*, 79, (11) 1538-1541

Nuttall, S.L., Routledge, H.C., & Manney, S. 2002. Circulating and exhaled markers of nitric oxide and antioxidant activity after smoking. *Circulation*, 106, (20) e145-e146

O'Riordan, E., Chen, J., Brodsky, S.V., Smirnova, I., Li, H., & Goligorsky, M.S. 2005. Endothelial cell dysfunction: the syndrome in making. *Kidney Int.*, 67, (5) 1654-1658

- Obeid, A.N., Barnett, N.J., Dougherty, G., & Ward, G. 1990. A critical review of laser Doppler flowmetry. *J.Med.Eng Technol.*, 14, (5) 178-181
- Orosz, Z., Csiszar, A., Labinsky, N., Smith, K., Kaminski, P.M., Ferdinandy, P., Wolin, M.S., Rivera, A., & Ungvari, Z. 2007. Cigarette smoke-induced proinflammatory alterations in the endothelial phenotype: role of NAD(P)H oxidase activation. *Am.J.Physiol Heart Circ.Physiol*, 292, (1) H130-H139
- Pajk, W., Schwarz, B., Knotzer, H., Friesenecker, B., Mayr, A., Dunser, M., & Hasibeder, W. 2002. Jejunal tissue oxygenation and microvascular flow motion during hemorrhage and resuscitation. *Am.J.Physiol Heart Circ.Physiol*, 283, (6) H2511-H2517
- Parthimos, D., Edwards, D.H., & Griffith, T.M. 1996. Comparison of chaotic and sinusoidal vasomotion in the regulation of microvascular flow. *Cardiovasc.Res.*, 31, (3) 388-399
- Peirce, S. M., Skalak, T.C., & Rodeheaver, G.T. 2000. Ischaemia-reperfusion injury in chronic pressure ulcer formation: a skin model in the rat. *Wound.Repair Regen.* 8, 68-76. 2000
- Peirce, S.M., Skalak, T.C., Rieger, J.M., Macdonald, T.L., & Linden, J. 2001. Selective A(2A) adenosine receptor activation reduces skin pressure ulcer formation and inflammation. *Am.J.Physiol Heart Circ.Physiol*, 281, (1) H67-H74
- Pellaton, C., Kubli, S., Feihl, F., & Waeber, B. 2002. Blunted vasodilatory responses in the cutaneous microcirculation of cigarette smokers. *Am.Heart J.*, 144, (2) 269-274
- Petersen, L.J., Pedersen, J.L., Skov, P.S., Nielsen, H.J., & Kehlet, H. 2009. Histamine is not released in acute thermal injury in human skin in vivo: a microdialysis study. *Inflamm.Res.*, 58, (7) 395-399
- Phillips, L. & Buttery, J. 2009. Exploring pressure ulcer prevalence and preventative care. *Nurs.Times*, 105, (16) 34-36
- Pittilo, R.M., Mackie, I.J., Rowles, P.M., Machin, S.J., & Woolf, N. 1982. Effects of cigarette smoking on the ultrastructure of rat thoracic aorta and its ability to produce prostacyclin. *Thromb.Haemost.*, 48, (2) 173-176

Pocock, G. & Richards, C.D. 2006. *Human Physiology: The Basis of Medicine*, 3rd ed. Oxford, Oxford University Press.

Pretto, E.A., Jr. 1991. Reperfusion injury of the liver. *Transplant.Proc.*, 23, (3) 1912-1914

Radi, R., Beckman, J.S., Bush, K.M., & Freeman, B.A. 1991. Peroxynitrite-induced membrane lipid peroxidation: the cytotoxic potential of superoxide and nitric oxide. *Arch.Biochem.Biophys.*, 288, (2) 481-487

Rasool, A.H., Ghazali, D.M., Abdullah, H., Halim, A.S., & Wong, A.R. 2009. Endothelial nitric oxide synthase G894T gene polymorphism and response to skin reactive hyperemia. *Microvasc.Res.*, 78, (2) 230-234

Reddy, N.P. & Cochran, G.V. 1981. Interstitial fluid flow as a factor in decubitus ulcer formation. *J.Biomech.*, 14, (12) 879-881

Reid, R.R., Sull, A.C., Mogford, J.E., Roy, N., & Mustoe, T.A. 2004. A novel murine model of cyclical cutaneous ischemia-reperfusion injury. *J.Surg.Res.*, 116, (1) 172-180

Rendell, M.S. & Wells, J.M. 1998. Ischemic and pressure-induced hyperemia: a comparison. *Arch.Phys.Med.Rehabil.*, 79, (11) 1451-1455

Reus, W.F., Robson, M.C., Zachary, L., & Heggors, J.P. 1984. Acute effects of tobacco smoking on blood flow in the cutaneous micro-circulation. *Br.J.Plast.Surg.*, 37, (2) 213-215

Rhodes, L.E., Belgi, G., Parslew, R., McLoughlin, L., Clough, G.F., & Friedmann, P.S. 2001. Ultraviolet-B-induced erythema is mediated by nitric oxide and prostaglandin E2 in combination. *J.Invest Dermatol.*, 117, (4) 880-885

Richardson, D. 1987. Effects of tobacco smoke inhalation on capillary blood flow in human skin. *Arch.Environ.Health*, 42, (1) 19-25

Rithalia, S.V.S., & Gonsalkorale, M. 2000. Quantification of pressure relief using interface pressure and tissue perfusion in alternating pressure air mattresses. *Arch.Phys.Med.Rehabil.*, 81, 1364-1369

- Rocchi, E., Bursi, F., Ventura, P., Ronzoni, A., Gozzi, C., Casalgrandi, G., Marri, L., Rossi, R., & Modena, M.G. 2007. Anti- and pro-oxidant factors and endothelial dysfunction in chronic cigarette smokers with coronary heart disease. *Eur.J.Intern.Med.*, 18, (4) 314-320
- Rossi, M., Ricco, R., & Carpi, A. 2004. Spectral analysis of skin laser Doppler blood perfusion signal during cutaneous hyperemia in response to acetylcholine iontophoresis and ischemia in normal subjects. *Clin.Hemorheol.Microcirc.*, 31, (4) 303-310
- Rossi, M. & Carpi, A. 2004. Skin microcirculation in peripheral arterial obliterative disease. *Biomed.Pharmacother.*, 58, (8) 427-431
- Rossi, M., Bertuglia, S., Varanini, M., Giusti, A., Santoro, G., & Carpi, A. 2005. Generalised wavelet analysis of cutaneous flowmotion during post-occlusive reactive hyperaemia in patients with peripheral arterial obstructive disease. *Biomed.Pharmacother.*, 59, (5) 233-239
- Rossi, M., Carpi, A., Galetta, F., Franzoni, F., & Santoro, G. 2006a. The investigation of skin blood flowmotion: a new approach to study the microcirculatory impairment in vascular diseases? *Biomed.Pharmacother.*, 60, (8) 437-442
- Rossi, M., Carpi, A., Di Maria, C., Galetta, F., & Santoro, G. 2006b. Spectral analysis of laser Doppler skin blood flow oscillations in human essential arterial hypertension. *Microvasc.Res.*, 72, (1-2) 34-41
- Rossi, M., Carpi, A., Di, M.C., Galetta, F., & Santoro, G. 2007. Absent post-ischemic increase of blood flowmotion in the cutaneous microcirculation of healthy chronic cigarette smokers. *Clin.Hemorheol.Microcirc.*, 36, (2) 163-171
- Rossi, M., Cupisti, A., Di, M.C., Galetta, F., Barsotti, G., & Santoro, G. 2008. Blunted post-ischemic increase of the endothelial skin blood flowmotion component as early sign of endothelial dysfunction in chronic kidney disease patients. *Microvasc.Res.*, 75, (3) 315-322
- Rossi, M., Carpi, A., Di, M.C., Franzoni, F., Galetta, F., & Santoro, G. 2009. Skin blood flowmotion and microvascular reactivity investigation in hypercholesterolemic patients without clinically manifest arterial diseases. *Physiol Res.*, 58, (1) 39-47

Rowell, L.B. 1977. Reflex control of the cutaneous vasculature. *J.Invest Dermatol.*, 69, (1) 154-166

Royal College of Nursing & National Institute for Health and Clinical Excellence. 2005. *The management of pressure ulcers in primary and secondary care: A clinical guideline.*

Rubanyi, G.M., Romero, J.C., & Vanhoutte, P.M. 1986. Flow-induced release of endothelium-derived relaxing factor. *Am.J.Physiol*, 250, (6 Pt 2) H1145-H1149

Rucker, M., Strobel, O., Vollmar, B., Roesken, F., & Menger, M.D. 2000. Vasomotion in critically perfused muscle protects adjacent tissues from capillary perfusion failure. *Am.J.Physiol Heart Circ.Physiol*, 279, (2) H550-H558

Rummery, N.M. & Hill, C.E. 2004. Vascular gap junctions and implications for hypertension. *Clin.Exp.Pharmacol.Physiol*, 31, (10) 659-667

Russell, L. 1998. Physiology of the skin and prevention of pressure sores. *Br.J.Nurs.*, 7, (18) 1084, 1088-1092, 1096

Sacks, A.H., O'Neill, H., & Perkas, I. 1985. Skin blood flow changes and tissue deformations produced by cylindrical indentors. *J.Rehabil.Res.Dev.*, 22, (3) 1-6

Sae-Sia, W., Wipke-Tevis, D.D., & Williams, D.A. 2007. The effect of clinically relevant pressure duration on sacral skin blood flow and temperature in patients after acute spinal cord injury. *Arch.Phys.Med.Rehabil.*, 88, (12) 1673-1680

Saumet, J.L., Kellogg, D.L., Jr., Taylor, W.F., & Johnson, J.M. 1988. Cutaneous laser-Doppler flowmetry: influence of underlying muscle blood flow. *J.Appl.Physiol*, 65, (1) 478-481

Sax, F.L., Cannon, R.O., III, Hanson, C., & Epstein, S.E. 1987. Impaired forearm vasodilator reserve in patients with microvascular angina. Evidence of a generalized disorder of vascular function? *N.Engl.J.Med.*, 317, (22) 1366-1370

Schubert, V. & Fagrell, B. 1989. Local skin pressure and its effects on skin microcirculation as evaluated by laser-Doppler fluxmetry. *Clin.Physiol*, 9, (6) 535-545

- Schubert, V. 1991. Hypotension as a risk factor for the development of pressure sores in elderly subjects. *Age Ageing*, 20, (4) 255-261
- Schubert, V. & Fagrell, B. 1991. Evaluation of the dynamic cutaneous post-ischaemic hyperaemia and thermal response in elderly subjects and in an area at risk for pressure sores. *Clin.Physiol*, 11, (2) 169-182
- Seeley, R., Stephens, T., & Tate, P. 2000. *Anatomy and Physiology*, McGraw-Hill Companies.
- Sell, M., Boldt, W., & Markwardt, F. 2002. Desynchronising effect of the endothelium on intracellular Ca<sup>2+</sup> concentration dynamics in vascular smooth muscle cells of rat mesenteric arteries. *Cell Calcium*, 32, (3) 105-120
- Shore, A.C., Price, K.J., Sandeman, D.D., Green, E.M., Tripp, J.H., & Tooke, J.E. 1991. Impaired microvascular hyperaemic response in children with diabetes mellitus. *Diabet.Med.*, 8, (7) 619-623
- Slaaf, D.W., Vrieling, H.H., Tangelder, G.J., & Reneman, R.S. 1988. Effective diameter as a determinant of local vascular resistance in presence of vasomotion. *Am.J.Physiol*, 255, (5 Pt 2) H1240-H1243
- Smith, S. 1997. *The scientist and engineers guide to DigitalSignalProcessing* California, Technical Publishing.
- Smith, C.J. & Fischer, T.H. 2001. Particulate and vapor phase constituents of cigarette mainstream smoke and risk of myocardial infarction. *Atherosclerosis*, 158, (2) 257-267
- Smith, B.M., Guihan, M., LaVela, S.L., & Garber, S.L. 2008. Factors predicting pressure ulcers in veterans with spinal cord injuries. *Am.J.Phys.Med.Rehabil.*, 87, (9) 750-757
- Soderstrom, T., Stefanovska, A., Veber, M., & Svensson, H. 2003. Involvement of sympathetic nerve activity in skin blood flow oscillations in humans. *Am.J.Physiol Heart Circ.Physiol*, 284, (5) H1638-H1646
- Sorensen, L.T., Jorgensen, S., Petersen, L.J., Hemmingsen, U., Bulow, J., Loft, S., & Gottrup, F. 2009. Acute effects of nicotine and smoking on blood flow, tissue oxygen, and aerobic metabolism of the skin and subcutis. *J.Surg.Res.*, 152, (2) 224-230

- Spilsbury, K., Nelson, A., Cullum, N., Iglesias, C., Nixon, J., & Mason, S. 2007. Pressure ulcers and their treatment and effects on quality of life: hospital inpatient perspectives. *J.Adv.Nurs.*, 57, (5) 494-504
- Sprigle, S., Linden, M., & Riordan, B. 2002. Characterizing reactive hyperemia via tissue reflectance spectroscopy in response to an ischemic load across gender, age, skin pigmentation and diabetes. *Med.Eng Phys.*, 24, (10) 651-661
- Stevens, A. & Lowe, J. 1997. *Human Histology*, 2nd ed. Philadelphia, Mosby.
- Stewart, J., Kohen, A., Brouder, D., Rahim, F., Adler, S., Garrick, R., & Goligorsky, M.S. 2004. Noninvasive interrogation of microvasculature for signs of endothelial dysfunction in patients with chronic renal failure. *Am.J.Physiol Heart Circ.Physiol*, 287, (6) H2687-H2696
- Stewart, J.M., Taneja, I., Goligorsky, M.S., & Medow, M.S. 2007. Noninvasive measure of microvascular nitric oxide function in humans using very low-frequency cutaneous laser Doppler flow spectra. *Microcirculation.*, 14, (3) 169-180
- Struck, B.D. & Wright, J.E. 2007. Pressure ulcers and endothelial dysfunction: is there a link? *J.Nutr.Elder.*, 26, (3-4) 105-117
- Stulc, T., Kasalova, Z., Prazny, M., Vrablik, M., Skrha, J., & Ceska, R. 2003. Microvascular reactivity in patients with hypercholesterolemia: effect of lipid lowering treatment. *Physiol Res.*, 52, (4) 439-445
- Suner, I.J., Espinosa-Heidmann, D.G., Marin-Castano, M.E., Hernandez, E.P., Pereira-Simon, S., & Cousins, S.W. 2004. Nicotine increases size and severity of experimental choroidal neovascularisation. *Invest.Ophthalmol.Vis.Sci.*, 45, (1) 311-317
- Suriadi, Sanada, H., Sugama, J., Thigpen, B., & Subuh, M. 2008. Development of a new risk assessment scale for predicting pressure ulcers in an intensive care unit. *Nurs.Crit Care*, 13, (1) 34-43
- Svalestad, J., Hellem, S., Vaagbo, G., Irgens, A., & Thorsen, E. 2010. Reproducibility of transcutaneous oximetry and laser Doppler flowmetry in facial skin and gingival tissue. *Microvasc.Res.*, 79, (1) 29-33

- Swain, I.D. & Grant, L.J. 1989. Methods of measuring skin blood flow. *Phys.Med.Biol.*, 34, (2) 151-175
- Taddei, S., Galetta, F., Viridis, A., Ghiadoni, L., Salvetti, G., Franzoni, F., Giusti, C., & Salvetti, A. 2000. Physical activity prevents age-related impairment in nitric oxide availability in elderly athletes. *Circulation*, 101, (25) 2896-2901
- Tagawa, T., Imaizumi, T., Endo, T., Shiramoto, M., Harasawa, Y., & Takeshita, A. 1994. Role of nitric oxide in reactive hyperemia in human forearm vessels. *Circulation*, 90, (5) 2285-2290
- Takenaka, T., Suzuki, H., Okada, H., Hayashi, K., Kanno, Y., & Saruta, T. 1998. Mechanosensitive cation channels mediate afferent arteriolar myogenic constriction in the isolated rat kidney. *J.Physiol*, 511 ( Pt 1), 245-253
- Tee, G.B., Rasool, A.H., Halim, A.S., & Rahman, A.R. 2004. Dependence of human forearm skin postocclusive reactive hyperemia on occlusion time. *J.Pharmacol.Toxicol.Methods*, 50, (1) 73-78
- Tenland, T., Salerud, E.G., Nilsson, G.E., & Oberg, P.A. 1983. Spatial and temporal variations in human skin blood flow. *Int.J.Microcirc.Clin.Exp.*, 2, (2) 81-90
- Thompson-Bishop, J.Y., & Mottola, C.M. 1992. Tissue interface pressure and estimated subcutaneous pressures of 11 different pressure reducing support surfaces. *Decubitus*. 5, 42-48
- Timar-Banu, O., Beaugard, H., Tousignant, J., Lassonde, M., Harris, P., Viau, G., Vachon, L., Levy, E., & Aribat, T. 2001. Development of noninvasive and quantitative methodologies for the assessment of chronic ulcers and scars in humans. *Wound.Repair Regen.*, 9, (2) 123-132
- Tingle, J. 1997. Pressure sores: counting the legal cost of nursing neglect. *Br.J.Nurs.*, 6, (13) 757-758
- Tortora, G.J. & Grabowski, S.R. 1996. *Principles of Anatomy and Physiology*, 8th ed. John Wiley & Sons Inc.
- Tortora, G.J. & Grabowski, S.R. 2000. *Principles of Anatomy and Physiology*, 9th ed. John Wiley & Sons Inc.

- Tortora, G. & Derrickson, B. 2009. *Principles of Anatomy and Physiology*, 12th ed. John Wiley & Sons Inc.
- Tousoulis, D., Antoniadis, C., Tentolouris, C., Tsioufis, C., Toutouza, M., Toutouzas, P., & Stefanadis, C. 2003. Effects of combined administration of vitamins C and E on reactive hyperemia and inflammatory process in chronic smokers. *Atherosclerosis*, 170, (2) 261-267
- Trandel, R.S., Lewis, D.W., & Verhonick, P.J. 1975. Thermographical investigation of decubitus ulcers. *Bull.Prosthet.Res.* (10-24) 137-155
- Tsai, A.G. & Intaglietta, M. 1993. Evidence of flowmotion induced changes in local tissue oxygenation. *Int.J.Microcirc.Clin.Exp.*, 12, (1) 75-88
- Tsuchiya, M., Asada, A., Kasahara, E., Sato, E.F., Shindo, M., & Inoue, M. 2002. Smoking a single cigarette rapidly reduces combined concentrations of nitrate and nitrite and concentrations of antioxidants in plasma. *Circulation*, 105, (10) 1155-1157
- Tur, E., Yosipovitch, G., & Oren-Vulfs, S. 1992. Chronic and acute effects of cigarette smoking on skin blood flow. *Angiology*, 43, (4) 328-335
- University of Southampton. 2005. *Demystifying Biomedical Signals: Principals and Applications*. Course Notes.
- Ursino, M., Cavalcanti, S., Bertuglia, S., & Colantuoni, A. 1996. Theoretical analysis of complex oscillations in multibranching microvascular networks. *Microvasc.Res.*, 51, (2) 229-249
- Vallance, P., & Chan, N. 2001. Endothelial function and nitric oxide: clinical relevance. *Heart*, 85, 342-350
- van Adrichem, L.N., Hovius, S.E., van, S.R., & van der Meulen, J.C. 1992. Acute effects of cigarette smoking on microcirculation of the thumb. *Br.J.Plast.Surg.*, 45, (1) 9-11
- van, d., V, Postma, D.S., Timens, W., Hylkema, M.N., Willemse, B.W., Boezen, H.M., Vonk, J.M., de Reus, D.M., Kauffman, H.F., & ten Hacken, N.H. 2005. Acute effects of cigarette smoking on inflammation in healthy intermittent smokers. *Respir.Res.*, 6, (22)

- Vangilder, C., Macfarlane, G.D., & Meyer, S. 2008. Results of nine international pressure ulcer prevalence surveys: 1989 to 2005. *Ostomy.Wound.Manage.*, 54, (2) 40-54
- Vangilder, C., MacFarlane, G., Meyer, S., & Lachenbruch, C. 2009. Body mass index, weight, and pressure ulcer prevalence: an analysis of the 2006-2007 International Pressure Ulcer Prevalence Surveys. *J.Nurs.Care Qual.*, 24, (2) 127-135
- Verma, S. & Anderson, T.J. 2002. Fundamentals of endothelial function for the clinical cardiologist. *Circulation*, 105, (5) 546-549
- Vinik, A.I., Erbas, T., Park, T.S., Pierce, K.K., & Stansberry, K.B. 2001. Methods for evaluation of peripheral neurovascular dysfunction. *Diabetes Technol.Ther.*, 3, (1) 29-50
- Wann-Hansson, C., Hagell, P., & Willman, A. 2008. Risk factors and prevention among patients with hospital-acquired and pre-existing pressure ulcers in an acute care hospital. *J.Clin.Nurs.*, 17, (13) 1718-1727
- Wardell, K., Braverman, I.M., Silverman, D.G., & Nilsson, G.E. 1994. Spatial heterogeneity in normal skin perfusion recorded with laser Doppler imaging and flowmetry. *Microvasc.Res.*, 48, (1) 26-38
- Warner, D.O., Joyner, M.J., & Charkoudian, N. 2004. Nicotine increases initial blood flow responses to local heating of human non-glabrous skin. *J.Physiol*, 559, (Pt 3) 975-984
- Whittington, K., Patrick, M., & Roberts, J.L. 2000. A national study of pressure ulcer prevalence and incidence in acute care hospitals. *J.Wound.Ostomy.Continence.Nurs.*, 27, (4) 209-215
- Wiernsperger, N. 2000. Defects in microvascular haemodynamics during prediabetes: contributor or epiphenomenon? *Diabetologia*, 43, (11) 1439-1448
- Widlansky, M.E. 2009. Shear stress and flow-mediated dilation: all shear responses are not created equally. *Am.J.Physiol.*, 296, H31-H32
- Wiesner, T.F., Berk, B.C., & Nerem, R.M. 1997. A mathematical model of the cytosolic-free calcium response in endothelial cells to fluid shear stress. *Proc.Natl.Acad.Sci.U.S.A*, 94, (8) 3726-3731

- Wiles, M.D., Dickson, E., & Moppett, I.K. 2008. Transient hyperaemic response to assess vascular reactivity of skin: effect of topical anaesthesia. *Br.J.Anaesth.*, 101, (3) 320-323
- Wilkin, J.K. 1986. Periodic cutaneous blood flow during postocclusive reactive hyperemia. *Am.J.Physiol*, 250, (5 Pt 2) H765-H768
- Wohlrab, J., Korting, R., Helmbold, P., & Marsch, W.C. 2001. The NO release test as a functional reference standard for laser Doppler fluxmetry in cutaneous microangiology. *Skin Res.Technol.*, 7, (3) 172-175
- Wong, B.J., Wilkins, B.W., Holowatz, L.A., & Minson, C.T. 2003. Nitric oxide synthase inhibition does not alter the reactive hyperemic response in the cutaneous circulation. *J.Appl.Physiol*, 95, (2) 504-510
- Wright, C. I., Kroner, C. I., & Draijer, R. 2006. Non-invasive methods and stimuli for evaluating the skin's microcirculation. *Journal of Pharmacological and Toxicological Methods*, 54, 1-25
- Wywiałowski, E.F. 1999. Tissue perfusion as a key underlying concept of pressure ulcer development and treatment. *J.Vasc.Nurs.*, 17, (1) 12-16
- Xakellis, G.C., Frantz, R.A., Arteaga, M., & Meletiou, S. 1993. Dermal blood flow response to constant pressure in healthy older and younger subjects. *J.Gerontol.*, 48, (1) M6-M9
- Yanbaeva, D.G., Dentener, M.A., Creutzberg, E.C., Wesseling, G., & Wouters, E.F. 2007. Systemic effects of smoking. *Chest*, 131, (5) 1557-1566
- Yin, L., Morita, A., & Tsuji, T. 2000. Alterations of extracellular matrix induced by tobacco smoke extract. *Arch.Dermatol.Res.* , 292, (4) 188-194
- Young, J.M., Shand, B.I., McGregor, P.M., Scott, R.S., & Frampton, C.M. 2006. Comparative effects of enzenol and vitamin C supplementation versus vitamin C alone on endothelial function and biochemical markers of oxidative stress and inflammation in chronic smokers. *Free Radic.Res.*, 40, (1) 85-94

Zhang, W.Z., Venardos, K., Chin-Dusting, J., & Kaye, D.M. 2006. Adverse effects of cigarette smoke on NO bioavailability: role of arginine metabolism and oxidative stress. *Hypertension*, 48, (2) 278-285

Zhao, J.L., Pergola, P.E., Roman, L.J., & Kellogg, D.L., Jr. 2004. Bioactive nitric oxide concentration does not increase during reactive hyperemia in human skin. *J.Appl.Physiol*, 96, (2) 628-632

Zhong, J., Seifalian, A.M., Salerud, G.E., & Nilsson, G.E. 1998. A mathematical analysis on the biological zero problem in laser Doppler flowmetry. *IEEE Trans.Biomed.Eng*, 45, (3) 354-364

